10-29-2019 4:15 PM

The Neural Circuitry of Sensory Processing in Post-traumatic Stress Disorder

Sherain Harricharan, *The University of Western Ontario*

Supervisor: Lanius, Ruth A., *The University of Western Ontario*

A thesis submitted in partial fulfillment of the requirements for the Doctor of Philosophy degree in Neuroscience

Abstract

Background: Traumatic experiences can have severe emotional and psychological consequences, which may affect the capacity to process both internal and external sensory information. Such aberrations may have cascading effects in individuals with post-traumatic stress disorder (PTSD), where alterations in sensory processing may hinder the capacity for higher-order executive functions, including emotion regulation. Delineating the neural circuitry of subcortical and cortical structures thought to be central to sensory processing is therefore critical to the study of PTSD and may help to develop an understanding of the neurobiological mechanisms underlying this often debilitating disorder.

Methods: Various neuroimaging approaches were employed to investigate sensory processing in PTSD, its dissociative subtype, and healthy controls. First, resting-state connectivity patterns of subcortical brainstem structures linked to interoceptive and exteroceptive sensory processing, including the periaqueductal gray and the vestibular nuclei, were examined (chapters 2 and 3). In addition, given that the insula is critical for relaying exteroceptive and interoceptive sensory information to other neurocognitive networks in the brain, resting-state whole brain seed-based connectivity patterns of different insula subregions were investigated (chapter 4). Furthermore, machine learning analyses were used to assess the utility of insula subregion resting-state connectivity patterns as a diagnostic predictor for classifying PTSD, its dissociative subtype, and healthy controls. Finally, a task-based paradigm using oculomotor stimuli with simultaneous traumatic autobiographical memory recall was employed to examine cortical brain structures involved in the convergence of exteroceptive and interoceptive sensory information (chapter 5).

Results and Discussion: As compared to controls, widespread periaqueductal gray connectivity was observed with cortical structures associated with emotional reactivity and defensive responding in PTSD and its dissociative subtype at rest. In addition, as compared to controls, decreased vestibular nuclei connectivity with cortical structures essential to exteroceptive sensory processing and multisensory integration was observed in individuals with the PTSD dissociative subtype. Moreover, PTSD showed limited cortical insula subregion resting-state connectivity with frontal lobe structures involved in the central executive network, which may be associated with impairment of higher-order executive functions, including emotion regulation, in PTSD. Finally, exposure to simultaneous exteroceptive and interoceptive sensory stimuli through oculomotor eye movements performed simultaneous to traumatic memory recall engaged the dorsal attentional network and default-mode frontoparietal networks that have been demonstrated to work in tandem to facilitate connectivity with structures in the central executive network, including the dorsolateral and dorsomedial prefrontal cortex, necessary for multisensory integration and emotion regulation. This effect was greater in individuals with PTSD and may provide a neurobiological account for how oculomotion may influence the frontoparietal cortical representation of traumatic memories. Overall, the findings of this dissertation reveal that individuals with PTSD experience aberrations in the neural circuitry necessary for processing both interoceptive and exteroceptive sensory information. We hypothesize that these observed alterations in interoceptive and exteroceptive neural processing may underlie, in part, the emotion dysregulation and maladaptive responses to chronic stress, including hypervigilance and dissociative symptoms, observed in PTSD and its dissociative subtype.

Keywords

post-traumatic stress disorder, dissociation, sensory processing, neuroimaging, brainstem, periaqueductal gray, vestibular system, insula, prefrontal cortex, frontoparietal network, multisensory integration, executive function, emotion regulation

Summary for Lay Audience

Post-traumatic stress disorder (PTSD) is a psychiatric disorder that is triggered by an individual experiencing or witnessing a traumatic event, which may precipitate persistent flashbacks and severe anxiety, causing individuals to be fearful and hypervigilant of their surroundings. Approximately 14-30% of traumatized individuals may present with a dissociative subtype of PTSD, which is often associated with repeated trauma or childhood trauma. These patients may present with additional symptoms, including depersonalization and derealization, where they may feel as if the world or self is “dream-like” and not real and/or describe “out-of-body” experiences. This dissertation explores potential neural alterations that may signify how traumatized individuals with PTSD and its dissociative subtype experience sensations differently, whether they are from the outside world (i.e. touch, auditory, visual sensations) or from the internal body (i.e. emotions, visceral sensations). It is hypothesized that alterations in neural pathways important for the processing of these sensations may have cascading effects on the performance of higher-order cognitive functions, including emotion regulation. Various functional magnetic resonance imaging techniques were employed to examine brain structures critical to sensory processing in individuals with PTSD, the PTSD dissociative subtype and healthy controls.

The cumulative findings from this dissertation have been summarized into a theoretical framework that hypothesizes a neurobiological account through which sensory processing may be impacted in traumatized individuals.

Co-Authorship Statement

Sherain Harricharan, Maria Densmore, Dr. Andrew Nicholson, Dr. Mischa Tursich, Dr. Jean Théberge, Dr. Margaret McKinnon, Dr. Paul Frewen, Dr. Richard Neufeld, Dr. Daniela Rabellino, Dr. Allan Schore Dr. Janine Thome, Dr. Bessel Van der Kolk, Dr. Ruth Lanius

As author of this thesis and the primary author of the four experimental chapters, Sherain Harricharan was responsible for designing the experiments, data analysis, and writing the completed thesis and manuscripts for each experiment. Maria Densmore helped supervise the statistical analysis used to investigate neuroimaging data (Chapters 2-5) and assisted in data analysis for Chapter 5. Dr. Andrew Nicholson supervised the machine learning neuroimaging analysis used in Chapter 4 and was consulted about the neuroscientific inferences made from experimental findings in Chapters 3 and 4. Dr. Mischa Tursich helped design the task-based paradigm used in Chapter 5. Dr. Jean Théberge oversaw the implementation of brain imaging acquisition methods used to collect neuroimaging data in Chapters 2-5. Dr. Margaret McKinnon was consulted about the neuroscientific inferences made from the experimental findings for Chapter 5 and helped revise the experimental manuscripts for Chapter 2-5. Dr. Paul Frewen was consulted about the neuroscientific inferences made from the experimental findings for Chapter 2,4 and 5. Dr. Richard Neufeld was consulted about the statistical analysis used to study neuroimaging data in Chapters 3 and 4. Dr. Daniela Rabellino and Dr. Allan Schore were consulted about the neuroscientific inferences made from the experimental findings for Chapter 2. Dr. Janine Thome was consulted about the neuroscientific inferences made from the experimental findings for Chapter 4. Dr. Bessel Van der Kolk was consulted about the neuroscientific inferences made from the experimental

findings for Chapter 5. Dr. Ruth Lanius supervised all stages of this thesis and assisted in experimental design and manuscript revisions for all four experimental chapters.

Acknowledgments

Foremost, I would like to thank my supervisor, Dr. Ruth Lanius. Thank you for taking a chance on me and providing me with an amazing opportunity that ignited my passion for studying post-traumatic stress disorder. I feel incredibly proud of the work done in our lab and it is because of the confidence and trust you instill in your staff and students.

Next, I would like to thank Suzy Southwell and Stephanie Nevill for all the hard work they do in recruiting and assessing participants for our numerous studies. In addition, I would like to thank Maria Densmore for her guidance and mentorship to ensure neuroimaging statistical models are implemented correctly. I would also like to thank Nancy Mazza for all the administrative work she does to make sure everything in our lab runs smoothly.

I would also like to acknowledge Dr. Margaret McKinnon and Dr. Paul Frewen for their guidance and mentorship throughout all stages of this dissertation, I am very grateful to have learned from you both.

I feel so grateful to have learned from the post-doctoral fellows and students in our lab, including Dr. Daniela Rabellino, Dr. Janine Thome, Dr. Andrew Nicholson, Chantelle Lloyd and Braeden Terpou. You are all brilliant, but more importantly, you are all incredible people who always manage to keep everything in perspective.

In addition, I would like to thank all my family and friends for their support throughout the past few years. In particular, to my sisters, Sharada and Monisha Harricharan, thank you for believing in me and for being my constant pillars of strength.

Finally, this body of work is dedicated to the memory of my beloved parents, Dr. Rajendra and Indira Harricharan, whose light will always guide and motivate me throughout everything I do in life.

Table of Contents

List of Tables

List of Figures

List of Appendices

Chapter 1

1 « Introduction and Overview»

Traumatic experiences are associated with not only drastic emotional and psychological consequences, but may also provoke aberrations in neural pathways essential to the cognitive control of stress. Critically, traumatic stress is thought to disrupt physiological homeostasis, with associated alterations in arousal, including hyperarousal and hypoarousal states (Brown et al., 1985; D'Andrea et al., 2013; Frewen & Lanius, 2006; Pitman et al., 2012; Southwick et al., 1999; Vieweg et al., 2006; Yehuda et al., 2015). Post-traumatic stress disorder (PTSD), arising in response to traumatic stressors, is a disorder characterized by extreme arousal states, emotion dysregulation, and commonly persistent negative alterations in cognition and mood (American Psychiatric Association, 2013). In addition, individuals with PTSD may experience intrusive memories of past traumatic experiences and may show persistent hypervigilance concerning their surroundings, even in the absence of threat (American Psychiatric Association, 2013; Ehlers & Clark, 2000; Taylor, Kuch, Koch, Crockett, & Passey, 1998; Van der Kolk & McFarlane, 1998, Yehuda et al., 2015). Notably, approximately 14-30% of traumatized individuals present with the dissociative subtype of PTSD characterized by depersonalization and derealization symptoms associated with emotional detachment and hypoarousal (Armour, Karstoft, & Richardson, 2014; Blevins, Weathers, & Witte, 2014; Bremner & Southwick, 1992; Briere, Scott, & Weathers, 2005; Cloitre, Petkova, Wang, & Lu, 2012; Feeny, Zoellner, Fitzgibbons, & Foa, 2000; Frewen & Lanius, 2006; Hansen, Ross, & Armour, 2017; Lanius et al., 2010; Pain, Bluhm, & Lanius, 2010; Sierra & Berrios, 1998; Stein et al., 2013; Steuwe, Lanius, & Frewen, 2012; Wolf et al., 2012).

In addition to these core cognitive and affective symptoms, individuals with PTSD have shown alterations in sensory processing patterns, often showing extreme hypersensitivity to reminders related to traumatic memories (Engel-Yeger, Palgy-Levin, & Lev-Wiesel, 2013; Grillon & Morgan III, 1999; Näätänen & Alho, 1995; Shalev et al., 2000). Here, it is possible that a compromised ability to utilize both internal and external sensory information necessary for multisensory integration at the level of the cortex may negatively influence the capacity to carry out higher-order executive functions. Accordingly, delineating the neural circuitry of subcortical and cortical structures central to sensory processing among individuals with PTSD is necessary to elucidate the neurobiological mechanisms underlying this psychiatric disorder. It is this topic that the current thesis addresses.

Sensory processing provides a contextual framework through which an individual may develop an internal depiction of the external world. Moreover, understanding the transmisson of incoming internal and external sensory information to higher-order areas of brain is central to the study of executive functions, including goal-oriented action, response inhibition, and emotion regulation (Alvarez & Emory, 2006; Chan, Shum, Toulopoulou, & Chen, 2008; Fernandez-Duque, Baird, & Posner, 2000; Mazoyer et al., 2001). Damasio & Carvalho (2013) theorized that affective feelings and sensations are mental experiences of bodily states driven by alterations in physiological homeostasis, which can potentiate large-scale neural systems that involve all areas of the brain, including the brainstem, the limbic system and the cortex. Together, the subcortical and cortical neural signatures associated with these affective feelings ultimately shape the cognitive framework underlying the human brain's ability to perform higher-order

executive functions such as decision making and emotion regulation (Bechara, Damasio & Damasio, 2000). Here, it is critical to note that the initiation of higher-order executive functions is thought, under some theories, to be dependent upon the raw affect and sensations evoked at the level of the brainstem (Buck, 1999; Damasio, 1998; Davidson & Irwin, 1999; Davidson, Jackson, & Kalin, 2000; Koelsch, 2015; Northoff et al., 2006).

For example, Paul MacLean (1990) described initially the Triune Brain Concept, which categorizes the brain into three distinct areas: the reptilian brain, the mammalian brain, and the human brain that together involve the brainstem, the limbic brain, and the cortex, respectively. According to MacLean, the reptilian brain is integral to generating raw affect and coordinating innate, reflexive responses in response to threat and evolutionarily-relevant stimuli. By contrast, whereas the mammalian brain is thought to evaluate subjective feelings, such as pleasure or distress, the human brain is thought responsible for carrying out higher-order executive functions that fit into mental constructs shaped by past experience (Schacter, Addis, & Buckner, 2007). Moreover, Jaak Panksepp (2004) expanded upon MacLean's Triune Brain Concept, emphasizing in particular the importance of the brainstem in affective neuroscience by suggesting that the midbrain's role in generating raw affect can be divided into several primary process emotional systems in the brain that carry out basal brain functioning. These systems are thought to evoke both positive and negative affect, including care, play, lust, seek, rage, fear, and panic (Panksepp, 1992, 1998, 2005). Together, these emotional systems are thought to originate in medial subcortical structures, including the periaqueductal grey in the brainstem, and are thought crucial for sensory and higher-order self-referential processing occurring in medial cortical areas, including the medial prefrontal cortex and

the posterior cingulate cortex (Northoff et al., 2006). Here, both Northoff & Panksepp (2008) suggest that emotionally salient stimuli may engage primitive affective responses that originate at subcortical brainstem structures, hypothesizing further that these structures may lay the foundation for neural transmission to both the limbic system and the cortex.

1.1 « Brainstem Sensory Processing »

Numerous accounts suggest that sensory information derived from interoceptive and exteroceptive processes enters the brain at the level of the brainstem initially (Craig, 2002; Craig, 2003; Critchley, 2009; Khalsa et al., 2018; Medford & Critchley, 2010; Pezzulo, Rigoli, & Friston, 2015; Simmons et al., 2013; Stein, 1998). At the brainstem level, incoming sensory information may, in turn, engage primary process emotional systems described by Panksepp (2004) to elicit raw affective responses, such as panic or rage (Cameron, 2001; Muir, Madill, & Brown, 2017; Owens, Allen, Ondobaka, & Friston, 2018; Wiens, 2005; Zaki, Davis, & Ochsner, 2012). Northoff and colleagues (2006) identified specific midbrain structures in the brainstem, including the periaqueductal gray, the ventral tegmentum areas and the superior colliculus as key for engaging primary process emotional systems that translate incoming sensory input to the viscerosensory and the medial prefrontal cortices for self-referential processing. The viscerosensory cortex includes the anterior cingulate cortex, the anterior insula, and the ventromedial prefrontal cortex, with these structures thought collectively to monitor continuously autonomic, metabolic, and immunological resources in the body necessary to maintain physiological homeostasis. These cortical areas are further hypothesized to maintain consistent top-down projections to brainstem areas, including the periaqueductal

grey, in order to initiate allostatic effects to maintain internal homeostasis (Barrett & Simmons, 2015; Critchley et al. 2004; Wiens, 2005). Consistent top-down viscerosensory cortical projections to the brainstem are thought to help minimize hyperreactivity to continuous sensory input, as humans are thought to have developed interoceptive coding, which predicts interoceptive input based on past experiences, such that allostatic effects are only initiated when there are prediction errors that can disrupt physiological homeostasis (Barrett & Simmons, 2015; Craig, 2002; Critchley, Mathias, & Dolan, 2001; Critchley, Wiens, Rotshtein, Öhman, & Dolan, 2004; Critchley, 2005; Füstös, Gramann, Herbert, & Pollatos, 2012; Herbert & Pollatos, 2012; Pollatos, Gramann, & Schandry, 2007).

When an individual perceives a threat that requires an immediate response, raw affect generated at the level of the brainstem can trigger adaptive survival instincts that evoke innate defensive behaviours (Holstege, 2014; Jansen, Van Nguyen, Karpitskiy, Mettenleiter, & Loewy, 1995; Liddell et al., 2005; Siegel & Victoroff, 2009). This response is often accompanied by a disruption of homeostasis within the brain and body and is associated frequently with altered functioning of the sympathetic and parasympathetic branches of the autonomic nervous system (Goldstein, 1987 Jansen et al., 1995; Selye, 1973; Porges, 2009). Critically, sudden autonomic nervous system changes may induce a stress response, which can elicit extreme hyperarousal and hypoarousal states (Jansen et al., 1995; Paulus & Stein, 2006; Porges, 2009). On balance, the evidence reviewed here suggests that alterations in arousal observed among traumatized individuals may result in neural aberrations at a subcortical level, thus

dysregulating the neural circuitry underlying transmission of affective information from the brainstem to the cortex.

Notably, persistent alterations in arousal may predispose traumatized individuals to be hypervigilant of their surroundings for fear of encountering trauma-related reminders. This state of defensive posturing may compromise further one's ability to interpret external sensory information continuously received at the supraliminal and subliminal level (Bryant et al., 2008; Felmingham et al., 2009), thus disrupting awareness of one's position in gravitational space (Ionta et al., 2011; Medford & Critchley, 2010). Here, the vestibular system is thought to be imperative not only for maintaining one's physical equilibrium but also aids in establishing the spatial orientation of one's position in gravitational space. External vestibular sensory information, necessary to spatial orienting, is thought to be relayed from the inner ear to the brainstem vestibular nuclei before eventually reaching the parieto-insular vestibular cortex (Day & Fitzpatrick, 2005; De Waele, Baudonnière, Lepecq, Tran Ba Huy, & Vidal, 2001; Guldin & Grüsser, 1998; Miller et al., 2008). This parieto-insular vestibular cortex spans primarily the posterior insula and the temporoparietal junction, which are thought critical for receiving both interoceptive and exteroceptive input, respectively (De Waele et al., 2001; Lenggenhager & Lopez, 2015). Whereas the posterior insula is thought to be important for receiving internal viscerosensory information, the temporoparietal junction is thought to be involved in understanding one's self-location and self-orientation in space (Craig, 2003; Heydrich & Blanke, 2013; Lanius et al., 2005; Simmons et al., 2013; Suzuki et al., 2013). Importantly, if traumatized individuals experience sustained hypervigilance to their surroundings in tandem with alterations in arousal, this posturing may influence not only

how the cortex receives information from the internal viscera but may also have cascading effects on brain structures involved in locating one's self in space.

Taken together, the literature reviewed here points to the brainstem as being critical for receiving incoming raw interoceptive and exteroceptive sensory information. Moreover, given that the brainstem is a critical relay point in the brain for neural transmission to the cortex, examining brainstem connectivity patterns in traumatized individuals may elucidate the underlying neural pathways associated with the alterations in cognitions and mood observed in PTSD.

1.2 « Cortical Sensory Processing »

When interoceptive and exteroceptive information is relayed from the brainstem to the cortex, it may have cascading effects on the three cortically-driven neurocognitive intrinsic networks within the brain: (1) the salience network; (2) the default-mode network; and (3) the central executive network (Menon, 2011; Seeley et al., 2007). The salience network involves the dorsal anterior cingulate cortex and the frontoinsular cortex and is thought to assist in filtering relevant interoceptive, autonomic, and emotional information (Menon, 2011; Seeley et al., 2007). By contrast, the default-mode network encompasses medial cortical structures, including the medial prefrontal cortex, the hippocampus, the precuneus and the posterior cingulate, and is thought to be critical for mediating self-referential processes relating to introspection and autobiographical memory (Menon, 2011; Seeley et al., 2007). Finally, the central executive network is thought to form a frontoparietal system, including the dorsolateral and the dorsomedial prefrontal cortices, the superior parietal lobule and the intraparietal sulcus, that is thought

to facilitate higher-order executive functions and goal-directed behaviours, including emotion regulation (Menon, 2011; Seeley et al., 2007).

Importantly, the insula is critical to mediating switching between the default mode- and executive networks (Mennon & Uddin, 2010). Here, it is thought that relevant viscerosensory information is filtered to the insular cortex for interoceptive processing, thus helping to identify emotional feeling states underlying incoming sensory information (Chang et al., 2013; Couto et al., 2013). In turn, viscerosensory information relayed to the insula is hypothesized to activate both salience processing and central-executive networks to facilitate higher-order executive functions that assist in coordinating goal-directed action to relevant external stimuli (Duerden et al., 2013; Kober et al., 2008; Menon & Uddin, 2010). Here, the lateral frontoparietal central executive network converges multiple modalities of sensory information (i.e., visual, spatial, emotional) into a coherent multisensory perception about the environment (Ghazanfar & Schroeder, 2006; Maculoso & Driver, 2005; Senkowski et al., 2008). Finally, when the default-mode network is eventually reactivated after responding to salient stimuli, it assists in integrating this sensory information into a contextual meaning that can be incorporated subsequently into the embodied representation of one's self (Couto et al., 2013; Menon & Uddin, 2010).

As described above, one of the hallmark symptoms of PTSD involves alterations in cognition and mood, where individuals with PTSD frequently experience persistent negative trauma-related emotions and associated changes in perception of the self and the world (Cox, Resnick, & Kilpatrick, 2014; Foa, Ehlers, Clark, Tolin, & Orsillo, 1999; Frewen, Thornley, Rabellino, & Lanius, 2017). Here, cognitive functions such as emotion regulation may be negatively impacted in individuals with PTSD, as multisensory

integration of internal and external sensory information, as described above, is necessary to form a coherent perception of one's self and surroundings (Boden, Bonn-Miller, Kashdan, Alvarez, & Gross, J.J., 2012; Cloitre, Miranda, Stovall-McClough, & Han, 2005; Ehring & Quack, 2010; Ford, 2017). Indeed, several neurophysiological studies in PTSD reveal that PTSD is often associated with extreme sensory processing patterns, including sensory hypersensitivity to stimuli associated with traumatic memories (such as specific sounds, images, touch stimulation) (Engel-Yeger, Palgy-Levin, & Lev-Wiesel, 2013; Grillon & Morgan III, 1999; Näätänen & Alho, 1995; Shalev et al., 2000). It is possible that such hypersensitivity may disrupt interoceptive signaling in individuals with PTSD, thus altering the neural trajectory required for translation of viscerosensory information from the brainstem to areas in the cortex linked to emotion regulation, including the insula and the frontoparietal executive control network. In line with this hypothesis, neuroimaging studies in individuals with PTSD point clearly to a decreased capacity for emotion regulation, where emotional stress may alter cognitive networks that process information about perception, salience processing and creating goal-oriented responses. This research points to aberrations at the prefrontal cortex that may play a role in disrupting emotion processing among individuals with PTSD, which may alter semantic encoding of traumatic memories and the cognitive control of behavioural responses to emotionally salient stimuli (Brown & Morey, 2012; Frewen et al., 2008; Hayes, VanElzakker, Shin, 2012; Helpman et al., 2016; Rolle, Chick, Trivedi, Monuszko, & Etkin, 2019).

Accordingly, delineating further the neural underpinnings of sensory processing at both the subcortical and cortical level in individuals with post-traumatic stress disorder

appears necessary to enhance our understanding the neurobiological mechanisms underlying this debilitating disorder.

1.3 « Objectives »

In keeping with this central objective, this thesis aimed to investigate the neural circuitry underlying brain structures thought to be involved in sensory processing in PTSD and its dissociative subtype. Firstly, whole brain resting state functional connectivity patterns of brainstem structures central to interoceptive and exteroceptive processing, including the periaqueductal gray (Chapter 2) and vestibular nuclei (Chapter 3), were examined. Secondly, given that the insula has been identified a critical node for relaying incoming exteroceptive and interoceptive sensory information to other neurocognitive networks in the brain, insula resting-state connectivity patterns with the whole brain were investigated (Chapter 4). Here, machine learning analyses were used to assess the utility of insula resting-state connectivity patterns as a diagnostic predictor for discriminating between individuals with PTSD, its dissociative subtype, and healthy individuals (Chapter 4). Finally, a task-based paradigm was employed to investigate the neural mechanisms associated with the presentation of both exteroceptive and interoceptive stimuli in individuals with PTSD (Chapter 5). Here, we evaluated the neural circuitry underlying horizontal eye movements (exteroceptive sensory stimulus) during simultaneous traumatic autobiographical memory recall (interoceptive sensory stimulus) in an effort to delineate the neurobiological mechanisms through which exteroceptive and interoceptive sensory processing may converge to engage higher-order executive functions, such as emotion regulation.

1.4 « References »

Alvarez, J. A., & Emory, E. (2006). Executive function and the frontal lobes: a meta analytic review. *Neuropsychology review*, *16*(1), 17-42.

American Psychiatric Association. (2013). Diagnostic and statistical manual of mental disorders (5th ed.). Arlington, VA: American Psychiatric Publishing.

Armour, C., Karstoft, K. I., & Richardson, J. D. (2014). The co-occurrence of PTSD and dissociation: Differentiating severe PTSD from dissociative-PTSD. *Social Psychiatry and Psychiatric Epidemiology*, *49*(8), 1297-1306.

Barrett, L. F., & Simmons, W. K. (2015). Interoceptive predictions in the brain. *Nature Reviews Neuroscience*, *16*(7), 419-429.

Bechara, A., Damasio, H., & Damasio, A. R. (2000). Emotion, decision making and the orbitofrontal cortex. *Cerebral cortex*, *10*(3), 295-307.

Blevins, C. A., Weathers, F. W., & Witte, T. K. (2014). Dissociation and posttraumatic stress disorder: A latent profile analysis. *Journal of Traumatic Stress*, *27*(4), 388 396.

Boden, M. T., Bonn-Miller, M. O., Kashdan, T. B., Alvarez, J., & Gross, J. J. (2012). The interactive effects of emotional clarity and cognitive reappraisal in posttraumatic stress disorder. *Journal of Anxiety Disorders*, *26*(1), 233-238.

Bremner, J. D., & Southwick, S. (1992). Dissociation and posttraumatic stress disorder in Vietnam combat veterans. *The American journal of psychiatry*, *149*(3), 328.

Briere, J., Scott, C., & Weathers, F. (2005). Peritraumatic and persistent dissociation in the presumed etiology of PTSD. *American Journal of Psychiatry*, *162*(12), 2295 2301.

Brown, M. R., Fisher, L. A., Webb, V., Vale, W. W., & Rivier, J. E. (1985). Corticotropin-releasing factor: a physiologic regulator of adrenal epinephrine secretion. *Brain research*, *328*(2), 355-357.

Brown, V. M. & Morey, R. (2012). Neural systems for cognitive and emotional processing in posttraumatic stress disorder. *Frontiers in psychology*, *3*, 449.

Buck, R. (1999). The biological affects: a typology. *Psychological review*, *106*(2), 301 336.

Cameron, O. G. (2001). Interoception: the inside story—a model for psychosomatic processes. *Psychosomatic medicine*, *63*(5), 697-710.

Chan, R. C., Shum, D., Toulopoulou, T., & Chen, E. Y. (2008). Assessment of executive functions: Review of instruments and identification of critical issues. *Archives of clinical neuropsychology*, *23*(2), 201-216.

Chang, L. J., Yarkoni, T., Khaw, M. W., & Sanfey, A. G. (2012). Decoding the role of the insula in human cognition: functional parcellation and large-scale reverse inference. *Cerebral cortex*, *23*(3), 739-749.

Cloitre, M., Miranda, R., Stovall-McClough, K. C., & Han, H. (2005). Beyond PTSD: Emotion regulation and interpersonal problems as predictors of functional impairment in survivors of childhood abuse. *Behavior Therapy*, *36*(2), 119-124.

Cloitre, M., Petkova, E., Wang, J., & Lu, F. (2012). An examination of the influence of a sequential treatment on the course and impact of dissociation among women with PTSD related to childhood abuse. *Depression and Anxiety*, *29*(8), 709-717.

Couto, B., Salles, A., Sedeño, L., Peradejordi, M., Barttfeld, P., Canales-Johnson, A., ... & Favaloro, R. (2013). The man who feels two hearts: the different pathways of interoception. *Social cognitive and affective neuroscience*, *9*(9), 1253-1260.

Cox K. S., Resnick H. S., & Kilpatrick D. G. (2014). Prevalence and correlates of posttraumautic distorted beliefs: Evaluating DSM-5 PTSD expanded cognitive symptoms in a national sample. *Journal of Traumatic Stress*, 27, 299–306.

Craig, A. D. (2002). How do you feel? Interoception: the sense of the physiological condition of the body. *Nature reviews neuroscience*, *3*(8), 655-656.

Craig, A. D. (2003). Interoception: the sense of the physiological condition of the body. *Current opinion in neurobiology*, *13*(4), 500-505.

Critchley, H. D. (2005). Neural mechanisms of autonomic, affective, and cognitive integration. *Journal of comparative neurology*, *493*(1), 154-166.

Critchley, H. D. (2009). Psychophysiology of neural, cognitive and affective integration: fMRI and autonomic indicants. *International Journal of Psychophysiology*, *73*(2), 88-94.

Critchley, H. D., Mathias, C. J., & Dolan, R. J. (2001). Neural activity in the human brain relating to uncertainty and arousal during anticipation. *Neuron*, *29*(2), 537-545.

Critchley, H. D., Wiens, S., Rotshtein, P., Öhman, A., & Dolan, R. J. (2004). Neural systems supporting interoceptive awareness. *Nature neuroscience*, *7*(2), 189-195.

d'Andrea, W., Pole, N., DePierro, J., Freed, S., & Wallace, D. B. (2013). Heterogeneity of defensive responses after exposure to trauma: Blunted autonomic reactivity in response to startling sounds. *International Journal of Psychophysiology*, *90*(1), 80-89.

Damasio, A. R. (1998). Emotion in the perspective of an integrated nervous system. *Brain research reviews*, *26*(2-3), 83-86.

Damasio, A., & Carvalho, G. B. (2013). The nature of feelings: evolutionary and neurobiological origins. *Nature Reviews Neuroscience*, *14*(2), 143.

Daniels, J. K., Frewen, P., Theberge, J., & Lanius, R. A. (2016). Structural brain aberrations associated with the dissociative subtype of post-traumatic stress disorder. *Acta Psychiatrica Scandinavica*, *133*(3), 232-240.

Davidson, R. J., & Irwin, W. (1999). The functional neuroanatomy of emotion and affective style. *Trends in cognitive sciences*, *3*(1), 11-21.

Davidson, R. J., Jackson, D. C., & Kalin, N. H. (2000). Emotion, plasticity, context, and regulation: perspectives from affective neuroscience. *Psychological bulletin*, *126*(6), 890-909.

Day, B. L., & Fitzpatrick, R. C. (2005). The vestibular system. *Current biology*, *15*(15), R583-R586.

De Waele, C., Baudonnière, P., Lepecq, J., Huy, P. T. B., & Vidal, P. (2001). Vestibular projections in the human cortex. *Experimental brain research*, *141*(4), 541-551.

Ehlers, A., & Clark, D. M. (2000). A cognitive model of posttraumatic stress disorder. *Behaviour research and therapy*, *38*(4), 319-345.

Ehring, T., & Quack, D. (2010). Emotion regulation difficulties in trauma survivors: The role of trauma type and PTSD symptom severity. *Behavior therapy*, *41*(4), 587 598.

Engel-Yeger, B., Palgy-Levin, D., & Lev-Wiesel, R. (2013). The sensory profile of people with post-traumatic stress symptoms. *Occupational Therapy in Mental Health*, *29*(3), 266-278.

Feeny, N. C., Zoellner, L. A., Fitzgibbons, L. A., & Foa, E. B. (2000). Exploring the roles of emotional numbing, depression, and dissociation in PTSD. *Journal of traumatic stress*, *13*(3), 489-498.

Fernandez-Duque, D., Baird, J. A., & Posner, M. I. (2000). Executive attention and metacognitive regulation. *Consciousness and cognition*, *9*(2), 288-307.

Foa E. B., Ehlers A., Clark D. M., Tolin D. F., & Orsillo S. M. (1999). The Posttraumatic Cognitions Inventory (PTCI): Development and validation. *Psychological Assessment*, 11, 303–314.

Ford, J. D. (2017). Treatment implications of altered affect regulation and information processing following child maltreatment. *Psychiatric Annals*, *35*(5), 410-419.

Frewen, P. A., & Lanius, R. A. (2006). Toward a psychobiology of posttraumatic self dysregulation: Reexperiencing, hyperarousal, dissociation, and emotional numbing. *Annals of the New York Academy of Sciences*, *1071*(1), 110-124.

Frewen, P. A., Lanius, R. A., Dozois, D. J., Neufeld, R. W., Pain, C., Hopper, J. W., ... & Stevens, T. K. (2008). Clinical and neural correlates of alexithymia in posttraumatic stress disorder. *Journal of Abnormal Psychology*, *117*(1), 171-181.

Frewen, P., Thornley, E., Rabellino, D., & Lanius, R. (2017). Neuroimaging the traumatized self: fMRI reveals altered response in cortical midline structures and occipital cortex during visual and verbal self- and other-referential processing in women with PTSD. *European journal of psychotraumatology*, *8*(1), 1314164.

Füstös, J., Gramann, K., Herbert, B. M., & Pollatos, O. (2012). On the embodiment of emotion regulation: interoceptive awareness facilitates reappraisal. *Social cognitive and affective neuroscience*, *8*(8), 911-917.

Goldstein, D. S. (1987). Stress-induced activation of the sympathetic nervous system. *Bailliere's clinical endocrinology and metabolism*, *1*(2), 253-278.

Grillon, C., & Morgan III, C. A. (1999). Fear-potentiated startle conditioning to explicit and contextual cues in Gulf War veterans with posttraumatic stress disorder. *Journal of abnormal psychology*, *108*(1), 134-142.

Guldin, W. O., & Grüsser, O. J. (1998). Is there a vestibular cortex?. *Trends in neurosciences*, *21*(6), 254-259.

Hansen, M., Ross, J., & Armour, C. (2017). Evidence of the dissociative PTSD subtype: A systematic literature review of latent class and profile analytic studies of PTSD. *Journal of Affective Disorders*, *213*, 59-69.

Hayes, J. P., VanElzakker, M. B., & Shin, L. M. (2012). Emotion and cognition interactions in PTSD: a review of neurocognitive and neuroimaging studies. *Frontiers in integrative neuroscience*, *6*, 89.

Helpman, L., Marin, M. F., Papini, S., Zhu, X., Sullivan, G. M., Schneier, F., ... & Lindquist, M. A. (2016). Neural changes in extinction recall following prolonged exposure treatment for PTSD: a longitudinal fMRI study. *Neuroimage: clinical*, *12*, 715-723.

Herbert, B. M., & Pollatos, O. (2012). The body in the mind: on the relationship between interoception and embodiment. *Topics in cognitive science*, *4*(4), 692-704

Heydrich, L., & Blanke, O. (2013). Distinct illusory own-body perceptions caused by damage to posterior insula and extrastriate cortex. *Brain*, *136*(3), 790-803.

Holstege, G. (2014). The periaqueductal gray controls brainstem emotional motor systems including respiration. *Progress in brain research*, *209*, 379-405.

Ionta, S., Heydrich, L., Lenggenhager, B., Mouthon, M., Fornari, E., Chapuis, D., ... & Blanke, O. (2011). Multisensory mechanisms in temporo-parietal cortex support self-location and first-person perspective. *Neuron*, *70*(2), 363-374.

Jansen, A. S., Van Nguyen, X., Karpitskiy, V., Mettenleiter, T. C., & Loewy, A. D. (1995). Central command neurons of the sympathetic nervous system: basis of the fight-or-flight response. *Science*, *270*(5236), 644-646.

Khalsa, S. S., Adolphs, R., Cameron, O. G., Critchley, H. D., Davenport, P. W., Feinstein, J. S., ... & Meuret, A. E. (2018). Interoception and mental health: a roadmap. *Biological Psychiatry: Cognitive Neuroscience and Neuroimaging*, *3*(6), 501-513.

Koelsch, S., Jacobs, A. M., Menninghaus, W., Liebal, K., Klann-Delius, G., von Scheve, C., & Gebauer, G. (2015). The quartet theory of human emotions: an integrative and neurofunctional model. *Physics of life reviews*, *13*, 1-27.

Lanius, R. A., Vermetten, E., Loewenstein, R. J., Brand, B., Schmahl, C., Bremner, J. D., & Spiegel, D. (2010). Emotion modulation in PTSD: Clinical and neurobiological evidence for a dissociative subtype. *American Journal of Psychiatry*, *167*(6), 640 647.

Lanius, R. A., Williamson, P. C., Boksman, K., Densmore, M., Gupta, M., Neufeld, R. W., ... & Menon, R. S. (2002). Brain activation during script-driven imagery induced dissociative responses in PTSD: a functional magnetic resonance imaging investigation. *Biological psychiatry*, *52*(4), 305-311.

Lanius, R. A., Williamson, P. C., Bluhm, R. L., Densmore, M., Boksman, K., Neufeld, R. W., ... & Menon, R. S. (2005). Functional connectivity of dissociative responses in posttraumatic stress disorder: a functional magnetic resonance imaging investigation. *Biological psychiatry*, *57*(8), 873-884.

Lenggenhager, Bigna; Lopez, Christophe (2015). Vestibular Contributions to the Sense of Body, Self, and Others. In: Metzinger, Thomas; Windt, Jennifer M. Open MIND. Frankfurt am Main: MIND Group, pp.1-38.

Liddell, B. J., Brown, K. J., Kemp, A. H., Barton, M. J., Das, P., Peduto, A., ... & Williams, L. M. (2005). A direct brainstem–amygdala–cortical 'alarm'system for subliminal signals of fear. *Neuroimage*, *24*(1), 235-243.

MacLean, P. D. (1990). *The triune brain in evolution: Role in paleocerebral functions*. New York, NY: Springer Science & Business Media.

Mazoyer, B., Zago, L., Mellet, E., Bricogne, S., Etard, O., Houdé, O., ... & Tzourio Mazoyer, N. (2001). Cortical networks for working memory and executive functions sustain the conscious resting state in man. *Brain researchbulletin*, *54*(3), 287-298.

Medford, N., & Critchley, H. D. (2010). Conjoint activity of anterior insular and anterior cingulate cortex: awareness and response. *Brain Structure and Function*, *214*(56), 535-549.

Menon, V. (2011). Large-scale brain networks and psychopathology: a unifying triple network model. *Trends in cognitive sciences*, *15*(10), 483-506.

Menon, V., & Uddin, L. Q. (2010). Saliency, switching, attention and control: a network model of insula function. *Brain Structure and Function*, *214*(5-6), 655-667.

Miller, W. L., Maffei, V., Bosco, G., Iosa, M., Zago, M., Macaluso, E., & Lacquaniti, F. (2008). Vestibular nuclei and cerebellum put visual gravitational motion in context. *Journal of neurophysiology*, *99*(4), 1969-1982.

Muir, K., Madill, A., & Brown, C. (2017). Individual differences in emotional processing and autobiographical memory: interoceptive awareness and alexithymia in the fading affect bias. *Cognition and Emotion*, *31*(7), 1392-1404.

Näätänen, R., & Alho, K. (1995). Mismatch negativity-a unique measure of sensory processing in audition. *International Journal of Neuroscience*, *80*(1-4), 317-337.

Nieuwenhuys, R. (2012). The insular cortex: a review. *Progress in brain research*, *195*, 123-163.

Northoff, G., Heinzel, A., De Greck, M., Bermpohl, F., Dobrowolny, H., & Panksepp, J. (2006). Self-referential processing in our brain—a meta-analysis of imaging studies on the self. *Neuroimage*, *31*(1), 440-457.

Northoff, G., & Panksepp, J. (2008). The trans-species concept of self and the subcortical–cortical midline system. *Trends in cognitive sciences*, *12*(7), 259-264.

Owens, A. P., Allen, M., Ondobaka, S., & Friston, K. J. (2018). Interoceptive inference: from computational neuroscience to clinic. *Neuroscience & Biobehavioral Reviews*, *90*, 174-183.

Pain, C., Bluhm, R. L., & Lanius, R. A. (2010). 23 Dissociation in Patients With Chronic PTSD: Hyperactivation and Hypoactivation Patterns, Clinical and Neuroimaging Perspectives. *Dissociation and the dissociative disorders: DSM-V and beyond*. New York, NY: Springer.

Panksepp, J. (1992). A critical role for" affective neuroscience" in resolving what is basic about basic emotions.

Panksepp, J. (1998). The periconscious substrates of consciousness: Affective states and the evolutionary origins of the SELF. *Journal of consciousness studies*, *5*(5-6), 566-582.

Panksepp, J. (2004). *Affective neuroscience: The foundations of human and animal emotions*. New York, NY: Oxford university press.

Panksepp, J. (2005). Affective consciousness: Core emotional feelings in animals and humans. *Consciousness and cognition*, *14*(1), 30-80.

Paulus, M. P., & Stein, M. B. (2006). An insular view of anxiety. *Biological psychiatry*, *60*(4), 383-387.

Pezzulo, G., Rigoli, F., & Friston, K. (2015). Active Inference, homeostatic regulation and adaptive behavioural control. *Progress in neurobiology*, *134*, 17-35.

Pitman, R. K., Rasmusson, A. M., Koenen, K. C., Shin, L. M., Orr, S. P., Gilbertson, M. W., ... & Liberzon, I. (2012). Biological studies of post-traumatic stress disorder. *Nature reviews neuroscience*, *13*(11), 769-787.

Pollatos, O., Gramann, K., & Schandry, R. (2007). Neural systems connecting interoceptive awareness and feelings. *Human brain mapping*, *28*(1), 9-18.

Porges, S. W. (2009). The polyvagal theory: new insights into adaptive reactions of the autonomic nervous system. *Cleveland Clinic journal of medicine*, *76*(Suppl 2), S86-S90.

Rolle, C., Chick, C. F., Trivedi, H. M., Monuszko, K., & Etkin, A. (2019). Transcranial magnetic stimulation demonstrates a role for the ventrolateral prefrontal cortex in emotion perception. *Psychiatry Research*, 112515.

Schacter, D. L., Addis, D. R., & Buckner, R. L. (2007). Remembering the past to imagine the future: the prospective brain. *Nature reviews neuroscience*, *8*(9), 657-661.

Seeley, W. W., Menon, V., Schatzberg, A. F., Keller, J., Glover, G. H., Kenna, H., ... & Greicius, M. D. (2007). Dissociable intrinsic connectivity networks for salience processing and executive control. *Journal of Neuroscience*, *27*(9), 2349-2356.

Selye, H. (1973). The evolution of the stress concept. *American Scientist, 61*, 692-699.

Shalev, A. Y., Peri, T., Brandes, D., Freedman, S., Orr, S. P., & Pitman, R. K. (2000). Auditory startle response in trauma survivors with posttraumatic stress disorder: a prospective study. *American Journal of Psychiatry*, *157*(2), 255-261.

Siegel, A., & Victoroff, J. (2009). Understanding human aggression: New insights from neuroscience. *International journal of law and psychiatry*, *32*(4), 209-215.

Sierra, M., & Berrios, G. E. (1998). Depersonalization: neurobiological perspectives. *Biological psychiatry*, *44*(9), 898-908.

Simmons, W. K., Avery, J. A., Barcalow, J. C., Bodurka, J., Drevets, W. C., & Bellgowan, P. (2013). Keeping the body in mind: insula functional organization and functional connectivity integrate interoceptive, exteroceptive, and emotional awareness. *Human brain mapping*, *34*(11), 2944-2958.

Southwick, S. M., Bremner, J. D., Rasmusson, A., Morgan III, C. A., Arnsten, A., & Charney, D. S. (1999). Role of norepinephrine in the pathophysiology and treatment of posttraumatic stress disorder. *Biological psychiatry*, *46*(9), 1192 1204.

Stein, B. E. (1998). Neural mechanisms for synthesizing sensory information and producing adaptive behaviors. *Experimental Brain Research*, *123*(1-2), 124-135.

Stein, D. J., Koenen, K. C., Friedman, M. J., Hill, E., McLaughlin, K. A., Petukhova, M., ... & Bunting, B. (2013). Dissociation in posttraumatic stress disorder: evidence from the world mental health surveys. *Biological psychiatry*, *73*(4), 302-312.

Steuwe, C., Lanius, R. A., & Frewen, P. A. (2012). Evidence for a dissociative subtype of PTSD by latent profile and confirmatory factor analyses in a civilian sample. *Depression and anxiety*, *29*(8), 689-700.

Suzuki, K., Garfinkel, S. N., Critchley, H. D., & Seth, A. K. (2013). Multisensory integration across exteroceptive and interoceptive domains modulates self-experience in the rubber-hand illusion. *Neuropsychologia*, *51*(13), 2909-2917.

Taylor, S., Kuch, K., Koch, W. J., Crockett, D. J., & Passey, G. (1998). The structure of posttraumatic stress symptoms. *Journal of abnormal psychology*, *107*(1), 154.

Van der Kolk, B. A., & McFarlane, A. C. (1998). *The Black Hole of Trauma* (p. 487) in *Traumatic stress: The effects of overwhelming experience on mind, body, and society*. Guilford Press.

Vieweg, W. V. R., Julius, D. A., Fernandez, A., Beatty-Brooks, M., Hettema, J. M., & Pandurangi, A. K. (2006). Posttraumatic stress disorder: clinical features, pathophysiology, and treatment. *The American journal of medicine*, *119*(5), 383 390.

Wiens, S. (2005). Interoception in emotional experience. *Current opinion in neurology*, *18*(4), 442-447.

Wolf, E. J., Lunney, C. A., Miller, M. W., Resick, P. A., Friedman, M. J., & Schnurr, P. P. (2012). The dissociative subtype of PTSD: A replication and extension. *Depression and anxiety*, *29*(8), 679-688.

Yehuda, R., Hoge, C. W., McFarlane, A. C., Vermetten, E., Lanius, R. A., Nievergelt, C. M., ... & Hyman, S. E. (2015). Post-traumatic stress disorder. *Nature Reviews Disease Primers*, *1*, 15057.

Zaki, J., Davis, J. I., & Ochsner, K. N. (2012). Overlapping activity in anterior insula during interoception and emotional experience. *Neuroimage*, *62*(1), 493-499.

Zilverstand, A., Parvaz, M. A., & Goldstein, R. Z. (2017). Neuroimaging cognitive reappraisal in clinical populations to define neural targets for enhancing emotion regulation. A systematic review. *Neuroimage*, *151*, 105-116.

Chapter 2

2 « fMRI functional connectivity of the periaqueductal gray in PTSD and its dissociative subtype»

Chapter 2 has been published in its entirety as:

Harricharan, S., Rabellino, D., Frewen, P. A., Densmore, M., Théberge, J., McKinnon, M. C., Schore, A.N., & Lanius, R. A. (2016). fMRI functional connectivity of the periaqueductal gray in PTSD and its dissociative subtype. *Brain and behavior, 6*(12), e00579. https: doi.org/10.1002/brb3.579

2.1 « Introduction»

Posttraumatic stress disorder (PTSD) involves re-experiencing, avoidance, and hyperarousal symptoms, where individuals tend to be hypervigilant of their surroundings to ensure their own safety and to avoid exposure to threatening stimuli (Dalgleish, Moradi, Taghavi, Nesha-Doost, & Yule, 2001; Taylor, Kuch, Koch, Crockett, & Passey, 1998; Ehlers & Clark, 2000; American Psychological Association, 2013). When a threat is detected, PTSD patients may display hyperarousal symptoms associated with active defensive fight and flight circuitry of the sympathetic nervous system as evidenced by increased heart rate, skin conductance, and blood pressure (Pole, 2007). By contrast, patients with the less common dissociative subtype of PTSD (14%) (Stein et al., 2013), characterized by symptoms of depersonalization, often exhibit passive or submissive defensive responses accompanied by autonomic blunting (Corrigan, Fisher, & Nutt, 2011; Lanius et al., 2005; Lanius, Bluhm, Lanius, & Pain, 2006, Lanius et al., 2010).

Schauer & Elbert (2010) recently proposed a defense cascade model aimed at explaining the typical defensive reaction of an organism. Here, the presence of

dissociative states in humans exposed to trauma are associated with a transition from fight or flight defensive responses to more primitive animal defensive responses. These defensive responses, evoked in passive or submissive responses to threats, include unresponsive immobility, emotional blunting and analgesia (Baldwin, 2013; Nijenhuis, Vanderlinden, & Spinhoven, 1998; Porges, 1995). Interestingly, Bandler and colleagues (2000) propose that the periaqueductal gray (PAG), a small structure in the midbrain that consists of multiple subdivisions that oppose each other in function, is a central structure for mediating autonomic responses and is thus responsible for coordinating defensive reactions when confronted with threatening stimuli. Specifically, this study suggested that whereas the dorsolateral and lateral periaqueductal gray (DL-PAG and L-PAG) are associated with sympathetic nervous system activation that evokes active defensive strategies, the ventrolateral PAG (VL-PAG) is associated with passive coping strategies via activation of the parasympathetic nervous system. A recent pre-clinical study by Adamec and colleagues (2012) supported this hypothesis, where the dorsolateral PAG was associated with anxiety-related responses to stress in rodents. By contrast, the ventrolateral PAG exhibited a contrasting immobility or passive reaction to stress.

Kozlowksa and colleagues (2015) explicitly applied the functions of the PAG subdivisions to the defense cascade model (Schauer & Elbert, 2010) suggesting that when a threat is detected, DL-PAG and L-PAG subdivisions coordinate hyperarousal symptoms, such as fight or flight responses associated with sympathetic nervous system activity in response to threat. Here, it is believed that endocannabinoids facilitate further release of cortisol to elicit an acute stress response from the organism. Concomitant activation of the locus coeruleus in the brainstem may induce vasoconstriction of

peripheral blood vessels and thus increase blood supply to muscles that would allow the organism to fight the predator (George et al., 2013; Goadsby, Lambert, & Lance, 1985; Gorzalka, Hill, & Hillard, 2008; Patel, Roelke, Rademacher, Cullinan, & Hillard, 2004). In cases where the threat becomes inescapeable, the VL-PAG predominates as parasympathetic nervous system activation overrides sympathetic nervous system activation through increased vagal efferents from the dorsal motor nucleus, which in turn may produce hypoarousal symptoms that cause a freezing or submissive shutdown response, sometimes referred to as ‘conservation withdrawal (An, Bandler, Ongur, & Price, 1998; Porges, 2001). Projections from the VL-PAG to the medulla may play a role in generating such defensive freezing behavior (Tovote et al., 2016), which may be associated with the recruitment of pre-synaptic opioid receptors that mediate analgesic relief (Musha, Satoh, Koyanagawa, Kimura, & Satoh, 1989).

Previous neuroimaging studies of the PAG (Linnman, Moulton, Barmettler, Becerra, & Borsook, 2012) have supported functional segregation of the structure into multiple subdivisions that vary in function, with the dorsal PAG associated with elevated blood pressure and the ventral PAG stimulating lower blood pressure and parasympathetic dominance. In particular, in resting-state functional connectivity studies of the PAG in healthy populations, connectivity has been observed with the cerebellum subcortical network as well as the thalamus and the amygdala (Tomasi & Volkow, 2011). Critically, however, the complex neural circuitry of the PAG has not yet been delineated in PTSD and its dissociative subtype.

Accordingly, the aim of the present study was to examine resting state functional connectivity patterns of the PAG subdivisions in PTSD, since it was hypothesized that

this patient population would exhibit greater defensive posturing even during the resting state. An additional aim was to compare patterns of activation between individuals with and without the dissociative subtype of PTSD. We hypothesized that all PTSD patients would demonstrate increased functional connectivity of both PAG subdivisions with brain regions involved in threat appraisal (dorsal anterior cingulate cortex, fusiform gyrus; see Milad et al., 2007; Porges, 2007). Moreover, given that both PTSD and its dissociative subtype are associated with fight-flight and concomitant hyperarousal responses, we hypothesized that both groups would demonstrate increased DL-PAG functional connectivity with brain structures associated with sympathetic nervous system activity and consequent active defensive strategies, including the anterior insula and pre-motor cortex (see Butler et al., 2007; Critchley, Nagai, Gray, & Mathias, 2011). We hypothesized, however, that only those with the dissociative subtype of PTSD would demonstrate VL-PAG functional connectivity with brain structures associated with depersonalization and passive defensive responses, including the temporoparietal junction and the rolandic operculum (see Blanke & Arzy, 2005; Daniels, Frewen, Théberge, & Lanius, 2016; Zaytseva et al., 2015).

2.2 «Methods»

2.2.1 Clinical and Demographic Information

One-hundred and thirty-seven age-matched subjects were included in the study: 60 patients with a primary diagnosis of PTSD without the dissociative subtype (PTSD), 37 PTSD patients with the dissociative subtype of PTSD (PTSD+DS), and 40 healthy controls. The participants were recruited by the LHSC (London Health Sciences Centre) Department of Psychiatry during 2009 to 2016 via referrals from family physicians,

mental health professionals, psychology/psychiatry clinics, community programs for traumatic-stress survivors and posters/advertisements within the London, Ontario community.

A primary PTSD diagnosis was determined using the CAPS-IV (Clinician-Administered PTSD Scale), which assesses 17 categorized symptoms associated with PTSD on separate frequency and intensity scales, with the diagnosis confirmed by the DSM-IV criteria with an additional minimum severity score of 50 (Blake et al., 1995). PTSD patients with the dissociative subtype had the additional requirement of scoring at least two on both the frequency and intensity scales for depersonalization or derealisation symptoms (as per Nicholson et al., 2015 and Steuwe et al., 2014). For each participant, co-morbid Axis-I disorders were diagnosed with the SCID (Structure Clinical Interview for DSM-IV Axis I disorders) (First, Spitzer, Gibbon, & Williams, 2002). A battery of questionnaires was also administered, including the Beck Depression Inventory (BDI; Beck et al., 1997) to assess depression symptoms, the Child Trauma Questionnaire (CTQ; Bernstein et al., 2003) to assess childhood trauma history [92 PTSD patients (PTSD+DS and PTSD; 85%) met criteria for interpersonal childhood trauma according to CTQ cut-off scores (Bernstein & Fink, 1998; DiLillo et al., 2006)] and the Multiscale Dissociative Inventory (MDI; Briere, Weathers, & Runtz, 2005) to assess further dissociative experiences. The demographic and clinical characteristics of study participants are outlined in Table 2.1.

A one-way ANOVA was performed to assess age differences across participant groups, and a Pearson’s chi-square test was used to determine the effect of gender differences across all three participant groups. A Kruskal-Wallis analysis was used to

assess the normal distribution of non-parametric psychological measures (CAPS, BDI, CTQ and averaged depersonalization and derealization scores from MDI) with -post-hoc tests to assess significant differences between groups (Kruskal & Wallis, 1952).

Exclusion criteria for all participants included metal implants that violate 3.0T scanner safety regulations, a previous head injury associated with loss of consciousness, current or past history of neurological disorders, significant untreated medical illness, and pervasive developmental mental disorders. PTSD patients were excluded if they met criteria for current or past history of bipolar or psychotic disorders, or if patients had alcohol/substance dependency or abuse that had not sustained full remission for at least 6 months prior to study entry. Control participants were excluded if lifetime criteria were met for any DSM-IV Axis-I psychiatric disorder

All scanning was conducted at either Robarts Research Institute's Center for Functional and Metabolic Mapping or Lawson Health Research Institute in London, Ontario, Canada. The study was approved by the Research Ethics Board at Western University of Canada. All participants provided written informed consent to partake in the study.

Table 2.1 *Clinical and Demographic Information*

Measure	PTSD	PTSD+DS	Controls
N	60	37	40
Age	37.8 ± 11.6	40.4 ± 13.7	35.0 ± 11.0
Sex	M=25, F=35	M=8, F=29	M=14,F=26
CAPS-Total	67.9 ± 13.4	81.6 ± 12.7	0.7 ± 3.1

CTQ – Total	56.3 ± 24.7	68.2 ± 19.1	31.6 ± 8.6
BDI	22.8 ± 7.5	33.0 ± 10.3	1.2 ± 2.1
MDI – Total	54.1 ± 15.2	77.2 ± 22.0	33.7 ± 3.4
MDI – Depersonalization	6.6 ± 2.7	12.0 ± 5.2	5.2 ± 0.6
MDI – Derealization	8.6 ± 3.4	12.7 ± 4.0	5.2 ± 0.5
MDD	n=11(24)	n=23(9)	-
Panic Disorder/Agoraphobia	n=10(6)	n=9(6)	-
Social Phobia	n=2(2)	n=6(0)	-
OCD	n=3(2)	n=0(2)	-
GAD	n=1(0)	n=0(0)	-

Age, sex, CAPS and self-report questionnaires (CTQ, MDI, BDI) are reported as mean ± SD. Psychiatric disorders assessed via SCID-I (MDD, Panic Disorder/Agoraphobia, Social Phobia, OCD and GAD) are reported in frequencies, as n = current(past) cases.

Abbreviations: PTSD, non-dissociative posttraumatic stress disorder patients; PTSD+DS, dissociative posttraumatic stress disorder patients; M, Males; F, Females; CAPS, Clinician-Administered PTSD Scale; CTQ, Child Trauma Questionnaire; BDI, Beck Depression Inventory; MDI, Multiscale Dissociation Inventory; MDD, Major Depression Disorder; OCD, Obsessive Compulsive Disorder; GAD, Generalized Anxiety Disorder.

2.2.2 Data Acquisition

Whole-brain fMRI (functional magnetic resonance) data was obtained using a 3.0T scanner (Magnetom Tim Trio, Siemens Medical Solutions, Erlangen, Germany) with a 32-channel phased array head coil where the participant's head was supported with foam padding. BOLD (blood-oxygen level dependent) fMRI data was collected using a manufacturer's standard gradient-echo planar imaging (EPI) pulse sequence (single-shot, blipped-EPI) with an interleaved slice acquisition order with the following parameters: Time Resolution (TR) = 3000 ms, Echo-Time (TE) = 20ms, voxel size= 2 x 2 x 2 mm^3, Field of View (FOV) = 192 x 192 x 128 mm^3 (94 x 94 matrix, 64 contiguous slices), Flip Angle (FA) =90°. High-resolution T1-weighted anatomical images were also obtained (MPRage: 192 slices, voxel size = 1 x 1 x 1 mm^3). To obtain resting-state data, subjects were asked to close their eyes and let their minds wander without focusing on anything in

particular for six minutes (as per standard methods in Fransson, 2005; also see Bluhm et al., 2009).

2.2.3 Resting-State fMRI Data Preprocessing

Image preprocessing and statistical analyses were performed using statistical parametric mapping software (SPM12, Wellcome Trust Center for Neuroimaging, London, UK: http:// www.fil.ion.ucl.ac.uk/spm) within MATLAB 8.6 (R2015b, Mathworks Inc., MA). Four dummy scans were omitted from the fMRI time-series to allow magnetization reach steady-state before the experiments commences and enhance the quality of realignment during image pre-processing. The functional images for each subject were realigned to the first functional image to correct for motion in the scanner and resliced. The mean functional image was created and subsequently co-registered to the T1-weighted structural image for each subject to spatially realign functional images to the subject's anatomical space. The co-registered images were segmented into gray matter, white matter, cerebrum spinal fluid, bone, soft tissue and air using the "New Segment" method implemented in SPM12, which uses T2-weighted and PD-weighted scans when generating tissue probability maps. The resulting forward deformation fields were generated and used to spatially normalize the functional images to MNI space without resampling the voxel size, and each subject was visually inspected to ensure precise normalization patterns given the small anatomical region being studied. The images were then smoothed with a three-dimensional isotropic Gaussian kernel of 4mm FWHM (full-width at half-maximum), in co-ordinance with a previous PAG functional neuroimaging study (Dunckley et al., 2005) and a PAG neuroimaging meta-analysis (Linnman, Moulton, Barmettler, Becerra, & Borsook, 2012) that suggested using a lower smoothing kernel facilitates higher voxel resolution and thus helps elicit optimal

functional connectivity patterns based on a smaller neuroanatomical area in the brain (Becerra, Harter, Gonzalez, & Borsook, 2006). Beissner, Deichmann, and Baudrexel (2011) investigated optimal smoothing and normalization patterns in the brainstem and also found that a relatively lower smoothing kernel may be necessary to obtain significant results given its small region in the brain. It is important to note that the present study still satisfies the theory of Gaussian fields developed by Friston et al. (1995), which recommends that Gaussian smoothing should be a least double the voxel size (2 mm voxel size to 4 mm smoothing).

The smoothed functional images were further motion corrected with ART software (version 2015-10; Gabrieli Lab, McGovern Institute for Brain Research, Cambridge, MA; http://www.nitrc.org/projects/artifact_detect/) at a motion threshold of 2mm, as motion artifacts may significantly affect the BOLD signal in resting-state functional connectivity studies (Power, Barnes, Snyder, Schlaggar, & Petersen, 2012). The outlier motion regressors identified with ART were used as a covariate of no interest during within-subject (first-level) analysis. The smoothed functional images were subsequently bandpass-filtered to reduce the signal to noise ratio using 0.012 and 0.1 Hz as the high-pass and low-pass frequency cut-offs, respectively (in-house software by co-author Jean Théberge, Lawson Health Research Institute).

2.2.4 Seed-Based Regions of Interest

Seed region-of-interest masks (ROI) were generated using PickAtlas software (WFU Pickatlas, version 3.0.5; Maldjian, Laurienti, Kraft, & Burdette, 2003; http://fmri.wfubmc.edu/software/pickatlas) in co-ordinance with a PAG atlas developed by Ezra, Faull, Jbadi, & Pattinson (2015). Ezra and his colleagues mapped the PAG

subdivisions via a column tractography study using diffusion MRI. Two box-shaped masks were created to define both the dorsolateral (MNI x: 0; y: -32; z: -8.5 plus 6 x 2 x 1.5 mm extensions) and ventrolateral (MNI x: 0; y: -27; z: -8 plus 3 x 1 x 1 mm extensions) subdivisions of the PAG (Figure 2.1).

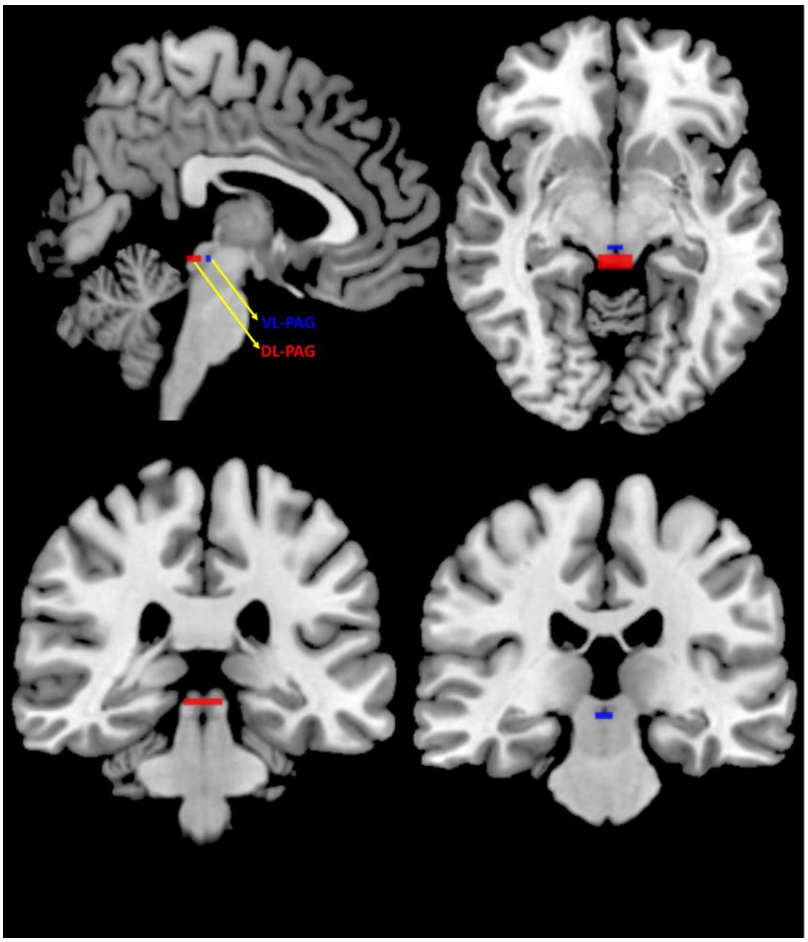

Figure 2.1 *Dorsolateral and Ventrolateral PAG Regions of Interest*. Two box-shaped masks were created to define both the dorsolateral (DL-PAG, red; MNI *x:* 0; *y*: −32; *z*: −8.5 plus 6 × 2 × 1.5 mm extensions) and ventrolateral (VL-PAG, blue; MNI *x*: 0; *y*: −27; *z*: −8 plus 3 × 1 × 1 mm extensions) subdivisions of the PAG. These masks are presented in sagittal (top left), axial (top right), and coronal (bottom) views.

2.2.5 fMRI Statistical Analyses

2.2.5.1 Within-Subject Analyses

The masks created in PickAtlas generated tables that provided region of interest seed activity for each subject based on whole-brain resting state data. In-house software developed by co-author Dr. Jean Théberge read these tables and generated a mean signal intensity time course to be used in a within-subject multiple regression model along with ART movement regressors. In addition, means of the number of outliers per subject in each group were compared in an effort to examine the potential influence they may have on any findings. Functional connectivity was then assessed using a voxel-wise approach by calculating both positive and negative correlations between ROIs and other voxels of the brain.

2.2.5.2 Between-Subject Analyses

A whole-brain 3 (subject group) x 2 (ROI) full-factorial analysis of variance (ANOVA) was conducted for the between-subject analyses, with and without using MDD diagnosis as a co-variate (MDD was diagnosed via SCID assessment for Axis-I psychiatric disorders, see Methods; Table I). The between-group factor consisted of three levels: non-dissociative PTSD patients (PTSD), dissociative PTSD patients (PTSD+DS) and healthy controls, whereas the within-group factor consisted of two levels: DL-PAG and VL-PAG. To determine significant clusters, a family-wise error (FWE) whole brain cluster corrected ($p< 0.05$, k=50) threshold was set for both interaction and post-hoc analyses. One-sample t-tests were used to assess connectivity patterns within each group and ROI, whereas two-sample t-tests assessed between-group comparisons for both the DL-PAG and VL-PAG as well as the differences between both ROIs. Brain regions were

identified using the AAL atlas (Tzourio-Mazoyer et al., 2002) via xjview software (http://www.nitrc.org/projects/xjview) and visually inspected using another anatomical atlas focusing on a dissected brain (Montemurro & Bruni, 2008). To more accurately distinguish between relevant anatomical areas in close proximity, such as the rolandic operculum and insula, masks of each area were created using PickAtlas software according to the AAL atlas and were inspected to ensure proper identification of brain regions. Brodmann areas of these brain regions were also identified using xjview software and the MNI2Tal atlas available online via the BioImage Suite at Yale University (http://bioimagesuite.yale.edu/mni2tal/; Lacadie, Fulbright, Constable, & Papademetris, 2008).

2.2.5.3 Clinical Correlations

Correlations between the fMRI data and clinical PTSD symptoms were examined by regressing CAPS (re-experiencing, avoidance and hyperarousal subscales, in addition to total CAPS score in all PTSD patients), CTQ, and MDI scores. Subsequent ROI analyses were carried out specifically for the left and the right fusiform gyrus (left: MNI x: -46, y: -42, z: -12; right: MNI x: 54, y: -38, z: -16) based on a meta-analysis of previous neuroimaging studies in PTSD (Patel, Spreng, Shin, & Girard, 2012). Each ROI analysis was conducted independently, drawing a 15-mm radius sphere around the given peak coordinate corrected at FWE $p < 0.05$ (cluster and peak corrected). Significant correlations were evaluated at FWE $p<0.05$ (cluster and peak corrected), with subsequent Pearson's correlation coefficients *(r)* calculated between clinical scores and the ROI used in the analysis, as defined above.

2.3 «Results»

2.3.1 Clinical and Demographic Measures

ANOVA analyses did not reveal significant differences in ages across all three participant groups (p=0.148, df=2), and a Pearson's chi-square test revealed no statistically significant association between gender and participant group (p=0.129, df=2). Kruskal-Wallis analysis of variance yielded significant values for all psychological measures, including CTQ, CAPS, MDI and BDI (all p<0.001). -Post-hoc Games-Howell comparisons revealed no significant differences between PTSD+DS and PTSD groups for CAPS (p=0.794) and BDI scores, but did reveal significantly higher CTQ and MDI (averaged depersonalization and derealization score) scores in PTSD+DS individuals (p<0.05). All psychological measures revealed significantly higher scores in both PTSD patient groups as compared to controls (all p<0.001). In addition, the mean number of outlier functional volumes per subject did not significantly differ across groups (p=0.327).

2.3.2 Full Factorial Design

The whole brain analysis of variance (3x2 ANOVA) revealed an interaction between group and region of interest, with significant main effects observed for each factor (see Appendix A). Using MDD diagnosis as a co-variate did not change the results. Post-hoc one-sample and two-sample t-tests based on the full-factorial ANOVA were carried out to assess differences observed within and between each variable of the two main factors, group (PTSD+DS, PTSD, control) and PAG region (DL and VL-PAG) at p<0.05-FWE whole brain cluster corrected, k=50.

2.3.3 Functional Connectivity of DL-PAG and VL-PAG within Participant Groups

2.3.3.1 Control Subjects

Control subjects demonstrated DL-PAG functional connectivity only with the left cerebellar lobule IV. Furthermore, VL-PAG connectivity was not observed beyond the VL-PAG itself (Figure 2.2; Appendix A). When comparing the functional connectivity of the DL-PAG to the VL-PAG (DL-PAG>VL-PAG), there was greater functional connectivity observed with the left cerebellar lobules IV and V, along with the cerebellar vermis. No greater functional connectivity was observed for the VL-PAG versus the DL-PAG (FWE whole brain cluster corrected at $p<0.05$, k=50).

2.3.3.2 PTSD

PTSD subjects showed extensive functional connectivity of both the DL-PAG and VL-PAG with the dACC, orbitomedial prefrontal cortex (OMPFC) and bilateral fusiform gyrus (see Appendix A). They also demonstrated DL-PAG connectivity with cerebellar lobule VI (Figure 2.2**;** Table 2.2). When comparing DL-PAG to VL-PAG connectivity (DL-PAG>VL-PAG), PTSD demonstrated increased functional connectivity with the right anterior insula, the left supplemental motor area and the right postcentral gyrus (Figure 2.3**;** Table 2.3). No greater functional connectivity was observed for the VL-PAG versus the DL-PAG -(FWE whole brain cluster corrected at $p<0.05$, k=50).

2.3.3.3 PTSD+DS

PTSD+DS subjects also demonstrated extensive functional connectivity of both the DL-PAG and VL-PAG, including with the OMPFC, left fusiform gyrus, and cerebellar lobule VI (Figure 2.2**;** Table 2.2). When comparing DL-PAG to VL-PAG connectivity (DL-

PAG>VL-PAG), PTSD+DS demonstrated increased functional connectivity with the left precentral and postcentral gyri (Figure 2.3**;** Table 2.3). No greater functional connectivity was observed for the VL-PAG versus the DL-PAG PAG (FWE whole brain cluster corrected at $p<0.05$, k=50).

Table 2.2 *Within Group DL-PAG and VL-PAG Connectivity Patterns in PTSD Patients*

Contrast	L/R	BA	Region	Cluster Size	p FWE	T Voxel	Z-Score	MNI Coordinates		
								x	y	z
Within PTSD DL-PAG	L		Cerebellar Lobules IV-V	47056	<0.001	8.30	7.81	-6	-38	-6
	R	54	Hippocampus			7.32	6.99	24	-36	-2
	L	32	Dorsal Anterior Cingulate			6.78	6.51	-10	18	36
	L	37	Fusiform Gyrus			5.78	5.50	-33	-52	-17
	R	37	Fusiform Gyrus	55	0.032	5.71	5.54	38	-54	-18
	L	46	Frontal Middle Gyrus	126	<0.001	4.74	4.64	-46	48	0
	L	10	Orbitomedial Prefrontal Cortex			4.44	4.35	-40	48	-12
Within PTSD VL-PAG	L	20	Inferior Temporal Gyrus	40354	<0.001	7.09	6.79	-48	40	4
	L	48	Caudate			6.82	6.54	-12	6	16
	L	32	Dorsal Anterior Cingulate Cortex			6.39	6.16	-6	26	30
	L		Cerebellar Lobule VI	1187	<0.001	5.62	5.46	-22	-54	-28
	L	37	Fusiform Gyrus			5.24	5.11	-44	-48	-20
	R		Cerebellar Vermis			5.10	4.98	2	-54	-6
	L	30	Precuneus	229	<0.001	5.46	5.31	-4	-52	14

	L	30	Calcarine Sulcus			5.16	5.03	-8	-58	4
	L	10	Orbitomedial Prefrontal Cortex	168	<0.001	5.44	5.30	-42	52	0
	L	19	Lingual Gyrus	77	0.006	4.39	4.31	-28	-54	-2
Within PTSD+DS DL-PAG	L	6	Superior Frontal Gyrus	37055	<0.001	6.40	6.16	-20	-4	50
	L		Cerebellar Lobule VI			6.35	6.13	-32	-54	-22
	R	6	Supplemental Motor			6.32	6.10	12	4	52
	R	8	Dorsal Anterior Cingulate			6.26	6.04	10	12	38
	L	37	Fusiform Gyrus			6.08	5.88	-34	-56	-14
	R	10	Orbitomedial Prefrontal Cortex	182	<0.001	4.61	4.52	30	52	-2
Within PTSD+DS VL-PAG	L	6	Middle Frontal Gyrus	33686	<0.001	6.44	6.20	30	52	-2
	L	37	Fusiform Gyrus			6.28	6.06	-20	-4	48
	L	6	Superior Frontal Gyrus			6.26	6.05	-36	-54	-14
	R	10	Middle Frontal Gyrus	161	<0.001	4.41	4.33	-16	4	54
	R	10	Orbitomedial Prefrontal Cortex			4.28	4.20	30	50	-4

Post-hoc one-sample t-tests to assess DL- and VL-PAG connectivity patterns within PTSD and PTSD+DS patient groups (FWE whole brain cluster corrected at $p<0.05$, k=50). Abbreviations: PTSD, non-dissociative posttraumatic stress disorder patients; PTSD+DS, dissociative posttraumatic stress disorder patients; DL-PAG, dorsolateral periaqueductal gray; VL-PAG, ventrolateral periaqueductal gray; L, left hemisphere; R, right hemisphere; BA, Brodmann Area.

Table 2.3 *DL-PAG versus VL-PAG Functional Connectivity Patterns*

Contrast	L/R	BA	Region	Cluster Size	p FWE	T Voxel	Z-Score	MNI Coordinates

								x	y	z
PTSD DL>VL-PAG	L		Cerebellar Lobules IV-V	414	<0.001	7.90	7.48	-6	-38	-6
	R		Cerebellar Vermis			6.02	5.83	6	-42	-8
	L	13	Rolandic Operculum	1131	<0.001	5.28	5.15	-40	-28	18
	R	28	Hippocampus	112	0.001	5.21	5.08	26	-34	2
	R	44	Inferior Frontal Operculum	141	<0.001	4.61	4.51	48	14	2
	R	13	Anterior Insula			3.85	3.79	46	6	-2
	L	28	Hippocampus	72	0.009	4.52	4.43	-18	-36	0
	L	32	Dorsal Anterior Cingulate	804	<0.001	4.48	4.39	-2	18	38
	L	32	Supplemental Motor			4.43	4.35	-2	10	44
	R	48	Caudate	81	0.005	4.41	4.33	16	16	2
	R	49	Putamen			4.21	4.13	26	14	-2
	R	6	Rolandic Operculum	60	0.022	4.32	4.24	58	6	10
	R	4	Post-central Gyrus			4.03	3.97	62	-2	16
PTSD+DS DL>VL-PAG	R	32	Mid-Cingulate Gyrus	910	<0.001	5.65	5.48	12	-4	44
	R	24	Mid-Cingulate Gyrus			5.31	5.17	8	-20	46
	L		Cerebellar Lobule IV-V	546	<0.001	5.26	5.13	-8	-46	-10
	L		Cerebellar Vermis			5.26	5.13	-2	-40	-6
	R		Lingual Gyrus	66	0.014	4.91	4.80	8	-58	6
	R		Precuneus			4.32	4.24	4	-54	6
	R		Calcarine Sulcus			3.63	3.58	18	-54	6
	L		Frontal Middle Gyrus	238	<0.001	4.86	4.76	-28	8	48

	L		Pre-central Gyrus			3.93	3.88	-36	2	38
	R		Lingual Gyrus	61	0.020	4.66	4.57	26	-52	-10
	R		Parahippocampal Gyrus			3.66	3.61	36	-32	-14
	L		Post-central Gyrus	181	<0.001	4.29	4.21	-38	-14	42
	L		Cerebellar Lobule VI	98	0.002	4.24	4.17	-32	-56	-22
	L		Fusiform Gyrus			4.11	4.05	-34	-62	-16
	R		Putamen	66	0.014	4.17	4.10	28	-2	6
	L		Putamen	66	0.014	4.06	3.99	-24	4	0

Post-hoc two-sample t-tests to compare DL-PAG and VL-PAG connectivity within PTSD and PTSD+DS patients (FWE whole brain cluster corrected at $p<0.05$, k=50).

Abbreviations: PTSD-DS, non-dissociative posttraumatic stress disorder patients; PTSD+DS, dissociative posttraumatic stress disorder patients; DL-PAG, dorsolateral periaqueductal gray; VL-PAG, ventrolateral periaqueductal gray; L, left hemisphere; R, right hemisphere; BA, Brodmann Area

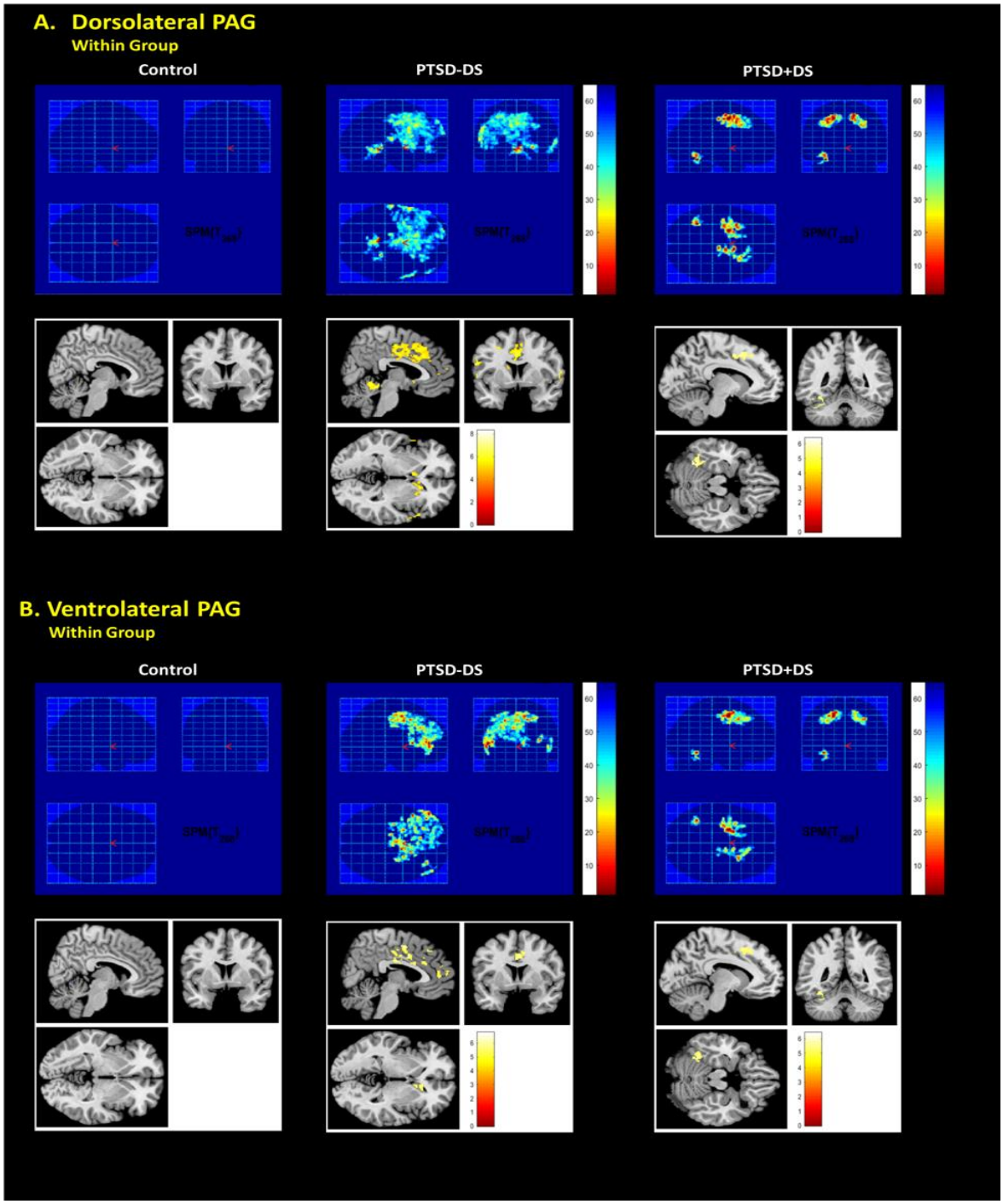

Figure 2.2 *Within Group Dorsolateral and Ventrolateral PAG Functional Connectivity Patterns*. Family-wise error whole brain corrected p<0.05, k=50; shown at x: 6, y: 0, z: 0 for PTSD and x:-10 y:-52 z:-16 for PTSD+DS based on MNI coordinates.

Abbreviations: PTSD, non-dissociative posttraumatic stress disorder patients; PTSD+DS, dissociative posttraumatic stress disorder patients.

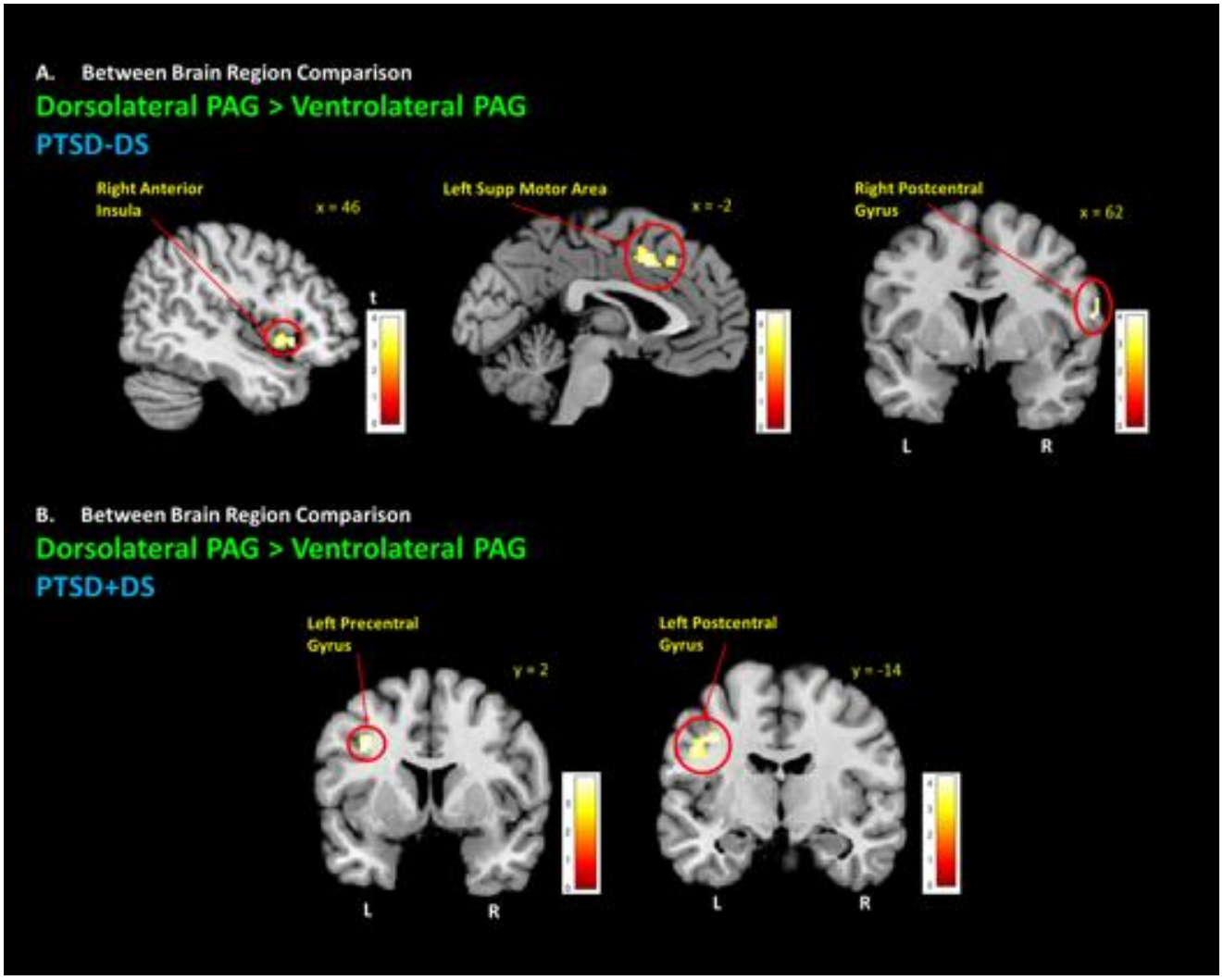

Figure 2.3 *Dorsolateral PAG Connectivity with Premotor Regions.*. Both PTSD and PTSD+DS demonstrated DL-PAG functional connectivity with premotor areas when comparing DL- to VL-PAG. (A) PTSD demonstrated greater VL-PAG connectivity with the right anterior insula, left supplemental motor area and right postcentral gyrus. (B) PTSD+DS demonstrated greater DL-PAG connectivity with the left pre- and post central gyri. FWE whole brain cluster corrected at $p<0.05$, $k=50$.

Abbreviations: PTSD, non-dissociative posttraumatic stress disorder patients; PTSD+DS, dissociative posttraumatic stress disorder patients; DL-PAG, dorsolateral periaqueductal gray; VL-PAG, ventrolateral periaqueductal gray; L, left hemisphere; R, right hemisphere.

2.3.4 Functional Connectivity Differences between Participant Groups

Between-group analyses confirmed that there was widespread cortical functional connectivity observed with DL-PAG and VL-PAG regions in both PTSD and PTSD+DS when compared to healthy controls (PTSD>Control; PTSD+DS>Control; see Appendix A). Moreover, there were no suprathreshold clusters observed where healthy controls exhibited greater functional connectivity than either PTSD patient group (Control>PTSD; Control>PTSD+DS) PAG (FWE whole brain cluster corrected at $p<0.05$, k=50).

When comparing PTSD to PTSD+DS (PTSD>PTSD+DS), there was no greater functional connectivity observed in either PAG subregion (Figure 2.4**;** Table 2.4). However, when comparing PTSD+DS to PTSD (PTSD+DS>PTSD), greater VL-PAG connectivity was observed within the right temporoparietal junction, right rolandic operculum, left fusiform gyrus and cerebellar lobule VI (FWE whole brain cluster corrected at $p<0.05$, k=50) (Figure 2.4**;** Table 2.4).

Table 2.4 *Between-Group PAG Functional Connectivity Patterns*

Contrast	L/R	BA	Region	Cluster Size	p FWE	T Voxel	Z-Score	MNI Coordinates		
								x	y	z
PTSD > PTSD+DS **DL-PAG**			No suprathreshold clusters							
PTSD+DS > PTSD **DL-PAG**	L	37	Fusiform Gyrus	148	<0.001	4.62	4.52	-36	-56	-12

	L		Cerebellar Lobule VI			4.00	3.94	-32	-54	-22
	L	37	Inferior Temporal Gyrus			3.53	3.49	-48	-50	-14
PTSD > PTSD+DS **VL-PAG**			No suprathreshold clusters							
PTSD+DS > PTSD **VL-PAG**	L	37	Fusiform Gyrus	211	<0.001	4.58	4.49	-34	-56	-14
	L		Cerebellar Lobule VI			4.38	4.30	-38	-58	-26
	R	1	Rolandic Operculum	60	0.022	3.95	3.89	58	-6	16
	R	44	Pre-central Gyrus			3.92	3.64	50	2	22
	R	40	Temporoparietal Junction			3.53	3.49	54	-12	18

Post-hoc two-sample t-tests to compare DL- and VL- PAG connectivity differences between PTSD and PTSD+DS patients (FWE whole brain cluster corrected at $p<0.05$, k=50).

Abbreviations: PTSD-DS, non-dissociative posttraumatic stress disorder patients; PTSD+DS, dissociative posttraumatic stress disorder patients; DL-PAG, dorsolateral periaqueductal gray; VL-PAG, ventrolateral periaqueductal gray; L, left hemisphere; R, right hemisphere; BA,

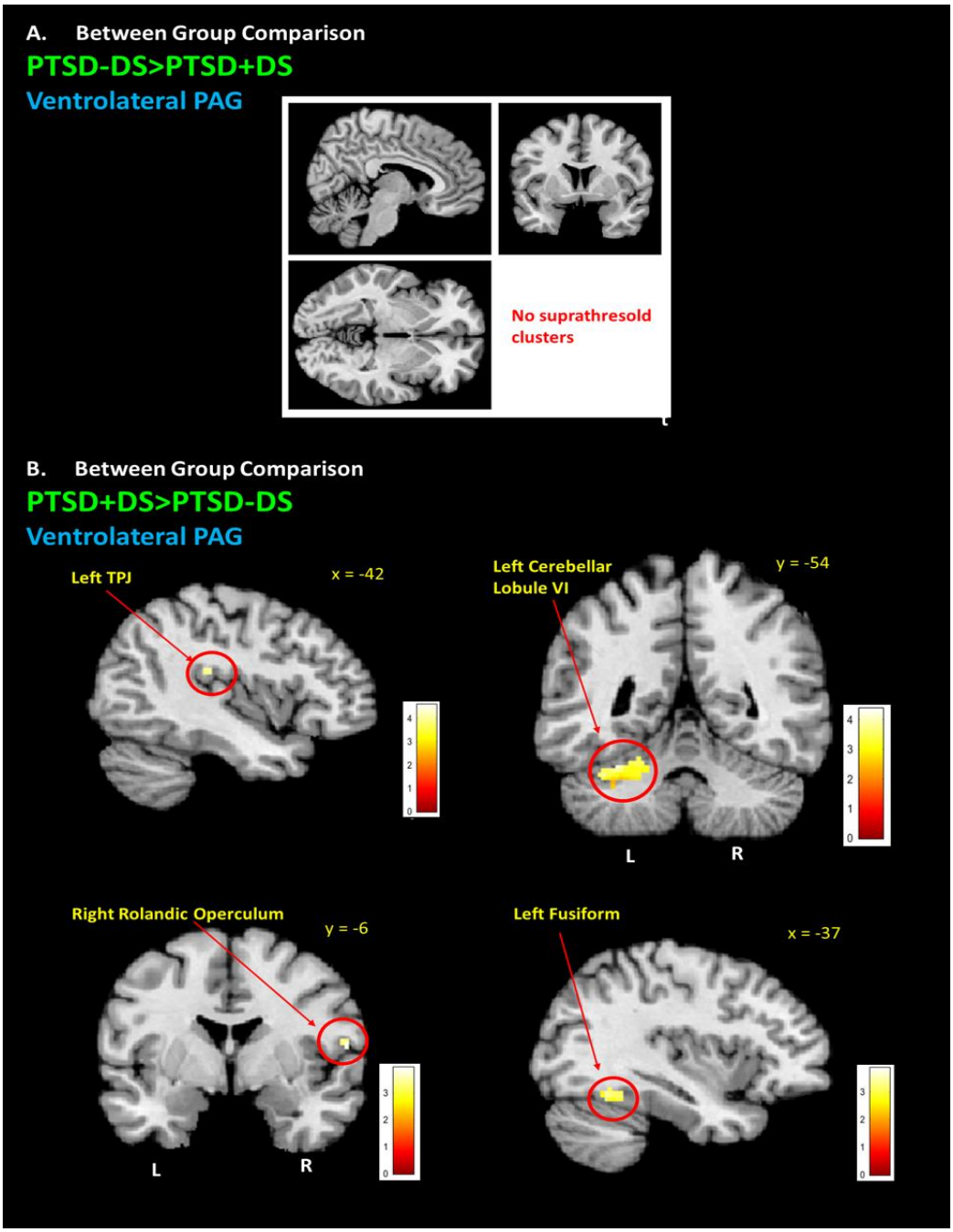

Figure 2.4 *PTSD+DS Ventrolateral PAG Connectivity with Brain Regions Implicated in Depersonalization.* (A) PTSD did not demonstrate VL-PAG functional connectivity when compared to PTSD+DS patients. (B) When compared to PTSD, PTSD+DS demonstrated greater VL-PAG functional connectivity with the left temporoparietal junction (lTPJ), left cerebellar lobule VI, the right rolandic operculum and the left fusiform gyrus. FWE whole brain cluster corrected at $p<0.05$, $k=50$.

Abbreviations: PTSD, non-dissociative posttraumatic stress disorder patients; PTSD+DS, dissociative posttraumatic stress disorder patients; DL-PAG, dorsolateral periaqueductal gray; VL-PAG, ventrolateral periaqueductal gray; L, left hemisphere; R, right hemisphere.

2.3.5 Clinical Score Correlations with Functional Connectivity Patterns in PTSD Patients

CAPS hyperarousal subscale scores were significantly correlated to the functional connectivity between the DL-PAG and the right fusiform gyrus (p=0.032, FWE-cluster corrected; k=29; r=0.359). Moreover, total CAPS severity score correlated with the functional connectivity between the DL-PAG and the left fusiform gyrus (p=0.039, FWE-cluster corrected; k=23; r=0.346). No significant correlations were observed between the functional connectivity of the DL-PAG or VL-PAG and the CTQ and MDI.

2.4 Discussion

The aim of the present study was to compare resting state connectivity patterns of the dorsolateral and ventrolateral PAG subdivisions between patients with and without the dissociative subtype of PTSD and controls. In line with our hypotheses, widespread DL- and VL-PAG functional connectivity to brain regions involved in emotional reactivity and defensive action was observed in both PTSD patient groups when compared to healthy participants, suggesting that PTSD patients may exhibit defensive posturing even at rest. Strikingly, even though both PTSD patient groups demonstrated DL-PAG connectivity to brain regions involved in coordinating active defense ‘fight or flight’ responses (e.g., dorsal anterior cingulate; insula; pre/post central gyri), only PTSD patients with the dissociative subtype demonstrated greater VL-PAG connectivity with brain regions related to passive defensive responses and increased levels of

depersonalization (left temporoparietal junction, rolandic operculum). We discuss these findings in turn.

2.4.1 PAG Connectivity with Brain Regions Involved in Autonomic Control

Both PTSD and PTSD+DS groups demonstrated DL-PAG functional connectivity with the dorsal ACC. In addition, PTSD patients demonstrated VL-PAG connectivity with this region. The dACC is an area associated with autonomic control of both the sympathetic nervous system and parasympathetic nervous system, and is implicated in the interpretation of contextual information about the safety of the environment (Bryant et al., 2005; Luu & Posner, 2003; Medford & Critchley, 2010; Shackman et al., 2011). Mobbs et al. (2009) elaborated further on the role of the mid-dorsal ACC during threat detection, where they demonstrated that increased connectivity between the mid-dorsal ACC and the midbrain during imminent danger is associated with automatic or 'hard-wired' defensive behaviours (also see Panksepp, 1998). Aberrant ACC activity is strongly associated with PTSD and is thought to contribute to re-experiencing, avoidance and hyperarousal symptoms (Felmingham et al., 2009; Shin et al., 2001; Rougemont-Bucking et al., 2011). Given that the PAG failed to show connectivity with the dACC in healthy participants, the increased VL-PAG and DL-PAG connectivity with the dACC in PTSD patients observed here suggests inadequate control of fear, which in turn may contribute to a predisposition to engage in reflexive defensive behaviours.

Both PTSD patient groups demonstrated increased DL- and VL-PAG functional connectivity with the orbitomedial prefrontal cortex (see Appendix A) within each patient group and when compared to controls. In support of these findings, Bandler and

colleagues (2000) suggested that the orbitomedial prefrontal cortices are responsible for inputs into autonomic control regions, such as the DL- and VL-PAG, and the hypothalamus.

It is also interesting to note that the areas of interest emerging from the main effect of ROI revealed lateralization to primarily areas in the right hemisphere (see Appendix A), particularly in the right anterior insula, right fusiform gyrus, right temporoparietal junction and right postcentral gyrus. The medulla oblongata is considered a major autonomic control center in the brainstem (Luiten, Ter Horst, Karst, & Steffens, 1985) and is located in the right hemisphere. Accordingly, lateralization to the right brain facilitates ipsilateral connections between autonomic-limbic structures that mediate arousal (i.e., medulla oblongata and right centromedial amydala) (Brake, Sullivan, & Gratton, 2000; Porges, Doussard-Roosevelt, & Maiti, 1994; Schore, 2002; 2009). These results support the notion that the right brain hemisphere may play a central role in mediating defensive behaviours in both non-dissociative and dissociative PTSD patients.

Given our findings of PAG connectivity with the dorsal anterior cingulate and orbitomedial prefrontal cortex in both patient groups, it appears probable that both VL-PAG and DL-PAG play a role in autonomic control in both PTSD and its dissociative subtype at rest. This pattern is in contrast to that observed in controls, who did not demonstrate any DL- or VL-PAG connectivity with any of the described areas.

2.4.2 PAG Connectivity with the Fusiform Gyrus

Both PTSD patient groups demonstrated DL and VL-PAG connectivity with the fusiform gyrus (see Appendix A), supporting Porges' Polyvagal Theory (2007) that this structure is critical in evaluating faces, movement, and vocalizations to determine whether or not an environment can be perceived as safe or trustworthy (Porges, 2011; also see Adolphs, 2002; Winston, Strange, O'Doherty, & Dolan, 2002). The involvement of the fusiform gyrus in PTSD was supported by our findings, as DL-PAG connectivity with both the left and right fusiform gyrus correlated with total CAPS and hyperarousal subscale scores, respectively. Given the role of the PAG in detecting threat, these findings may suggest that in contrast to healthy individuals, even during rest, patients with PTSD are consistently evaluating the safety of their environment. Porges' theorizes further that during threat detection, the fusiform gyrus may initiate top-down limbic control to generate defensive responses to fear (also see Pessoa, 2002). In line with this hypothesis, Williams et al. (2006) reported right amygdala functional connectivity with the fusiform gyrus during conscious attention to fear.

It is interesting to note that the current study revealed greater VL-PAG and DL-PAG connectivity with the left fusiform gyrus in PTSD+DS as compared to PTSD. Here, Shaw et al. (2009) found increased activation of the left fusiform gyrus corresponded with inefficient working memory systems in PTSD patients. Indeed, impaired working memory performance has been observed in patients with depersonalization-derealization disorders (Papageorgieu, Lykouras, Ventouras, Uzunoglu, & Christodoulou, 2002). Furthermore, left fusiform gyrus activity appears to vary with high frequency in HRV (Critchley et al. 2003), typically corresponding to increased parasympathetic nervous

system activity, as well as of bradycardia (Critchley, Corfield, Chandler, Mathias, & Dolan, 2000). Consistent with the defense cascade model (Schauer & Elbert, 2010), these results provide support for the notion that greater VL-PAG connectivity with the left fusiform gyrus in PTSD+DS may be associated with increased parasympathetic arousal (VL-PAG connectivity was observed in both PTSD+DS and PTSD) and could thus contribute to passive defensive strategies through parasympathetic nervous system activity.

PTSD patients also demonstrated DL-PAG connectivity with the right fusiform gyrus, a pattern also observed in studies assessing posttraumatic flashbacks often associated with hyperarousal symptoms (Osuch et al., 2001; Lanius, Bluhm, Lanius, & Pain, 2006). In the present study, more severe hyperarousal symptoms were associated with increased DL-PAG functional connectivity with the right fusiform gyrus. Taken together, these findings suggest that the DL-PAG may be responsible for initiating hyperarousal responses in PTSD patients that evoke active defensive strategies associated with movement as previously suggested by Bandler et al. (2000), and a corresponding sympathetic 'fight or flight' response that occurs despite the absence of an external threat stimulus during resting state.

2.4.3 PAG Connectivity with the Cerebellum

All groups (controls, PTSD+DS, PTSD+) demonstrated DL-PAG connectivity with cerebellar lobules IV and V, a structure thought to play a critical role in assessing a trustworthy environment and in fine motor movement (Schutter, 2013; see Appendix A). Critically, this finding is consistent with the Universal Cerebellar Transform theory (Schmahmann, Weilburg, & Sherman, 2007), which suggests the cerebellum may play an

unconscious regulatory role in all aspects of brain functioning, including autonomic homeostasis. Although PTSD and PTSD+DS patient groups demonstrated VL-PAG functional connectivity with cerebellar lobule VI, connectivity with this structure was greater in PTSD+DS patients. Interestingly, activity in this region was also associated with processing of fearful faces and trauma-related words in PTSD (Rabellino, Densmore, Frewen, Théberge, & Lanius, 2016). Although autonomic control has been shown to be associated with successful fear conditioning (Critchley, Melmed, Featherstone, Mathias, & Dolan, 2002), cerebellar lobule VI lesions have also been implicated in fear learning during animal studies and thus maintaining unconditioned responses to fear stimuli (i.e., startle response) (Attwell, Cooke, & Yeo, 2002; Bellebaum & Daum, 2011; Lange et al., 2015; Lavond & Steinmetz, 1989). Our findings suggest that this modulatory role of the cerebellum may be sustained at rest in both controls and PTSD patients. Individuals with PTSD, however, may develop aberrations in PAG-cerebellar connectivity (i.e., with lobule VI) that may affect the ability of the cerebellum to maintain homeostasis in response to stressors. Future studies are –required urgently to confirm this hypothesis.

2.4.4 PAG Connectivity with Motor Regions

In keeping with our hypothesis, both PTSD patient groups demonstrated DL-PAG connectivity with motor areas thought responsible for generating ‘fight or flight’ movements mediated by sympathetic nervous system activity. PTSD, however, also showed greater DL-PAG connectivity with the right anterior insula when compared to its VL-PAG connectivity. This finding points towards a key association between the DL-PAG and sympathetic nervous system activity, where the right anterior insula is thought

to play a critical role in controlling sympathetic arousal in the central autonomic network across numerous studies (Benarroch, 1993; Critchley, Wiens, Rotshtein, & Ohman, Dolan, 2004; Critchley, 2009; de Morree, Rutten, Szabó, Sitskoorn, & Kop, 2016; Saper, 2002). Both PTSD patient groups also demonstrated DL-PAG connectivity with supplemental pre-motor areas and pre- and post-central gyri, regions implicated in generating motor movement.

2.4.5 PAG Connectivity with Regions Involved in Depersonalization

The PTSD+DS patient group demonstrated greater VL-PAG connectivity (when compared to PTSD) with regions associated with depersonalization responses, including the right rolandic operculum and the left temporoparietal junction (TPJ). Interestingly, the rolandic operculum has recently been shown to be a neural correlate of depersonalization in a case of schizotypal disorder (Zaytseva et al., 2015), and is also thought susceptible to alterations stemming from childhood maltreatment (Dannlowski et al., 2012), the prevalence of which is increased in PTSD+DS (Stein et al., 2013). The TPJ is an area implicated in depersonalization experiences, as it is thought to contribute to discrimination between self and non-self (Blanke & Arzy, 2005; Murray, 2015). Whereas the right TPJ is important for evaluating self-location and bodily consciousness (Blanke et al. 2005; Olivé, Tempelmann, Berthoz, & Heinze, 2015), the left TPJ is thought to play an important role in self-processing, where it may assist in discerning self-involvement during past autobiographical events (Muscatelli, Addis, & Kensinger, 2010). Here, previous studies examining gray matter alterations as a function of dissociative traits found changes in the inferior parietal cortex, which is also implicated in

bodily consciousness (Nardo et al., 2013). Taken together, these findings may help to explain why individuals with PTSD can feel emotionally detached from their traumatic memories during states of depersonalization (Krystal, Bennett, Bremner, Southwick, & Charney, 1995; Spiegel, 1997; Lanius et al., 2010). It should also be noted that these structures contribute to numerous general functions of the brain that are not limited to depersonalization responses; however, the present findings provide a basis for further exploration of PAG functional connectivity in those with dissociative traits in order to further delineate neural correlates associated with depersonalization responses.

2.4.6 Limitations and Future Directions

Some limitations of the present study need to be considered. Firstly, we did not include a trauma-exposed control group without PTSD, since individuals with matching trauma histories often meet lifetime criteria for one or more psychiatric disorders. Although previous studies have also reported sex-related differences during resting state in healthy individuals (Gur et al., 1995; Tian, Wang, Yan, & He, 2011), these results are conflicting, with numerous authors suggesting it is not necessary to control for sex (Damoiseaux et al., 2006; Weissman-Fogel, Moayedi, Taylor, Pope, & Davis, 2010). Unfortunately, the current study was not powered to examine sex differences; which have been observed in a previous pain-related functional PAG connectivity study (Linnman, Beucke, Jensen, Gollub, & Kong, 2011); this issue warrants exploration in future studies as these differences may influence clinical symptoms. Furthermore, additional measures designed to reduce physiological noise from the fMRI scanner, such as a component-based approach, should be examined in future studies (Behzadi, Restom, Liau, & Liu, 2007). Finally, it is also important to note that the current study is cross-sectional in nature and

can therefore not make conclusions about cause and effect. Future studies should also explore the use of a greater magnetic field strength to explore PAG subdivision functional connectivity with greater temporal resolution and assess how these patterns of functional connectivity may vary in response to a stressor, as demonstrated in previous animal studies (Adamec, Berton, & Abdul-Razek, 2009).

2.4.7 Conclusions

On balance, this study reveals novel findings highlighting the importance of examining altered subcortical functional connectivity networks in PTSD patients and its dissociative subtype during resting state. Even during resting state, patients with PTSD showed extensive VL-PAG and DL-PAG functional connectivity with areas associated with emotional reactivity and defensive action. It is possible that these findings reflect greater defensive posturing observed in PTSD even at rest. Our findings further indicate that patients with the dissociative subtype of PTSD show unique patterns of PAG functional connectivity when compared to those without the subtype. Here, although all patients with PTSD demonstrated DL-PAG functional connectivity with areas linked to hyperarousal and the initiation of active coping strategies through sympathetic nervous system activation (e.g., dACC; right insula; pre/post central gyri), only PTSD patients with the subtype demonstrated greater VL-PAG functional connectivity with brain regions associated with passive coping strategies and increased levels of depersonalization (e.g., left TPJ; right rolandic operculum; left fusiform gyrus). Taken together, these findings represent an important first step to identifying neural and behavioural targets for therapeutic interventions that address both active and passive defensive strategies in trauma-related disorders.

2.5 References

Adamec, R., Berton, O., & Abdul-Razek, W. (2009). Viral vector induction of CREB expression in the periaqueductal gray induces a predator stress-like pattern of changes in pCREB expression, neuroplasticity, and anxiety in rodents. *Neural Plasticity*, Article ID 904568, 15 pages.

Adamec, R., Toth, M., Haller, J., Halasz, J., & Blundell, J. (2012). Activation patterns of cells in selected brain stem nuclei of more and less stress responsive rats in two animal models of PTSD–predator exposure and submersion stress. *Neuropharmacology*, *62*(2), 725-736.

Adolphs, R. (2002). Trust in the brain. *Nature neuroscience*, *5*(3), 192-193.

An, X., Bandler, R., Öngür, D., & Price, J. L. (1998). Prefrontal cortical projections to longitudinal columns in the midbrain periaqueductal gray in macaque monkeys. *Journal of Comparative Neurology*, *401*(4), 455-479.

Attwell, P. J., Cooke, S. F., & Yeo, C. H. (2002). Cerebellar function in consolidation of a motor memory. *Neuron*, *34*(6), 1011-1020.

Baldwin, D. V. (2013). Primitive mechanisms of trauma response: an evolutionary perspective on trauma-related disorders. *Neuroscience & Biobehavioral Reviews*, *37*(8), 1549-1566.

Bandler, R., Keay, K. A., Floyd, N., & Price, J. (2000). Central circuits mediating patterned autonomic activity during active vs. passive emotional coping. *Brain research bulletin*, *53*(1), 95-104.

Becerra, L., Harter, K., Gonzalez, R. G., & Borsook, D. (2006). Functional magnetic resonance imaging measures of the effects of morphine on central nervous system circuitry in opioid-naive healthy volunteers. *Anesthesia & Analgesia*, *103*(1), 208 216.

Beck, A. T., Guth, D., Steer, R. A., & Ball, R. (1997). Screening for major depression disorders in medical inpatients with the Beck Depression Inventory for Primary Care. *Behaviour research and therapy*, *35*(8), 785-791.

Beissner, F., Deichmann, R., & Baudrexel, S. (2011). fMRI of the brainstem using dual echo EPI. *NeuroImage*, *55*(4), 1593-1599.

Behzadi, Y., Restom, K., Liau, J., & Liu, T. T. (2007). A component based noise correction method (CompCor) for BOLD and perfusion based fMRI. *Neuroimage*, *37*(1), 90-101.

Bellebaum, C., & Daum, I. (2011). Mechanisms of cerebellar involvement in associative learning. *Cortex: A Journal Devoted to the Study of the Nervous System and Behavior*.

Benarroch, E.E. (1993). The central autonomic network: Functional organization dysfunction and perspective. *Mayo Clinic Proceedings*, *68*(10), 988-1001.

Bernstein, D.P., Fink, L. (1998). Childhood trauma questionnaire: A retrospective self report manual. San Antonio, TX: The Psychological Corporation.

Bernstein, D. P., Stein, J. A., Newcomb, M. D., Walker, E., Pogge, D., Ahluvalia, T., ... & Zule, W. (2003). Development and validation of a brief screening version of the Childhood Trauma Questionnaire. *Child abuse & neglect*, *27*(2), 169-190.

Blake, D. D., Weathers, F. W., Nagy, L. M., Kaloupek, D. G., Gusman, F. D., Charney, D. S., & Keane, T. M. (1995). The development of a clinician-administered PTSD scale. *Journal of traumatic stress*, *8*(1), 75-90.

Blanke, O., & Arzy, S. (2005). The out-of-body experience: disturbed self-processing at the temporo-parietal junction. *The Neuroscientist*, *11*(1), 16-24.

Blanke, O., Mohr, C., Michel, C. M., Pascual-Leone, A., Brugger, P., Seeck, M., ... & Thut, G. (2005). Linking out-of-body experience and self processing to mental

own-body imagery at the temporoparietal junction. *Journal of Neuroscience*, *25*(3), 550-557.

Bluhm, R. L., Williamson, P. C., Osuch, E. A., Frewen, P. A., Stevens, T. K., Boksman, K., ... & Lanius, R. A. (2009). Alterations in default network connectivity in posttraumatic stress disorder related to early-life trauma. *Journal of psychiatry & neuroscience*, *34*(3), 187-194.

Brake, W. G., Sullivan, R. M., & Gratton, A. (2000). Perinatal distress leads to lateralized medial prefrontal cortical dopamine hypofunction in adult rats. *Journal of Neuroscience*, *20*(14), 5538-5543.

Briere, J., Weathers, F. W., & Runtz, M. (2005). Is dissociation a multidimensional construct? Data from the Multiscale Dissociation Inventory. *Journal of Traumatic Stress*, *18*(3), 221-231.

Bryant, R. A., Felmingham, K. L., Kemp, A. H., Barton, M., Peduto, A. S., Rennie, C., ... & Williams, L. M. (2005). Neural networks of information processing in posttraumatic stress disorder: a functional magnetic resonance imaging study. *Biological psychiatry*, *58*(2), 111-118.

Bryant, R. A., Kemp, A. H., Felmingham, K. L., Liddell, B., Olivieri, G., Peduto, A., ... & Williams, L. M. (2008). Enhanced amygdala and medial prefrontal activation during nonconscious processing of fear in posttraumatic stress disorder: an fMRI study. *Human brain mapping*, *29*(5), 517-523.

Butler, T., Pan, H., Tuescher, O., Engelien, A., Goldstein, M., Epstein, J., ... & Chang, L. (2007). Human fear-related motor neurocircuitry. *Neuroscience*, *150*(1), 1-7.

Corrigan, F. M., Fisher, J. J., & Nutt, D. J. (2011). Autonomic dysregulation and the window of tolerance model of the effects of complex emotional trauma. *Journal of Psychopharmacology*, *25*(1), 17-25.

Critchley, H. D., Corfield, D. R., Chandler, M. P., Mathias, C. J., & Dolan, R. J. (2000). Cerebral correlates of autonomic cardiovascular arousal: a functional

neuroimaging investigation in humans. *The Journal of physiology*, *523*(1), 259 270.

Critchley, H. D., Melmed, R. N., Featherstone, E., Mathias, C. J., & Dolan, R. J. (2002). Volitional control of autonomic arousal: a functional magnetic resonance study. *Neuroimage*, *16*(4), 909-919.

Critchley, H. D., Mathias, C. J., Josephs, O., O'Doherty, J., Zanini, S., Dewar, B. K., ... & Dolan, R. J. (2003). Human cingulate cortex and autonomic control: converging neuroimaging and clinical evidence. *Brain*, *126*(10), 2139-2152.

Critchley, H. D., Wiens, S., Rotshtein, P., Öhman, A., & Dolan, R. J. (2004). Neural systems supporting interoceptive awareness. *Nature neuroscience*, *7*(2), 189-195.

Critchley, H. D. (2009). Psychophysiology of neural, cognitive and affective integration: fMRI and autonomic indicants. *International Journal of Psychophysiology*, *73*(2), 88-94.

Critchley, H. D., Nagai, Y., Gray, M. A., & Mathias, C. J. (2011). Dissecting axes of autonomic control in humans: insights from neuroimaging. *Autonomic Neuroscience*, *161*(1-2), 34-42.

Dalgleish, T., Moradi, A. R., Taghavi, M. R., Neshat-Doost, H. T., & Yule, W. (2001). An experimental investigation of hypervigilance for threat in children and adolescents with post-traumatic stress disorder. *Psychological medicine*, *31*(3), 541-547.

Damoiseaux, J. S., Rombouts, S. A. R. B., Barkhof, F., Scheltens, P., Stam, C. J., Smith, S. M., & Beckmann, C. F. (2006). Consistent resting-state networks across healthy subjects. *Proceedings of the national academy of sciences*, *103*(37), 13848-13853.

Daniels, J. K., Frewen, P., Theberge, J., & Lanius, R. A. (2016). Structural brain aberrations associated with the dissociative subtype of post-traumatic stress disorder. *Acta Psychiatrica Scandinavica*, *133*(3), 232-240.

Dannlowski, U., Stuhrmann, A., Beutelmann, V., Zwanzger, P., Lenzen, T., Grotegerd, D., ... & Lindner, C. (2012). Limbic scars: long-term consequences of childhood maltreatment revealed by functional and structural magnetic resonance imaging. *Biological psychiatry*, *71*(4), 286-293.

de Morree, H. M., Rutten, G. J., Szabó, B. M., Sitskoorn, M. M., & Kop, W. J. (2016). Effects of insula resection on autonomic nervous system activity. *Journal of neurosurgical anesthesiology*, *28*(2), 153-158.

DiLillo, D., Fortier, M. A., Hayes, S. A., Trask, E., Perry, A. R., Messman-Moore, T., ... & Nash, C. (2006). Retrospective assessment of childhood sexual and physical abuse: A comparison of scaled and behaviorally specific approaches. *Assessment*, *13*(3), 297-312.

Dunckley, P., Wise, R. G., Fairhurst, M., Hobden, P., Aziz, Q., Chang, L., & Tracey, I. (2005). A comparison of visceral and somatic pain processing in the human brainstem using functional magnetic resonance imaging. *Journal of Neuroscience*, *25*(32), 7333-7341.

Ehlers, A., & Clark, D. M. (2000). A cognitive model of posttraumatic stress disorder. *Behaviour research and therapy*, *38*(4), 319-345.

Ezra, M., Faull, O. K., Jbabdi, S., & Pattinson, K. T. (2015). Connectivity-based segmentation of the periaqueductal gray matter in human with brainstem optimized diffusion MRI. *Human brain mapping*, *36*(9), 3459-3471.

Felmingham, K., Kemp, A. H., Williams, L., Falconer, E., Olivieri, G., Peduto, A., & Bryant, R. (2008). Dissociative responses to conscious and non-conscious fear impact underlying brain function in post-traumatic stress disorder. *Psychological medicine*, *38*(12), 1771-1780.

Felmingham, K. L., Williams, L. M., Kemp, A. H., Rennie, C., Gordon, E., & Bryant, R. A. (2009). Anterior cingulate activity to salient stimuli is modulated by autonomic arousal in posttraumatic stress disorder. *Psychiatry Research: Neuroimaging*, *173*(1), 59-62.

First, M.B., Spitzer, R.L., Gibbon, M., Williams, J.B. (2002). Structured Clinical Interview for DSM-IV Axis I Disorders, Research Version, Non–patient Edition (SCID–I/NP) New York, NY: Biometrics Research, New York State Psychiatric Institute.

Fransson, P. (2005). Spontaneous low-frequency BOLD signal fluctuations: An fMRI investigation of the resting-state default mode of brain function hypothesis. *Human brain mapping*, *26*(1), 15-29.

Friston, K. J., Ashburner, J., Frith, C. D., Poline, J. B., Heather, J. D., & Frackowiak, R.S. (1995). Spatial registration and normalization of images. *Human brain mapping*, *3*(3), 165-189.

George, S. A., Knox, D., Curtis, A. L., Aldridge, J. W., Valentino, R. J., & Liberzon, I. (2013). Altered locus coeruleus–norepinephrine function following single prolonged stress. *European journal of Neuroscience*, *37*(6), 901-909.

Goadsby, P. J., Lambert, G. A., & Lance, J. W. (1985). The mechanism of cerebrovascular vasoconstriction in response to locus coeruleus stimulation. *Brain research*, *326*(2), 213-217.

Gorzalka, B. B., Hill, M. N., & Hillard, C. J. (2008). Regulation of endocannabinoid signaling by stress: implications for stress-related affective disorders. *Neuroscience & Biobehavioral Reviews*, *32*(6), 1152-1160.

Gur, R. C., Mozley, L. H., Mozley, P. D., Resnick, S. M., Karp, J. S., Alavi, A., ... & Gur, R. E. (1995). Sex differences in regional cerebral glucose metabolism during a resting state. *Science*, *267*(5197), 528-531.

Kozlowska, K., Walker, P., McLean, L., & Carrive, P. (2015). Fear and the defense cascade: clinical implications and management. *Harvard review of psychiatry*, *23*(4), 263-287.

Kruskal, W. H., & Wallis, W. A. (1952). Use of ranks in one-criterion variance analysis. *Journal of the American statistical association*, *47*(260), 583-621.

Krystal, J. H., Bennett, A. L., Bremner, J. D., Southwick, S. M., & Charney, D. S. (1995). Toward a cognitive neuroscience of dissociation and altered memory functions in post-traumatic stress disorder: Neurobiological and clinical consequences of stress. In: Friedman, M.J., Charney, D.S., Deutsch, A.Y. (Eds.). Normal adaptions to PTSD. New York, NY: Raven Press.

Lacadie, C. M., Fulbright, R. K., Rajeevan, N., Constable, R. T., & Papademetris, X. (2008). More accurate Talairach coordinates for neuroimaging using non-linear registration. *Neuroimage*, *42*(2), 717-725.

Lange, I., Kasanova, Z., Goossens, L., Leibold, N., De Zeeuw, C. I., van Amelsvoort, T., & Schruers, K. (2015). The anatomy of fear learning in the cerebellum: a systematic meta-analysis. *Neuroscience & Biobehavioral Reviews*, *59*, 83-91.

Lanius, R. A., Williamson, P. C., Bluhm, R. L., Densmore, M., Boksman, K., Neufeld, R. W., ... & Menon, R. S. (2005). Functional connectivity of dissociative responses in posttraumatic stress disorder: a functional magnetic resonance imaging investigation. *Biological psychiatry*, *57*(8), 873-884.

Lanius, R. A., Bluhm, R., Lanius, U., & Pain, C. (2006). A review of neuroimaging studies in PTSD: heterogeneity of response to symptom provocation. *Journal of psychiatric research*, *40*(8), 709-729.

Lanius, R. A., Vermetten, E., Loewenstein, R. J., Brand, B., Schmahl, C., Bremner, J. D., & Spiegel, D. (2010). Emotion modulation in PTSD: Clinical and neurobiological evidence for a dissociative subtype. *American Journal of Psychiatry*, *167*(6), 640 647.

Lavond, D. G., & Steinmetz, J. E. (1989). Acquisition of classical conditioning without cerebellar cortex. *Behavioural brain research*, *33*(2), 113-164.

Linnman, C., Beucke, J. C., Jensen, K. B., Gollub, R. L., & Kong, J. (2012). Sex similarities and differences in pain-related periaqueductal gray connectivity. *Pain*, *153*(2), 444-454.

Linnman, C., Moulton, E. A., Barmettler, G., Becerra, L., & Borsook, D. (2012). Neuroimaging of the periaqueductal gray: state of the field. *Neuroimage*, *60*(1), 505-522.

Luiten, P. G. M., Ter Horst, G. J., Karst, H., & Steffens, A. B. (1985). The course of paraventricular hypothalamic efferents to autonomic structures in medulla and spinal cord. *Brain research*, *329*(1-2), 374-378.

Luu, P., & Posner, M. I. (2003). Anterior cingulate cortex regulation of sympathetic activity. *Brain*, *126*, 2119-2120.

Maldjian, J. A., Laurienti, P. J., Kraft, R. A., & Burdette, J. H. (2003). An automated method for neuroanatomic and cytoarchitectonic atlas-based interrogation of fMRI data sets. *Neuroimage*, *19*(3), 1233-1239.

Medford, N., & Critchley, H. D. (2010). Conjoint activity of anterior insular and anterior cingulate cortex: awareness and response. *Brain Structure and Function*, *214*(5 6), 535-549.

Milad, M. R., Quirk, G. J., Pitman, R. K., Orr, S. P., Fischl, B., & Rauch, S. L. (2007). A role for the human dorsal anterior cingulate cortex in fear expression. *Biological psychiatry*, *62*(10), 1191-1194.

Mobbs, D., Petrovic, P., Marchant, J. L., Hassabis, D., Weiskopf, N., Seymour, B., ... & Frith, C. D. (2007). When fear is near: threat imminence elicits prefrontal periaqueductal gray shifts in humans. *Science*, *317*(5841), 1079-1083.

Montemurro, D.G., Bruni, J.E. (2008). The human brain in dissection. New York, NY: Oxford University Press.

Murray, R. J., Debbané, M., Fox, P. T., Bzdok, D., & Eickhoff, S. B. (2015). Functional connectivity mapping of regions associated with self-and other processing. *Human Brain Mapping*, *36*(4), 1304-1324.

Muscatell, K. A., Addis, D. R., & Kensinger, E. A. (2009). Self-involvement modulates the effective connectivity of the autobiographical memory network. *Social cognitive and affective neuroscience*, *5*(1), 68-76.

Musha, T., Satoh, E., Koyanagawa, H., Kimura, T., Satoh, S. (1989): Effects of opioid agonists on sympathetic and parasympathetic transmission to the dog heart. *Journal of Pharmacology and Experimental Therapeutics*, *250*(3), 1087 1091.

Nardo, D., Högberg, G., Lanius, R. A., Jacobsson, H., Jonsson, C., Hällström, T., & Pagani, M. (2013). Gray matter volume alterations related to trait dissociation in PTSD and traumatized controls. *Acta Psychiatrica Scandinavica*, *128*(3), 222 233.

Nicholson, A. A., Densmore, M., Frewen, P. A., Théberge, J., Neufeld, R. W., McKinnon, M. C., & Lanius, R. A. (2015). The dissociative subtype of posttraumatic stress disorder: unique resting-state functional connectivity of basolateral and centromedial amygdala complexes. *Neuropsychopharmacology*, *40*(10), 2317-2326.

Nijenhuis, E. R., Vanderlinden, J., & Spinhoven, P. (1998). Animal defensive reactions as a model for trauma-induced dissociative reactions. *Journal of Traumatic Stress*, *11*(2), 243-260.

Olive, I., Tempelmann, C., Berthoz, A., & Heinze, H. J. (2015). Increased functional connectivity between superior colliculus and brain regions implicated in bodily

self-consciousness during the rubber hand illusion. *Human brain mapping*, *36*(2), 717-730.

Osuch, E. A., Benson, B., Geraci, M., Podell, D., Herscovitch, P., McCann, U. D., & Post, R. M. (2001). Regional cerebral blood flow correlated with flashback intensity in patients with posttraumatic stress disorder. *Biological psychiatry*, *50*(4), 246-253.

Panksepp, J. (1998). Affective neuroscience. New York, NY: Oxford University Press.

Papageorgiou, C., Lykouras, L., Ventouras, E., Uzunoglu, N., & Christodoulou, G. N. (2002). Abnormal P300 in a case of delusional misidentification with coinciding Capgras and Fregoli symptoms. *Progress in Neuro-Psychopharmacology and Biological Psychiatry*, *26*(4), 805-810.

Patel, R., Spreng, R. N., Shin, L. M., & Girard, T. A. (2012). Neurocircuitry models of posttraumatic stress disorder and beyond: a meta-analysis of functional neuroimaging studies. *Neuroscience & Biobehavioral Reviews*, *36*(9), 2130-2142.

Patel, S., Roelke, C. T., Rademacher, D. J., Cullinan, W. E., & Hillard, C. J. (2004). Endocannabinoid signaling negatively modulates stress-induced activation of the hypothalamic-pituitary-adrenal axis. *Endocrinology*, *145*(12), 5431-5438.

Pessoa, L., McKenna, M., Gutierrez, E., & Ungerleider, L. G. (2002). Neural processing of emotional faces requires attention. *Proceedings of the National Academy of Sciences*, *99*(17), 11458-11463.

Pole, N. (2007). The psychophysiology of posttraumatic stress disorder: a meta analysis. *Psychological bulletin*, *133*(5), 725.

Porges, S. W. (1995). Orienting in a defensive world: Mammalian modifications of our evolutionary heritage. A polyvagal theory. *Psychophysiology*, *32*(4), 301-318.

Porges, S. W. (2001). The polyvagal theory: phylogenetic substrates of a social nervous system. *International journal of psychophysiology*, *42*(2), 123-146.

Porges, S. W. (2007). The polyvagal perspective. *Biological psychology*, *74*(2), 116-143.

Porges, S.W. (2011). The polyvagal theory: Neurophysiological foundations of emotions, attachment, communication and self-regulation. New York: WW Norton & Company.

Porges, S. W., Doussard-Roosevelt, J. A., & Maiti, A. K. (1994). Vagal tone and the physiological regulation of emotion. *Monographs of the society for research in child development*, *59*(2-3), 167-186.

Power, J. D., Barnes, K. A., Snyder, A. Z., Schlaggar, B. L., & Petersen, S. E. (2012). Spurious but systematic correlations in functional connectivity MRI networks arise from subject motion. *Neuroimage*, *59*(3), 2142-2154.

Rabellino, D., Densmore, M., Frewen, P. A., Théberge, J., & Lanius, R. A. (2016). The innate alarm circuit in post-traumatic stress disorder: Conscious and subconscious processing of fear-and trauma-related cues. *Psychiatry Research: Neuroimaging*, *248*, 142-150.

Rougemont-Bücking, A., Linnman, C., Zeffiro, T. A., Zeidan, M. A., Lebron-Milad, K., Rodriguez-Romaguera, J., ... & Milad, M. R. (2011). Altered processing of contextual information during fear extinction in PTSD: an fMRI study. *CNS neuroscience & therapeutics*, *17*(4), 227-236.

Saper, C. B. (2002). The central autonomic nervous system: conscious visceral perception and autonomic pattern generation. *Annual review of neuroscience*, *25*(1), 433-469.

Schauer, M., & Elbert, T. (2015). Dissociation following traumatic stress. *Zeitschrift für Psychologie/Journal of Psychology*. *218*, 109-127.

Schmahmann, J. D., Weilburg, J. B., & Sherman, J. C. (2007). The neuropsychiatry of the cerebellum—insights from the clinic. *The cerebellum*, *6*(3), 254-267.

Schore, A. N. (2002). Dysregulation of the right brain: a fundamental mechanism of traumatic attachment and the psychopathogenesis of posttraumatic stress disorder. *Australian and New Zealand Journal of Psychiatry*, *36*(1), 9-30.

Schore, A.N. (2009). Attachment trauma and the developing right brain: Origins of pathological dissociation. In: Dell PF, O'Neil JA (Eds.). *Dissociation and the dissociative disorders*.New York, NY: Routledge.

Schutter DJ (2013): Human cerebellum in motivation and emotion. In: Manto M, Gruol DL, Schmahmann J, Koibuchi N, Rossi F (Eds.). *Handbook of the cerebellum and cerebellar disorders* Netherlands: Springer.

Shackman, A. J., Salomons, T. V., Slagter, H. A., Fox, A. S., Winter, J. J., & Davidson, R. J. (2011). The integration of negative affect, pain and cognitive control in the cingulate cortex. *Nature Reviews Neuroscience*, *12*(3), 154-167.

Shaw, M. E., Moores, K. A., Clark, R. C., McFarlane, A. C., Strother, S. C., Bryant, R. A., ... & Taylor, J. D. (2009). Functional connectivity reveals inefficient working memory systems in post-traumatic stress disorder. *Psychiatry Research: Neuroimaging*, *172*(3), 235-241.

Shin, L. M., Whalen, P. J., Pitman, R. K., Bush, G., Macklin, M. L., Lasko, N. B., ... & Rauch, S. L. (2001). An fMRI study of anterior cingulate function in posttraumatic stress disorder. *Biological psychiatry*, *50*(12), 932-942.

Spiegel, D. (1997). Trauma, dissociation, and memory. *Annals of New York Academy of Sciences*, *821*, 225-237.

Stein, D. J., Koenen, K. C., Friedman, M. J., Hill, E., McLaughlin, K. A., Petukhova, M., ... & Bunting, B. (2013). Dissociation in posttraumatic stress disorder: evidence from the world mental health surveys. *Biological psychiatry*, *73*(4), 302-312.

Steuwe, C., Daniels, J. K., Frewen, P. A., Densmore, M., Pannasch, S., Beblo, T., ... & Lanius, R. A. (2012). Effect of direct eye contact in PTSD related to interpersonal

trauma: an fMRI study of activation of an innate alarm system. *Social Cognitive and Affective Neuroscience*, *9*(1), 88-97.

Taylor, S., Kuch, K., Koch, W. J., Crockett, D. J., & Passey, G. (1998). The structure of posttraumatic stress symptoms. *Journal of abnormal psychology*, *107*(1), 154.

Tian, L., Wang, J., Yan, C., & He, Y. (2011). Hemisphere-and gender-related differences in small-world brain networks: a resting-state functional MRI study. *Neuroimage*, *54*(1), 191-202.

Tomasi, D., & Volkow, N. D. (2011). Association between functional connectivity hubs and brain networks. *Cerebral cortex*, *21*(9), 2003-2013.

Tovote, P., Esposito, M. S., Botta, P., Chaudun, F., Fadok, J. P., Markovic, M., ... & \ Herry, C. (2016). Midbrain circuits for defensive behaviour. *Nature*, *534*(7606), 206-212.

Tzourio-Mazoyer, N., Landeau, B., Papathanassiou, D., Crivello, F., Etard, O., Delcroix, N., ... & Joliot, M. (2002). Automated anatomical labeling of activations in SPM using a macroscopic anatomical parcellation of the MNI MRI single-subject brain. *Neuroimage*, *15*(1), 273-289.

Weissman-Fogel, I., Moayedi, M., Taylor, K. S., Pope, G., & Davis, K. D. (2010). Cognitive and default-mode resting state networks: Do male and female brains "rest" differently?. *Human brain mapping*, *31*(11), 1713-1726.

Williams, L. M., Kemp, A. H., Felmingham, K., Barton, M., Olivieri, G., Peduto, A., ... & Bryant, R. A. (2006). Trauma modulates amygdala and medial prefrontal responses to consciously attended fear. *Neuroimage*, *29*(2), 347-357.

Winston, J. S., Strange, B. A., O'Doherty, J., & Dolan, R. J. (2002). Automatic and intentional brain responses during evaluation of trustworthiness of faces. *Nature neuroscience*, *5*(3), 277-283.

Zaytseva, Y., Szymanski, C., Gutyrchik, E., Pechenkova, E., Vlasova, R., & Wittmann, M. (2015). A disembodied man: A case of somatopsychic depersonalization in schizotypal disorder. *PsyCh journal*, *4*(4), 186-198.

Chapter 3

3 « Sensory overload and imbalance: Resting-state vestibular connectivity in PTSD and its dissociative subtype»

The findings from Chapter 2 provide a clear demonstration that when compared to healthy individuals, individuals with PTSD and its dissociative subtype exhibit significantly altered periaqueductal gray neural connectivity patterns with the whole brain during rest. Specifically, during rest, all traumatized individuals demonstrated widespread dorsolateral periaqueductal gray connectivity with cortical structures associated with emotional reactivity and defensive responding. Furthermore, individuals with the dissociative subtype of PTSD showed additional ventrolateral periaqueductal grey connectivity with brain structures involved in depersonalization. The periaqueductal gray has been identified as a critical structure for autonomic nervous system regulation. It is therefore possible that the distinctive periaqueductal grey connectivity patterns observed in individuals with PTSD and its dissociative subtype when compared to healthy individuals are illustrative of extreme arousal states exhibited at rest. Moreover, we hypothesize that the widespread periaqueductal gray resting-state connectivity patterns observed with brain structures associated with defensive responses is indicative of hypervigilance responses during rest in PTSD. This hypervigilance may, in turn, alter the perceptions and navigation of the external world and impact not only exteroceptive processing but also self-representation in space. Here, the vestibular system is central to the understanding of one’s position in gravitational space and relies on the continuous acquisition of interoceptive and exteroceptive sensory information from the environment,

even at a subconscious level. This system may therefore be a critical factor underlying aberrations in interoceptive and exteroceptive sensory processing observed in individuals with PTSD.

Chapter 3 has been published in its entirety as:

Harricharan, S., Nicholson, A. A., Densmore, M., Théberge, J., McKinnon, M. C., Neufeld, R. W.J., & Lanius, R. A. (2017). Sensory overload and imbalance: Resting-state vestibular connectivity in PTSD and its dissociative subtype. *Neuropsychologi*a, 106, 169-178.

3.1 « Introduction »

The vestibular system operates subconsciously, consistently monitoring one's position in gravitational space and being influenced by one's own interoceptive awareness (Berthoz & Weiss, 2000; Day & Fitzpatrick, 2005; Heydrich & Blanke, 2013; Lopez, 2016; Lopez & Blanke, 2011; Zu Eulenburg, Baumgärtner, Treede, & Dieterich, 2013). Most literature regarding the vestibular system emphasizes its role in bodily consciousness, where it is viewed as broadly integrating cognitive processes with multisensory input to maintain awareness of the bodily self, including physical balance (Blanke, 2012; De Waele, Baudonnière, Lepecq, Tran Ba Huy, & Vidal, 2001; Hitier, Besnard, & Smith, 2014; Lenggenhager & Lopez, 2015; Pfeiffer, Serino, & Blanke, 2014). Maintenance of physical equilibrium relies upon continuous proprioceptive input used to respond to changes in one's gravitational balance, and it is derived from both exteroceptive signals, including tactile and visual external stimuli, as well as interoceptive signals stemming from more visceral sensations in the body (Aspell et al., 2013; Balaban & Thayer, 2001; Suzuki, Garfinkel, Critchley, & Seth, 2013; Tsakiris, Tajadura-Jiménez, & Costantini,

2011). Taken together, the vestibular system plays a critical role in guiding the body through the physical world and in the interpretation of sensory stimuli. Accordingly, its disruption may signal profound alterations in key processes such as balance and sensory integration.

Neurobiologically, in non-human primates, vestibular multisensory input relating to one's position in the gravitational field travels through the vestibular nuclei of the brainstem and reaches its relevant cortical areas for multisensory processing, known as the parieto-insular vestibular cortex (PIVC; includes posterior insula, inferior parietal lobule – supramarginal and angular gyri), as well as somatosensory and motor areas (Akbarian, Grüsser, & Guldin 1994; Boisacq-Schepens & Hanus, 1972; Guldin & Grüsser, 1998; Lopez & Blanke, 2011). The definition of the human PIVC is less concrete, as it is sometimes referred to broadly as the temporo-peri-Sylvian vestibular network; however, some areas of the non-human PIVC are thought to be overlap with its human homologue, such as the posterior insula and the temporoparietal junction (Dieterich et al., 2003; Kahane, Hoffmann, Minotti, & Berthoz, 2003; Khan & Chang, 2013; Lopez & Blanke, 2011).

The cortical regions of the PIVC are critical for vestibular afferent processing, with each region playing an intricate role in organizing multisensory input to maintain vestibular function. Here, the posterior insula serves as a multisensory integration site to bring awareness to one's internal affective state, where it is critical to coordinating behavioral responses to exteroceptive vestibular input and contributes to one's own interoceptive awareness (Baier et al., 2013; Mazzola et al., 2014; Serino et al., 2013; Tsakiris, Hesse, Boy, Haggard, & Fink, 2007). The entire insula is considered

collectively the primary interoceptive cortex. Whereas the anterior insula plays a role in emotional regulation, the posterior insula is thought to be more involved with internal physiological homeostasis reactions to pain, cardiac signals and visceral sensations (Craig, 2002; Craig, 2003; Critchley, Wiens, Rotshtein, Öhman, & Dolan, 2004) . Importantly, the temporoparietal junction, which encompasses the supramarginal gyrus, as well as the posterior superior temporal gyrus/sulcus and angular gyrus, is also critical for receiving vestibular afferents and for integrating multisensory input related to bodily and visual spatial orientation relating to one's surroundings (Arzy, Thut, Mohr, Michel, & Blanke, 2006; Blanke, 2012; Blanke & Arzy, 2005; Burgess, Maguire, Spiers, & O'Keefe, 2001; Decety & Lamm, 2007; Igelström, Webb, & Graziano, 2015).

Neurobiological models of PTSD suggest that physiological homeostasis is disrupted due to chronic stress, which may promote hyperarousal symptoms, such as hypervigilance or irritability observed in PTSD patients (Kendall-Tackett, 2000; Vieweg et al., 2006; Yehuda, 2002; Yehuda & LeDoux, 2007; Yehuda & McFarlane, 1995), or alternatively, hypoarousal symptoms associated with emotional detachment, including symptoms of depersonalization/derealization in patients with its dissociative subtype (Frewen & Lanius, 2006; Lanius et al., 2010; Pain, Bluhm, & Lanius, 2010; Van Der Kolk, 2006). Moreover, depersonalization/derealization symptoms have been reported in vestibular disorders such as vertigo, where compromised sensorimotor processing can influence the relation between one's self and environment and affect negatively integration with other senses, particularly during acute episodes of severe stress (Yen Pik Sang, Jauregui-Renaud, Green, Bronstein, & Gresty, 2006). Moreover, aberrant functioning of the insula has been reported repeatedly in neuroimaging studies of PTSD

and its dissociative subtype (Brown & Morey, 2012; Herringa, Phillips, Almeida, Insana, & Germain, 2013; Hopper, Frewen, Sack, Lanius, & Van Der Kolk, 2007; Lanius et al., 2005; Nicholson et al., 2016; Simmons, Strigo, Matthews, Paulus, & Stein, 2009). Finally, altered activation of the temporo-parietal junction has been observed in patients with depersonalization disorder (Simeon et al., 2000), and is associated with dissociative symptoms observed in vestibular and psychiatric disorders, including dissociative PTSD (Ionta et al., 2011; Kennis, van Rooij, van den Heuvel, Kahn, & Geuze, 2016; Lanius et al., 2005, Lanius et al., 2002; Smith & Darlington, 2013; Steuwe et al., 2014; Voon et al., 2010). Critically, however, despite the close relationship between regions of the parieto-vestibular insular cortex and symptom profiles observed in PTSD and its dissociative subtype, the neural circuitry underlying the vestibular system in relation to PTSD has yet to be elucidated.

Accordingly, the objective of the current study was to examine functional connectivity of the vestibular system in PTSD, its dissociative subtype, and healthy controls. Using resting-state fMRI to determine the vestibular neural circuitry with key cortical regions overlapping with PTSD neurophenomenology, we performed a seed-based functional connectivity analysis of the vestibular nuclei with the whole-brain. Since the vestibular system operates subconsciously, continuous multisensory vestibular afferents monitoring one's position in the gravitational field are not dependent conscious or localizable stimuli as employed in task-based paradigms; we thus predicted that changes in the neural circuitry of the vestibular system in PTSD would be detectable during rest. Given that brainstem-cortical functional connectivity is essential for multisensory processing, we hypothesized that as compared to PTSD, healthy individuals

would demonstrate enhanced vestibular nuclei functional connectivity with relevant vestibular cortices (PIVC and prefrontal cortex) at rest. We further hypothesized that PTSD patient groups would differ in functional connectivity patterns. Specifically, we hypothesized that both PTSD groups would demonstrate altered multisensory integration patterns unique to the symptom profiles these groups experience. Specifically, we predicted that individuals with the dissociative subtype of PTSD would demonstrate significantly less vestibular nuclei functional connectivity with key vestibular cortices essential to understanding one's bodily self-awareness (e.g., supramarginal gyrus), due to their disposition to experiencing depersonalization/derealization symptoms.

3.2 Methods

3.2.1 Clinical and Demographic Information

The study consisted of one-hundred and forty-one participants, including 60 PTSD patients (PTSD), 41 PTSD patients with the dissociative subtype (PTSD+DS), and 40 healthy controls. London Health Sciences Centre recruited participants from 2009-2016 via referrals from family physicians, mental health professionals, psychology/psychiatric clinics, community programs for traumatic stress, and posters/advertisements within the London, Ontario community.

Inclusion criteria for PTSD and its dissociative subtype was based on the CAPS interview, which assesses the frequency and intensity of PTSD symptoms [CAPS; versions IV and 5 (for 18 participants); CAPS IV cut-off score >50, CAPS-5 uses a different scoring system with no definitive cut-off)] (Blake et al., 1995; Weathers et al., 2013). Individuals meeting criteria for the dissociative subtype scored at least two in

frequency and intensity for depersonalization and/or derealization symptoms as per standard methods (Harricharan et al., 2016; Nicholson et al., 2015; Steuwe et al., 2014). For all participants, the SCID was administered (Structured Clinical Interview for DSM-IV Axis-I disorders) (First, Spitzer, Gibbon, & Williams, 2002), along with a battery of questionnaires: Beck Depression Inventory (BDI) (Beck, Guth, Steer, & Ball, 1997), Child Trauma Questionnaire (CTQ; 87% of all PTSD patients had histories of childhood trauma, confirmed if patient scored above the 'none/minimal' threshold for any trauma category according to the CTQ scoring manual) (Bernstein & Fink, 1998), as well as the Multiscale Dissociation Inventory (MDI) (Briere, Weathers, & Runtz, 2005).

Clinical and demographic information are detailed in Table I. Age differences were assessed via a one-way ANOVA, and a Pearson's chi-square was performed to calculate gender differences across all three participant groups. If Levene's test violated homogeneity of variance assumptions, a Kruskal-Wallis analysis followed by post-hoc Games-Howell comparisons was performed to assess the significance of nonparametric psychological measures (CAPS, BDI, CTQ, and averaged depersonalization and derealization MDI scores) across groups (Kruskal & Wallis, 1952).

Participants were excluded if they could not adhere to the safety regulations required for the 3.0T scanner, including metal implants, previous head trauma associated with a period of unconsciousness, current or past history of neurological disorders, significant untreated medical illness, and/or pervasive developmental mental disorders. Additional exclusion criteria for PTSD patients included current or past history of bipolar or psychotic disorders, or if patients had alcohol/substance dependency or abuse for at least six months prior to participation in the study, as determined by the SCID. Control

participants were screened for prior trauma exposure and were excluded if lifetime criteria were met for any DSM-IV Axis-I psychiatric disorder. Approximately 35 patients (PTSD, n=20; PTSD+DS, n=15) were using psychotropic medications at the time of the study. The medications included antidepressants (n=32: SSRIs, n=13; SNRIs, n=7; NDRIs, n=9; MAOI, n=1; SARIs, n=4; tricyclics, n=1; tetracyclics, n=2), atypical antipsychotics (n=9), and sedative drugs (n=13: benzodiazepines, n=11; cyclopyrrolone, n=2). Moreover, 89% of participants were right-handed (n=126), while 11 participants were left-handed (Controls, n=2; PTSD, n=5; PTSD+DS, n=4) and 4 participants' handedness were unknown. If eligible, subjects provided written informed consent to participate in the study. All scanning was conducted in London, Ontario, Canada at either Robarts Research Institute's Center for Functional and Metabolic Mapping or Lawson Health Research Institute. The study was approved by the Research Ethics Board at Western University of Canada.

Table 3.1 *Clinical and Demographic Information*

Age, gender, CAPS, and self-report questionnaires (CTQ, MDI, BDI) are reported as mean ± SD. Psychiatric disorders assessed via SCID-I (MDD, Panic Disorder/Agoraphobia, Social Phobia, OCD and GAD) are reported in frequencies, as n = current (past) cases.

Abbreviations: PTSD, posttraumatic stress disorder; PTSD + DS, posttraumatic stress disorder with the dissociative subtype; M, Males; F, Females; CAPS, Clinician-Administered PTSD Scale; CTQ, Child Trauma Questionnaire; BDI, Beck Depression Inventory; MDI, Multiscale Dissociation Inventory; MDD, Major Depression Disorder; OCD, Obsessive Compulsive Disorder; GAD, Generalized Anxiety Disorder.**s**

3.2.2 Data Acquisition

Whole-brain fMRI (functional magnetic resonance) data were collected in a 3.0T scanner (Magnetom Tim Trio, Siemens Medical Solutions, Erlangen, Germany) with a 32-channel phased array head coil. BOLD (blood oxygen level dependent) fMRI data were collected using a manufacturer's standard gradient-echo planar imaging (EPI) pulse sequence (single-shot, blipped-EPI) with an interleaved slice acquisition order per the following specifications: Time Resolution (TR) = 3000 ms, Echo Time (TE) = 20 ms, voxel size = $2 \times 2 \times 2$ mm^3, Field of View (FOV) = $192 \times 192 \times 128$ mm^3 (94×94 matrix, 64 contiguous slices), and Flip Angle (FA) = 90°. High-resolution T1-weighted anatomical images were also collected (MPRage: 192 slices, voxel size = $1 \times 1 \times 1$ mm3). To obtain resting-state data, subjects were asked to close their eyes and let their minds wander without focusing on anything in particular for 6 min as per standard methods (Bluhm et al., 2009; Fransson, 2005; Harricharan et al., 2016), with follow-up post-scan clinical state measures, including the State-Trait Anxiety Inventory (STAI) (Spielberger, 2010) and the Responses to Script-Driven Imagery Scale (RSDI) (Hopper, Frewen, Sack, Lanius, & Van Der Kolk, 2007) to assess the participants' state clinical symptoms during the scan.

3.2.3 Resting-State fMRI Data Preprocessing

Image preprocessing and statistical analyses were performed using statistical parametric mapping software (SPM12, Wellcome Trust Center for Neuroimaging, London, UK: http:// www.fil.ion.ucl.ac.uk/spm; RRID:SCR_007037) within MATLAB 8.6 (R2015b, Mathworks Inc., MA; RRID:SCR_001622). The functional images for each subject were realigned to the first functional image, after four dummy scans were omitted to allow

magnetization to reach steady state, to correct for motion in the scanner and were resliced. The resulting mean functional image was co-registered to the T1-weighted anatomical image to spatially realign BOLD data with the subject's anatomical space. The co-registered images were segmented using the "New Segment" method implemented in SPM12, which uses T2-weighted and PD-weighted scans when generating tissue probability maps. The functional images were registered to a MNI template using the forward deformation field, with additional visual inspection of precise brainstem normalization in each subject, and were subsequently smoothed with a three-dimensional isotropic Gaussian kernel of 6 mm full-width half maximum [FWHM; as guided by previous fMRI vestibular nuclei studies which range from 4 mm-8 mm FWHM smoothing kernels (Kirsch et al., 2016; Miller et al., 2008)]. The images were further motion corrected with ART software (version 2015-10; Gabrieli Lab, McGovern Institute). The means of the total motion outliers per subject in each group were compared to assess any potential influence on the results of the present study and did not vary significantly across groups (p=0.327, *ns*). Physiological denoising of the data was done through bandpass filtering of the smoothed functional volumes to isolate frequencies of interest and reduce respiratory and other physiological noises, ranging from 0.012 to 0.1 Hz. Bandpass filtering isolates low frequencies associated with spontaneous fluctuations within the gray matter of the brain at rest, while adjusting for proper sampling of cardiac and respiratory noise for frequencies of physiological interest (Fox et al., 2005; Zuo et al., 2010). While low frequencies are associated with low MR scanner noise (i.e. slow scanner drifts), high frequencies are thought to correspond to

white matter, as well as cardiac and respiratory signals (Cordes et al., 2001; Van Den Heuvel, Stam, Boersma, & Hulshoff Pol, 2008).

3.2.4 fMRI Statistical Analyses

3.2.4.1 Within-Subject Analysis

A within-subject general linear model was used to assess resting-state functional connectivity patterns for each subject. The model included the mean signal intensity time course for the resting-state scan, with ART motion outliers used as regressors. The left and right vestibular nuclei (LVN and RVN) [***x*:** ±16, ***y*:** -36, ***z*:** -32] were used as spherical (5mm radii) seed regions-of-interest (Figure 3.1), in concordance with previous studies (Kirsch et al., 2016; Miller et al., 2008), and generated using PickAtlas software (WFU Pickatlas, version 3.0.5 (Maldjian, Laurienti, Kraft, & Burdette, 2003); http://fmri.wfubmc.edu/software/pickatlas; RRID:SCR_007378). The mean signal intensity time course was created via in-house software, developed by co-author Jean Théberge, which read LVN and RVN seed activity from PickAtlas in each resting-state functional volume per subject. A voxel-wise approach was used to calculate positive and negative correlations between LVN and RVN signal time courses with other voxels of the brain.

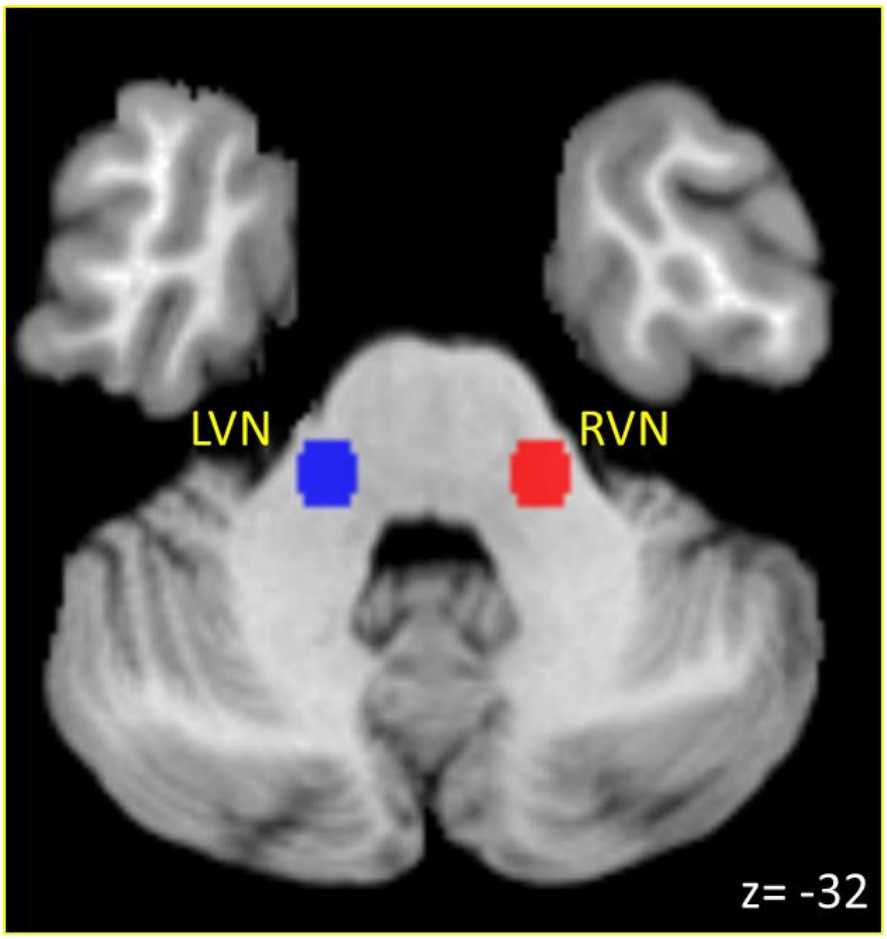

Figure 3.1 *Vestibular Nuclei Seed Regions-of-Interest.* Left (LVN) and right (RVN) vestibular nuclei regions-of-interest [MNI: *x*: ±16 y: -36 *z*: -32; 5 mm sphere] used to generate seed time courses for within-subject analysis.

3.2.4.2 Between-Subject Analysis

A full-factorial analysis of variance (ANOVA) was performed to examine the 3x2 interaction between participant group (PTSD, PTSD+DS and controls) and regions-of-interest (left and right vestibular nuclei; L/R VN) as well as main effects. Separate ANOVAs were performed using either MDD diagnosis (determined via SCID assessment; see Methods; Table I) or participants on medications as covariates. Post-hoc one-sample t-tests and two-sample t-tests were used to assess functional connectivity patterns within and between each group and region-of-interest, respectively. Correlations between PTSD seed-based analysis and psychological measures (CAPS, CTQ and averaged depersonalization and derealization MDI scores) and post-scan clinical state measures (STAI and averaged depersonalization and derealization RSDI scores) were assessed. Subsequent ROI analyses of key parieto-vestibular cortical areas [posterior insula (***x:*** -42, ***y:*** -12, ***z:*** 10) and supramarginal gyrus (***x:*** 59, ***y:*** -36, ***z:*** 30)] based on anatomical data from a previous vestibular-related resting-state neuroimaging study (Göttlich et al., 2014) were performed to look at results from the full-factorial analysis and regression analyses of clinical correlations with seed-based analysis. Brain regions were identified using the AAL atlas (Tzourio-Mazoyer et al., 2002) via xjview software (http://www.nitrc.org/projects/xjview), the MNI2Tal atlas available online via the BioImage Suite at Yale University (http://bioimagesuite.yale.edu/mni2tal/) (Lacadie, Fulbright, Constable, & Papademetris, 2008) and visually inspected using an additional anatomical atlas (Montemurro & Bruni, 1988).

In order to determine significant clusters, the FWE-corrected alpha was set to p=0.05, resulting in a calculated FWE corrected cluster size of k=10 based on random

field theory in SPM (Friston et al., 1994; Hayasaki & Nichols, 2003; Lui et al., 2011; Nicholson et al., 2015). Significant clusters identified in ROI analyses were adjusted for multiple comparisons at a voxel-wise FWE-corrected threshold set at $p \leq 0.025$, k=10.

3.3 Results

3.3.1 Overview

Overall, the present study revealed altered vestibular nuclei functional connectivity patterns across PTSD, PTSD+DS and healthy control groups. More specifically, bilateral vestibular nuclei functional connectivity with the parieto-vestibular insular cortex (posterior insula, supramarginal gyrus) and the dorsolateral prefrontal cortex was observed in both PTSD and healthy controls whereas the PTSD+DS group in contrast showed minimal functional connectivity with these areas. Interestingly, the PTSD group showed greater vestibular nuclei functional connectivity with the right angular and supramarginal gyri than both the PTSD+DS and healthy control groups. Conversely, healthy controls demonstrated greater RVN connectivity with the left posterior insula than the PTSD group. Finally, PTSD symptom severity negatively correlated with vestibular nuclei functional connectivity with the prefrontal cortex, while averaged depersonalization/derealization MDI and RSDI scores negatively correlated with vestibular nuclei connectivity with the right supramarginal gyrus.

3.3.2 Clinical and Demographic Measures

ANOVA analysis did not reveal significant differences in ages across all three participant groups (p=0.073, df = 2), and a Pearson's chi-square test failed to reveal a statistically significant association between gender and participant group (p=0.066, df = 2). Kruskal–

Wallis analysis of variance yielded significant values for all psychological test measures, including CTQ, CAPS, MDI, and BDI, as well as resting-state clinical measures RSDI and STAI (all $p< 0.001$). Post-hoc Games-Howell comparisons revealed no significant differences between PTSD+DS and PTSD groups for CAPS-IV ($p = .794$) and BDI scores, but did reveal significantly higher CTQ and MDI (averaged depersonalization and derealization) scores in PTSD+DS individuals ($p< 0.05$). For resting-state clinical measures, Games-Howell comparisons revealed no significant differences between PTSD+DS and PTSD for STAI scores ($p=0.064$), but did reveal significantly higher RSDI (averaged depersonalization and derealization score) in PTSD+DS as compared to PTSD ($p<0.05$) during the scan. All psychological measures and resting-state clinical measures revealed significantly higher scores in both PTSD patient groups as compared to controls (all $p< 0.01$).

3.3.3 Full Factorial Design

The 3x2 full factorial ANOVA conducted for the seed-based analysis revealed an interaction between participant group (PTSD+DS, PTSD, healthy controls) and region-of-interest (left and right vestibular nuclei; LVN, RVN, respectively) as well as main effects for each factor; results are shown in Appendix B. Post-hoc one-sample and two-sample t-tests were used to assess group and region-of-interest differences [all results are reported as FWE-voxel corrected, $p<0.05$, $df = (1, 276)$]. Separate full-factorial analyses using either MDD diagnosis or patients on medications as a covariate did not change the results of the original full-factorial ANOVA analysis.

3.3.3.1 Within Group Functional Connectivity

Figure 3.2 depicts vestibular nuclei functional connectivity patterns with previously identified key vestibular cortical regions (posterior insula, supramarginal gyrus) and the dorsolateral prefrontal cortex within each participant group. A more comprehensive explanation of within group vestibular nuclei functional connectivity patterns are detailed in Appendix B.

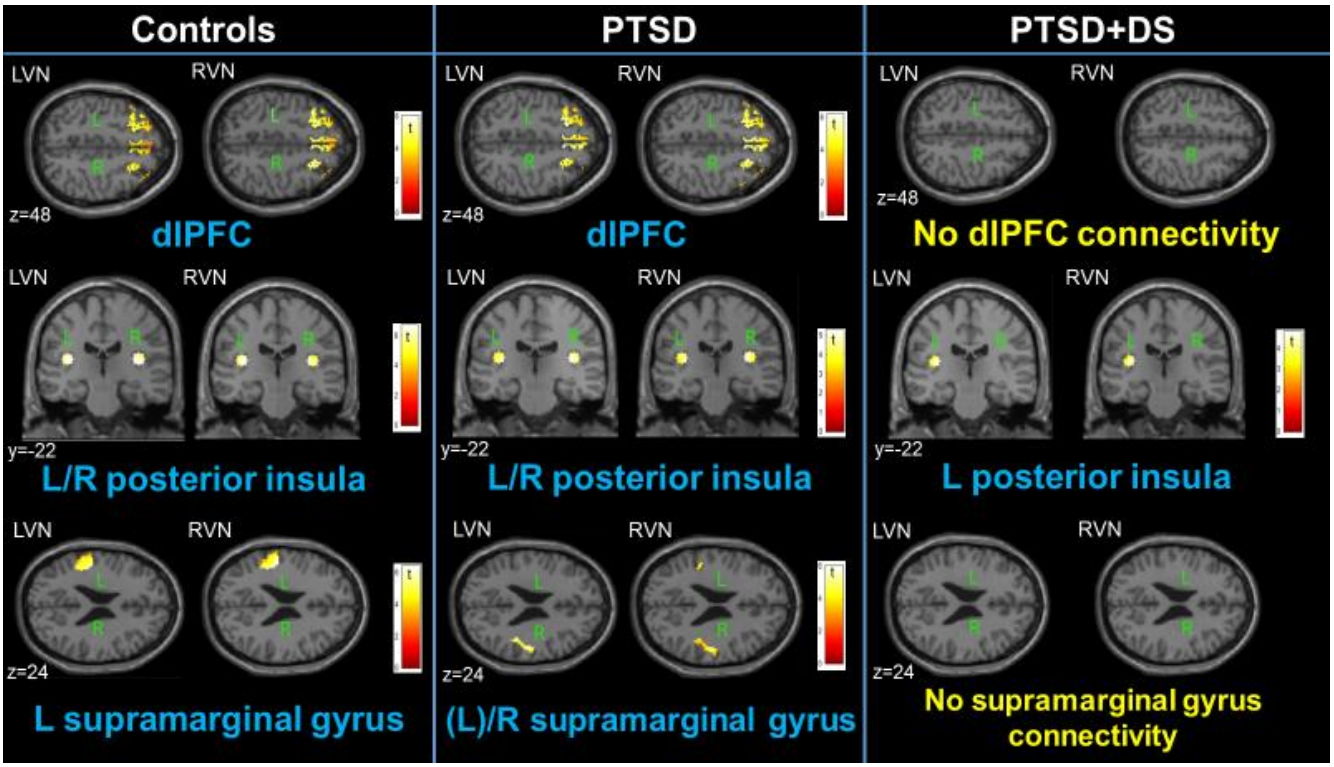

Figure 3.2 *Within-Group Vestibular Nuclei Functional Connectivity Patterns.* Left and right vestibular nuclei functional connectivity patterns with key cortical regions relevant to the vestibular system based on seed-based analysis within all three participant groups (controls, PTSD and PTSD+DS), including the parieto-insular vestibular cortical regions (posterior insula, supramarginal gyrus), and the dorsolateral prefrontal cortex. Notably, healthy controls and PTSD demonstrated connectivity with all three brain regions shown (dlPFC, posterior insula, supramarginal gyrus), whereas PTSD+DS demonstrated neither LVN nor RVN functional connectivity with neither the dlPFC nor the supramarginal gyrus.

Abbreviations: PTSD posttraumatic stress disorder patients non-subtype; PTSD+DS, PTSD patients with the dissociative subtype; LVN, left vestibular nuclei; RVN, right vestibular nuclei; L, left hemisphere; R, right hemisphere; dlPFC, dorsolateral prefrontal cortex.

3.3.3.2 Between-Group Functional Connectivity

3.3.3.2.1 PTSD > PTSD+DS and Healthy Controls

PTSD demonstrated greater bilateral vestibular nuclei connectivity with the right angular and supramarginal gyri, as well as the right middle temporal gyrus as compared to PTSD+DS, with additional increased LVN connectivity with the superior and middle frontal gyri (BA 9,10), the medial orbitofrontal cortex, the right fusiform and the right inferior occipital gyrus as compared to PTSD+DS (Table 3.2). Moreover, the PTSD group demonstrated greater LVN connectivity with the right angular gyrus and greater RVN connectivity with the right supramarginal gyrus as compared to healthy controls (Table 3.2).

3.3.3.2.2 PTSD+DS > PTSD and Healthy Controls

The PTSD+DS group did not demonstrate greater bilateral vestibular nuclei connectivity with any area as compared to PTSD and healthy controls.

3.3.3.2.3 Healthy Controls > PTSD and PTSD+DS

Healthy controls demonstrated increased LVN connectivity with the middle temporal gyrus as compared to the PTSD group, as well as increased RVN connectivity with the left posterior insula upon subsequent ROI analyses as compared to PTSD (Table 3.2). In addition, controls demonstrated greater bilateral vestibular nuclei connectivity with the left precuneus as compared to PTSD+DS, with additional increased LVN connectivity with the left supramarginal gyrus, precentral gyrus, middle temporal gyrus and middle frontal gyrus as compared to PTSD+DS (BA 6) (Table 3.2**)**.

Table 3.2 *Between-Group LVN and RVN Functional Connectivity Patterns*

Contrast	**L R**	**B A**	**Region**	**K**	**vFWE**	**Z**	**MNI Coordinates x y z**		
PTSD>PTSD+DS LVN	R	40	Angular Gyrus	1970	<0.001	5.88	56	-62	28
	R	40	Supramarginal Gyrus		<0.001	5.67	64	-28	28
	R	39	Middle Temporal Gyrus		<0.001	5.66	52	-70	18
	R	37	Inferior Occipital Gyrus		0.002	5.16	50	-66	-14
	R	37	Fusiform Gyrus		0.006	4.89	52	-58	-18
	L	10	Middle Frontal Gyrus	104	0.005	4.90	-42	54	14
	R	10	Middle Frontal Gyrus	364	0.007	4.83	38	54	20
	R	9	Superior Frontal Gyrus		0.013	4.70	28	48	38
	L	40	Supramarginal Gyrus	44	0.010	4.75	-62	-28	42
	R	10	Medial Orbitofrontal	16	0.011	4.74	6	68	-4

			Cortex						
PTSD>PTSD+DS RVN	R	40	Angular Gyrus	1099	0.001	5.40	58	-60	28
	R	40	Supramarginal Gyrus		0.001	5.29	66	-28	28
	R	39	Middle Temporal Gyrus		0.024	4.56	56	-64	18
PTSD>Ctrl LVN	R	39	Angular Gyrus	175	0.048	4.38	56	-62	28
PTSD>Ctrl RVN	R	40	Supramarginal Gyrus	187	0.004	4.96	66	-28	30
PTSD+DS>PTSD LVN			None						
PTSD+DS>PTSD RVN			None						
PTSD+DS>Ctrl LVN			None						

PTSD+DS>Ctrl RVN			None						
Ctrl>PTSD LVN	L	22	Middle Temporal Gyrus	81	0.014	4.68	-68	-22	-4
Ctrl>PTSD RVN	L	41	*ROI Analysis** Posterior Insula	51	0.02	3.04	-52	-12	10
Ctrl>PTSD+DS LVN	L	40	Supramarginal Gyrus	330	0.006	4.87	-52	-26	42
	L	6	Precentral Gyrus	964	0.008	4.81	-26	-20	74
	L	6	Middle Frontal Gyrus		0.014	4.69	-34	8	62
	L	21	Middle Temporal Gyrus	92	0.016	4.65	-68	-34	-8
	L	5	Precuneus	252	0.023	4.56	-2	-36	56

Ctrl>PTSD+DS RVN	L	5	Precuneus	3612	0.023	4.57	-4	-36	-56

Post-hoc two-sample t-tests based on full-factorial analysis (reported at family-wise error whole-brain voxel-corrected at $p<.05$, $k=10$). Peak coordinates without *k* (cluster size) values listed are subpeaks of the nearest *k* value listed above. *ROI analysis is adjusted for multiple comparisons and is reported at vFWE $p \leq 0.025$, $k=10$.

Abbreviations: PTSD posttraumatic stress disorder; PTSD+DS, posttraumatic stress disorder with the dissociative subtype; Ctrl, healthy controls; LVN, left vestibular nuclei; RVN, right vestibular nuclei; L, left hemisphere; R, right hemisphere; BA, Brodmann Area; *k*, Cluster Size; vFWE, family-wise error voxel-corrected

3.3.3.3 Between-Seed Region Functional Connectivity

Functional connectivity patterns between region-of-interest differences demonstrated greater PTSD+DS RVN connectivity with the bilateral superior frontal gyrus (BA 10), middle frontal gyrus (BA 8), and the inferior frontal triangularis as compared to LVN functional connectivity patterns (Table III). In addition, greater RVN functional connectivity was observed with the left middle temporal gyrus and the superior temporal pole as compared to LVN in PTSD+DS (Table 3.3). LVN and RVN regions-of-interest differences were not observed in PTSD and controls.

Table 3.3 *LVN versus RVN Functional Connectivity Within Participant Groups*

Contrast	**L R**	**B A**	**Region**	**k**	**pFWE**	**Z**	**MNI Coordinates**		
							x	**y**	**z**
PTSD LVN>RVN			None						
PTSD RVN>LVN			None						

PTSD+DS LVN>RVN			None						
PTSD+DS RVN>LVN	R	10	Superior Frontal Gyrus	249	0.001	5.30	30	66	0
	R	38	Superior Temporal Pole	87	0.016	4.58	34	16	-30
	L	21	Middle Temporal Gyrus	194	0.027	4.44	-58	-30	-18
	L	8	Middle Frontal Gyrus	249	0.032	4.40	-38	16	58
	L	44	Inferior Frontal Triangularis		0.042	4.33	-56	24	26
	L	10	Superior Frontal Gyrus	37	0.046	4.31	-12	68	6
Ctrl LVN>RVN			None						
Ctrl RVN>LVN			None						

Post-hoc two-sample t-tests based on full-factorial analysis (reported at family-wise error whole-brain voxel-corrected at $p<.05$, $k=10$). Peak coordinates without *k* (cluster size) values listed are subpeaks of the nearest *k* value listed above.

Abbreviations: PTSD, posttraumatic stress disorder; PTSD+DS, posttraumatic stress disorder with the dissociative subtype; Ctrl, healthy controls; LVN, left vestibular nuclei; RVN, right vestibular nuclei; L, left hemisphere; R, right hemisphere; BA, Brodmann Area; *k*, Cluster Size; vFWE, family-wise error voxel-corrected.

3.3.3.4 Clinical Measure Correlations with Functional Connectivity Patterns in PTSD Patients

CAPS-IV total scores correlated negatively with the middle frontal gyrus in all PTSD patients (both PTSD and PTSD+DS groups) for both LVN [(***x:*** 44, ***y:*** 40, ***z:*** 30), *k*=320, *p*FWE=0.013) and RVN [(***x:*** 42, ***y:*** 42, ***z:*** 30), *k*=319, *p*FWE=0.017] functional connectivity patterns. In addition, averaged depersonalization/derealization RSDI and MDI scores correlated negatively with the right supramarginal gyrus upon ROI analysis for the LVN [(***x:*** 54, ***y:*** -28, ***z:*** 30), *k*=162, *p*FWE=0.009] and RVN [(***x:*** 62, ***y:*** -38, ***z:*** 34), *k*=188, *p*FWE=0.002] connectivity patterns, respectively. There were no correlations observed with other psychological test scores (CTQ, BDI) and clinical state measure (STAI).

3.4 Discussion

The aim of the present study was to delineate the neural circuitry of the vestibular system by examining functional connectivity patterns of the brainstem vestibular nuclei in PTSD and its dissociative subtype, as well as in healthy controls during resting-state. The cortical areas implicated in the vestibular system neural circuitry overlap with areas identified as aberrant during resting-state in previous PTSD literature. We therefore predicted that altered neural circuitry in PTSD would be detectable at resting-state as vestibular function relies on continuous multisensory input for awareness of one's own position in the gravitational field. Moreover, given the role of the vestibular system in integrating proprioceptive input based on both interoceptive and exteroceptive multisensory information to inform bodily experience, we predicted that PTSD and its dissociative subtype would display unique sensory processing patterns based on their

distinctive symptom profiles. On balance, this proved the case. Specifically, as compared to PTSD patients with the dissociative subtype, PTSD patients without the dissociative subtype and healthy controls demonstrated increased functional connectivity with key vestibular cortical brain regions identified in previous literature [parieto-insular vestibular cortex (PIVC) and dorsolateral prefrontal cortex]. Interestingly, whereas controls demonstrated increased vestibular nuclei connectivity with the posterior insula as compared to PTSD, the PTSD group demonstrated greater connectivity with the right temporoparietal junction as compared to both controls and PTSD+DS. These findings suggest PTSD patients may display differing multisensory integration patterns that influence uniquely vestibular function in PTSD based on the presence of the dissociative subtype during resting-state. We discuss these findings in turn.

3.4.1 Vestibular Nuclei and Parieto-Insular Vestibular Cortex Connectivity

3.4.1.1 Posterior Insula

Both groups of PTSD patients, as well as healthy individuals, demonstrated bilateral vestibular nuclei functional connectivity with the left posterior insula; however, only PTSD patients without the dissociative subtype and healthy controls showed bilateral functional connectivity with the right posterior insula. Moreover, the control group showed increased RVN connectivity with the posterior insula as compared to the PTSD group. Here, the posterior insula is critical to one's interoceptive awareness as multimodal sensory integration of afferent stimuli is essential for physiological homeostasis to maintain one's affective state in response to external environmental cues and sensory-evoked emotions (Baier et al., 2013; Craig, 2003; Critchley, Wiens,

Rotshtein, Öhman, & Dolan, 2004; Flynn, 1999; Wager & Barrett, 2004). Direct brainstem vestibular nuclei connectivity with the posterior insula observed in PTSD and healthy controls reflects this, as sensory processing can subconsciously integrate both exteroceptive and interoceptive information to maintain physiological homeostasis. However, decreased RVN connectivity with the left posterior insula observed in PTSD as compared to the healthy controls may suggest deficient sensory integration of exteroceptive and interoceptive cues, as exteroceptive information relayed from the vestibular nuclei to the posterior insula may be subject to the influence of additional neural networks involving the posterior insula in relation to PTSD symptomatology. Interestingly, Nicholson et al. (2016) observed increased posterior insula connectivity with the basolateral amygdala in PTSD patients during rest and postulated its association with increased sensory processing during hyperarousal and hypervigilant symptoms, which exist irrespective of the presence of a threat present, and would thus be detectable during resting-state (Kimble et al., 2014). Aberrant sensory integration in the PTSD group can trigger physiological dysregulation, which may contribute to increased sympathetic tone observed in PTSD patients as well as alter a patient's ability to appraise threat (Lipov & Kelzenberg, 2012; Révész et al., 2014; Sbarra & Hazan, 2008; Tsigos & Chrousos, 1994).

PTSD+DS did not demonstrate vestibular nuclei functional connectivity with the right posterior insula, perhaps suggesting weakened interoceptive awareness in these patients as well, given that additional depersonalization symptoms render one more prone to experience emotional detachment and to developing an altered sense of bodily self-consciousness that can alter the ability to navigate the physical world and integrate

sensory stimuli (Frewen et al., 2008; Heydrich & Blanke, 2013; Lanius et al., 2010; Lopez, 2013). Interestingly, state depersonalization/derealization symptoms (RSDI) were elevated during the resting state scan in PTSD+DS as compared to PTSD. It is therefore possible that the emotional detachment these individuals experience may re-direct or stagnate overwhelming sensory/emotional input associated with their interpretation of surroundings, thus obstructing the vestibular nuclei connectivity with the posterior insula (Frewen & Lanius, 2006).

3.4.1.2 Supramarginal Gyrus

The temporoparietal junction, which encompasses the supramarginal gyrus, is critical for multisensory processing; specifically, the right temporoparietal junction is thought to be critical for discriminating between one's self versus non-self, thereby contributing to feelings of body ownership (Blanke & Arzy, 2005; Igelström, Webb, & Graziano, 2015; Tsakiris, Costantini, & Haggard, 2008). Both PTSD and healthy controls demonstrated vestibular nuclei functional connectivity with the supramarginal gyrus as compared to PTSD+DS, which did not demonstrate any connectivity.

Given the role of the supramarginal gyrus in integrating multisensory information in terms of bodily orientation, brainstem vestibular nuclei functional connectivity with the supramarginal gyrus observed in healthy individuals aligns with the observation that they are less susceptible than patients with PTSD with the dissociative subtype to feelings of disembodiment and are thus better able to maintain adequate integration of tactile and proprioceptive external cues, a pattern similar to that observed in PTSD patients without the dissociative subtype (Blanke, 2012; Lopez, 2016; Lopez, Halje, & Blanke, 2008; Vieweg et al., 2006). Interestingly, the PTSD group demonstrated increased vestibular

nuclei functional connectivity with the right suprarmarginal gyrus as well as the right angular gyrus, also part of the temporoparietal junction, as compared to healthy individuals and PTSD+DS. Recruitment of additional areas of the right temporoparietal junction may reflect a greater effort required for PTSD patients to process tactile and proprioceptive sensory information pertaining to external cues because of their hypervigilance symptoms, which may heighten one's concern for knowledge of his/her own position in gravitational space to fulfill the need to consistently evaluate one's own safety in relation to his/her environment (Engel-Yeger et al., 2013; McFarlane, Weber, & Clark, 1993; Porges, 2011). In contrast, the depersonalization/derealization symptom profile observed in PTSD+DS may be responsible for altered processing of tactile and proprioceptive sensory information, as deficient functional connectivity between the vestibular nuclei and the supramarginal gyrus can compromise proper assessment of one's own bodily orientation in space. This may also contribute to elevated RSDI - depersonalization/derealization symptoms observed during the resting-state scan in PTSD+DS patients, as compared to PTSD and controls (Blanke, 2012; Serino et al., 2013), where previous studies have also linked altered right supramarginal gyrus function to provocation of out-of-body experiences, which may be related to depersonalization experiences in the dissociative subtype of PTSD (Blanke, Ortigue, Landis, & Seeck, 2002; Lopez, Halje, & Blanke, 2008; Lopez, 2013; De Ridder, Van Laere, Dupont, Menovsky, & Van De Heyning, 2007). Additional clinical resting-state measures also revealed significantly higher state anxiety clinical measures in PTSD+DS as compared to healthy controls during the resting-state scan, which itself has been suggested to intensify depersonalization/derealization symptoms in those with vestibular dysfunction (Kolev,

Georgieva-Zhostova, & Berthoz, 2014) . Future research is warranted to principally investigate the role of anxiety on vestibular function and its relation to symptoms of depersonalization/derealization.

3.4.2 Vestibular Nuclei and Dorsolateral Prefrontal Cortex Functional Connectivity

PTSD and healthy individuals demonstrated significant functional connectivity with the prefrontal cortex, particularly with the dorsolateral prefrontal cortex (BA 8, 9, 46). De Waele and colleagues (2001) suggested that vestibular nerve stimulation leads to egomotion processing at the level of the prefrontal cortex thus facilitating planning for motor responses in response to disruptions in balance (both voluntary and involuntary) and contributing to knowledge of one's own physical equilibrium. Here, PTSD seed-based functional connectivity correlations also revealed that increased CAPS-IV scores negatively correlated with prefrontal cortex functional connectivity, as increased PTSD symptom severity may compromise one's ability to properly integrate exteroceptive and interoceptive information relating one's own position in gravitational space (see Figure 3.3). Critically, within group, PTSD+DS did not demonstrate connectivity with *any* area of the prefrontal cortex, and PTSD demonstrated greater LVN connectivity with the dorsolateral prefrontal cortex (BA 9) as compared to PTSD+DS. Symptoms of disembodiment and vestibular dysfunction may therefore hinder the ability to conduct ego-motion processing and may contribute to gait unsteadiness reported previously in dissociative conversion disorders (Holmes et al., 2005; Janet, 1907). Interestingly, Janet (1889) proposed that following intense trauma, psychological disorganization ("*déagréation psychologique*") can lead to altered states of consciousness that manifest as

somatic symptoms (Gottlieb, 2003; Janet, 1889), which may not be limited to feelings of disembodiment as have been discussed in relation to altered states of consciousness associated with PTSD (Frewen & Lanius, 2015).

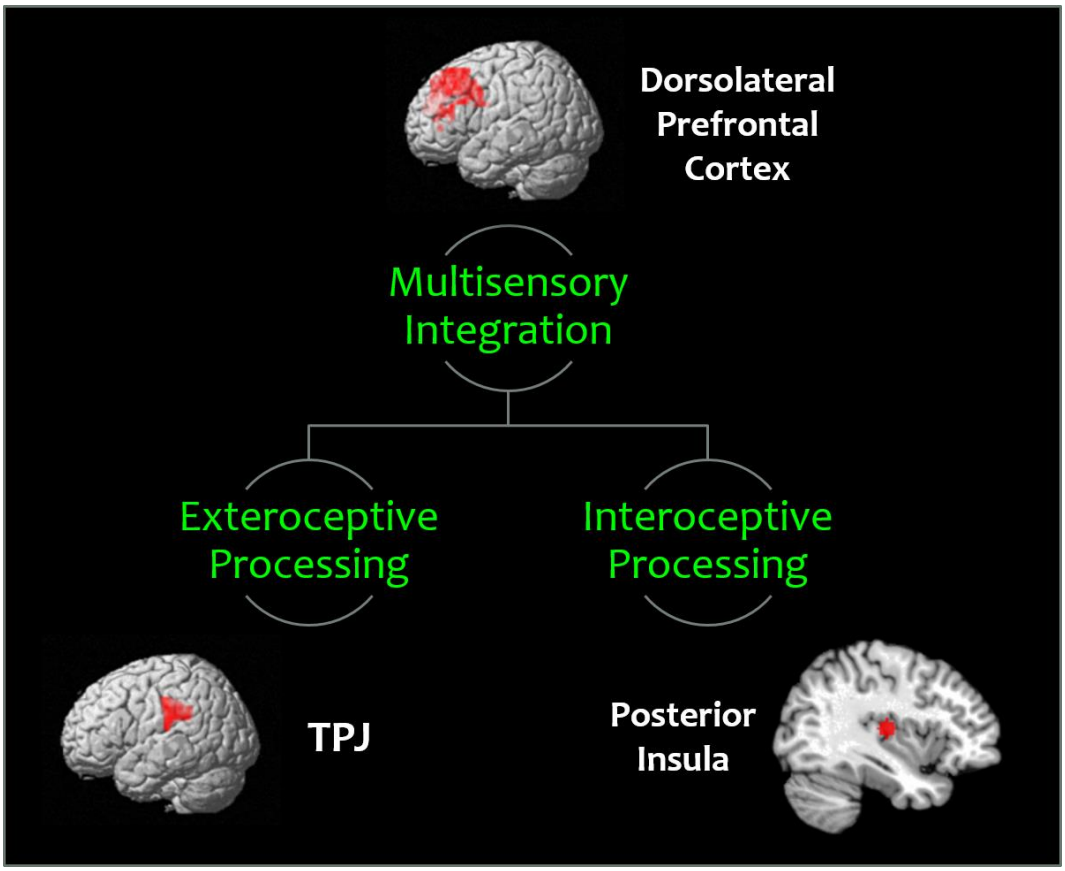

Figure 3.3 *Multisensory Integration.* Multisensory integration is thought to be dependent upon exteroceptive and interoceptive processing, as vestibular multisensory input pertaining to one's awareness in gravitational space requires understanding of both the physical and mental self to navigate through the physical world with appropriate context of one's surroundings. Here, PTSD patients with and without the dissociative subtype seem to display unique neural connectivity patterns involving key structures for sensory processing as compared to healthy controls based on their distinctive symptom profiles.

3.4.3 Limitations and Future Directions

Several limitations of this study need to be considered. First, previous studies have reported gender-related differences during resting state in healthy individuals (Gur et al., 1995; Tian, Wang, Yan, & He, 2011), but see also (Damoiseaux et al., 2006; Weissman-Fogel, Moayedi, Taylor, Pope, & Davis, 2010). Future studies should therefore explore the gender-specific neural circuitry of the vestibular system in relation to trauma. Secondly, although the data has been corrected for general effects of heart rate through filtering grey matter frequencies, this may not fully account for the physiological influence on the BOLD signal [e.g., EEG, COMPCOR (Behzadi, Restom, Liau, & Liu, 2007), RETROICOR (Glover, Li, & Ress, 2000)]. Future studies investigating the brainstem should therefore explore optimal methods of correcting for physiological noise as the brainstem is comprised of a unique grey and white matter distribution. Thirdly, this study was only powered to examine brainstem vestibular nuclei functional connections with the whole brain; however, further investigation of the influence of the parieto-insular vestibular cortex on its neural correlates and vice-versa, is required to eventually assist in delineating the neural circuitry underlying the vestibular system in PTSD using dynamic causal modelling. In addition, we intend to further explore the effect of task-based fMRI paradigms on the vestibular network in post-traumatic stress disorder to delineate how conscious multisensory information processing affect vestibular function. Moreover, future research is warranted to explore other aspects of the vestibular system, such as the vestibular link with anxiety symptoms, and its role in autonomic regulation addressed in previous studies (Balaban, 1999; Biaggioni, Costa, & Kaufmann, 1998). Finally, the present study did not identify a right-dominant hemispheric laterality

component to the vestibular system as described in previous studies (Bottini et al., 2001; Fasold et al., 2002). Future studies should therefore investigate whether this absence of laterality is more pronounced in PTSD patients, or, alternatively, whether hemispheric laterality is greater under experimental conditions as compared to resting-state conditions.

3.4.4 Conclusions

On balance, the current findings lay the groundwork for future studies examining the vestibular system in PTSD and its dissociative subtype, where alterations in one's interoceptive awareness and sense of bodily orientation can compromise multisensory integration of vestibular signals critical for understanding one's relationship with his/her surroundings. Moreover, PTSD symptom severity negatively correlated with prefrontal cortex functional connectivity, as well as between clinical dissociative measures and the right supramarginal gyrus connectivity. Taken together, these findings suggest altered multisensory integration patterns in PTSD patients may distort the intricate relationship between one's surroundings, interoceptive awareness and bodily self-consciousness. This disruption may, in turn, compromise vestibular function and contribute to the neurophenomenology of the unique symptom profiles observed in PTSD and its dissociative subtype. Decreased vestibular functional connectivity with the posterior insula in PTSD patients as compared to healthy individuals suggest a weakened interoceptive awareness, which may impair one's attunement with his/her surroundings and promote hypervigilance symptoms to consistently evaluate one's own safety in his/her environment. Moreover, limited vestibular functional connectivity with key vestibular cortical regions (parieto-insular vestibular cortex, dorsolateral prefrontal

cortex) in the PTSD dissociative subtype as compared to PTSD and healthy controls suggests that depersonalization/derealization and emotional numbing symptoms may further intensify vestibular dysfunction. This dysfunction may, in turn, hinder one's cognitive capability to integrate multisensory information and, ultimately, facilitate disengagement from one's environment. Hence, there is an urgent need to study the neural circuitry of the vestibular system in PTSD patients, an effort that may be critical not only to further delineating the neural underpinnings of PTSD symptomatology but to identifying psychotherapeutic interventions that target symptoms of interoceptive awareness and disembodiment related to vestibular dysfunction.

3.5 References

Akbarian, S., Grüsser, O. J., & Guldin, W. O. (1994). Corticofugal connections between the cerebral cortex and brainstem vestibular nuclei in the macaque monkey. *Journal of Comparative Neurology*, *339*(3), 421-437.

Arzy, S., Thut, G., Mohr, C., Michel, C. M., & Blanke, O. (2006). Neural basis of embodiment: distinct contributions of temporoparietal junction and extrastriate body area. *Journal of Neuroscience*, *26*(31), 8074-8081.

Aspell, J. E., Heydrich, L., Marillier, G., Lavanchy, T., Herbelin, B., & Blanke, O. (2013). Turning body and self inside out: visualized heartbeats alter bodily self consciousness and tactile perception. *Psychological science*, *24*(12), 2445-2453.

Baier, B., Eulenburg, P. Z., Best, C., Geber, C., Müller-Forell, W., Birklein, F., & Dieterich, M. (2013). Posterior insular cortex–a site of vestibular–somatosensory interaction?. *Brain and behavior*, *3*(5), 519-524.

Balaban, C. D. (1999). Vestibular autonomic regulation (including motion sickness and the mechanism of vomiting). *Current opinion in neurology*, *12*(1), 29-33.

Balaban, C. D., & Thayer, J. F. (2001). Neurological bases for balance–anxiety links. *Journal of anxiety disorders*, *15*(1-2), 53-79.

Beck, A. T., Guth, D., Steer, R. A., & Ball, R. (1997). Screening for major depression disorders in medical inpatients with the Beck Depression Inventory for Primary Care. *Behaviour research and therapy*, *35*(8), 785-791.

Behzadi, Y., Restom, K., Liau, J., & Liu, T. T. (2007). A component based noise correction method (CompCor) for BOLD and perfusion based fMRI. *Neuroimage*, *37*(1), 90-101.

Bernstein, D., Fink, L. (1998). Childhood trauma questionnaire: a retrospective self report: Manual. San Antonio, TX: The Psychological Corporation.

Berthoz, A., Weiss, G. (2000). The brain's sense of movement., Perspectives in cognitive neuroscience. Cambridge, MA: Harvard University Press.

Biaggioni, I., Costa, F., & Kaufmann, H. (1998). Vestibular influences on autonomic cardiovascular control in humans. *Journal of Vestibular Research*, *8*(1), 35-41.

Blake, D. D., Weathers, F. W., Nagy, L. M., Kaloupek, D. G., Gusman, F. D., Charney, D. S., & Keane, T. M. (1995). The development of a clinician-administered PTSD scale. *Journal of traumatic stress*, *8*(1), 75-90.

Blanke, O. (2012). Multisensory brain mechanisms of bodily self-consciousness. *Nature Reviews Neuroscience*, *13*(8), 556.

Blanke, O., & Arzy, S. (2005). The out-of-body experience: disturbed self-processing at the temporo-parietal junction. *The Neuroscientist*, *11*(1), 16-24.

Blanke, O., Ortigue, S., Landis, T., & Seeck, M. (2002). Neuropsychology: stimulating illusory own-body perceptions. *Nature*, *419*(6904), 269-270.

Bluhm, R. L., Williamson, P. C., Osuch, E. A., Frewen, P. A., Stevens, T. K., Boksman, K., ... & Lanius, R. A. (2009). Alterations in default network connectivity in posttraumatic stress disorder related to early-life trauma. *Journal of psychiatry & neuroscience: JPN*, *34*(3), 187-194.

Boisacq-Schepens, N., & Hanus, M. (1972). Motor cortex vestibular responses in the chloralosed cat. *Experimental brain research*, *14*(5), 539-549.

Bottini, G., Karnath, H. O., Vallar, G., Sterzi, R., Frith, C. D., Frackowiak, R. S., & Paulesu, E. (2001). Cerebral representations for egocentric space: functional anatomical evidence from caloric vestibular stimulation and neck vibration. *Brain*, *124*(6), 1182-1196.

Briere, J., Weathers, F. W., & Runtz, M. (2005). Is dissociation a multidimensional construct? Data from the Multiscale Dissociation Inventory. *Journal of Traumatic Stress*, *18*(3), 221-231.

Morey, R., & Brown, V. M. (2012). Neural systems for cognitive and emotional processing in posttraumatic stress disorder. *Frontiers in psychology*, *3*, 449.

Burgess, N., Maguire, E. A., Spiers, H. J., & O'Keefe, J. (2001). A temporoparietal and prefrontal network for retrieving the spatial context of lifelike events. *Neuroimage*, *14*(2), 439-453.

Cordes, D., Haughton, V. M., Arfanakis, K., Wendt, G. J., Turski, P. A., Moritz, C. H., ... & Meyerand, M. E. (2000). Mapping functionally related regions of brain with functional connectivity MR imaging. *American Journal of Neuroradiology*, *21*(9), 1636-1644.

Craig, A. D. (2002). How do you feel? Interoception: the sense of the physiological condition of the body. *Nature reviews neuroscience*, *3*(8), 655.

Craig, A. D. (2003). Interoception: the sense of the physiological condition of the body. *Current opinion in neurobiology*, *13*(4), 500-505.

Critchley, H. D., Wiens, S., Rotshtein, P., Öhman, A., & Dolan, R. J. (2004). Neural systems supporting interoceptive awareness. *Nature neuroscience*, *7*(2), 189-195.

Damoiseaux, J. S., Rombouts, S. A. R. B., Barkhof, F., Scheltens, P., Stam, C. J., Smith, S. M., & Beckmann, C. F. (2006). Consistent resting-state networks across healthy subjects. *Proceedings of the national academy of sciences*, *103*(37), 13848-13853.

Day, B. L., & Fitzpatrick, R. C. (2005). The vestibular system. *Current biology*, *15*(15), R583-R586.

De Ridder, D., Van Laere, K., Dupont, P., Menovsky, T., & Van de Heyning, P. (2007). Visualizing out-of-body experience in the brain. *New England Journal of Medicine*, *357*(18), 1829-1833.

De Waele, C., Baudonnière, P., Lepecq, J., Huy, P. T. B., & Vidal, P. (2001). Vestibular projections in the human cortex. *Experimental brain research*, *141*(4), 541-551.

Decety, J., & Lamm, C. (2007). The role of the right temporoparietal junction in social interaction: how low-level computational processes contribute to meta cognition. *The Neuroscientist*, *13*(6), 580-593.

Dieterich, M., Bense, S., Lutz, S., Drzezga, A., Stephan, T., Bartenstein, P., & Brandt, T. (2003). Dominance for vestibular cortical function in the non-dominant hemisphere. *Cerebral cortex*, *13*(9), 994-1007.

Engel-Yeger, B., Palgy-Levin, D., & Lev-Wiesel, R. (2013). The sensory profile of people with post-traumatic stress symptoms. *Occupational Therapy in Mental Health*, *29*(3), 266-278.

Fasold, O., von Brevern, M., Kuhberg, M., Ploner, C. J., Villringer, A., Lempert, T., & Wenzel, R. (2002). Human vestibular cortex as identified with caloric stimulation in functional magnetic resonance imaging. *Neuroimage*, *17*(3), 1384-1393.

First, M., Spitzer, R., Gibbon, M., Williams, J. (2002). Structured clinical interview for DSM-IV-TR axis I disorders, research version, non-patient edition. New York, NY: Biometrics Research, New York Psychiatric Institute.

Friston, K. J., Worsley, K. J., Frackowiak, R. S., Mazziotta, J. C., & Evans, A. C. (1994). Assessing the significance of focal activations using their spatial extent. *Human brain mapping*, *1*(3), 210-220.

Flynn, F. G. (1999). Anatomy of the insula functional and clinical correlates. *Aphasiology*, *13*(1), 55-78.

Fox, M. D., Snyder, A. Z., Vincent, J. L., Corbetta, M., Van Essen, D. C., & Raichle, M. E. (2005). The human brain is intrinsically organized into dynamic, anticorrelated functional networks. *Proceedings of the National Academy of Sciences*, *102*(27), 9673-9678.

Fransson, P. (2005). Spontaneous low-frequency BOLD signal fluctuations: An fMRI investigation of the resting-state default mode of brain function hypothesis. *Human brain mapping*, *26*(1), 15-29.

Frewen, P.A., Lanius, R.A. (2015). Healing the traumatized self. New York, NY: W.W. Norton & Company.

Frewen, P. A., & Lanius, R. A. (2006). Toward a psychobiology of posttraumatic self dysregulation: Reexperiencing, hyperarousal, dissociation, and emotional numbing. *Annals of the New York Academy of Sciences*, *1071*(1), 110-124.

Frewen, P. A., Lanius, R. A., Dozois, D. J., Neufeld, R. W., Pain, C., Hopper, J. W., ... & Stevens, T. K. (2008). Clinical and neural correlates of alexithymia in posttraumatic stress disorder. *Journal of Abnormal Psychology*, *117*(1), 171-181.

Friston, K. J., Holmes, A. P., Worsley, K. J., Poline, J. P., Frith, C. D., & Frackowiak, R. S. (1994). Statistical parametric maps in functional imaging: a general linear approach. *Human brain mapping*, *2*(4), 189-210.

Glover, G. H., Li, T. Q., & Ress, D. (2000). Image-based method for retrospective correction of physiological motion effects in fMRI: RETROICOR. *Magnetic Resonance in Medicine*, *44*(1), 162-167.

Göttlich, M., Jandl, N. M., Wojak, J. F., Sprenger, A., von der Gablentz, J., Münte, T. F., ... & Helmchen, C. (2014). Altered resting-state functional connectivity in patients with chronic bilateral vestibular failure. *NeuroImage: Clinical*, *4*, 488-499.

Gottlieb, R. M. (2003). Psychosomatic medicine: The divergent legacies of Freud and Janet. *Journal of the American Psychoanalytic Association*, *51*(3), 857-881.

Guldin, W. O., & Grüsser, O. J. (1998). Is there a vestibular cortex?. *Trends in neurosciences*, *21*(6), 254-259.

Gur, R. C., Mozley, L. H., Mozley, P. D., Resnick, S. M., Karp, J. S., Alavi, A., ... & Gur, R. E. (1995). Sex differences in regional cerebral glucose metabolism during a resting state. *Science*, *267*(5197), 528-531.

Harricharan, S., Rabellino, D., Frewen, P. A., Densmore, M., Théberge, J., McKinnon, M. C., ... & Lanius, R. A. (2016). fMRI functional connectivity of the periaqueductal gray in PTSD and its dissociative subtype. *Brain and behavior*, *6*(12), e00579.

Hayasaka, S., & Nichols, T. E. (2003). Validating cluster size inference: random field and permutation methods. *Neuroimage*, *20*(4), 2343-2356.

Herringa, R., Phillips, M., Almeida, J., Insana, S., & Germain, A. (2012). Post-traumatic stress symptoms correlate with smaller subgenual cingulate, caudate, and insula volumes in unmedicated combat veterans. *Psychiatry Research: Neuroimaging*, *203*(2-3), 139-145.

Heydrich, L., & Blanke, O. (2013). Distinct illusory own-body perceptions caused by damage to posterior insula and extrastriate cortex. *Brain*, *136*(3), 790-803.

Hitier, M., Besnard, S., & Smith, P. F. (2014). Vestibular pathways involved i cognition. *Frontiers in integrative neuroscience*, *8*, 59.

Holmes, E. A., Brown, R. J., Mansell, W., Fearon, R. P., Hunter, E. C., Frasquilho, F., & Oakley, D. A. (2005). Are there two qualitatively distinct forms of dissociation? A review and some clinical implications. *Clinical psychology review*, *25*(1), 1-23.

Hopper, J. W., Frewen, P. A., Sack, M., Lanius, R. A., & Van der Kolk, B. A. (2007). The Responses to Script-Driven Imagery Scale (RSDI): assessment of state posttraumatic symptoms for psychobiological and treatment research. *Journal of Psychopathology and Behavioral Assessment*, *29*(4), 249-268.

Igelström, K. M., Webb, T. W., & Graziano, M. S. (2015). Neural processes in the human temporoparietal cortex separated by localized independent component analysis. *Journal of Neuroscience*, *35*(25), 9432-9445.

Ionta, S., Heydrich, L., Lenggenhager, B., Mouthon, M., Fornari, E., Chapuis, D., ... & Blanke, O. (2011). Multisensory mechanisms in temporo-parietal cortex support self-location and first-person perspective. *Neuron*, *70*(2), 363-374.

Janet, P. (1907). The major symptoms of hysteria. *Boston Medical Surgery Journal 155*, 595-598.

Janet, P. (1889). L'automatisme psychologique: essai de psychologie expérimentale sur les formes inférieures de l'activité humaine (Vol. 2). impr. Ch. Hérissey.

Kahane, P., Hoffmann, D., Minotti, L., & Berthoz, A. (2003). Reappraisal of the human vestibular cortex by cortical electrical stimulation study. *Annals of Neurology: Official Journal of the American Neurological Association and the Child Neurology Society*, *54*(5), 615-624.

Kendall-Tackett, K. A. (2000). Physiological correlates of childhood abuse: chronic hyperarousal in PTSD, depression, and irritable bowel syndrome. *Child abuse & neglect*, *24*(6), 799-810.

Kennis, M., Van Rooij, S. J. H., Van Den Heuvel, M. P., Kahn, R. S., & Geuze, E. (2016). Functional network topology associated with posttraumatic stress disorder in veterans. *NeuroImage: Clinical*, *10*, 302-309.

Khan, S., & Chang, R. (2013). Anatomy of the vestibular system: a review. *NeuroRehabilitation*, *32*(3), 437-443.

Kimble, M., Boxwala, M., Bean, W., Maletsky, K., Halper, J., Spollen, K., & Fleming, K. (2014). The impact of hypervigilance: Evidence for a forward feedback loop. *Journal of anxiety disorders*, *28*(2), 241-245.

Kirsch, V., Keeser, D., Hergenroeder, T., Erat, O., Ertl-Wagner, B., Brandt, T., & Dieterich, M. (2016). Structural and functional connectivity mapping of the vestibular circuitry from human brainstem to cortex. *Brain Structure and Function*, *221*(3), 1291-1308.

Kolev, O. I., Georgieva-Zhostova, S. O., & Berthoz, A. (2014). Anxiety changes depersonalization and derealization symptoms in vestibular patients. *Behavioural neurology*.

Kruskal, W. H., & Wallis, W. A. (1952). Use of ranks in one-criterion variance analysis. *Journal of the American statistical Association*, *47*(260), 583-621.

Lacadie, C. M., Fulbright, R. K., Rajeevan, N., Constable, R. T., & Papademetris, X. (2008). More accurate Talairach coordinates for neuroimaging using non-linear registration. *Neuroimage*, *42*(2), 717-725.

Lanius, R. A., Vermetten, E., Loewenstein, R. J., Brand, B., Schmahl, C., Bremner, J. D., & Spiegel, D. (2010). Emotion modulation in PTSD: Clinical and neurobiological evidence for a dissociative subtype. *American Journal of Psychiatry*, *167*(6), 640 647.

Lanius, R. A., Williamson, P. C., Bluhm, R. L., Densmore, M., Boksman, K., Neufeld, R. W., ... & Menon, R. S. (2005). Functional connectivity of dissociative responses in posttraumatic stress disorder: a functional magnetic resonance imaging investigation. *Biological psychiatry*, *57*(8), 873-884.

Lanius, R. A., Williamson, P. C., Boksman, K., Densmore, M., Gupta, M., Neufeld, R. W., ... & Menon, R. S. (2002). Brain activation during script-driven imagery induced dissociative responses in PTSD: a functional magnetic resonance imaging investigation. *Biological psychiatry*, *52*(4), 305-311.

Lenggenhager, Bigna; Lopez, Christophe (2015). Vestibular Contributions to the Sense of Body, Self, and Others. In: Metzinger, Thomas; Windt, Jennifer M. Open MIND. Frankfurt am Main: MIND Group, pp.1-38.

Lipov, E., & Kelzenberg, B. (2012). Sympathetic system modulation to treat post traumatic stress disorder (PTSD): a review of clinical evidence and neurobiology. *Journal of affective disorders*, *142*(1-3), 1-5.

Lopez, C. (2016). The vestibular system: balancing more than just the body. *Current opinion in neurology*, *29*(1), 74-83.

Lopez, C. (2013). A neuroscientific account of how vestibular disorders impair bodily self-consciousness. *Frontiers in integrative neuroscience*, *7*, 91.

Lopez, C., & Blanke, O. (2011). The thalamocortical vestibular system in animals and humans. *Brain research reviews*, *67*(1-2), 119-146.

Lopez, C., Halje, P., & Blanke, O. (2008). Body ownership and embodiment: vestibular and multisensory mechanisms. *Neurophysiologie Clinique/Clinical Neurophysiology*, *38*(3), 149-161.

Lui, S., Wu, Q., Qiu, L., Yang, X., Kuang, W., Chan, R. C., ... & Gong, Q. (2011). Resting-state functional connectivity in treatment-resistant depression. *American Journal of Psychiatry*, *168*(6), 642-648.

Maldjian, J. A., Laurienti, P. J., Kraft, R. A., & Burdette, J. H. (2003). An automated method for neuroanatomic and cytoarchitectonic atlas-based interrogation of fMRI data sets. *Neuroimage*, *19*(3), 1233-1239.

Mazzola, L., Lopez, C., Faillenot, I., Chouchou, F., Mauguière, F., & Isnard, J. (2014). Vestibular responses to direct stimulation of the human insular cortex. *Annals of neurology*, *76*(4), 609-619.

McFarlane, A. C., Weber, D. L., & Clark, C. R. (1993). Abnormal stimulus processing in posttraumatic stress disorder. *Biological Psychiatry*, *34*(5), 311-320.

Miller, W. L., Maffei, V., Bosco, G., Iosa, M., Zago, M., Macaluso, E., & Lacquaniti, F. (2008). Vestibular nuclei and cerebellum put visual gravitational motion in context. *Journal of neurophysiology*, *99*(4), 1969-1982.

Montemurro, D., Bruni, J. (1988). The human brain in dissection. New York, NY:Oxford University Press.

Nicholson, A. A., Densmore, M., Frewen, P. A., Théberge, J., Neufeld, R. W., McKinnon, M. C., & Lanius, R. A. (2015). The dissociative subtype of posttraumatic stress disorder: unique resting-state functional connectivity of basolateral and centromedial amygdala complexes. *Neuropsychopharmacology*, *40*(10), 2317-2326.

Nicholson, A. A., Sapru, I., Densmore, M., Frewen, P. A., Neufeld, R. W., Théberge, J., ... & Lanius, R. A. (2016). Unique insula subregion resting-state functional connectivity with amygdala complexes in posttraumatic stress disorder and its dissociative subtype. *Psychiatry Research: Neuroimaging*, *250*, 61-72.

Pain, C., Bluhm, R.L., Lanius, R.A. (2010). Dissociation and the dissociative disorders: DSM-V and beyond. New York, NY: Routledge.

Pfeiffer, C., Serino, A., & Blanke, O. (2014). The vestibular system: a spatial reference for bodily self-consciousness. *Frontiers in integrative neuroscience*, *8*, 31.

Porges, S.W. (2011). The polyvagal theory: neurophysiologcal foundations of emotions, attachment, communication and self-regulation. New York, NY: WW Norton & Company,.

Révész, D., Verhoeven, J. E., Milaneschi, Y., de Geus, E. J., Wolkowitz, O. M., & Penninx, B. W. (2014). Dysregulated physiological stress systems and accelerated cellular aging. *Neurobiology of aging*, *35*(6), 1422-1430.

Sbarra, D. A., & Hazan, C. (2008). Coregulation, dysregulation, self-regulation: An integrative analysis and empirical agenda for understanding adult attachment, separation, loss, and recovery. *Personality and Social Psychology Review*, *12*(2), 141-167.

Serino, A., Alsmith, A., Costantini, M., Mandrigin, A., Tajadura-Jimenez, A., & Lopez, C. (2013). Bodily ownership and self-location: components of bodily self consciousness. *Consciousness and cognition*, *22*(4), 1239-1252.

Simeon, D., Guralnik, O., Hazlett, E. A., Spiegel-Cohen, J., Hollander, E., & Buchsbaum, M. S. (2000). Feeling unreal: a PET study of depersonalization disorder. *American Journal of Psychiatry*, *157*(11), 1782-1788.

Simmons, A., Strigo, I. A., Matthews, S. C., Paulus, M. P., & Stein, M. B. (2009). Initial evidence of a failure to activate right anterior insula during affective set-shifting in PTSD. *Psychosomatic medicine*, *71*(4), 373.

Smith, P., & Darlington, C. (2013). Personality changes in patients with vestibular dysfunction. *Frontiers in human neuroscience*, *7*, 678.

Spielberger, C.D. (2010). State-Trait Anxiety Inventory, in: *The Corsini Encyclopedia of Psychology*. Hoboken, NJ: John Wiley & Sons, Inc.

Steuwe, C., Daniels, J. K., Frewen, P. A., Densmore, M., Pannasch, S., Beblo, T., ... & Lanius, R. A. (2012). Effect of direct eye contact in PTSD related to interpersonal trauma: an fMRI study of activation of an innate alarm system. *Social Cognitive and Affective Neuroscience*, *9*(1), 88-97.

Suzuki, K., Garfinkel, S. N., Critchley, H. D., & Seth, A. K. (2013). Multisensory integration across exteroceptive and interoceptive domains modulates self experience in the rubber-hand illusion. *Neuropsychologia*, *51*(13), 2909-2917.

Tian, L., Wang, J., Yan, C., & He, Y. (2011). Hemisphere-and gender-related differences in small-world brain networks: a resting-state functional MRI study. *Neuroimage*, *54*(1), 191-202.

Tsakiris, M., Costantini, M., Haggard, P., 2008. The role of the right temporo-parietal junction in maintaining a coherent sense of one's body. Neuropsychologia 46, 3014–3018. doi:10.1016/j.neuropsychologia.2008.06.004

Tsakiris, M., Hesse, M. D., Boy, C., Haggard, P., & Fink, G. R. (2006). Neural signatures of body ownership: a sensory network for bodily self-consciousness. *Cerebral cortex*, *17*(10), 2235-2244.

Tsakiris, M., Jiménez, A. T., & Costantini, M. (2011). Just a heartbeat away from one's body: interoceptive sensitivity predicts malleability of body representations. *Proceedings of the Royal Society: Biological Sciences*, *278*(1717), 2470-2476.

Tsigos, C., & Chrousos, G. P. (1994). Physiology of the hypothalamic-pituitary-adrenal axis in health and dysregulation in psychiatric and autoimmune disorders. *Endocrinology and metabolism clinics of North America*, *23*(3), 451 466.

Tzourio-Mazoyer, N., Landeau, B., Papathanassiou, D., Crivello, F., Etard, O., Delcroix, N., ... & Joliot, M. (2002). Automated anatomical labeling of activations in SPM using a macroscopic anatomical parcellation of the MNI MRI single-subject brain. *Neuroimage*, *15*(1), 273-289.

Van den Heuvel, M. P., Stam, C. J., Boersma, M., & Pol, H. H. (2008). Small-world and scale-free organization of voxel-based resting-state functional connectivity in the human brain. *Neuroimage*, *43*(3), 528-539.

Van Der Kolk, B.A. (2006). Clinical implications of neuroscience research in PTSD. *Annals of the New York Academy of Sciences*. 1071, 277–293.

Vieweg, W. V. R., Julius, D. A., Fernandez, A., Beatty-Brooks, M., Hettema, J. M., & Pandurangi, A. K. (2006). Posttraumatic stress disorder: clinical features, pathophysiology, and treatment. *The American journal of medicine*, *119*(5), 383 390.

Voon, V., Gallea, C., Hattori, N., Bruno, M., Ekanayake, V., & Hallett, M. (2010). The involuntary nature of conversion disorder. *Neurology*, *74*(3), 223-228.

Wager, T.D., Barrett, L.F. (2004). From affect to control: functional specialization of the insula in motivation and regulation. *Emotion, 129*, 2865.

Weathers, F. W., Bovin, M. J., Lee, D. J., Sloan, D. M., Schnurr, P. P., Kaloupek, D. G., ... & Marx, B. P. (2013). The Clinician-Administered PTSD Scale for DSM–5 (CAPS-5): Development and initial psychometric evaluation in military veterans. *Psychological Assessment*, *30*(3), 383.

Weissman-Fogel, I., Moayedi, M., Taylor, K. S., Pope, G., & Davis, K. D. (2010). Cognitive and default-mode resting state networks: Do male and female brains "rest" differently?. *Human brain mapping*, *31*(11), 1713-1726.

Yehuda, R. (2002). Post-traumatic stress disorder. *New England journal of medicine, 346*(2), 108-114.

Yehuda, R., & LeDoux, J. (2007). Response variation following trauma: a translational neuroscience approach to understanding PTSD. *Neuron, 56*(1), 19-32.

Yehuda, R., McFarlane, A.C. (1995). Conflict between current knowledge about posttraumatic stress disorder and its original conceptual basis. *The American Journal of Psychiatry 152,* 1705–1713.

Yen-Pik Sang, F. Y. P., Jauregui-Renaud, K., Green, D. A., Bronstein, A. M., & Gresty, M. A. (2006). Depersonalisation/derealisation symptoms in vestibular disease. *Journal of Neurology, Neurosurgery & Psychiatry*, *77*(6), 760-766.

Zu Eulenburg, P., Baumgärtner, U., Treede, R. D., & Dieterich, M. (2013). Interoceptive and multimodal functions of the operculo-insular cortex: tactile, nociceptive and vestibular representations. *Neuroimage*, *83*, 75-86.

Zuo, X. N., Di Martino, A., Kelly, C., Shehzad, Z. E., Gee, D. G., Klein, D. F., ... & Milham, M. P. (2010). The oscillating brain: complex and reliable. *Neuroimage*, *49*(2), 1432-1445.

Chapter 4

4 « PTSD and its dissociative subtype through the lens of the insula: Anterior and posterior insula resting-state functional connectivity and its predictive validity using machine learning»

The vestibular system is consistently activated, even during rest, to maintain one's awareness of his/her position in gravitational space. It relays exteroceptive and interoceptive sensory information from the brainstem to the parieto-insular vestibular cortex, a region spanning the temporoparietal junction and the posterior insula, to maintain both physical equilibrium and physiological homeostasis. While the decreased vestibular nuclei connectivity with the posterior insula observed in individuals with PTSD as compared to healthy individuals (Chapter 3) suggests weakened interoceptive awareness among traumatized individuals, these findings also offer critical insight into how exteroceptive sensory processing may be negatively impacted in the PTSD dissociative subtype. In addition, in Chapter 3, individuals with the dissociative subtype demonstrated limited brainstem vestibular nuclei connectivity with the temporoparietal junction, an area linked previously to depersonalization and identified as crucial for understanding one's own self-location in space. Moreover, individuals with the dissociative subtype showed limited vestibular nuclei connectivity with the dorsolateral prefrontal cortex, a brain region critical to multisensory integration of vestibular signals. These neural aberrations may have further cascading effects on key higher-order cognitive functions, including emotion regulation. Here, the insula is thought to be critical to emotion processing, where it is believed to assist in identifying emotional feeling states that underlie viscerosensory input to the cortex. It is therefore critical to

investigate patterns of insula subregion neural connectivity in an effort to delineate the neural signatures that may contribute to emotion dysregulation observed in PTSD.

Chapter 4 has been published in its entirety as:

Harricharan, S., Nicholson, A.A., Thome, J., Densmore, M., McKinnon, M.C.M.,Theberge, J., Frewen, P.A., Neufeld, R.W.J., & Lanius, R. A. (2019). PTSD and its dissociative subtype through the lens of the insula: Anterior and posterior insula resting-state functional connectivity and its predictive using machine learning. *Psychophysiology, in press.* https://doi.org/10.1111/psyp.13472

4.1 « Introduction »

Posttraumatic stress disorder (PTSD) is characterized by emotion dysregulation, including prominently states of reliving and of hypervigilance, which are thought to be mediated, in part, by decreased prefrontal inhibition on limbic (e.g., amygdala) and brainstem (e.g., periaqueductal grey) regions (Fenster, Lebois, Ressler, & Suh, 2018; Lanius et al., 2010; Shalev, Liberzon, & Marmar, 2017; Yehuda et al., 2015; Corrigan, Fisher, & Nutt, 2011; Lanius et al., 2010; Litz, 1992; Nicholson et al., 2017). By contrast, the dissociative subtype of PTSD (PTSD+DS) is associated with symptoms of depersonalization and derealization and concomitant emotional detachment (Daniels, Frewen, Theberge, & Lanius, 2016; Lanius et al., 2010; Melara, Ruglass, Fertuck, & Hien, 2018; Sierra & Berrios, 1998), which is thought to be mediated by increased top-down prefrontal inhibition on limbic and brainstem regions (Nicholson et al., 2017). Notably, brain connectivity patterns consistent with emotion dysregulation in PTSD and its dissociative subtype are present even at rest (Harricharan et al., 2016; Nicholson et al., 2016; Nicholson et al., 2017; Thome et al., 2016). Indeed, the prefrontal cortex, as well as subcortical limbic and brainstem regions have been described as central to the neural underpinnings of emotion dysregulation in PTSD; however, more recent work has sought

to expand this neurobiological framework through identification of other structures critical to emotion processing, including the insula (Etkin & Wager, 2007; Nicholson et al., 2016; Stark et al., 2015; Stein, Simmons, Feinstein, & Paulus, 2007).

The insula is thought to be central to the processing of emotional feeling states (Chang, Yarkoni, Khaw, & Sanfey, 2013; Couto et al., 2013; Craig, 2002), where this region is well situated as an intermediary structure between subcortical brain regions that receive visceral sensations from within the body and frontal lobe regions that help determine the affective and motivational significance underlying these sensations. Notably, the insula is parcellated into posterior, mid and anterior subregions, each unique in function and working in tandem to identify emotional feeling states (Chang et al., 2013; Couto et al., 2013; Craig, 2002; Craig, 2009). Specifically, the posterior insula aids in recognizing internal changes within the body and is thought to receive affective input from thalamic, limbic and brainstem structures (Craig, 2009). By contrast, the mid-insula is an intermediary structure that interacts with both anterior and posterior portions of the insula to aid in translating visceral sensory input to structures involved in emotion processing (Craig, 2009). Finally, the anterior insula is thought to assist in identifying emotional states underlying visceral sensations, and interacts with higher-order frontal brain regions to develop a subjective evaluation of one's own social and emotional interactions with the environment (Craig, 2009).

In addition to these functional subregions, the dorsal and ventral aspects of the insula are thought to play distinct roles in evaluating subjective information (Cloutman, Binney, Drakesmith, Parker, & Lambon Ralph, 2012; Craig, 2002; Kurth, Zilles, Fox, Laird, & Eickhoff, 2010; Liotti et al., 2000; Simmons et al., 2013). Whereas the ventral

insula appears to assist with the emotion processing of incoming sensory information, the dorsal insula shapes the direction of goal-oriented action in response to salient information requiring higher-order sensorimotor processing (Simmons et al., 2009).

Notably, the insula's involvement in emotion and social processing relies not only on activation of this region but also on its wider connectivity to functional neural networks (Couto et al., 2013). Here, the insula is thought to modulate two resting-state networks: (1) an anterior insula-based network that works in tandem with the anterior cingulate cortex to influence brain regions in both the default-mode network, involved in introspection, and in the central executive network, involved centrally in emotional appraisal (Akiki et al., 2018; Bressler & Menon, 2010; Cauda et al., 2011; Chen et al., 2013; Fox et al., 2005; Simmons et al., 2013); and (2) a posterior insula-based network that maintains connections with sensorimotor areas involved in environmental monitoring (e.g., pre- and post-central gyri, and the mid-cingulate) (Deen, Pitskel, & Pelphrey, 2011; Simmons et al., 2013; Taylor, Seminowicz, & Davis, 2009). Moreover, the insula, the ventral frontoparietal areas (e.g., the inferior frontal gyrus and the temporoparietal junction), and the subcortical structures form a right-lateralized ventral attention network that is thought to mediate bottom-up attentional processes and salience processing (Corbetta, Patel, & Shulman, 2008; Frank & Sabatinelli, 2012). Notably, this network shows hyper-connectivity during rest in healthy individuals under stress (Soares et al., 2013).

Numerous studies describe hyperactivation of the insula among individuals with PTSD exposed to negative or trauma-related stimuli (Bremner et al., 2003; Etkin & Wager, 2007; Germain et al., 2013; Hopper, Frewen, Van Der Kolk, & Lanius, 2007;

Shin et al., 2001) and during the anticipation of negative events (Aupperle et al., 2012; Simmons et al., 2008). Paulus & Stein (2006) postulate that this observed pattern of insular hyperactivity may relate, in part, to overactive threat detection mediated by limbic structures, resulting together in the hypervigilance and avoidance symptoms observed among individuals with PTSD. Interestingly, Hopper et al. (2007) reported that hyperactivation of the right anterior insula correlated *positively* with state re-experiencing scores and *negatively* with state dissociation scores, suggesting that dissociative symptoms may alter the insula's capacity to engage in processing emotional feeling states. Moreover, a pilot study examining functional connectivity between subregions of the insula and the amygdala during resting-state in PTSD and its dissociative subtype found increased insula connectivity with the basolateral amygdala when patients with PTSD+DS were compared to PTSD and healthy individuals (Nicholson et al., 2016). However, the study was performed on a smaller sample size and was powered to examine functional connectivity between insular subregions and the amygdala only. Taken together, the insula shows not only altered activation and connectivity as a function of dissociation, but also serves as a central hub that mediates other larger-scale neurocognitive networks (Chang et al., 2013; Diekhof, Geier, Falkai, & Gruber, 2011; Kober et al., 2008; Kohn et al., 2014; Menon & Uddin, 2010; Seeley et al., 2007). As such, it appears critical to examine whole brain resting-state insula subregion connectivity in an effort to elucidate further the neural networks underlying PTSD and its dissociative subtype.

Accordingly, we examined insula subregion resting-state functional connectivity patterns in PTSD, its dissociative subtype (PTSD+DS), and healthy controls, using a

seed-based approach that allowed for the examination of whole brain neural connectivity. Subsequently, these data were inputted into machine learning algorithms to assess the predictive validity of insula subregion resting-state functional connectivity patterns in discriminating between individuals with PTSD, PTSD+DS, and healthy controls. We hypothesized that individuals with PTSD, characterized predominantly by sustained hypervigilance and hyperarousal symptoms, would show increased insula subregion resting-state functional connectivity with subcortical and limbic structures. By contrast, we hypothesized that individuals with the dissociative subtype, characterized predominantly by emotional detachment, including depersonalization and derealization, would exhibit limited insula subregion functional connectivity with subcortical structures involved in hyper-emotionality. Finally, we predicted that univariate group differences would translate into high predictive accuracy when classifying individual subjects via multivariate machine learning algorithms based on insula subregion functional connectivity.

4.2 Methods

4.2.1 Clinical and Demographic Information

One-hundred and eighty-four participants, including 84 PTSD patients (PTSD), 49 PTSD patients with the dissociative subtype (PTSD+DS), and 51 healthy controls were included in the study. Participants were recruited to the study from 2009-2018 through referrals from family physicians, mental health professionals, psychology/psychiatric clinics, community programs for traumatic stress, and posters/advertisements within the London, Ontario community.

A primary PTSD diagnosis was determined using the Clinician-Administered PTSD Scale [CAPS; versions IV (for 156 participants) and 5 (for 28 participants); CAPS IV: cut-off score > 50 (Blake et al., 1995); CAPS-5: no cut-off score is used for the DSM-5 version (Weathers et al., 2013)]. Individuals meeting the criteria for the dissociative subtype scored at least two in frequency and intensity on the CAPS-IV scale, or at least two in symptom severity on the CAPS-5 scale for depersonalization and/or derealization symptoms [as per previous studies (Harricharan et al., 2017; Rabellino et al., 2018; Terpou et al., 2018)]. For all participants, the SCID was administered (Structured Clinical Interview for DSM-IV Axis-I disorders; First, Spitzer, Gibbon, & Williams, 2002), along with a battery of questionnaires: Beck Depression Inventory (BDI; Beck, Guth, Steer, & Ball, 1997), Child Trauma Questionnaire (CTQ; 87% of all PTSD patients had histories of childhood trauma, confirmed if patient scored above the 'none/minimal' threshold for any trauma category according to the CTQ scoring manual; Bernstein & Fink, 1998), as well as the Multiscale Dissociation Inventory (MDI; Briere, Weathers, & Runtz, 2005).

Clinical and demographic information are detailed in Table 1. Participant groups were age- and sex- matched. Age differences were assessed via a one-way ANOVA and a Pearson's chi-square was performed to calculate sex differences across all three participant groups. A Kruskal-Wallis analysis was performed followed by post-hoc Games-Howell comparisons to assess nonparametric psychological measures (CAPS, BDI, CTQ, and averaged depersonalization and derealization MDI scores) and significance across groups (Kruskal & Wallis, 1952).

Participants were excluded if they could not adhere to the safety regulations required for the 3.0 T scanner, including metal implants, previous head trauma associated with a period of unconsciousness, current or past history of neurological disorders, significant untreated medical illness, and/or pervasive developmental mental disorders. Additional exclusion criteria for PTSD patients included current or past history of bipolar or psychotic disorders, or if patients had alcohol/substance dependency or abuse for at least six months prior to participation in the study, as determined by the SCID. Control participants were screened for prior trauma exposure and were excluded if lifetime criteria were met for any DSM-IV Axis-I psychiatric disorder. If eligible, subjects provided written informed consent to participate in the study[1]. All scanning was conducted in London, Ontario, Canada at either Robarts Research Institute's Center for Functional and Metabolic Mapping or Lawson Health Research Institute. The study was approved by the Research Ethics Board at Western University of Canada.

Table 4.1 *Clinical and Demographic Information*

[1] No eligible participants were subsequently excluded from the study nor did any of the participants drop out over the course of the study.

Measure	PTSD	PTSD+DS	Controls
N	84	49	51
Age	39.3 ± 11.9	4.0 ± 13.6	35.0 ± 11.0
Sex	M = 38, F = 46	M = 11, F = 38	M = 17, F = 34
CAPS-IV Total (*n* =156)	67.9 ± 13.4 (*n* = 75)	81.6 ± 12.7 (*n* = 30)	0.6 ± 2.7 (*n* = 51)
CAPS-5 Total (*n* =28)	36.3 ± 9.6 (*n* = 9)	42.8 ± 6.3 (*n* = 19)	n/a
CTQ – Total	56.1 ± 23.0	69.0 ± 18.9	32.3 ± 9.1
BDI	23.2 ± 8.3	34.9 ± 11.7	1.0 ± 2.0
MDI – Total	53.7 ± 14.8	79.7 ± 21.0	34.0 ± 4.0
MDI – Depersonalization	6.7 ± 2.6	12.6 ± 5.3	5.2 ± 0.6
MDI – Derealization	8.5 ± 3.2	13.0 ± 4.0	5.2 ± 0.6
MDD	*n* = 12(24)	*n* = 23(9)	-
Panic Disorder/Agoraphobia	*n* = 10(6)	*n* = 9(6)	-
Social Phobia	*n* = 2(2)	*n* = 6(0)	-
OCD	*n* = 3(2)	*n* = 0(2)	-
GAD	*n* = 1(0)	*n* = 0(0)	-
STAI	5.7 ± 2.2	6.2 ± 2.5	3.3 ± 0.6
CADSS	3.7 ± 1.2	4.7 ± 2.9	3.1 ± 0.5
RSDI-Dissociation	3.6 ± 1.4	4.9 ± 2.0	2.7 ± 0.6
RSDI-Emotional Distress	3.1 ± 1.4	3.5 ± 1.6	2.3 ± 0.6

RSDI-Reliving Experiences	2.9 ± 1.2	3.3 ± 1.5	2.1 ± 0.3
RSDI-Visceral Sensations	3.5 ± 1.2	3.8 ± 1.7	2.5 ± 0.9

Age, sex, CAPS, self-report questionnaires (CTQ, MDI, BDI), and state clinical measures taken during the scan (STAI, CADSS, RSDI) are reported as mean ± SD. Psychiatric disorders assessed via SCID-I (MDD, Panic Disorder/Agoraphobia, Social Phobia, OCD and GAD) are reported in frequencies, as *n* = current (past) cases.

Abbreviations: PTSD, posttraumatic stress disorder; PTSD + DS, posttraumatic stress disorder with the dissociative subtype; M, Males; F, Females; CAPS, Clinician-Administered PTSD Scale (CAPS-IV = version 4; CAPS-5 = version 5); CTQ, Child Trauma Questionnaire; BDI, Beck Depression Inventory; MDI, Multiscale Dissociation Inventory; MDD, Major Depression Disorder; OCD, Obsessive Compulsive Disorder; GAD, Generalized Anxiety Disorder; STAI, State Trait Anxiety Inventory; CADSS, The Clinician-Administered Dissociative States Scale; RSDI, Responses to Script-Driven Imagery Scale.

4.2.2 Data Acquisition

Whole-brain fMRI (functional magnetic resonance) data were collected in a 3.0 T scanner (Magnetom Tim Trio, Siemens Medical Solutions, Erlangen, Germany) with a 32-channel phased array head coil. BOLD (blood oxygen level dependent) fMRI data were collected using a manufacturer's standard gradient-echo planar imaging (EPI) pulse sequence (single-shot, blipped-EPI) with an interleaved slice acquisition order per the following specifications: Time Resolution (TR) = 3000 ms, Echo Time (TE) = 20 ms, voxel size = 2 × 2 × 2 mm^3, Field of View (FOV) = 192 × 192 × 128 mm^3 (94 × 94 matrix, 64 contiguous slices), and Flip Angle (FA) = 90°. High-resolution T1-weighted anatomical images were also collected (MPRAGE: 192 slices, voxel size = 1 × 1 × 1

mm^3). For the resting-state procedure, participants were instructed to close their eyes and let their minds wander while trying not to focus on anything in particular for 6 minutes, as per standard methods (Bluhm et al., 2009; Fransson, 2005; Harricharan et al., 2016). Immediately following, the on-site research coordinator confirmed with all participants that they remained awake during the resting-state scan. In addition, The Responses to Script-Driven Imagery Scale (RSDI; Hopper et al., 2007), State-Trait Anxiety Inventory (STAI; Spielberger, 2010), and the Clinician-Administered Dissociative States Scale (CADSS; Bremner et al., 1998) questionnaires were administered after the scan to assess the participants' self-reported state clinical symptoms experienced during the scan. Consistent with psychological measures collected prior to the scan, Kruskal-Wallis analyses with post-hoc Games-Howell comparisons were also performed on participants' responses to post-scan questionnaires.

4.2.3 Resting-State fMRI Data Preprocessing

Image preprocessing and statistical analyses were performed using statistical parametric mapping software (SPM12, Wellcome Trust Center for Neuroimaging, London, UK: https:// www.fil.ion.ucl.ac.uk/spm; RRID:SCR_007037) within MATLAB 8.6 (R2015b, Mathworks Inc., MA; RRID:SCR_001622). Preprocessing was performed according to the default instructions provided in the updated SPM12 manual. The functional images for each subject were realigned to the first functional image and resliced. The resulting mean functional image was co-registered to the T1-weighted anatomical image template to spatially realign BOLD data with the subject's anatomical space. The co-registered images were segmented using the "New Segment" method implemented in SPM12, which uses T2-weighted and PD-weighted scans when generating tissue probability

maps. The functional images were normalized to an MNI (Montréal Neurological Institute) template using the forward deformation field and were subsequently smoothed with a three-dimensional isotropic Gaussian kernel of 6 mm FWHM (full-width at half-maximum) (Wang et al., 2018). Motion regressors were created with Artifact Removal Tool (ART) software (version 2015-10; Gabrieli Lab, McGovern Institute).

4.2.4 fMRI Statistical Analyses

4.2.4.1 Within-Subject Analysis

A within-subject multiple regression model was used to derive insula functional connectivity patterns for each subject. For each subject, this model included the mean signal intensity time course for the resting-state scan, with ART motion outliers used as regressors-of-no-interest. The seed regions-of-interest were defined via the Brainnetome atlas (Fan et al., 2016), which parcellates the insula into 12 regions based on its subregions (anterior, mid, posterior), axes (dorsal, ventral) and hemispheres (left, right). Seed time courses were generated using REST software (RRID:SCR_009641; Song et al., 2011). A mean signal intensity time course was generated for each seed region-of-interest, which was subsequently used in a voxel-wise approach to calculate positive correlations between each insula parcellation with other voxels of the whole-brain.

4.2.4.2 Between-Subject Analysis

We conducted a 3 x 12 full-factorial analysis of variance (ANOVA) that principally focused on the interaction between participant groups (PTSD+DS, PTSD and healthy controls) and the 12 parcellations of the insula. Post-hoc two-sample *t*-tests were used to evaluate differences in functional connectivity patterns between participant groups with regard to parcellations of the insula. To determine significant peak coordinates, a *whole-*

brain family-wise error (FWE) corrected threshold using *voxel-wise inference* (*pFWE* < .05, *k* = 10) was set for the ANOVA interactions, main effects, and all post-hoc analyses. Similarly, all seed-based analysis correlations performed with self-reported psychological measures collected at the time of scanning (RSDI, STAI, CADSS - used to assess symptoms at time of scanning) and prior to scanning (CAPS, CTQ, MDI, BDI) were evaluated at the same voxel-wise *pFWE* < .05, *k* = 10 threshold. Separately, we conducted a 3 x 2 x 2 x 3 full factorial ANOVA, which grouped parcellations of the insula together based on additional factors, including (1) hemisphere (left and right); (2) axis (dorsal and ventral); and (3) subregions (anterior, mid, posterior). This analysis was performed to examine more closely how each factor interacts with the others and with the factor of group. For brevity, this analysis is included in Appendix C. Seed-based analysis correlations with self-reported psychological measures used to assess state symptoms at the time of scanning (RSDI, STAI, CADSS) and trait symptoms prior to scanning (CAPS, CTQ, MDI, BDI were performed in both the PTSD and PTSD+DS groups (significant peak coordinates were evaluated at the same voxel-wise *pFWE* < .05, *k* = 10 threshold). Although the Brainnetome atlas was used to parcellate the insula into its subregions (not captured in the AAL atlas and MNI2Tal atlas), brain regions from the results of the seed-based analysis were identified using the AAL atlas (Tzourio-Mazoyer et al., 2002) via xjview software (https://www.nitrc.org/projects/xjview), the MNI2Tal atlas (https://bioimagesuite.yale.edu/mni2tal; Lacadie, Fulbright, Constable, & Papademetris, 2008), and visual inspection using an additional anatomical atlas (Montemurro & Bruni, 1988). This approach is consistent with our previous studies (Harricharan et al., 2016; Rabellino et al. 2018; Terpou et al., 2018).

4.2.5 Multiclass Gaussian Process Classification Machine Learning

A Multiclass Gaussian Process Classification (MGPC) machine learning analysis was carried out using the Pattern Recognition for Neuroimaging Toolbox (PRoNTo; Schrouff et al., 2013; 2018) within SPM12. Here, MGPC is able to predict group classification across multiple classes using fMRI feature sets (Rasmussen et al., 2006; Schrouff et al., 2013; 2018). We employed MGPC using a resting-state design with no conditions, in order to calculate a supervised pattern of classification that discriminates multiple clinical samples (PTSD+DS, PTSD and healthy controls) based on insula resting-state functional connectivity patterns. We performed MGPC analyses using 8 of the insula seed ROI maps (left/right, dorsal/ventral anterior and posterior insula) as input modalities, in which we applied the DARTEL (Ashburner, 2007) gray matter mask. A feature set was built using first-level spatial maps of insula seed connectivity patterns that were mean-centered, where individual kernels were built for each of the 8 seed maps. These spatial maps were later concatenated during the MGPC computation. In order to assess generalizability, we conducted a leave-one-subject-out cross-validation procedure. The MGPC analysis was evaluated using balanced accuracy measures in order to account for differences in group size (Schrouff et al., 2018). Statistical significance of these measures was determined by way of permutation testing ($n = 1000$; $p < .012$). Using the Automated Anatomical Labeling (AAL) brain atlas, weights for each anatomical region were computed in order to illustrate the regional pattern of decision function weights used by the machine to classify each group (Haufe et al., 2014; Schrouff et al., 2018).

4.3 Results

4.3.1 Overview

Overall, healthy controls, PTSD and PTSD+DS showed specific patterns of bilateral anterior and posterior insula functional connectivity that were unique to each group. Interestingly, however, when considering functional connectivity patterns of dorsal and ventral portions of insula subregions between participant groups, such distinctions were not consistently observed. A visual depiction of these results is shown in Figure 4.1.

Specifically, as compared to PTSD and PTSD+DS groups, the healthy control group showed increased right anterior and posterior insula connectivity with cortical sensorimotor structures in the brain, including the left pre- and post- central gyri. By contrast, as compared to PTSD+DS and healthy control groups, the PTSD group showed increased bilateral posterior insula connectivity with subcortical limbic and brainstem structures, including the left ventral pallidum and the periaqueductal gray. In addition, as compared to PTSD and healthy control groups, the PTSD+DS group showed increased bilateral posterior insula connectivity with posterior brain regions, specifically with the left lingual gyrus, as well as increased right posterior insula connectivity with the left precuneus. Finally, the multivariate machine learning analysis using insula subregion functional connectivity patterns was able to classify the three participant groups (PTSD, PTSD+DS and healthy controls) with 80.4% accuracy. We present a more comprehensive description of these results below.

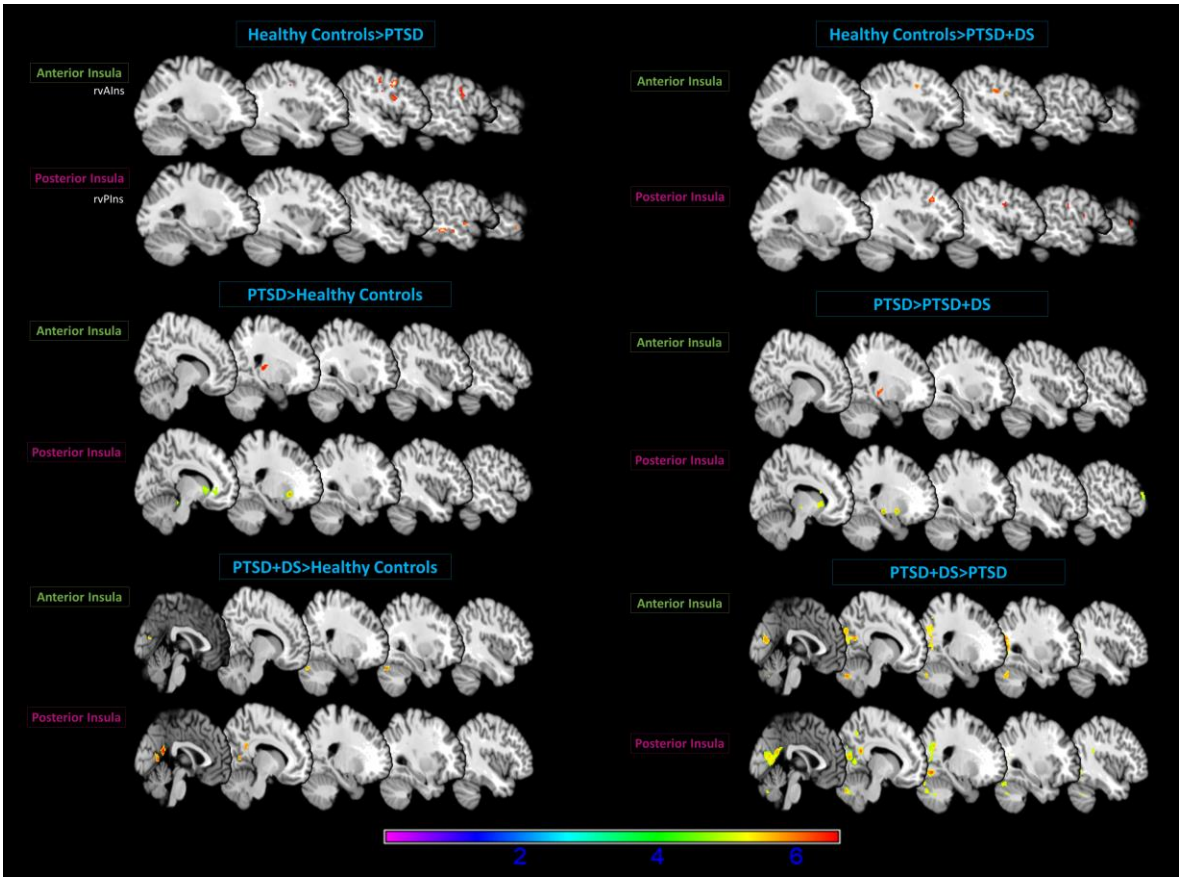

Figure 4.1 *Summary Figure of Right Ventral Anterior and Posterior Insula Functional Connectivity Patterns.* This figure provides a visual depiction that summarizes the main results of the present study. Here, we observe that, as compared to PTSD and PTSD+DS, healthy controls showed increased right ventral anterior and posterior insula connectivity with anterior neocortical structures involved in sensorimotor processing, including the left pre- and post-central gyri. Conversely, as compared to healthy controls and PTSD+DS, PTSD showed limited right ventral anterior insula connectivity with the whole-brain. However, PTSD did show increased right ventral posterior insula connectivity with the lower-order subcortical limbic and brainstem structures, including the left ventral pallidum and the periaqueductal gray, when compared to healthy controls and PTSD+DS. By contrast, as compared to healthy controls and PTSD, PTSD+DS showed increased right ventral anterior and posterior insula connectivity with posterior brain regions, including the left lingual gyrus, the left precuneus and the cerebellum. *Reported at family-wise error whole-brain voxel-corrected at $pFWE < .05$, $k = 10$

4.3.2 Clinical and Demographic Measures

An ANOVA conducted across the three participant groups (PTSD+DS, PTSD and healthy controls) revealed non-significant differences in age [F (2,179) = 2.77, *ns*], and a Pearson's chi-square test revealed no statistically significant association between sex and participant group [X^2 (2, N = 184) = 3.55, *ns*]. Kruskal-Wallis analysis of variance yielded significant values ($p < .001$) for all self-reported trait psychological measures collected prior to (CAPS, CTQ, MDI and BDI) and during (RSDI, STAI, CADSS) the scan. Post-hoc Games-Howell comparisons showed, as compared to the PTSD group, PTSD+DS scored significantly higher on trait psychological measures collected prior to the scan (CTQ, MDI and BDI; $p < .001$) and state measures during the scan (RSDI-dissociation subscale $p < .05$). By contrast, scores for STAI and RSDI subscales assessing emotional distress, reliving previous traumas, and visceral sensations obtained during the scan did not differ between the PTSD and PTSD+DS groups ($p < .05$). However, all psychological measures collected prior to and during the scan in both the PTSD and PTSD+DS groups were significantly higher when compared to healthy controls ($p < .05$).

4.3.3 Full Factorial Design

Results from the omnibus 3 x 12 (participant group x insula parcellation) full-factorial ANOVA are detailed in the Appendix C. In the present study, we focus our discussion on the subsequent post-hoc two-sample *t*-tests detailing participant group differences (PTSD, PTSD+DS, and healthy controls) in functional connectivity patterns among the bilateral anterior and posterior insula, including both their dorsal and ventral axes. Given that the mid-insula subregion is considered an intermediary structure between the anterior and posterior insula subregions (Craig, 2009), we elected to detail mid-insula functional

connectivity patterns in Appendix C. In addition, for brevity, one-sample *t*-tests delineating insula functional connectivity within each participant group are listed in Appendix C.

4.3.4 Between-Group Functional Connectivity

4.3.4.1 Healthy Controls> PTSD and PTSD+DS

4.3.4.1.1 Anterior Insula

As compared to the PTSD and PTSD+DS groups, the healthy control group showed increased right dorsal/ventral anterior insula connectivity with the left pre- and post-central gyri (Figure 4.2). In addition, as compared to PTSD group, the healthy control group showed increased right ventral anterior insula connectivity with the left dorsolateral prefrontal cortex. By contrast, as compared to the PTSD and PTSD+DS groups, the healthy control group did not show increased left dorsal and ventral anterior insula connectivity with the whole brain. A full description of these results can be found in Table 4.2.

4.3.4.1.2 Posterior Insula

As compared to both the PTSD and PTSD+DS groups, the healthy control group showed increased right ventral posterior insula connectivity with the left postcentral gyrus (Figure 4.2). In addition, as compared to the PTSD+DS group, the healthy control group showed increased right ventral posterior insula connectivity with the left dorsolateral prefrontal cortex. A full description of these results can be found in Table 4.2.

Table 4.2 *Healthy Controls versus PTSD and PTSD+DS Insula Subregion Functional Connectivity*

Contrast	**L R**	**B A**	**Region**	**k**	**vFWE**	**Z**	**MNI Coordinates**		
							x	**y**	**z**
healthy controls > PTSD									
rdAIns	L	6	Precentral Gyrus	92	< .001	5.89	-46	0	44
	L	6	Postcentral Gyrus	138	< .001	5.74	-48	0	24
rvAIns	L	6	Precentral Gyrus	156	< .001	6.57	-46	0	44
	L	6	Postcentral Gyrus	522	< .001	5.89	-48	0	24
	L	6	Postcentral Gyrus	Of 522	< .001	5.81	-52	-14	36
	L	6	Precentral Gyrus	Of 522	< .001	5.65	-50	0	22
	L	8	Dorsolateral Prefrontal Cortex	25	.004	5.00	-44	14	36
ldAIns			*ns*						

.lvAIns			*ns*						
rdPIns	L	22	Superior Temporal Gyrus	503	< .001	6.35	-64	-16	-6
	L	21	Middle Temporal Gyrus	Of 503	< .001	5.73	-58	-38	-8
	L	21	Middle Temporal Gyrus	Of 503	< .001	5.60	-60	-24	-10
	L	6	Postcentral Gyrus	50	< .001	5.52	-58	-8	28
	L	44	Inferior Frontal Gyrus	33	.004	4.98	-60	12	12
rvPIns	L	21	Middle Temporal Gyrus	262	< .001	6.08	-56	-40	-10
	L	22	Middle Temporal Gyrus	Of 262	< .001	5.65	-60	-24	-10
	L	37	Middle Temporal Gyrus	Of 262	< .001	5.51	-64	-14	-6
	L	6	Postcentral Gyrus	27	< .001	5.23	-58	-8	28
	L	7	Superior Parietal Lobule	66	.002	5.13	-32	-64	58

ldPIns			*ns*						
lvPIns	R	39	Angular Gyrus	66	< .001	5.39	34	-70	52
	R	7	Superior Parietal Lobule	Of 66	.004	5.01	26	-74	52
	L	7	Superior Parietal Lobule	93	.001	5.25	-30	-66	58
	L	7	Superior Parietal Lobule	152	.002	5.21	-18	-72	52
healthy controls > PTSD+DS									
rdAIns	L	6	Precentral Gyrus	267	< .001	569	-40	-2	32
	L	6	Precentral Gyrus	Of 267	< .001	5.46	-40	-6	42
	L	6	Precentral Gyrus	Of 267	< .001	5.42	-42	2	22
	L	6	Postcentral Gyrus	63	.002	5.22	-48	-16	32
	L	6	Postcentral Gyrus	45	.003	5.10	-34	-20	42
	L	24	Mid-Cingulate	26	.003	5.06	-8	-2	44

rvAIns	L	6	Postcentral Gyrus	376	< .001	5.60	-50	-14	34
	L	6	Precentral Gyrus	Of 376	.001	5.44	-40	-6	42
ldAIns			*ns*						
lvAIns			*ns*						
rdPIns	L	37	Middle Temporal Gyrus	77	< .001	5.77	-62	-42	-16
	R	21	Middle Temporal Gyrus	22	.001	5.26	68	-36	-12
rvPIns	L	41	Superior Temporal Gyrus	437	< .001	6.61	-62	-4	4
	L	6	Precentral Gyrus	Of 437	< .001	5.70	-62	12	22
	L	6	Postcentral Gyrus	Of 437	< .001	5.62	-62	-8	24
	L	8	Dorsolateral Prefrontal Cortex	88	< .001	6.06	-36	14	38

	L	6	Postcentral Gyrus	58	< .001	5.90	-52	-22	30
	R	6	Precentral Gyrus	37	< .001	5.86	42	-8	36
	L	4	Central Operculum	51	.002	5.18	-46	-12	18
ldPIns	L	22	Superior Temporal Gyrus	47	< .001	6.14	-67	-8	2
lvPIns	L	22	Superior Temporal Gyrus	52	< .001	7.10	-64	-8	2

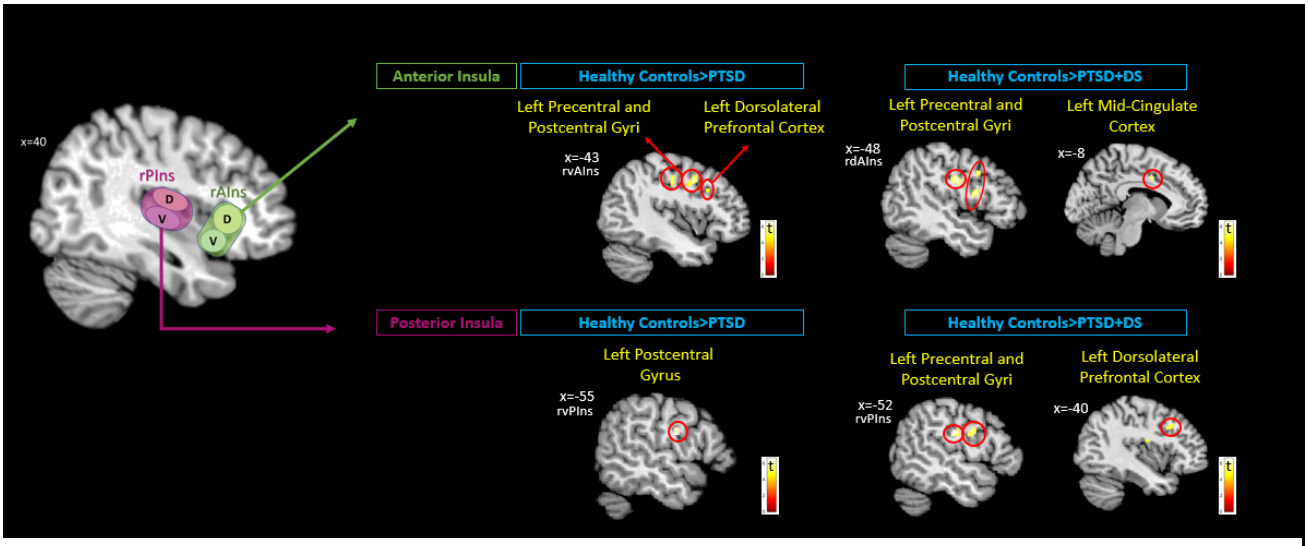

Figure 4.2 *Healthy Control Insula Subregion Connectivity Patterns.* Specifically, as compared to PTSD and PTSD+DS, healthy controls showed increased right anterior insula connectivity with higher-order sensorimotor processing areas, including the left pre- and post-central gyri. In addition, as compared to PTSD and PTSD+DS, healthy controls showed increased right anterior insula connectivity with the left dorsolateral prefrontal cortex and the left mid-cingulate cortex, respectively. Moreover, as compared to PTSD and PTSD+DS, healthy controls showed increased right posterior insula connectivity with the left postcentral gyrus. Furthermore, as compared to the PTSD+DS group, healthy controls showed increased right posterior insula connectivity with the left precentral gyrus and the left dorsolateral prefrontal cortex. This figure depicts right insula connectivity patterns only; however, interestingly, as compared to PTSD and PTSD+DS, healthy controls did not show increased left anterior and posterior insula connectivity with higher-order sensorimotor processing areas (see Table 2 for full description). *Reported at family-wise error whole-brain voxel-corrected at $pFWE < .05$, $k = 10$

4.3.4.2 PTSD>PTSD+DS and healthy controls

4.3.4.2.1 Anterior Insula

As compared to the PTSD+DS group, the PTSD group did not show increased bilateral dorsal or ventral anterior insula connectivity with the whole brain (Figure 4.3). By contrast, as compared to the healthy control group, the PTSD group showed increased bilateral dorsal anterior insula connectivity with the right pulvinar thalamic nuclei, as well as increased right dorsal anterior insula connectivity with the right hippocampus (Figure 4.3). A full description of these results can be found in Table 4.3.

4.3.4.2.2 Posterior Insula

As compared to the PTSD+DS and healthy control groups, the PTSD group showed increased bilateral dorsal/ventral posterior insula connectivity with the left ventral pallidum, as well as increased right dorsal/ventral posterior insula connectivity with the periaqueductal gray (Figure 4.3). Moreover, as compared to the healthy control group, the PTSD group showed increased bilateral dorsal and ventral posterior insula connectivity with the right caudate (Figure 4.3). A full description of these results can be found in Table 4.3.

Table 4.3 *PTSD versus PTSD+DS and Healthy Controls Insula Subregion Functional Connectivity*

Contrast	LR	BA	Region	k	vFWE	Z	MNI Coordinates		
							x	y	z
PTSD > PTSD+DS									
rdAIns			*ns*						
rvAIns			*ns*						
ldAIns			*ns*						
lvAIns			*ns*						
rdPIns	R	10	Mid-Cingulate Cortex	56	< .001	5.46	12	-20	42
	R	10	Postcentral Gyrus	231	< .001	5.37	34	-16	40
	R	10	Orbitolateral Prefrontal Cortex	26	.002	5.14	38	60	-2
	L	51	Pallidum	22	.003	5.12	-20	-6	-6
rvPIns	L	36	Parahippocampal Gyrus	279	< .001	6.67	-16	-32	-8
			Ventral	Of 279	< .001	6.05	-22	-26	-6

			Tegmental Area						
			Periaqueductal Gray	Of 279	.002	5.20	-10	-22	0
	R	6	Precentral Gyrus	62	< .001	6.51	42	-10	36
	R	48	Caudate	1011	< .001	6.50	16	8	4
	L	51	Pallidum	Of 1011	< .001	6.46	-20	-2	-4
	R	50	Pulvinar Thalamus	86	< .001	6.07	16	-32	-2
	L	24	Dorsal Anterior Cingulate	206	< .001	5.63	-2	36	4
	R		Cerebellar Lobule IV (Vermis)	150	< .001	5.82	2	-42	-10
	L	46	Dorsolateral Prefrontal Cortex	65	< .001	5.42	-50	36	18
	R	10	Orbitolateral Prefrontal Cortex	105	< .001	5.35	38	58	-2
	R	24	Mid-Cingulate Cortex	110	< .001	5.32	12	-20	42
ldPIns	L	51	Pallidum	227	< .001	6.62	-16	6	-2
	L	51	Pallidum	Of 227	< .001	5.75	-22	-4	-2
	L	38	Temporal Pole	53	< .001	5.94	-56	8	-24
	R	51	Pallidum	69	< .001	5.77	18	6	2
lvPIns	L	38	Temporal Pole	95	< .001	7.74	-58	6	-24
	L	51	Pallidum	249	< .001	7.09	-14	4	-2

	R	50	Pulvinar Thalamus	46	< .001	6.12	16	-32	0
	R	41	Temporal Pole	27	< .001	5.82	62	2	-22
	R	50	Anterior Thalamus	64	< .001	5.68	14	8	-2
PTSD > healthy controls									
rdAIns	R	50	Pulvinar Thalamus	478	< .001	7.00	20	-32	12
	R	54	Hippocampus	Of 478	.001	5.28	26	-28	-8
	R	50	Mediodorsal Thalamus	Of 478	.001	4.82	10	-22	18
rvAIns			*ns*						
ldAIns	R	50	Pulvinar Thalamus	200	.004	4.98	12	-24	16
	R	50	Anterior Thalamus	76	.001	5.28	6	2	-4
lvAIns	R	50	Anterior Thalamus	81	< .001	5.45	6	2	-4
rdPIns	R	48	Caudate	2110	< .001	6.61	10	10	0
	L	51	Pallidum	Of	< .001	5.9	-18	0	-6

				2110		3			
	R	13	Ventral Anterior Insula	86	< .001	5.76	42	16	-10
			Superior Colliculus /Periaqueductal Gray	45	< .001	5.32	-2	-38	-2
rvPIns	R	48	Caudate	2225	< .001	6.94	10	10	0
	R	13	Ventral Anterior Insula	Of 2225	< .001	6.30	42	18	-10
	L	49	Putamen	Of 2225	< .001	6.21	-22	10	-2
	L	51	Pallidum	Of 2225	< .001	6.06	-18	-4	0
	L		Cerebellar Lobule III	195	< .001	5.85	-6	-38	-12
			Periaqueductal Gray	Of 195	< .001	5.77	-2	-38	-4
	R		Cerebellar Lobule IV	117	< .001	5.62	20	-34	-22
			Periaqueductal Gray	27	.002	5.22	-6	-24	-8
	R	54	Hippocampus	20	.004	5.01	30	-18	-8
ldPIns	R	51	Pallidum	1090	< .001	7.31	6	4	-4
	R	48	Caudate	Of 1090	< .001	6.69	10	8	4
	L	50	Anterior	Of	< .001	5.9	-2	2	-2

			Thalamus	1090		6			
			Superior Colliculus /Periaqueductal Gray	26	< .001	5.39	-4	-28	0
	L	51	Pallidum	100	.002	5.22	-14	4	0
	L	54	Hippocampus	30	.002	5.20	-26	-34	0
lvPIns	R	50	Anterior Thalamus	2943	< .001	7.12	4	2	-4
	R	49	Putamen	Of 2943	< .001	6.89	18	6	6
	R	48	Caudate	Of 2943	< .001	6.42	8	12	4
	R	45	Ventrolateral Prefrontal Cortex	312	< .001	6.40	54	32	0
	R	9	Dorsolateral Prefrontal Cortex	Of 312	< .001	6.01	56	26	14
	-		Ventral Diencephalon	230	< .001	5.67	0	-24	-10
	L		Superior Colliculus	Of 230	< .001	5.48	-4	-34	-6
	L	51	Pallidum	78	< .001	5.94	-12	6	0
	L	54	Hippocampus	32	.001	5.24	-34	-26	-12
	R	47	Inferior Frontal Gyrus	49	.002	5.13	38	22	-10

Between group post-hoc two-sample *t*-tests detailing differences in insula subregion functional connectivity patterns between PTSD versus PTSD+DS and healthy controls based on the 3 x 12 full-factorial analysis (reported at family-wise error whole-brain voxel-corrected at $pFWE < .05$, $k = 10$). Cluster sizes (*k*) listed as "Of *x*" are subpeaks of the nearest "*x*" *k*-value listed above.

Abbreviations: PTSD posttraumatic stress disorder; PTSD+DS, posttraumatic stress disorder with the dissociative subtype; rdAIns, right dorsal anterior insula; rvAIns, right ventral anterior insula; ldAIns, left dorsal anterior insula; lvAIns, left ventral anterior insula; rdPIns, right dorsal posterior insula rvPIns, right ventral posterior insula; ldPIns, left dorsal posterior insula; lvPIns, left ventral posterior insula; L, left hemisphere; R, right hemisphere; BA, Brodmann Area; *k*, Cluster Size; *vFWE*, family-wise error voxel-corrected; MNI, Montréal Neurological Institute.

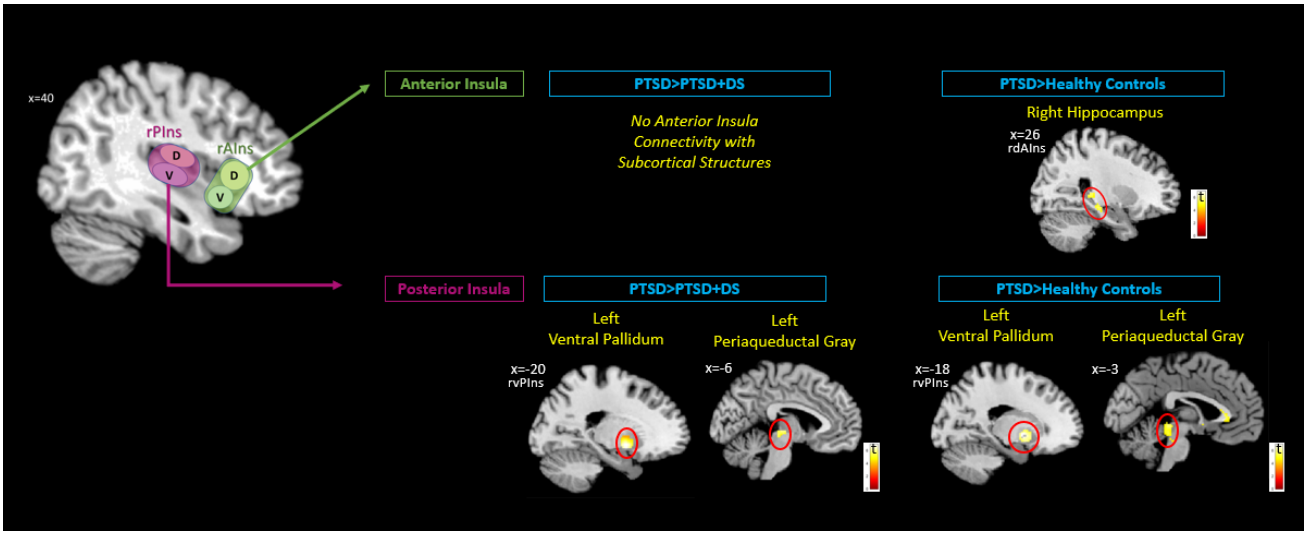

Figure 4.3 *PTSD Insula Subregion Connectivity Patterns.* Specifically, as compared to healthy controls, PTSD showed increased right anterior insula connectivity with the right hippocampus in the limbic system and the right pulvinar thalamic nuclei. In addition, as compared to PTSD+DS and healthy controls, PTSD showed increased right posterior insula connectivity with the left ventral pallidum in the limbic system and with the periaqueductal gray in the midbrain. Moreover, as compared to healthy controls, PTSD showed also increased right posterior insula connectivity with the right caudate. This figure depicts right insula connectivity patterns only; however, left insula patterns showed connectivity with similar regions, including the bilateral pallidum and the periaqueductal gray (see Table 3 for full description). *Reported at family-wise error whole-brain voxel-corrected at $pFWE < .05$, $k = 10$

4.3.4.3 PTSD+DS>PTSD and Healthy Controls

4.3.4.3.1 Anterior Insula

As compared to the PTSD and healthy control groups, the PTSD+DS group showed increased right dorsal/ventral anterior insula connectivity with the left lingual gyrus (Figure 4.4). A full description of these results can be found in Table 4.4.

4.3.4.3.2 Posterior Insula

As compared to the PTSD and healthy control groups, the PTSD+DS group showed increased bilateral dorsal/ventral posterior insula connectivity with the left lingual gyrus, as well as increased right dorsal/ventral posterior insula connectivity with the left precuneus (Figure 4.4). In addition, as compared to the PTSD group, PTSD+DS showed increased right ventral posterior insula connectivity with the left superior parietal lobule. A full description of these results can be found in Table 4.4.

Table 4.4 *PTSD+DS versus PTSD and Healthy Controls Insula Subregion Functional Connectivity*

Contrast	**L R**	**B A**	**Region**	**k**	**vFWE**	**Z**	**MNI Coordinates**		
							x	**y**	**z**
PTSD+DS > PTSD									
rdAIns	L		Cerebellar Lobule II	122	< .001	5.37	-8	-80	-28
rvAIns	L	19	Middle Occipital Gyrus	1789	< .001	5.56	-38	-74	12
	L	18	Lingual Gyrus	59	.001	5.28	-18	-68	-4
	L		Cerebellum Lobule I	255	.002	5.18	-34	-72	-26
ldAIns			*ns*						
lvAIns			*ns*						

rdPIns	L		Cerebellar Lobule II	3799	< .001	6.75	-6	-80	-28
	L		Cerebellar Lobule I	Of 3799	< .001	6.17	-16	-80	-26
	L	18	Lingual Gyrus	Of 3799	< .001	5.97	-16	-68	-4
	L	40	Supramarginal Gyrus	61	< .001	5.56	-48	-44	22
	L	23	Posterior Cingulate Cortex	74	< .001	5.45	-12	-54	24
	L	7	Precuneus	26	.004	5.00	-8	-62	50
rvPIns	L	18	Lingual Gyrus	4523	< .001	6.63	-18	-72	-4
	L	18	Cuneus	Of 4523	< .001	6.20	-6	-74	18
	L	19	Inferior Occipital Gyrus	Of 4523	< .001	6.18	-40	-72	0
	L	40	Supramarginal Gyrus	147	< .001	6.24	-50	-44	22
	L	7	Precuneus	61	< .001	5.50	-10	-60	50
	L	7	Superior Parietal Lobule	49	< .001	5.31	-30	-52	38
	L	37	Middle Temporal Gyrus	24	.002	5.17	-48	-58	0
	R		Cerebellar Lobule VI	31	.002	5.13	36	-70	-22
ldPIns	L		Cerebellar Lobule I	805	< .001	6.12	-40	-64	-24
	L		Cerebellar	Of 805	< .001	6.08	-12	-68	-32

			Lobule IX (Uvula)						
	L	18	Lingual Gyrus	425	< .001	6.02	-18	-70	-4
	L		Cerebellar Lobule IV (Vermis)	Of 425	.002	5.19	-6	-64	-10
	L	19	Fusiform Gyrus	Of 425	.004	5.01	-36	-80	-12
	R	7	Precuneus	110	.001	5.31	12	-64	48
	R	23	Posterior Cingulate Cortex	31	.003	5.08	10	-54	28
	R	13	Mid Ventral Insula	22	.004	5.00	48	-4	-4
lvPIns	L	18	Lingual Gyrus	17282	< .001	7.35	-18	-72	-4
	L		Cerebellar Lobule I	Of 17282	< .001	7.01	-38	-64	-26
	L	6	Supplementary Motor Cortex	430	< .001	6.18	-2	-4	60
	R	6	Premotor Cortex	Of 17282	< .001	5.89	10	14	68
	R	22	Temporal Pole	617	< .001	6.14	52	2	-16
	R	13	Ventral Anterior Insula	Of 617	< .001	5.87	48	12	-8
	R	6	Premotor Cortex	70	< .001	5.54	22	10	56
	L	4	Precentral Gyrus	58	< .001	5.44	-4	-28	62
	L	5	Postcentral Gyrus	104	.001	5.34	-26	-38	60
	R	21	Middle Temporal Gyrus	92	.001	5.30	60	-32	-12
	R	21	Inferior	Of 92	.002	5.13	54	-38	-16

			Temporal Gyrus						
	L	6	Precentral Gyrus	117	.001	5.27	-20	-16	70
	L	6	Premotor Cortex	47	.001	5.23	-12	18	62
	R	6	Precentral Gyrus	30	.003	5.06	34	-10	54
PTSD+DS > healthy controls									
rdAIns	L	18	Cuneus	1811	< .001	5.74	-2	-82	18
	R	19	Middle Occipital Gyrus	Of 1811	< .001	5.47	32	-76	16
	L	19	Lingual Gyrus	351	< .001	5.55	-16	-68	-4
	R	18	Lingual Gyrus	Of 351	.002	5.15	12	-74	0
	R	18	Inferior Occipital Gyrus	140	< .001	5.32	36	-82	0
	L		Cerebellar Lobule VI	126	.001	5.30	-32	-68	-22
	R		Cerebellar Lobule VI	65	.001	5.25	-28	-78	-22
rvAIns	L	19	Lingual Gyrus	106	< .001	5.69	-16	-68	-4
	L		Cerebellar Lobule VI	98	< .001	5.38	-28	-78	-22
ldAIns	L	19	Lingual Gyrus	36	.004	5.05	-8	-64	-8
	R	19	Cuneus	73	.004	5.02	10	-78	34

lvAIns	L		Cerebellar Lobule IV (Vermis)	379	< .001	5.55	-8	-62	-6
	L	18	Lingual Gyrus	Of 379	.001	5.21	-16	-68	-6
	L		Cerebellar Lobule I	Of 379	.004	5.03	-20	-80	-22
	L		Cerebellar Lobule VI	25	.003	5.07	-36	-66	-24
rdPIns	R	13	Ventral Anterior Insula	254	< .001	6.47	46	14	-8
	R	18	Lingual Gyrus	539	< .001	5.70	2	-64	8
	R	38	Temporal Pole	20	< .001	5.56	36	10	-18
	L	19	Lingual Gyrus	135	< .001	5.51	-14	-66	-6
	R	18	Lingual Gyrus	23	< .001	5.40	12	-74	0
	L	17	Cuneus	Of 539	.002	5.21	-10	-64	12
	L	23	Posterior Cingulate Cortex	32	.002	5.21	-4	-56	20
	L	19	Superior Occipital Gyrus	23	.004	5.02	-26	-84	12
	L	18	Cuneus	33	.004	5.02	-12	-64	26
	R	18	Cuneus	40	.004	4.98	18	-72	28
rvPIns	R	13	Ventral Anterior Insula	82	< .001	5.86	46	14	-8
	R	38	Temporal Pole	Of 82	.002	5.16	44	14	-24
	L	31	Precuneus	518	< .001	5.76	-2	-58	22

	LR	17	Lingual Gyrus	Of 518	< .001	5.62	0	-68	10
	L	18	Lingual Gyrus	34	.004	4.97	-18	-72	-6
ldPIns	R	18	Lingual Gyrus	2693	< .001	6.25	10	-62	12
	R	44	Dorsal Anterior Insula	106	< .001	5.44	44	20	8
	R	13	Ventral Anterior Insula	Of 106	.002	5.15	46	12	-10
	L	37	Fusiform Gyrus	32	< .001	5.43	-38	-64	-24
	L		Cerebellar Lobule VI	48	.001	5.15	-18	-64	-32
lvPIns	R	6	Premotor Cortex	742	< .001	6.78	12	2	70
	R	1	Postcentral Gyrus	264	< .001	5.61	44	-28	38
	L		Cerebellar Lobule IV (Vermis)	194	< .001	6.23	-6	-64	-10
	L		Cerebellar Lobule I	51	< .001	5.81	-50	-52	-30
	R	18	Lingual Gyrus	224	< .001	5.76	10	-62	12
	L	17	Cuneus	Of 224	< .001	5.39	-2	-68	14
	L		Cerebellar Lobule VI	92	< .001	5.40	-18	-64	-30
	L	31	Posterior Cingulate Cortex	87	.002	5.22	-12	-54	30

Between group post-hoc two-sample *t*-tests detailing differences in insula subregion functional connectivity patterns in PTSD+DS versus PTSD and healthy controls based on

the 3 x 12 full-factorial analysis (reported at family-wise error whole-brain voxel-corrected at *pFWE* < .05, *k* = 10). Cluster sizes (*k*) listed as "Of *x*" are subpeaks of the nearest "*x*" k-value listed above.

Abbreviations: PTSD posttraumatic stress disorder; PTSD+DS, posttraumatic stress disorder with the dissociative subtype; rdAIns, right dorsal anterior insula; rvAIns, right ventral anterior insula; ldAIns, left dorsal anterior insula; lvAIns, left ventral anterior insula; rdPIns, right dorsal posterior insula rvPIns, right ventral posterior insula; ldPIns, left dorsal posterior insula; lvPIns, left ventral posterior insula; L, left hemisphere; R, right hemisphere; BA, Brodmann Area; *k*, Cluster Size; vFWE, family-wise error voxel-corrected; MNI, Montréal Neurological Institute.

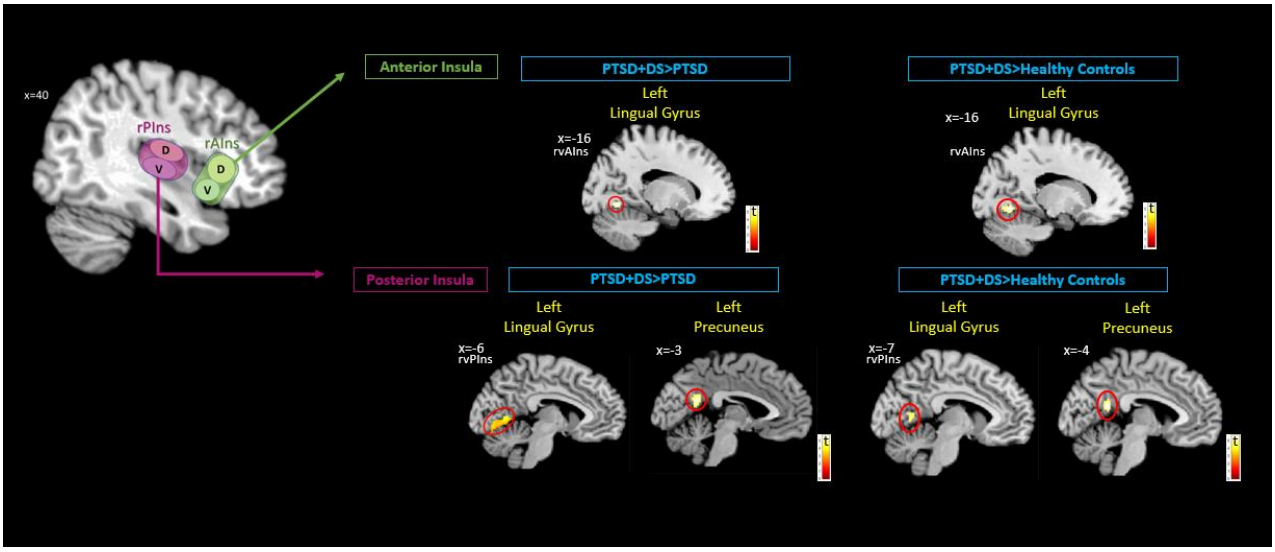

Figure 4.4 *PTSD+DS Insula Subregion Connectivity Patterns.* Specifically, as compared to PTSD and healthy controls, PTSD+DS showed increased right anterior and posterior connectivity with the left lingual gyrus. Moreover, as compared to PTSD and healthy controls, PTSD+DS showed increased right posterior insula connectivity with the left

precuneus. This figure depicts right insula connectivity patterns only; however, left insula patterns showed connectivity with similar regions, including the left lingual gyrus (see Table 4 for full description). *Reported at family-wise error whole-brain voxel-corrected at *pFWE* < .05, *k* = 10

4.3.5 Clinical Measure Correlations with Functional Connectivity Patterns in PTSD Patients

In the cumulative PTSD sample (PTSD and PTSD+DS), higher self-reported state dissociation scores reported during the scan (RSDI scale) were associated with increased left ventral posterior insula connectivity with the left fusiform gyrus (*pFWE* < .05, *k* = 10). Similarly, higher self-reported dissociation scores assessed prior to the scan (MDI scale) were associated with increased left dorsal posterior insula connectivity with the right fusiform gyrus (*pFWE* < .05, *k* = 10). These self-reported dissociative symptoms are consistent with insula functional connectivity patterns observed in the seed-based analysis, as the left dorsal posterior insula showed connectivity with the left fusiform gyrus in PTSD+DS as compared to both PTSD and healthy controls. Moreover, higher levels of self-reported reliving of past experiences during the scan (RSDI scale) were associated with decreased right dorsal anterior insula connectivity with the right ventromedial prefrontal cortex (Table 4.5; Figure 4.5). Insula functional connectivity patterns were not correlated with PTSD symptom clusters assessed by the CAPS scale nor with depression and childhood trauma as assessed by BDI and CTQ, respectively.

Table 4.5 *Clinical Score Correlations with Insula Subregion Connectivity Patterns in PTSD Patients*

Contrast	**L**	**B**	**Region**	**k**	**vFWE**	**Z**	**MNI**

	R	A					Coordinates x	y	z
RSDI Dissociative Score									
Positive correlation									
lvPIns	L	19	Fusiform Gyrus	30705	.02	4.65	-34	-66	-10
MDI Dissociative Score									
Positive correlation									
ldPIns	R	19	Fusiform Gyrus	9122	.04	4.47	38	-68	-22
RSDI Reliving Experiences									
Negative correlation									
rdAIns	R	10	Ventromedial Prefrontal Cortex	356	.04	4.51	12	68	4

Significant positive and negative correlations of psychological clinical measures taken prior to (MDI) and during (RSDI-Dissociation, RSDI-Reliving Experiences) the scan with insula subregion functional connectivity patterns of the cumulative PTSD sample (PTSD and PTSD+DS) (reported at family-wise error whole-brain voxel-corrected at $pFWE < .05$, $k = 10$).

Abbreviations: PTSD posttraumatic stress disorder; PTSD+DS, posttraumatic stress disorder with the dissociative subtype; rvAIns, right ventral anterior insula; ldAIns;

ldPIns, left dorsal posterior insula; lvPIns, left ventral posterior insula; L, left hemisphere; R, right hemisphere; BA, Brodmann Area; *k*, Cluster Size; *vFWE*, family-wise error voxel-corrected; MNI, Montréal Neurological Institute.

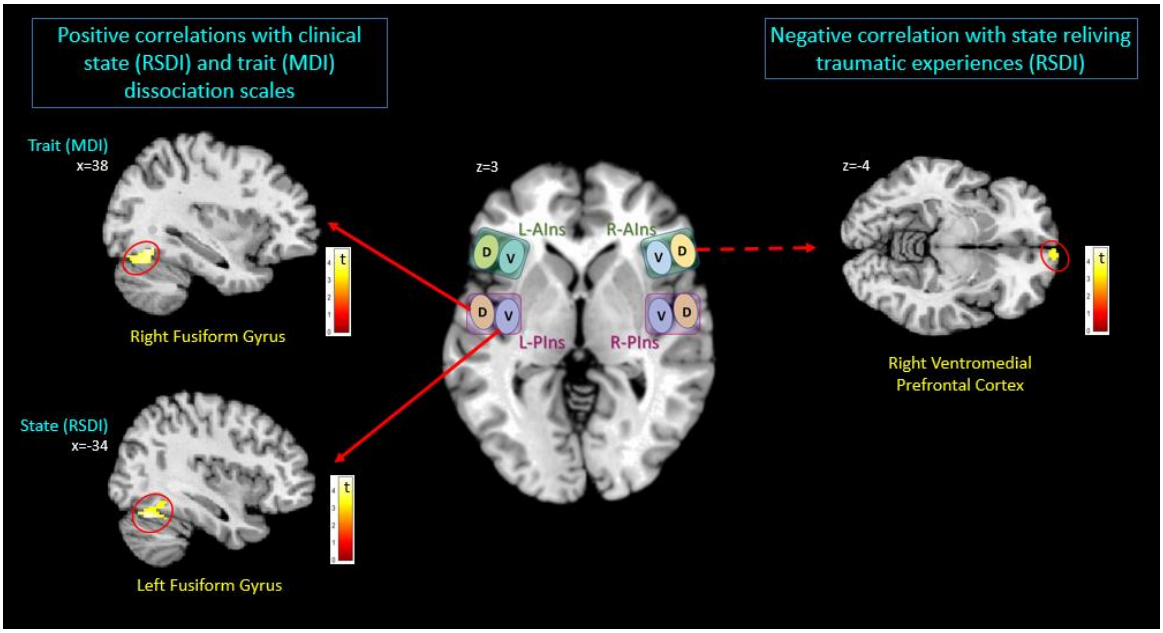

Figure 4.5 *Clinical Score Correlations with Insula Subregion Functional Connectivity Patterns in PTSD Patients.* In the cumulative PTSD sample (PTSD and PTSD+DS), increasing self-reported dissociation experienced during the scan measured by the RSDI scale, correlated positively with left ventral posterior insula connectivity with the left fusiform gyrus (pFWE < .05, k = 10). Similarly, increasing self-reported dissociation scores collected prior to the scan through the MDI scale correlated positively with left dorsal posterior insula connectivity with the right fusiform gyrus ($pFWE$ < .05, k = 10). Correlations from dissociation measures collected prior to and during the scan are consistent with the left dorsal posterior insula functional connectivity patterns observed in the seed-based analysis. Moreover, increasing self-reports of reliving past experiences during the scan measured also through the RSDI scale correlated negatively with right dorsal anterior insula connectivity with the right ventromedial prefrontal cortex.

*Reported at family-wise error whole-brain voxel-corrected at $pFWE$ < .05, k = 10

4.3.6 Machine Learning Results

The MGPC analysis was able to classify the three participant groups (healthy controls, PTSD, and PTSD+DS) with 80.4% balanced accuracy, based on feature sets extracted from bilateral dorsal/ventral anterior and posterior insula functional connectivity maps. Specifically, class accuracy was 82% (42/51) for healthy controls, 80% (65/84) for PTSD, and 80% (39/49) for PTSD+DS. In addition, class predictive value was 80% for healthy controls, 83% for PTSD, and 77% for PTSD+DS. The MGPC analysis identified several anatomical regions with relatively high weights used by the decision function of the machine to predict group classification, including bilateral dorsal/ventral anterior and posterior insula connectivity with the bilateral orbital prefrontal cortex, the bilateral ventral pallidum of the limbic system, and the bilateral temporal pole (Figure 4.6). However, as all voxels inputted into the algorithm within this multivariate analysis will contribute to the machine's prediction, it is not possible to single out whether any one region is predictive in isolation (Haufe et al. 2014).

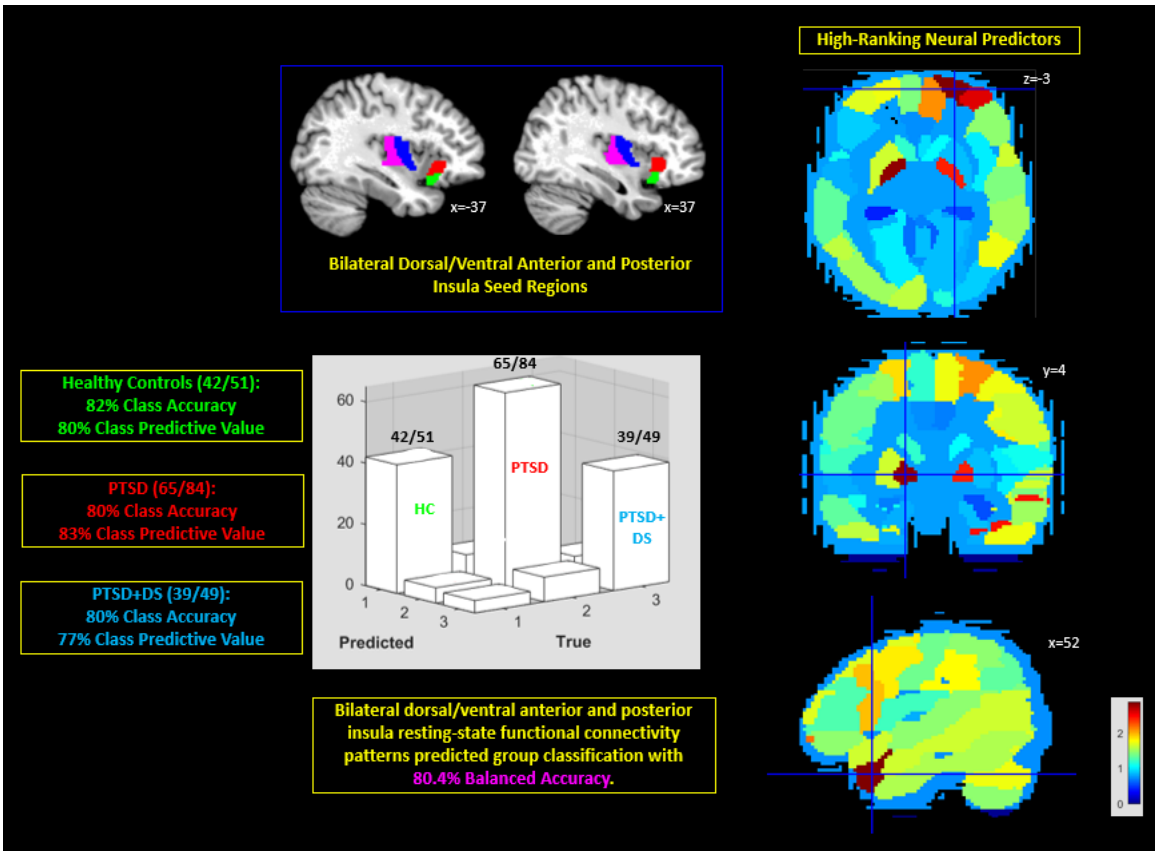

Figure 4.6 *Multiclass Gaussian Process Classification Machine Learning Analysis*. The bottom-left corner of this figure shows the confusion matrix from the machine learning analysis. The Multiclass Gaussian Process Classification (MGPC) predicted group classification based on resting-state insula subregion functional connectivity patterns derived from the seed-based analysis with 80.4% balanced accuracy. Specifically, class accuracy was 82% (42/51) for healthy individuals, 80% (65/84) for PTSD and 80% (39/49) for PTSD+DS. In addition, class predictive value was 80% for healthy controls, 83% for PTSD and 77% for PTSD+DS. As the MGPC machine learning analysis is multivariate, all inputted voxels from the insula functional connectivity maps will contribute to the decision function of the machine. This figure depicts high-ranking regional contributions of insula subregion functional connectivity for visualization purposes only. Here, regions ranked with high weights in classifying the three participant groups were the right orbitofrontal cortex, the bilateral ventral pallidum and the right temporal pole.

4.4 Discussion

The present study investigated the utility of insular subregion resting-state functional connectivity patterns in elucidating differences between individuals with PTSD, its dissociative subtype, and healthy controls. Here, a number of provocative findings emerged.

Specifically, as compared to PTSD and PTSD+DS groups, healthy controls showed increased right anterior and posterior insula functional connectivity with contralateral higher-order sensorimotor processing areas, including the left pre- and post-central gyri. In addition, as compared to the PTSD+DS group, the healthy control group showed increased right ventral posterior insula connectivity with the left dorsolateral prefrontal cortex. Taken together, these findings suggest that among healthy controls, as compared to individuals with PTSD and its dissociative subtype, the right insula shows increased connectivity for relaying sensory input to higher-order cortical areas involved in: (1) environmental monitoring, including the pre- and post-central gyri; and (2) appraising the emotional relevance of sensory information at the level of the dorsolateral prefrontal cortex.

A number of key differences also emerged between the PTSD and PTSD+DS groups. Specifically, as compared to PTSD+DS, individuals with PTSD showed increased right posterior insula connectivity with lower-level limbic and brainstem brain regions, including the left ventral pallidum and the periaqueductal gray, which are involved in evoking instinctual defensive responses and maintaining autonomic control. These findings are consistent with the heightened levels of emotional distress and reliving symptoms that were reported at rest by individuals with PTSD. By contrast, as compared

to PTSD, individuals with the dissociative subtype exhibited: (1) bilateral anterior and posterior insula connectivity to posterior brain regions associated with implicit memory processing (i.e., the left precuneus, the left lingual gyrus and the cerebellum), and (2) left ventral posterior insula functional connectivity with the right temporal pole, a region involved in processing visceral sensations. Notably, no distinctive differences emerged consistently when comparing functional connectivity patterns of dorsal and ventral portions of insula subregions between participant groups.

Notably, the multivariate machine learning analysis revealed that anterior and posterior insula resting-state functional connectivity features derived from the seed-based analysis were able to classify the three participant groups with 80.4% balanced accuracy ($p < .01$). This powerful multivariate analysis allowed us to make clinical predictions on the individual subject level, in contrast to the univariate seed-based analyses that allowed for group-wise inferences only (Cohen et al., 2017; Woo et al., 2017). Taken together, these findings suggest that distinct patterns of insular subregion functional connectivity may be useful in classifying individual patient populations with PTSD versus PTSD+DS.

4.4.1 Insula Subregion Connectivity in PTSD

The present study revealed increased right anterior insula connectivity with higher-order sensorimotor cortical areas in healthy controls, including the left pre- and post-central gyri and the left dorsolateral prefrontal cortex. This finding is consistent with current literature that suggests viscero-sensory information from limbic and brainstem regions may direct information upstream to more anterior portions of the insula in order to identify emotional feeling states that are later processed by higher-order frontal lobe structures (Cauda et al., 2011; Craig, 2009).

Interestingly, however, as compared to both PTSD+DS and healthy controls during rest, individuals with PTSD showed increased bilateral dorsal and ventral posterior insula functional connectivity with lower-order subcortical limbic and brainstem regions involved in hyperarousal and hypervigilance, including the left ventral pallidum and the periaqueductal gray. The posterior insula is considered the primary interoceptive cortex and receives viscero-sensory input from subcortical limbic and midbrain structures regarding physiological visceral sensations emanating from within the body (Craig, 2002). Here, elevated emotional and physiological distress experienced by individuals with PTSD at rest may be associated with altered posterior insula connectivity. Specifically, enhanced posterior insula connectivity with limbic and midbrain structures, including the ventral pallidum and the periaqueductal gray, may be related to sustained subcortical loops that promote instinctual fight-or-flight defensive behaviours, thereby limiting the translation of viscero-sensory information to higher-order cortical structures involved in emotion processing. These findings are also consistent with sustained activation of a subcortical innate alarm circuit in PTSD that responds to the perception of imminent threat (Lanius et al., 2017; Liddell et al., 2005; Rabellino, Densmore, Frewen, Théberge, & Lanius, 2016; Steuwe et al., 2014), a pattern that has been observed repeatedly in individuals with PTSD during rest (Harricharan et al., 2016; Lanius et al., 2017; Nicholson et al., 2017; 2018).

Interestingly, as compared to the PTSD+DS group, the PTSD group showed increased right dorsal and ventral posterior insula connectivity with cortical areas in the frontal lobe involved in sensorimotor processing and monitoring of the environment, including the dorsal anterior- and mid- cingulate cortices, the right postcentral gyrus, and

the right orbitolateral prefrontal cortex. Although, individuals with PTSD show weaker insula connectivity with cortical areas central to apprehending salient stimuli when compared to healthy individuals during rest. This finding suggests that individuals with the PTSD dissociative subtype may show greater limitations than do individuals with PTSD in their capacity to use higher-order cortical processing to appraise their surroundings.

4.4.2 Insula Subregion Connectivity in PTSD+DS

While depersonalization and derealization symptoms are thought to stem, in part, from increased top-down prefrontal inhibition of lower-order limbic and brainstem structures, PTSD+DS showed limited anterior and posterior insula connectivity with prefrontal structures during rest as compared to PTSD and healthy control groups. Instead, when compared to PTSD and healthy controls, the PTSD+DS group showed increased bilateral anterior and posterior insula connectivity with posterior cortical structures associated with the dorsal and ventral attention networks involved in the monitoring of *both* top-down (the superior parietal lobule, the precuneus) and bottom-up (the precuneus, the cuneus, and the lingual gyrus) neural processes (Burianová, Ciaramelli, Grady, & Moscovitch, 2012; Cabeza, 2008). Sun and colleagues (2001) demonstrated that bottom-up neural processing may facilitate the development of implicit skills; increased insula subregion connectivity in PTSD+DS with brain regions involved in bottom-up attentional networks may therefore suggest a role for the insula in developing connections with networks involved in implicit neural processes (Sun et al., 2001).

Interestingly, as compared to PTSD and healthy controls, PTSD+DS also showed increased anterior and posterior insula subregion connectivity during rest with posterior

cortical structures involved in implicit neural processes (Grèzes et al., 2003; Reber et al., 2013). Here, increased insula subregion connectivity with ventral posterior brain regions observed in the PTSD+DS group overlaps with neural markers associated with implicit memory processes (Rugg et al., 1998; Schott et al., 2005; Vuilleumier, Schwartz, Duhoux, Dolan, & Driver, 2005). Whereas implicit memory guides behaviours of perceptions of one's surroundings based on past experiences without conscious awareness (Squire & Dede, 2015; Tulving, 1985), explicit memory relies upon conscious awareness to guide retrieval of episodic (i.e., autobiographical experiences) or semantic (i.e., facts/concepts) memories (Squire & Dede, 2015; Tulving, 1985). In addition, whereas explicit memory tends to correlate with activity along the anterior cortical midline during introspection, including the medial prefrontal cortex, implicit memory tends to rely on more posterior brain regions, including the precuneus (Rugg et al., 1998). Implicit memory is particularly relevant to the study of PTSD, where traumatic experiences may subliminally guide behaviour and the individuals' perception of surroundings (Amir, McNally, & Wiegartz, 1996; Brewin, 2001; Golier, Yehuda, Lupien, & Harvey, 2003; Krikorian & Layton, 1998; Rabellino et al., 2016; van der Kolk & Fisler, 1995; Zeitlin & McNally, 1991). Furthermore, state dissociation scores correlated positively with left dorsal posterior insula connectivity with the left fusiform gyrus. Notably, visual cortex activation has been observed consistently in studies involving individuals with the dissociative subtype of PTSD (see Daniels et al., 2012, 2016; Lanius et al., 2005; Lanius et al., 2002), and forms part of an occipital resting-state network that facilitates visual mental imagery (Wang et al., 2008). Here, whereas implicit memory responses to visual priming cues appear intact among individuals that experience

dissociation, explicit memory processes are relatively impaired (Devilly et al., 2007; Eich, Macaulay, Loewenstein, & Patrice, 1997; Elzinga, Phaf, Ardon, & Van Dyck, 2003; Fenster et al., 2018; Kihlstrom, 2005). Taken together, these results point towards the need for additional research to clarify the role of implicit memory in the processing of salient environmental stimuli among individuals with PTSD+DS.

4.4.3 Limitations and Future Directions

There are several limitations to the present study. First, the insula seed regions-of-interest were taken from the Brainnetome anatomical atlas, thus lacking sensitivity to identify individual anatomical differences given the relative proximity of seed regions. Nonetheless, the insula parcellations derived from this atlas have been used successfully in numerous insula functional connectivity studies (see Xu et al., 2018; Yu et al., 2017; Zhang et al., 2018). Secondly, while our three participant groups were sex-matched, we did not examine insula resting-state connectivity patterns as a function of sex. Thirdly, we cannot infer directionality from the insula seed-based connectivity analyses conducted in the present study. Accordingly, future studies should employ cross-spectral dynamic causal modelling techniques to incorporate the insula into neurobiological frameworks describing the effective functional connectivity patterns involved in maintaining both top-down and bottom-up neural processes during rest.

4.4.4 Conclusions

On balance, insula subregion functional connectivity patterns observed during rest suggest a neurobiological distinction between PTSD, its dissociative subtype, and healthy controls. Specifically, as compared to PTSD and PTSD+DS, healthy controls demonstrated increased insula connectivity with higher cortical brain regions involved in

environmental monitoring and emotional appraisal, including the left postcentral gyrus and the left dorsolateral prefrontal cortex. Conversely, as compared to healthy controls and PTSD+DS, we observed increased posterior insula functional connectivity with subcortical structures in individuals with PTSD that may contribute to sustaining hypervigilance and hyperarousal symptoms. In stark contrast to PTSD and healthy controls, PTSD+DS showed limited insula subregion connectivity with prefrontal structures and increased connectivity with posterior brain regions involved in both top-down and bottom-up attentional processes, including implicit networks. Future studies should therefore aim to delineate how the dynamic between these opposing networks may uniquely impact individuals with the dissociative subtype and point towards the need to further investigate the neural underpinnings of implicit neural processes in PTSD+DS. Finally, the machine learning analysis demonstrated that insula subregion resting-state functional connectivity patterns may be utilized as diagnostic markers for classifying individuals with PTSD and its dissociative subtype. Identifying neural classifiers of insula resting-state functional connectivity patterns may offer valuable clinical insight into guiding treatments for the contrasting symptom profiles observed in individuals with PTSD and its dissociative subtype.

4.5 References

Akiki, T. J., Averill, C. L., Wrocklage, K. M., Scott, J. C., Averill, L. A., Schweinsburg, B., … Abdallah, C. G. (2018). Default mode network abnormalities in posttraumatic stress disorder: a novel network-restricted topology approach. *NeuroImage*, *176*, 489–498.

Amir, N., Mcnally, R. J., & Wiegartz, P. S. (1996). Implicit memory bias for threat in

posttraumatic stress disorder. *Cognitive Therapy and Research*, *20*(6), 625–635.

Ashburner, J. (2007). A fast diffeomorphic image registration algorithm. *NeuroImage*, *38*(1), 95–113.

Aupperle, R. L., Allard, C. B., Grimes, E. M., Simmons, A. N., Flagan, T., Behrooznia, M., … Stein, M. B. (2012). Dorsolateral prefrontal cortex activation during emotional anticipation and neuropsychological performance in posttraumatic stress disorder. *Archives of General Psychiatry*, *69*(4), 360–371.

Beck, A. T., Guth, D., Steer, R. A., & Ball, R. (1997). Screening for major depression disorders in medical inpatients with the Beck Depression Inventory for Primary Care. *Behaviour Research and Therapy*, *35*(8), 785–791.

Bernstein, D., & Fink, L. (1998). Childhood trauma questionnaire: A retrospective self-report: Manual. San Antonio, TX: The Psychological Corporation,.

Blake, D. D., Weathers, F. W., Nagy, L. M., Kaloupek, D. G., Gusman, F. D., Charney, D. S., & Keane, T. M. (1995). The development of a clinician-administered PTSD scale. *Journal of Traumatic Stress*, 8(1), 75-90.

Bluhm, R. L., Williamson, P. C., Osuch, E. A., Frewen, P. A., Stevens, T. K., Boksman, K., … Lanius, R. A. (2009). Alterations in default network connectivity in posttraumatic stress disorder related to early-life trauma. *Journal of Psychiatry and Neuroscience*, *34*(3), 187–194.

Bremner, J. D., Krystal, J. H., Putnam, F. W., Southwick, S. M., Marmar, C., Charney, D.

S., & Mazure, C. M. (1998). Measurement of dissociative states with the clinician-administered dissociative states scale (CADSS). *Journal of Traumatic Stress, 11*(1), 125–136.

Bremner, J. D., Vythilingam, M., Vermetten, E., Southwick, S. M., Mcglashan, T., Staib, L. H., … Charney, D. S. (2003). Neural correlates of declarative memory for emotionally valenced words in women with posttraumatic stress disorder related to early childhood sexual abuse. *Biological Psychiatry*, *53*(10), 879–889.

Bressler, S. L., & Menon, V. (2010). Large-scale brain networks in cognition: emerging methods and principles. *Trends in Cognitive Sciences*, *14*(6), 277–290.

Brewin, C. R. (2001). A cognitive neuroscience account of posttraumatic stress disorder and its treatment. *Behaviour Research and Therapy*, *39*, 373–393.

Briere, J., Weathers, F. W., & Runtz, M. (2005). Is dissociation a multidimensional construct? Data from the Multiscale Dissociation Inventory. *Journal of Traumatic Stress*, *18*(3), 221–231.

Burianová, H., Ciaramelli, E., Grady, C. L., & Moscovitch, M. (2012). Top-down and bottom-up attention-to-memory: Mapping functional connectivity in two distinct networks that underlie cued and uncued recognition memory. *NeuroImage*, *63*(3), 1343–1352.

Cauda, F., D'Agata, F., Sacco, K., Duca, S., Geminiani, G., & Vercelli, A. (2011). Functional connectivity of the insula in the resting brain. *NeuroImage*, *55*(1), 8–23.

Chang, L. J., Yarkoni, T., Khaw, M. W., & Sanfey, A. G. (2013). Decoding the role of the insula in human cognition : functional parcellation and large-scale reverse inference. *Cerebral Cortex*, *23*(3), 739–749.

Chen, A. C., Oathes, D. J., Chang, C., Bradley, T., Zhou, Z.-W., Williams, L. M., … Etkin, A. (2013). Causal interactions between fronto-parietal central executive and default-mode networks in humans. *Proceedings of the National Academy of Sciences*, *110*(49), 19944–19949.

Cloutman, L. L., Binney, R. J., Drakesmith, M., Parker, G. J. M., & Lambon Ralph, M. A. (2012). The variation of function across the human insula mirrors its patterns of structural connectivity: evidence from in vivo probabilistic tractography. *NeuroImage*, *59*(4), 3514–3521.

Cohen, J. D., Daw, N., Engelhardt, B., Hasson, U., Li, K., Niv, Y., ... & Willke, T. L. (2017). Computational approaches to fMRI analysis. *Nature neuroscience*, *20*(3), 304.

Corbetta, M., Patel, G., & Shulman, G. L. (2008). The reorienting system of the human brain: from environment to theory of mind. Neuron, 58(3), 306-324.

Corrigan, F. M., Fisher, J. J., & Nutt, D. J. (2011). Autonomic dysregulation and the window of tolerance model of the effects of complex emotional trauma. *Journal of Psychopharmacology*, *25*(1), 17–25.

Couto, B., Sedeño, L., Sposato, L. A., Sigman, M., Riccio, P. M., Salles, A., … Ibanez, A. (2013). Insular networks for emotional processing and social cognition:

comparison of two case reports with either cortical or subcortical involvement. *Cortex, 49*(5), 1420–1434.

Craig, A. D. (2002). How do you feel? Interoception: the sense of the physiological condition of the body. *Nature Reviews Neuroscience, 3*(8), 655–666.

Craig, A. D. (2009). How do you feel — now? The anterior insula and human awareness. *Nautre Reviews Neuroscience, 10*(1), 59–70.

Daniels, J. K., Coupland, N. J., Hegadoren, K. M., Rowe, B. H., Densmore, M., Neufeld, R. W. J., & Lanius, R. A. (2012). Neural and behavioral correlates of peritraumatic dissociation in an acutely traumatized sample. *Journal of Clinical Psychiatry, 73*(4), 420–426.

Daniels, J. K., Frewen, P., Theberge, J., & Lanius, R. A. (2016). Structural brain aberrations associated with the dissociative subtype of post-traumatic stress disorder. *Acta Psychiatrica Scandinavica, 133*(3), 232–240.

Deen, B., Pitskel, N. B., & Pelphrey, K. A. (2011). Three systems of insular functional connectivity identified with cluster analysis. *Cerebral Cortex, 21*(7), 1498–1506.

Devilly, G. J., Ciorciari, J., Piesse, A., Sherwell, S., Zammit, S., Cook, F., & Turton, C. (2007). Dissociative tendencies and memory performance on directed forgetting tasks. *Psychological Science, 18*(3), 212–217.

Diekhof, E. K., Geier, K., Falkai, P., & Gruber, O. (2011). Fear is only as deep as the mind allows: a coordinate-based meta-analysis of neuroimaging studies on the

regulation of negative affect. *NeuroImage*, *58*(1), 275–285.

Eich, E., Macaulay, D., Loewenstein, R. J., & Dihle, P.H. (1997). Memory, amnesia , and dissociative identity disorder. *Psychological Medicine*, *8*(6), 417–422.

Elzinga, B. M., Phaf, R. H., Ardon, A. M., & Van Dyck, R. (2003). Directed forgetting between, but not within, dissociative personality states. *Journal of Abnormal Psychology*, *112*(2), 237–243.

Etkin, A., & Wager, T. D. (2007). Functional neuroimaging of anxiety: a meta-analysis of emotional processing in PTSD, social anxiety disorder, and specific phobia. *American Journal of Psychiatry*, *164*(10), 1476-1488.

Fan, L., Li, H., Zhuo, J., Zhang, Y., Wang, J., Chen, L., … Jiang, T. (2016). The human brainnetome atlas: A new brain atlas based on connectional architecture. *Cerebral Cortex*, *26*(8), 3508–3526.

Felmingham, K. L., Williams, L. M., Kemp, A. H., Rennie, C., Gordon, E., & Bryant, R. A. (2009). Anterior cingulate activity to salient stimuli is modulated by autonomic arousal in posttraumatic stress disorder. *Psychiatry Research: Neuroimaging*, *173*(1), 59–62.

Fenster, R. J., Lebois, L. A. M., Ressler, K. J., & Suh, J. (2018). Brain circuit dysfunction in post-traumatic stress disorder: from mouse to man. *Nature Reviews Neuroscience*, 1.

First, M., Spitzer, R., Gibbon, M., & Williams, J. (2002). Structured clinical interview for

DSM-IV-TR axis I disorders, research version, patient edition. New York City, New York: Biometrics Research, New York State Psychiatric Institute.

Fox, M. D., Snyder, A. Z., Vincent, J. L., Corbetta, M., van Essen, D. C., & Raichle, M. E. (2005). The human brain is intrinsically organized into dynamic, anticorrelated functional networks. *Proceedings of the National Academy of Sciences*, *102*(27), 9673–9678.

Frank, D. W., & Sabatinelli, D. (2012). Stimulus-driven reorienting in the ventral frontoparietal attention network: the role of emotional content. F*rontiers in human neuroscience*, *6*, 116.

Fransson, P. (2005). Spontaneous low-frequency BOLD signal fluctuations: an fMRI investigation of the resting-state default mode of brain function hypothesis. *Human Brain Mapping*, *26*(1), 15–29.

Germain, A., James, J., Insana, S., Herringa, R. J., Oomen, M., Price, J., & Nofzinger, E. (2013). A window into the invisible wound of war: Functional neuroimaging of REM sleep in returning combat verterans with PTSD. *Psychiatry Research: Neuroimaging*, *211*(2), 176–179.

Golier, J. A., Yehuda, R., Lupien, S. J., & Harvey, P. D. (2003). Memory for trauma-related information in Holocaust survivors with PTSD. *Psychiatry Research*, *121*(2), 133–143.

Grèzes, J., Tucker, M., Armony, J., Ellis, R., & Passingham, R. E. (2003). Objects automatically potentiate action: an fMRI study of implicit processing. European

Journal of Neuroscience, 17(12), 2735-2740.

Harricharan, S., Nicholson, A. A., Densmore, M., Théberge, J., McKinnon, M. C., Neufeld, R. W. J., & Lanius, R. A. (2017). Sensory overload and imbalance: Resting-state vestibular connectivity in PTSD and its dissociative subtype. *Neuropsychologia*, *106*, 169-178.

Harricharan, S., Rabellino, D., Frewen, P. A., Densmore, M., Théberge, J., Mckinnon, M. C., … Lanius, R. A. (2016). fMRI functional connectivity of the periaqueductal gray in PTSD and its dissociative subtype. *Brain and Behavior*, e00579.

Haufe, S., Meinecke, F., Görgen, K., Dähne, S., Haynes, J.D., Blankertz, B., Biebmann, F. (2014). On the interpretation of weight vectors of linear models in multivariate neuroimaging. *NeuroImage*, *87*, 96–110.

Hopper, J. W., Frewen, P. A., Van Der Kolk, B. A., & Lanius, R. A. (2007). Neural correlates of reexperiencing, avoidance, and dissociation in PTSD: symptom dimensions and emotion dysregulation in responses to script-driven trauma imagery. *Journal of Traumatic Stress*, *20*(5), 713–725.

Kihlstrom, J. F. (2005). Dissociative disorders. *Annual Review of Clinical Psychology*, *1*(1), 227–253.

Kober, H., Barrett, L. F., Joseph, J., Bliss-Moreau, E., Lindquist, K., & Wager, T. D. (2008). Functional grouping and cortical-subcortical interactions in emotion: A meta-analysis of neuroimaging studies. *NeuroImage*, *42*(2), 998–1031.

Kohn, N., Eickhoff, S. B., Scheller, M., Laird, A. R., Fox, P. T., & Habel, U. (2014). Neural network of cognitive emotion regulation - an ALE meta-analysis and MACM analysis. *NeuroImage*, *87*, 345–355.

Krikorian, R., & Layton, B. (1998). Implicit memory in posttraumatic stress disorder with amnesia for the traumatic event. *The Journal of Neuropsychiatry and Clinical Neurosciences*, *10*(3), 359–362.

Kruskal, W. H., & Wallis, W. A. (1952). Use of ranks in one-criterion variance analysis. *Journal of the American Statistical Association*, *47*(260), 583–621

Kurth, F., Zilles, K., Fox, P. T., Laird, A. R., & Eickhoff, S. B. (2010). A link between the systems: functional differentiation and integration within the human insula revealed by meta-analysis. *Brain Structure and Function*, *214*(5–6), 519–534.

Lacadie, C. M., Fulbright, R. K., Constable, R. T., & Papademetris, X. (2008). More accurate talairach coordinates for neuroImaging using nonlinear registration. *NeuroImage*, *42*(2), 717–725.

Lanius, R. A., Rabellino, D., Boyd, J. E., Harricharan, S., Frewen, P. A., & McKinnon, M. C. (2017). The innate alarm system in PTSD: conscious and subconscious processing of threat. *Current Opinion in Psychology*, *14*, 109-115.

Lanius, R. A., Vermetten, E., Loewenstein, R. J., Brand, B., Schmahl, C., Bremner, J. D., & Spiegel, D. (2010). Emotion modulation in PTSD: Clinical and neurobiological evidence for a dissociative subtype. *American Journal of Psychiatry*, *167*(6), 640–647.

Lanius, R. A., Williamson, P. C., Bluhm, R. L., Densmore, M., Boksman, K., Neufeld, R. W., … Menon, R. S. (2005). Functional connectivity of dissociative responses in posttraumatic stress disorder: a functional magnetic resonance imaging investigation. *Biological Psychiatry*, *57*(8), 873–884.

Lanius, R. A., Williamson, P. C., Boksman, K., Densmore, M., Gupta, M., Neufeld, R. W. J., … Menon, R. S. (2002). Brain activation during script-driven imagery induced dissociative responses in PTSD : a functional magnetic resonance imaging investigation. *Biological Psychiatry*, *52*(4), 305–311.

Liddell, B. J., Brown, K. J., Kemp, A. H., Barton, M. J., Das, P., Peduto, A., … Williams, L. M. (2005). A direct brainstem – amygdala – cortical "alarm" system for subliminal signals of fear. *NeuroImage*, *24*(1), 235–243.

Liotti, M., Mayberg, H. S., Brannan, S. K., McGinnis, S., Jerabek, P., & Fox, P. T. (2000). Differential limbic-cortical correlates of sadness and anxiety in healthy subjects: implications for affective disorders. *Biological Psychiatry*, *48*(1), 30–42.

Litz, B. T. (1992). Emotional numbing in combat-related post-traumatic stress disorder: A critical review and reformulation. *Clinical Psychology Review*, *12*(4), 417–432.

Melara, R. D., Ruglass, L. M., Fertuck, E. A., & Hien, D. A. (2018). Regulation of threat in post-traumatic stress disorder: Associations between inhibitory control and dissociative symptoms. *Biological Psychology*, *133*, 89–98.

Menon, V., & Uddin, L. Q. (2010). Saliency, switching, attention and control: a network model of insula function. *Brain Structure and Function*, *214*(5), 655–667.

Montemurro, D., & Bruni, J. (1988). The human brain in dissection. New York City, New York, US: Oxford University Press,

Nicholson, A. A., Friston, K. J., Zeidman, P., Harricharan, S., McKinnon, M. C., Densmore, M., … Lanius, R. A. (2017). Dynamic causal modeling in PTSD and its dissociative subtype: Bottom–up versus top–down processing within fear and emotion regulation circuitry. *Human Brain Mapping*, *38*(11), 5551-5561.

Nicholson, A. A., Densmore, M., McKinnon, M. C., Neufeld, R. W., Frewen, P. A., Théberge, J., ... & Lanius, R. A. (2018). Machine learning multivariate pattern analysis predicts classification of posttraumatic stress disorder and its dissociative subtype: a multimodal neuroimaging approach. *Psychological medicine*, *49*(12), 2049-2059.

Nicholson, A. A., Sapru, I., Densmore, M., Frewen, P. A., Neufeld, R. W. J., Théberge, J., … Lanius, R. A. (2016). Unique insula subregion resting-state functional connectivity with amygdala complexes in posttraumatic stress disorder and its dissociative subtype. *Psychiatry Research: Neuroimaging*, *250*, 61–72.

Paulus, M. P., & Stein, M. B. (2006). An insular view of anxiety. *Biological Psychiatry*, *60*(4), 383–387.

Rabellino, D., Densmore, M., Frewen, P. A., Théberge, J., & Lanius, R. A. (2016). The innate alarm circuit in post-traumatic stress disorder : conscious and subconscious processing of fear- and trauma-related cues. *Psychiatry Research: Neuroimaging*, *248*, 142–150.

Rabellino, D., Densmore, M., Harricharan, S., Jean, T., McKinnon, M. C., & Lanius, R. A. (2018). Resting-state functional connectivity of the bed nucleus of the stria terminalis in post-traumatic stress disorder and its dissociative subtype. *Human Brain Mapping*, *39*(3), 1367-1379.

Rasmussen C.E., Williams, C.K.I. (2006). GPML Toolbox. Adaptive computation and machine learning 11, 1 online resource xviii, 248 p.

Reber, P. J. (2013). The neural basis of implicit learning and memory: a review of neuropsychological and neuroimaging research. Neuropsychologia, 51(10), 2026-2042.

Rugg, M., Mark, R. E., Walla, P., Schloerscheidt, A. M., Birch, C. S., & Allan, K. (1998). Dissociation of the neural correlates of implicit and explicit memory. *Nature*, *392*, 595–598.

Schott, B. H., Henson, R. N., Richardson-Klavehn, A., Becker, C., Thoma, V., Heinze, H.-J., & Duzel, E. (2005). Redefining implicit and explicit memory: the functional neuroanatomy of priming, remembering, and control of retrieval. *Proceedings of the National Academy of Sciences*, *102*(4), 1257–1262.

Schrouff, J., Rosa, M. J., Rondina, J. M., Marquand, A. F., Chu, C., Ashburner, J., … Mourão-Miranda, J. (2013). PRoNTo: Pattern recognition for neuroimaging toolbox. *Neuroinformatics*, *11*(3), 319–337. https://doi.org/10.1007/s12021-013-9178-1

Schrouff, J., Monteiro, J. M., Portugal, L., Rosa, M. J., Phillips, C., & Mourão-Miranda, J. (2018). Embedding anatomical or functional knowledge in whole-brain multiple

kernel learning models. *Neuroinformatics*, *16*(1), 117-143.

Seeley, W. W., Menon, V., Schatzberg, A. F., Keller, J., Gary, H., Kenna, H., … Greicius, M. D. (2007). Dissociable intrinsic connectivity networks for salience processing and executive control. *Journal of Neurosciences*, *27*(9), 2349–2356.

Shalev, A., Liberzon, I., & Marmar, C. (2017). Post-traumatic stress disorder. *New England Journal of Medicine*, *376*(25), 2459–2469.

Shin, L. M., Whalen, P. J., Pitman, R. K., Bush, G., Macklin, M. L., Lasko, N. B., … Rauch, S. L. (2001). An fMRI Study of anterior cingulate function in posttraumatic stress disorder. *Biological Psychiatry*, *50*(12), 932-942.

Sierra, M., & Berrios, G. E. (1998). Depersonalization: neurobiological perspectives. *Biological Psychiatry*, *44*(9), 898–908.

Simmons, A., Paulus, M. P., Thorp, S. R., Matthews, S. C., Norman, S. B., & Stein, M. B. (2008). Functional activation and neural networks in women with posttraumatic stress disorder related to intimate partner violence. *Biological Psychiatry*, *64*(8), 681–690.

Simmons, A., Strigo, I. A., Matthews, S. C., Paulus, M. P., & Stein, M. B. (2009). Initial evidence of a failure to activate right anterior insula during affective set-shifting in PTSD. *Psychosomatic Medicine*, *71*(4), 373–377.

Simmons, W. K., Avery, J. A., Barcalow, J. C., Bodurka, J., Drevets, W. C., & Bellgowan, P. (2013). Keeping the body in mind: insula functional organization and

functional connectivity integrate interoceptive, exteroceptive, and emotional awareness. *Human Brain Mapping*, *34*(11), 2944–2958.

Soares, J. M., Sampaio, A., Ferreira, L. M., Santos, N. C., Marques, P., Marques, F., … Sousa, N. (2013). Stress impact on resting state brain networks. *PLoS ONE*, *8*(6), e66500.

Song, X. W., Dong, Z. Y., Long, X. Y., Li, S. F., Zuo, X. N., Zhu, C. Z., … Zang, Y. F. (2011). REST: A Toolkit for resting-state functional magnetic resonance imaging data processing. *PLoS ONE*, *6*(9), e25031.

Spielberger, C. D. (2010). State-Trait Anxiety Inventory. In *The Corsini Encyclopedia of Psychology*. Hoboken, NJ, USA: John Wiley & Sons, Inc,

Squire, L. R., & Dede, A. J. (2015). Conscious and unconscious memory systems. *Cold Spring Harbor Perspectives in Biology*, *7*(3), a021667.

Stark, E. A., Parsons, C. E., Van Hartevelt, T. J., Charquero-Ballester, M., McManners, H., Ehlers, A., … Kringelbach, M. L. (2015). Post-traumatic stress influences the brain even in the absence of symptoms: A systematic, quantitative meta-analysis of neuroimaging studies. *Neuroscience and Biobehavioral Reviews*, *56*, 207–221.

Stein, M. B., Simmons, A. N., Feinstein, J. S., & Paulus, M. P. (2007). Increased amygdala and insula activation during emotion processing in anxiety-prone subjects. *American Journal of Psychiatry*, *164*(2), 318–327.

Steuwe, C., Daniels, J. K., Frewen, P. A., Densmore, M., Pannasch, S., Beblo, T., …

Lanius, R. A. (2014). Effect of direct eye contact in PTSD related to interpersonal trauma : an fMRI study of activation of an innate alarm system. *Social Cognitive and Affective Neuroscience*, *9*(1), 88–97.

Sun, R., Merrill, E., & Peterson, T. (2001). From implicit skills to explicit knowledge: a bottom-up model of skill learning. *Cognitive Science*, 25(2), 203-244.

Taylor, K. S., Seminowicz, D. A., & Davis, K. D. (2009). Two systems of resting state connectivity between the insula and cingulate cortex. *Human Brain Mapping*, *30*(9), 2731–2745. https://doi.org/10.1002/hbm.20705

Terpou, B. A., Densmore, M., Théberge, J., Frewen, P., McKinnon, M. C., & Lanius, R. A. (2018). Resting-state pulvinar-posterior parietal decoupling in PTSD and its dissociative subtype. *Human Brain Mapping*, 1–13.

Thome, J., Densmore, M., Frewen, P. A., McKinnon, M. C., Théberge, J., Nicholson, A. A., ... & Lanius, R. A. (2017). Desynchronization of autonomic response and central autonomic network connectivity in posttraumatic stress disorder. *Human brain mapping*, 38(1), 27-40.

Tulving, E. (1985). Memory and consciousness. *Canadian Psychology*, *26*(1), 1–12.

Tzourio-Mazoyer, N., Landeau, B., Papathanassiou, D., Crivello, F., Etard, O., Delcroix, N., … Joliot, M. (2002). Automated anatomical labeling of activations in SPM using a macroscopic anatomical parcellation of the MNI MRI single-subject brain. *NeuroImage*, *15*(1), 273–289.

Van der Kolk, B. A., & Fisler, R. (1995). Dissociation and the fragmentary nature of traumatic memories : overview and exploratory study. *Journal of Traumatic Stress*, *8*(4), 505–525.

Vuilleumier, P., Schwartz, S., Duhoux, S., Dolan, R. J., & Driver, J. (2005). Selective attention modulates neural substrates of repetition priming and "implicit" visual memory: suppressions and enhancements revealed by FMRI. *Journal of Cognitive Neuroscience*, *17*(8), 1245–1260.

Wang, K., Jiang, T., Yu, C., Tian, L., Li, J., Liu, Y., … Li, K. (2008). Spontaneous activity associated with primary visual cortex: A resting-state fMRI study. *Cerebral Cortex*, *18*(3), 697–704.

Wang, C., Wu, H., Chen, F., Xu, J., Li, H., Li, H., & Wang, J. (2018). Disrupted functional connectivity patterns of the insula subregions in drug-free major depressive disorder. *Journal of Affective Disorders*, 234, 297-304.

Weathers, F. W., Blake, D. D., Schnurr, P. P., Kaloupek, D. G., Marx, B. P., & Keane, T. M. (2013). The clinician-administered PTSD scale for DSM-5 (CAPS-5). Interview available from the National Center for PTSD at www.ptsd.va.gov.

Woo, C. W., Chang, L. J., Lindquist, M. A., & Wager, T. D. (2017). Building better biomarkers: brain models in translational neuroimaging. *Nature neuroscience*, *20*(3), 365.

Xu, J., Wang, H., Zhang, L., Xu, Z., Li, T., Zhou, Z., … Hu, Q. (2018). Both hypo-connectivity and hyper-connectivity of the insular subregions associated with

severity in children with autism spectrum disorders. *Frontiers in Neuroscience, 12*, 1–9.

Yehuda, R., Hoge, C. W., McFarlane, A. C., Vermetten, E., Lanius, R. A., Nievergelt, C. M., … Hyman, S. E. (2015). Post-traumatic stress disorder. *Nature Reviews Disease Primers, 1*, 15057.

Yu, Z., Lv, Y., Song, L., Liu, D., Huang, X., Hu, X., … Li, H. (2017). Functional connectivity differences in the insular sub-regions in migraine without aura: a resting-state functional magnetic resonance imaging study. *Frontiers in Behavioral Neuroscience, 11*, 1–10.

Zeitlin, S. B., & McNally, R. J. (1991). Implicit and explicit memory bias for threat in post-traumatic stress disorder. *Behaviour Research and Therapy*, *29*(5), 451–457.

Zhang, Y., Zhou, W., Wang, S., Zhou, Q., Wang, H., Zhang, B., … Wang, X. (2018). The roles of subdivisions of human insula in emotion perception and auditory processing. *Cerebral Cortex*,

Chapter 5

5 « A pilot study examining overlapping frontoparietal networks in response to oculomotion and traumatic autobiographical memory retrieval: Implications for eye movement desensitization and reprocessing »

Chapter 4 investigated insula subregion resting-state connectivity patterns with the whole brain in an effort to identify brain regions that may contribute to emotion dysregulation in individuals with PTSD and its dissociative subtype. In Chapter 4, when compared to healthy individuals, individuals with PTSD and its dissociative subtype demonstrated limited connectivity with frontal lobe structures thought critical for higher-order cognitive functions, including emotion regulation. Moreover, consistent with the emotion dysregulation observed in this disorder, even at rest, individuals with PTSD showed increased insula subregion connectivity with subcortical structures thought to evoke innate defensive responses, including hyperemotionality and hypervigilance. By contrast, the dissociative subtype showed increased insula subregion connectivity with ventral posterior brain regions implicated in implicit memory. Interestingly, machine learning analyses indicated further that insula subregion resting-state connectivity patterns may be a used as a potential diagnostic predictor for discriminating between individuals with PTSD, its dissociative subtype, and healthy individuals, where they classified the patterns for each group with 80% balanced accuracy.

The insula has been identified as a critical node that aids in the switching between the default mode network and the central executive network (Dixon et al., 2018; Menon & Uddin, 2010). In the previous chapter, limited insula subregion connectivity with

frontal lobe structures involved in the central executive network in PTSD may point toward a decreased capacity for higher-order executive functions, including emotion regulation. Here, it is important to recall that the insula is hypothesized to play a critical role not only in emotion regulation but is also thought to be a central structure for receiving both interoceptive and exteroceptive sensory information. Thus, investigating the neural circuitry underlying sensory processing through explicit exposure to simultaneous interoceptive and exteroceptive input using a task-based paradigm may delineate further the neurobiological underpinnings of emotion dysregulation in PTSD.

Chapter 5 has been published in its entirety as:

Harricharan, S., McKinnon, M. C., Tursich, M., Densmore, M., Frewen, P., Théberge, J., van der Kolk, B.A., & Lanius, R. A. (2019). Overlapping frontoparietal networks in response to oculomotion and traumatic autobiographical memory retrieval: implications for eye movement desensitization and reprocessing. *European Journal of Psychotraumatology*, *10*(1), 1586265. https://doi.org/10.1080/20008198.2019.1586265

5.1 « Introduction »

In post-traumatic stress disorder (PTSD), traumatic memories tend to be re-experienced as flashbacks of sensory elements of the memory (images, sounds, smells or physical sensations) that are accompanied by intense negative affect (Brewin, Huntley, & Whalley, 2012; Ehlers, Hackmann, & Michael, 2004; van der Kolk & Fisler, 1995). To reduce frequent re-experiencing of traumatic memories and their associated negative affect in PTSD, therapeutic strategies such as eye movement desensitization and reprocessing (EMDR) use eye movements in an attempt to facilitate the reprocessing of traumatic memories (Shapiro, 1989; van der Kolk et al., 2007). Eye movements, i.e.,

oculomotion, have been shown to reduce not only sympathetic activity upon retrieval of a traumatic memory (Barrowcliff, Gray, Freeman, & MacCulloch, 2004), but also to diminish intrusive memories and the vividness associated with them (Andrade, Kavanagh, & Baddeley, 1997; Barrowcliff et al., 2004; Cotter et al., 2017). To date, however, little is known about the possible neurobiological underpinnings of these effects. In this pilot study, we examine specifically the relation between oculomotion and episodic memory by investigating patterns of brain activation in healthy controls and individuals with PTSD during retrieval of traumatic/stressful and neutral memories while performing simultaneously contrasting patterns of oculomotor movements (i.e., saccadic, smooth pursuit, stationary dot fixation). Here, we propose several key neural networks and brain regions central not only to episodic memory retrieval, but also to oculomotion and to accompanying emotional regulation strategies, that may heighten reprocessing of traumatic memories during EMDR.

5.1.1 Dorsal Attentional Network

The dorsal attentional network consists of dorsal frontoparietal brain regions, including the frontal and supplementary eye fields and the intraparietal sulcus. In conjunction with other sensory modalities, including auditory, vestibular and tactile stimuli, eye movements are a key component of the dorsal attentional network, and are critical for probing extrapersonal space to inform one's internal perspective of the world (Corbetta & Shulman, 2002). Sensory information obtained from oculomotion travels to the superior colliculus in the midbrain (Vernet, Quentin, Chanes, Mitsumasu, & Valero-Cabré, 2014). The superior colliculus is then responsible for projections to the frontal eye field in the lateral frontal lobe, which aid in visuospatial attentional processes and visuomotor

movements (see Figure 5.1 for details; also see Grosbras & Paus, 2002; Vernet et al. 2014). The frontal eye field in turn projects to the lateral posterior parietal cortex, which is involved in perceiving spatial information pertaining to one's viewer-centered egocentric space, and thus helps to identify self-location and mental navigation through one's surroundings (Figure 5.1; also see Burgess, 2006; Szczepanski, Pinsk, Douglas, Kastner, & Saalmann, 2013). In addition, the frontal eye fields aid in the evaluation of the environment from a spatial perspective through interactions with the supplementary eye field, which projects to both the lateral and medial posterior parietal cortices to inform both one's viewer (egocentric) and observer (allocentric) perspective (Figure 5.1; also see Szczepanski et al. 2013).

Although eye movements are critical to gathering current visuospatial information required for the optimal functioning of attentional processes that guide working memory (Beck & Hollingworth, 2017; Pearson & Sahraie, 2003; Shipstead et al., 2012), short-term working memory interacts further with long-term episodic memory such that previous experiences provide context to salient stimuli (Baddeley & Hitch 1974; Eriksson et al., 2015; Souza & Oberauer, 2017; Uncapher & Wagner, 2009). Taken together, these findings suggest that salient visuospatial sensory information, guided, in part, by oculomotion, informs perspective on the relevance of incoming sensory input. Interestingly, previous studies have indicated that eye movements performed simultaneously with episodic memory retrieval tax working memory resources; such interference may reduce the capacity to engage in other higher-order tasks reliant upon executive functioning (Maxfield et al., 2008; Op den Kelder et al., 2018).

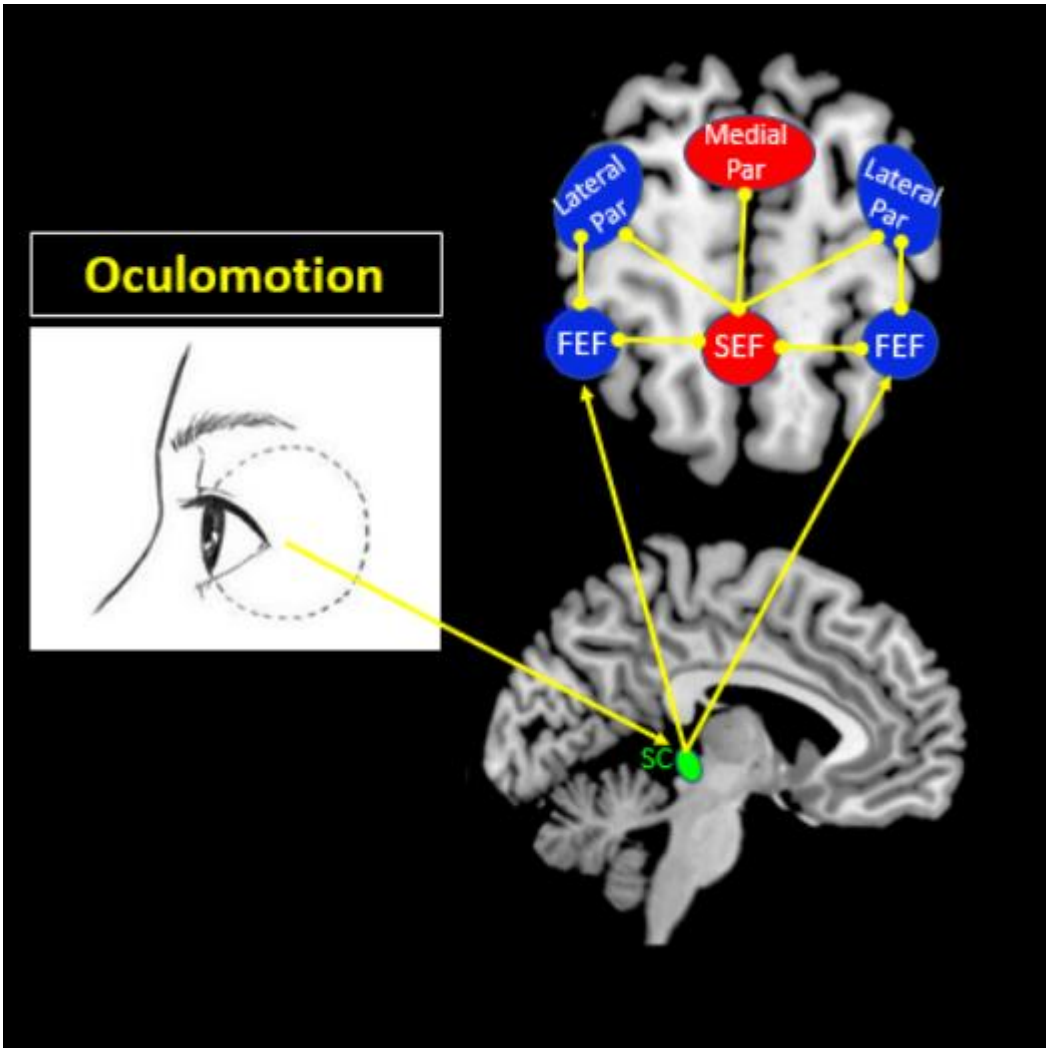

Figure 5.1 *Oculomotor Network.* Visuospatial sensory information obtained from oculomotion travels to the superior colliculus in the midbrain via cranial nerves III, IV and VI. The superior colliculus can project visuospatial afferents to the frontal eye field to engage the dorsal visual stream, which is a functional component of the dorsal attentional network that helps guide one's visuospatial processing of the external environment. The frontal eye field functionally connects with the lateral posterior parietal cortex, where one can process visuospatial details related to one's viewer-centered egocentric perspective (i.e., identifying one's self-location). The frontal eye field also interacts with the supplementary eye field, which maintains connections with both the lateral and medial parietal cortices. The supplementary eye field through its connections with the parietal cortex can process visuospatial details from both an egocentric and

observer-centered allocentric perspective, as it can identify one's self-location based on identifying objects or external locations in the environment. The eye clipart image was retrieved and adapted from a free public domain (clker.com, Rolera LLC).

5.1.2 Frontoparietal Executive Control Network

This dynamic relationship between working memory and long-term episodic memory depends critically on the ability to use salient sensory information to guide retrieval of episodic autobiographical memories (Baddeley, 2010; Burianova, McIntosh, & Grady, 2010). Dixon et al. (2018) describes a frontoparietal executive control network comprised of two functional subdivisions involved in sensorimotor and introspective processes, respectively. Here, the sensorimotor frontoparietal subdivision is thought to orient, via oculomotor movements, to salient multisensory cues in the external environment, (Corbetta and Shulman, 2002), thus assisting in mapping sensory information in the environment through visual search. This subdivision overlaps with neural regions implicated in the dorsal attentional network, including the frontal/supplementary eye fields and the right inferior parietal lobule. By contrast, the introspective frontoparietal subdivision is thought to mediate internally-based mental thoughts and emotion processing and overlaps with areas involved in autobiographical memory and self-referential processing, including the medial prefrontal cortex. These functional subdivisions of a larger frontoparietal cognitive control network are thought to work in tandem to carry out higher-order cognitive tasks, including emotion regulation.

5.1.3 The Role of Oculomotion in Integration of Autobiographical Memories

Commonly, autobiographical memories are appraised on a continuum of positive to negative valence, a process associated with changes in physiological homeostasis in response to internal and/or external reminders of the memory (Morawetz, Bode, Derntl, & Heekeren, 2017; Picó-Pérez, Radua, Steward, Menchón, & Soriano-Mas, 2017). Here, individuals may modulate emotional appraisal of a negative memory by introducing emotion regulation strategies, where one attempts to adjust the internal affective representation of a subjective memory (Morawetz et al., 2017; Picó-Pérez et al., 2017; Zilverstand, Parvaz, & Goldstein, 2017). Critically, in traumatic memory, reappraisal strategies target the down-regulation of negative affective representations associated with the memory in an attempt to reduce its emotional impact. This conscious top-down emotion regulation is thought to engage a frontoparietal network involving brain regions similar to those implicated in oculomotion and in autobiographical memory, including the right dorsolateral and ventrolateral prefrontal cortex, which may work in tandem to attenuate the intense negative affect underlying traumatic memories (Zilverstand et al., 2017).

Previous studies have demonstrated that the vividness of traumatic memories are reduced when memory retrieval is performed simultaneous to horizontal eye movements (Andrade et al., 1997; Barrowcliff et al., 2004; Littel et al., 2017; Thomaes, Engelhard, Sijbrandij, Cath, & Van den Heuvel, 2016). However, no study has sought to investigate the neural underpinnings of this effect, where significant overlap is observed in the

frontoparietal networks believed involved in oculomotion, autobiographical memory and emotional regulation. Identification of frontal and parietal neural regions common to these processes may assist in delineating the neurobiological mechanisms contributing to traumatic memory reprocessing using eye movements and provide an organizing framework to identify neural targets for EMDR.

5.1.4 Objectives

Accordingly, we sought to identify the neural architecture associated with traumatic/stressful autobiographical memory retrieval during simultaneous performance of horizontal smooth pursuit or saccadic eye movements in patients with PTSD and in healthy controls. Specifically, we hypothesized that: 1) traumatic/stressful memory retrieval during performance of horizontal eye movements would engage the two functional subdivisions of the larger frontoparietal executive control network proposed by Dixon et al. (2018) and thought to be involved in sensorimotor and introspective processing. We hypothesized: 2) a) that oculomotor eye movements would activate sensorimotor brain regions in the dorsal attentional network, including the frontal and supplementary eye fields; b) that activation of the dorsal attention network in conjunction with traumatic/stressful autobiographical memory retrieval would recruit frontal and parietal brain regions involved in introspective processing; and c) that dual sensorimotor and introspective processing would initialize a larger frontoparietal executive control network that recruits areas involved in higher-order cognitive demands, including emotion regulation. In keeping with our own work (Lanius et al., 2004), we hypothesized further that: 3) individuals with PTSD would show group differences during traumatic

memory retrieval as compared to those without PTSD. Furthermore, we hypothesized that: 4) in individuals with PTSD, as compared to controls, activation of the dorsal attentional network through eye movements would enhance the recruitment of regions involved in self-referential processing and emotion regulation, thus laying a foundation for understanding of the neurobiological mechanisms underlying EMDR.

5.2 Methods

5.2.1 Clinical and Demographic Information

Thirty-nine participants participated in the present study, including 20 patients with PTSD and 19 age- and gender-matched healthy controls. Recruitment for the study took place during 2014-2016, via referrals from family physicians, mental health professionals, psychology/psychiatric clinics, community programs for traumatic stress, and posters/advertisements within the London, Ontario community.

Inclusion criteria for the study included a PTSD diagnosis based on the Clinician-Administered PTSD Scale (CAPS), versions IV (Blake et al., 1995; n=26, PTSD diagnosis if score>50) and 5 (Weathers et al. 2013; n=13, different scoring system with no definitive cut-off). For all participants, a Structured-Clinical Interview for DSM-IV Axis-I disorders (SCID; First, Spitzer, Gibbon, & Williams, 2002) was administered, along with a battery of questionnaires assessing trait psychological symptoms, including the Beck Depression Inventory (BDI; Beck, Guth, Steer, & Ball, 1997), Child Trauma Questionnaire (CTQ; Bernstein & Fink, 1998; 94% of participants had histories of childhood trauma, i.e., they scored above the ‘none/minimal’ threshold for any trauma category), and the Multiscale Dissociation Inventory (MDI; Briere, Weathers, & Runtz,

2005). In addition, during the scan, the Responses to Script-Driven Imagery scale (RSDI; Hopper et al., 2007), State-Trait Anxiety Inventory (STAI; Spielberger, 2010), and the Clinician-Administered Dissociative States Scale (CADSS; Bremner et al., 1998) were used to assess state-based psychological responses. The clinical and demographic characteristics of the study sample are detailed in Table 5.1.

Participants were excluded if 3.0T scanner safety regulations were violated, including the presence of metal implants, and/or if participants experienced previous head trauma associated with a loss of consciousness, significant untreated medical illness, and/or pervasive developmental disorders. Additional exclusion criteria for PTSD patients included current or past history of bipolar or psychotic disorders, and/or alcohol/substance dependency or abuse for at least six months prior to partaking in the study. Control participants were ineligible if lifetime criteria were met for any Axis-I psychiatric disorder from the SCID assessment. If eligible, participants provided written informed consent to participate in the study. No eligible participants were subsequently excluded from study nor did any of the participants drop out over the course of the study. All scanning was conducted in London, Ontario at Robarts Research Institute's Centre for Functional Metabolic Mapping. The study was approved by the Research Ethics Board at Western University of Canada.

Table 5.1 ***Clinical and Demographic Information***

Measure	**PTSD**	**Healthy Controls**	**t-test/χ^2(P)**
N	20	19	
Sex	M=8, F=12	M=8, F=11	0.894
Age	38.8 ± 14.3	39.3 ± 13.5	0.908

CAPS-IV Total (n=26)	82.7 ± 16.3	0.6 ± 1.3	<0.001*
CAPS-5 Total (n=13)	34.7 ± 9.6	0	<0.001*
CTQ-Total	65.8 ± 21.0	34.8 ± 13.6	<0.001*
BDI-Total	27.0 ± 7.0	1.2 ± 2.0	<0.001*
MDI-Total	61.2 ± 12.7	33.3 ± 13.0	<0.001*
MDI-Depersonalization	7.9 ± 2.5	5 ± 0	<0.001*
MDI-Derealization	9.7 ± 3.8	6.3 ± 1.0	<0.001*
Initial RSDI-Total	22.4 ± 6.6	15.5 ± 3.0	0.002*
Initial RSDI-Dissociation^{avg}	2.6 ± 0.2	5.0 ± 3.3	0.011*
MDD	n=3(3)	-	
Panic Disorder/Agoraphobia	n=3	-	
Social Phobia	None	-	
OCD	n=(2)	-	
GAD	None	-	
Ratings of Emotional Experience After Traumatic Memory Retrieval (Scale of 1-6)			
Fear	3.1±2.3	0.6±1.1	<0.001*
Anger	3.6±2.2	0.6±1.2	<0.001*
Guilt	2.4±2.3	0.5±1.3	0.003*
Happiness	0.2±0.6	0.2±0.6	0.96
Sadness	3.7±2.1	1.7±2.4	0.01*

Shame	2.7±2.2	0.2±0.7	<0.001*
Disgust	2.7±2.4	0.3±0.8	<0.001*

Age, sex, CAPS, and self-report questionnaires (CTQ, MDI, BDI) are reported as mean±SD. Psychiatric illnesses assessed via SCID-I (MDD, Panic Disorder/Agoraphobia, Social Phobia, OCD and GAD) are reported in frequencies, as n = current(past) cases. *Dissociation*^{avg} indicates averaged depersonalization and derealization symptom measures based on responses to the RSDI scale.

Abbreviations: PTSD, post-traumatic stress disorder; CAPS, Clinician-Administered PTSD Scale; CTQ, Child Trauma Questionnaire; BDI, Beck Depression Inventory; MDI, Multiscale Dissociation Inventory; RSDI, Responses to State-Driven Imagery Scale; MDD, Major Depressive Disorder; OCD, Obsessive Compulsive Disorder; GAD, Generalized Anxiety Disorder. (* = $p<0.05$).

5.2.2 Data Acquisition

Whole-brain functional magnetic resonance imaging (fMRI) data were collected in a 3.0T scanner (Magnetom Tim Trio, Siemens Medical Solutions, Erlangen, Germany) with a 32-channel phased array head coil. BOLD (blood oxygen level dependent) fMRI were collected using a manufacturer's standard gradient-echo planar imaging (EPI) pulse sequence (single-shot, blipped-EPI) with an interleaved slice acquisition per the following specifications: Time Resolution (TR) = 3000 ms, Echo Time (TE) = 20 ms, voxel size = 2 × 2 × 2 mm^3, Field of View (FOV) = 192 × 192 × 128 mm^3 (94 × 94 matrix, 64 contiguous slices), and Flip Angle (FA) = 90°. High-resolution T1-weighted anatomical images were also collected (MPRage: 192 slices, voxel size = 1 × 1 × 1 mm^3).

5.2.3 Eye Movement Scan Procedure

All participants were asked to retrieve both neutral and traumatic/stressful autobiographical memories via a single personalized word cue associated with each memory (chosen by participants prior to the study; whereas PTSD participants retrieved traumatic memories, controls retrieved their most stressful memories) while following a moving dot to guide eye movements across the screen (see Figure 5.2). In order to maintain safety, participants were instructed to select a word representing a traumatic/stressful memory that would be distressing upon retrieval, but not to an extent that a particular memory would inhibit a participant's capacity to partake in the study. All participants were video recorded throughout the experiment and the recordings were visually inspected to ensure they were performing eye movements while in the scanner. In total, there were three conditions, each lasting 13 minutes, conducted in the following order: no memory retrieval, neutral memory retrieval and traumatic/stressful memory retrieval. Each condition consisted of twelve runs, separated into four blocks that were presented in a randomized order. For each block, *one* of four types of oculomotor stimuli (either a stationary fixation dot, a horizontal smooth pursuit, a horizontal saccadic pursuit, or a vertical saccadic pursuit) was presented in three consecutive runs. Each run lasted 39 seconds, which included: (i) collection of an implicit baseline measure (6 seconds); (ii) display of a personalized word cue for neutral or traumatic/stressful memory retrieval (e.g. "comb" for a neutral memory, "knife" for a traumatic memory) (3 seconds); and (iii) presentation of an oculomotor stimulus (30 seconds). Firstly, a black central stationary dot was displayed for 6 seconds to obtain an implicit baseline measure (explained below; see Bremner et al., 1999; Lanius et al., 2004). After the implicit

baseline was collected, participants were then instructed to retrieve autobiographical memories after reading a personalized word cue displayed on the screen for 3 seconds (replaced with a '+' symbol in the no memory retrieval condition). Subsequently, the oculomotor stimulus, coloured circles to guide eye movements across the screen, was presented for 30 seconds while participants continued to engage with the memory. After three consecutive runs involving the same oculomotor stimulus, participants were asked to rate the severity of PTSD symptoms they experienced during memory retrieval with the specific adjunctive oculomotor stimulus, including emotional intensity, numbing, dissociation, re-experiencing and vividness of memory. Afterwards, an 18-second rest interval using a black stationary fixation '+' led to a transition into a new block that presented a different oculomotor stimulus. This process was repeated four times to evaluate each type of oculomotor stimulus. Both prior to the experiment and after each condition (no memory retrieval, neutral memory retrieval and traumatic/stressful memory retrieval), participants were asked to rate the severity of reexperiencing, avoidance and dissociative symptoms experienced in the scanner based on the Responses to Script-Driven Imagery Scale (see Table 1; RSDI; Hopper, Frewen, Sack, Lanius, & Van Der Kolk, 2007). In addition, participants were asked to report intensity ratings (on a Likert scale of 1 to 6) of different negative emotions experienced after each memory retrieval condition (see Table 1). After the scan, a brief interview was administered to assess whether participants were successful in retrieving the memories during the scanning protocol.

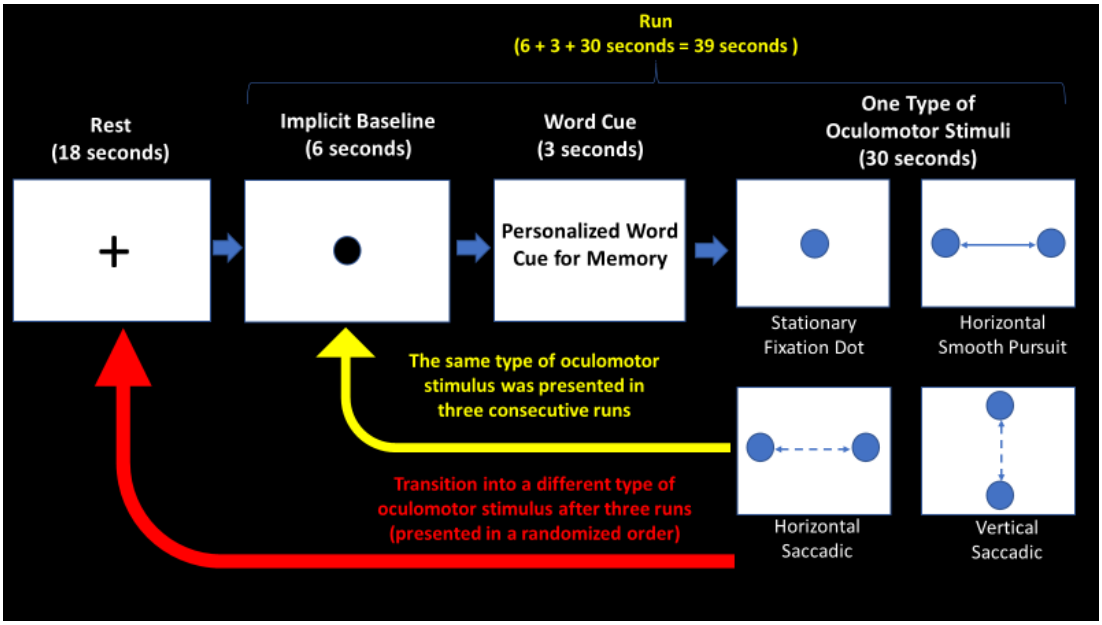

Figure 5.2 *Experimental Paradigm*. All participants were asked to retrieve both neutral and traumatic autobiographical memories via a personalized word cue associated with each memory, while following a moving dot to guide eye movements across the screen. In total, there were three conditions, each lasting 13 minutes, conducted in the following order: no memory retrieval, neutral memory retrieval and traumatic memory retrieval. Each condition consisted of twelve runs, separated into four blocks to present each type of oculomotor stimulus in three consecutive runs (stationary fixation dot, a horizontal smooth pursuit, a horizontal saccadic pursuit and a vertical saccadic pursuit). Each run lasted (6 + 3 + 30) 39 seconds, where a black central stationary dot was displayed for 6 seconds to obtain an implicit baseline measure, after which participants were instructed to retrieve autobiographical memories while reading a single personalized word cue displayed on the screen for 3 seconds (replaced with a '+' symbol in the no memory retrieval condition). Immediately following, participants were asked to continue retrieving the memory while 30 seconds of one type of oculomotor stimulus was presented using coloured circles to guide eye movements across the screen. After three consecutive runs using the same type of oculomotor stimulus, participants were then asked to rate the severity of PTSD symptoms they experienced during memory retrieval with the specific adjunctive oculomotor stimulus, including emotional intensity, numbing, dissociation, re-experiencing and vividness of memory. Afterwards, an 18-

second rest interval using a black stationary fixation '+' led to a transition into a new type of oculomotion. This process was repeated four times to evaluate the effects of each type of oculomotor stimulus.

5.2.3.1 Implicit Baseline

The implicit baseline measure is a quantitative estimation of a null period during the experiment where the participant is not engaged in task-related activities, and it can also be used as a reset period to obtain a baseline measure between tasks (Bremner et al., 1999; Lanius et al., 2004). In the present study, the implicit baseline measure was a black stationary fixation dot displayed for 6 seconds before the oculomotor stimulus was presented within each run.

5.2.4 fMRI Preprocessing

Image preprocessing and statistical analyses were performed using Statistical Parametric Mapping software (SPM12; Wellcome Trust Centre for Neuroimaging) within MATLAB 8.6 (R2015b; MathWorks). The functional images collected for each condition were realigned to the first volume of the scan. The images were then normalized to an MNI anatomical template and spatially smoothed to a Gaussian kernel of 8mm full-width half maximum (FWHM).

5.2.5 fMRI Statistical Analysis

Voxel-wise general linear models were used to investigate activation patterns during each condition. For each subject, a BOLD-contrast map was developed for each type of oculomotor stimulus within each memory retrieval condition (e.g. no memory horizontal smooth pursuit, traumatic/stressful memory horizontal saccadic pursuit etc.). ART (version 2015-10; Gabrieli Lab, McGovern Institute) motion parameters were included as

covariates in all within-subject analyses for all statistical analyses (including subtraction analysis and subsequent psychophysiological interactions). A 2x3x4 full-factorial subtraction analysis was employed to examine interaction effects of group (PTSD, controls), memory retrieval (no memory, neutral memory and stressful/traumatic memory) and oculomotion (horizontal smooth pursuit, horizontal saccadic pursuit, vertical saccadic pursuit, stationary dot fixation) versus the implicit baseline as described above, thus all results obtained from this analysis are based on comparisons to no oculomotor stimuli. Results were reported at family-wise error (FWE) voxel-wise whole-brain corrected threshold of $p<0.05$, with a cluster extent threshold of $k=10$, in accordance with Eklund et al. (2016). In order to examine our primary question concerning the correlation of oculomotion with frontal and parietal neural correlates involved in autobiographical memory retrieval and top-down emotion regulation, the right frontal and supplementary eye fields were observed as peak areas of activation across all factors and were therefore selected as seed regions in psychophysiological interaction (PPI) analyses to explore their functional connectivity patterns with the whole brain.

A region-of-interest (ROI) approach was used to investigate group comparisons in the PPI analyses between seed regions and four brain regions, identified *a priori* using coordinates from various meta-analyses employing activation likelihood estimation methodology: (1) the right dorsomedial prefrontal cortex [*x:*10, *y:*40, *z:*52] associated with mentalization of autobiographical memories (Andrews-Hanna, Saxe, & Yarkoni, 2014); (2) the right dorsolateral prefrontal cortex [*x:*40, *y:*23, *z:*44] and (3) the right anterior insula [*x:*44, *y:*16, *z:*4] linked to cognitive reappraisal emotion regulation

strategies (Morawetz et al., 2017); and (4) the right posterior insula [*x:*-35, *y:*-13, *z:*9] associated with interoception based on insular functional mapping (Kurth, Zilles, Fox, Laird, & Eickhoff, 2010). A 10mm sphere was created around the coordinates listed above using PickAtlas software (Maldjian, Laurienti, Kraft, & Burdette, 2003) and was used in a ROI-correction analysis for clusters that did not survive the family-wise error voxel-wise threshold $p<0.05$, $k=10$. Significant clusters identified in the ROI analyses were adjusted for multiple comparisons at a voxel-wise FWE-corrected threshold set at $p\leq0.0125$, k=10, calculated by dividing the original *p*FWE <0.05 threshold by four to account for each ROI used. Finally, we correlated neuroimaging data from the PPI analyses with self-reported clinical state symptom scores collected in the scanner (RSDI, STAI, CADSS) and trait symptom scores collected prior to experiment (MDI, BDI, CAPS).

5.3 Results

5.3.1 fMRI Statistical Analyses

The peak coordinates of activation in the omnibus ANOVA test included the right frontal eye field (FEF) [**x**:46, **y**:0, **z**:56] and the right supplementary eye field (SEF) [**x**:2, **y**:2, **z**:62], which were used subsequently as seed regions for psychophysiological interaction analyses (PPIs) to explore their functional connectivity with the frontal and parietal brain regions listed as regions-of-interest above (right dorsomedial prefrontal cortex, right dorsolateral prefrontal cortex, right anterior insula and right posterior insula). Additional cortical regions that were activated in the ANOVA effect, interactions and main factor effects are listed in Appendix D. Although we present inclusively all post-hoc results from the ANOVA in Appendix D, including all measures from each factor, we discuss

here horizontal saccadic and smooth pursuit eye movements in the context of traumatic/stressful memory only, as these are of primary interest for studying the underpinnings of emotion regulation using horizontal eye movements during EMDR. All results are based on comparisons to the implicit baseline measure (without oculomotor stimuli).

5.3.2 Psychophysiological Interactions

5.3.2.1 Right Frontal Eye Field

Significant regions in the PPI omnibus ANOVA test are listed in the supplementary material. There were no significant two-way or three-way interactions observed between the memory, oculomotion or participant group factors, and no significant clusters within the main effect for each factor. Post-hoc one-sample t-tests within each variable did not yield significant connectivity with the frontal and parietal brain regions studied.

5.3.2.1.1 Between Participant Group, Within Motion, Between Memory

As compared to the PTSD group, the healthy control group showed increased right FEF connectivity with the right posterior insula during horizontal smooth pursuit eye movements in the traumatic/stressful memory retrieval versus neutral memory retrieval condition (Table 5.2a; Figure 5.3a).

5.3.2.1.2 Between Participant Group, Between Motion, Between Memory

As compared to the healthy control group, the PTSD group showed increased right FEF connectivity with the right dorsolateral prefrontal cortex during horizontal smooth

pursuit>horizontal saccadic eye movements in the traumatic/stressful memory retrieval versus no memory retrieval condition (Table 5.2a; Figure 5.3a).

Table 5.2 *Right frontal and supplementary eye field psychophysiological interaction post-hoc two-sample t-tests and correlations with clinical dissociative symptoms*

	LR	**BA**	**Region**	**k**	**vFWE**	**Z-Score**	**MNI Coordinates**		
							x	**y**	**z**
A. Right Frontal Eye Field Psychophysiological Interaction Post-hoc Analysis									
Between Group, Within Motion, Between Memory									
Control>PTSD Traumatic/stressful>Neutral Memory Smooth Pursuit	R	13	Posterior Insula	18	0.007*	4.08	36	4	14
Between Group, Between Motion, Between Memory									
PTSD>Control Traumatic/stressful>No Memory Smooth Pursuit>Saccadic	R	9	Dorsolateral Prefrontal Cortex	12	0.005*	4.19	48	28	38
B. Right Supplementary Eye Field Psychophysiological Interaction Post-hoc Analysis									

Between Group, Within Motion, Within Memory									
Control>PTSD Traumatic/stressful Memory Saccadic	L/R	7	Precuneus	161	0.020	5.07	0	-70	56
PTSD>Control Traumatic/stressful Memory Smooth Pursuit	R	8	Dorsomedial Prefrontal Cortex	42	0.002*	4.06	10	36	58
Between Group, Within Motion **Between Memory**									
Control>PTSD Traumatic/stressful>No Memory Saccadic	L/R	7	Precuneus	376	0.017	5.19	0	-70	56
Between Group, **Between Motion, Within Memory**									
PTSD>Control Traumatic/stressful Memory Smooth Pursuit>Fixation Dot	R	8	Dorsolateral Prefrontal Cortex	43	0.001*	4.40	36	24	38
PTSD>Control Traumatic/stressful Memory Smooth Pursuit>Saccadic	R	9	Dorsomedial Prefrontal Cortex	50	0.001*	4.45	8	34	56

	R	8	Dorsolateral Prefrontal Cortex	57	0.008*	3.93	42	22	44
Between Group, Between Motion, Between Memory									
PTSD>Control Traumatic/stressful>Neutral Memory Saccadic>Fixation Dot	R	44	Anterior Insula	10	0.002*	4.49	48	14	14
C. Negative Supplementary Eye Field Connectivity with Dissociation Measures									
MDI-Total Trait Dissociative Measures									
	R	9	Dorsolateral Prefrontal Cortex	14	0.004*	4.35	42	34	42
RSDI-Dissociative State Dissociative Measures									
	R	9	Dorsolateral Prefrontal Cortex	11	0.002*	4.40	44	32	42

Exploratory functional connectivity analyses (psychophysiological interaction) of the (A) right frontal eye field and (B) right supplementary eye field seed regions during traumatic memory retrieval with concurrent horizontal smooth pursuit and horizontal saccadic eye movements versus the implicit baseline. Section (C) shows negative supplementary eye field exploratory functional connectivity correlations with increasing clinical trait

dissociative and state dissociative measures in PTSD during traumatic memory retrieval with simultaneous horizontal smooth pursuit eye movements.

Results are listed at *p*FWE<0.05, those marked with an * are region-of-interest corrected at *p*FWE≤0.0125 with adjusting for multiple comparisons.

Abbreviations: LR, left/right hemisphere; BA, Brodmann Area; k, cluster size; vFWE, voxel-wise family-wise error corrected; MNI, Montréal Neurological Institute; MDI, Multiscale Dissociation Inventory; RSDI, Responses to Script-Driven Imagery Scale.

5.3.2.2 Right Supplementary Eye Field

Significant regions in the PPI omnibus ANOVA test, interactions and main factor effects are listed in the supplementary material. Post-hoc one-sample t-tests within each variable did not yield significant connectivity with the frontal and parietal brain regions studied.

5.3.2.2.1 Between Participant Group, Within Motion, Within Memory

As compared to the healthy control group, the PTSD group showed increased right SEF connectivity with the right dorsomedial prefrontal cortex during horizontal smooth pursuit eye movements in the traumatic/stressful memory retrieval condition. By contrast, as compared to the PTSD group, the healthy control group showed increased right SEF connectivity with the medial precuneus during horizontal saccadic eye movements in the traumatic/stressful memory retrieval condition (Table 5.2b; Figure 5.3b).

5.3.2.2.2 Between Participant Group, Within Motion, Between Memory

As compared to the PTSD group, the healthy control group showed increased right SEF connectivity with the medial precuneus during horizontal saccadic eye movements in the

traumatic/stressful memory retrieval versus no memory retrieval condition (Table 5.2b; Figure 5.3b).

5.3.2.2.3 Between Participant Group, Between Motion, Within Memory

As compared to the healthy control group, the PTSD group showed increased right supplementary eye field connectivity with the right dorsolateral prefrontal cortex during horizontal smooth pursuit eye movements as compared to *both* the stationary central fixation dot stimulus and the horizontal saccadic eye movements in the traumatic/stressful memory retrieval condition. In addition, as compared to the healthy control group, the PTSD group showed increased right SEF connectivity with the right dorsomedial prefrontal cortex during horizontal smooth pursuit as compared to horizontal saccadic eye movements during the traumatic/stressful memory retrieval condition (Table 5.2b; Figure 5.3b).

5.3.2.2.4 Between Participant Group, Between Motion, Between Memory

As compared to the healthy control group, the PTSD group showed increased right SEF connectivity with the right anterior insula during horizontal saccadic eye movements>the stationary central fixation dot stimulus in the traumatic/stressful versus neutral memory retrieval condition (Table 5.2b; Figure 5.3b).

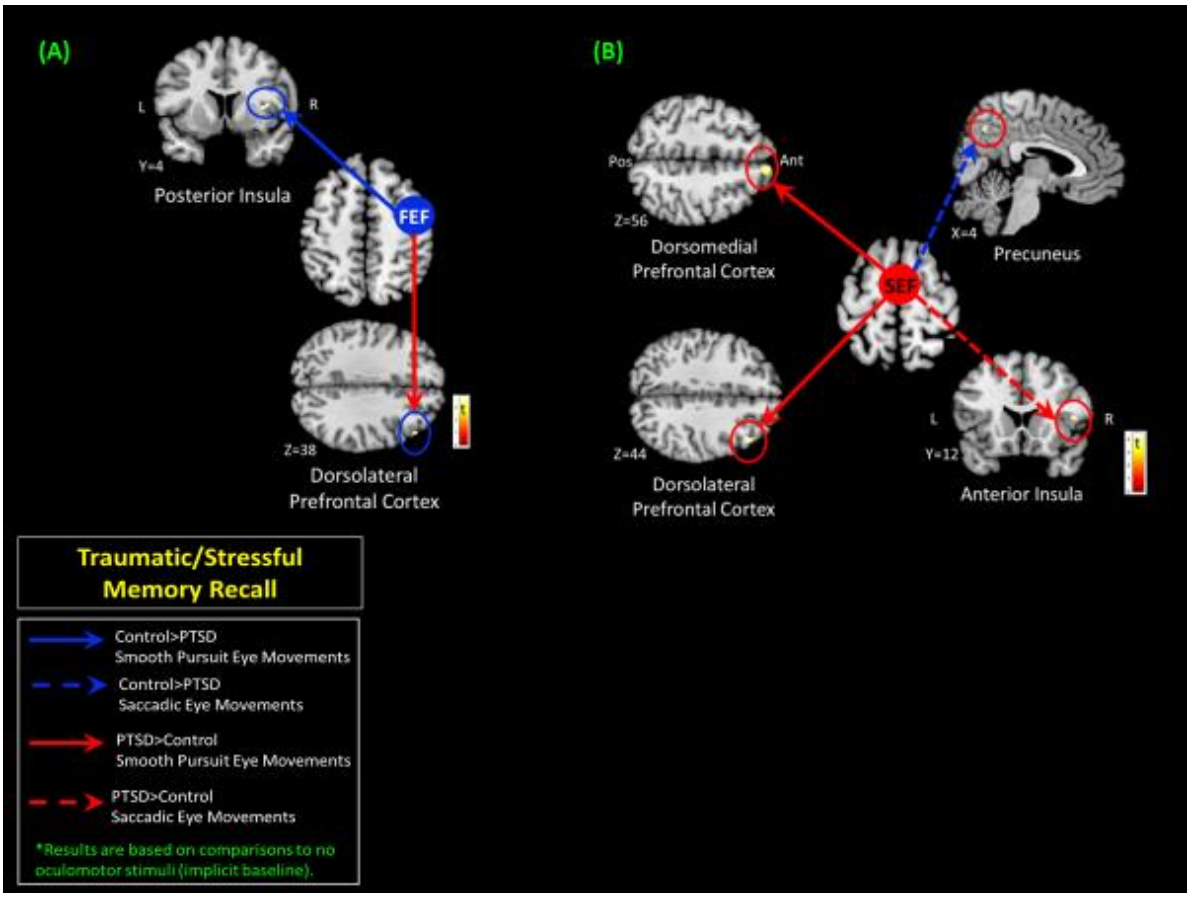

Figure 5.3 *Explorative functional connectivity analyses (psychophysiological interaction) of the (A) right frontal eye field [FEF; (x: 46, y: 0, z: 56)] and the (B) right supplementary eye field [SEF; (x: 2, y: 2, z: 62)] seed regions during the traumatic memory retrieval condition.* (A) During retrieval of a traumatic/stressful memory, as compared to the PTSD patient group, healthy controls demonstrated increased right FEF connectivity with the right posterior insula with simultaneous smooth pursuit eye movements. In contrast, as compared to healthy controls, PTSD patients demonstrated increased right FEF connectivity with the right dorsolateral prefrontal cortex during retrieval of a traumatic memory with simultaneous smooth pursuit eye movements. (B) During retrieval of a traumatic/stressful memory with smooth pursuit eye movements, as compared to healthy controls, PTSD patients showed increased right SEF connectivity with the right dorsomedial and the right dorsolateral prefrontal cortices. In addition, as compared to controls, PTSD showed increased right SEF connectivity with the right anterior insula during retrieval of a traumatic memory with concurrent saccadic eye

movements. All results are shown at pFWE≤0.0125, k=10, to correct for multiple comparisons; however, the precuneus is pFWE whole-brain corrected at p<0.05, k=10.

5.3.2.2.5 Clinical Correlations

Trait dissociative symptoms, measured by the self-reported MDI scale prior to the study, correlated negatively with right SEF connectivity with the right dorsolateral prefrontal cortex in the PTSD group during traumatic memory retrieval while performing concurrent horizontal smooth pursuit eye movements. Moreover, dissociative symptoms reported by the PTSD group in the scanner just prior to the experiment and measured by the RSDI scale correlated negatively with right SEF connectivity with the right dorsolateral prefrontal cortex during traumatic memory retrieval with concurrent horizontal smooth pursuit eye movements (Table 2c; Figure 5.4). No significant correlations emerged between dissociative symptoms and right FEF connectivity patterns.

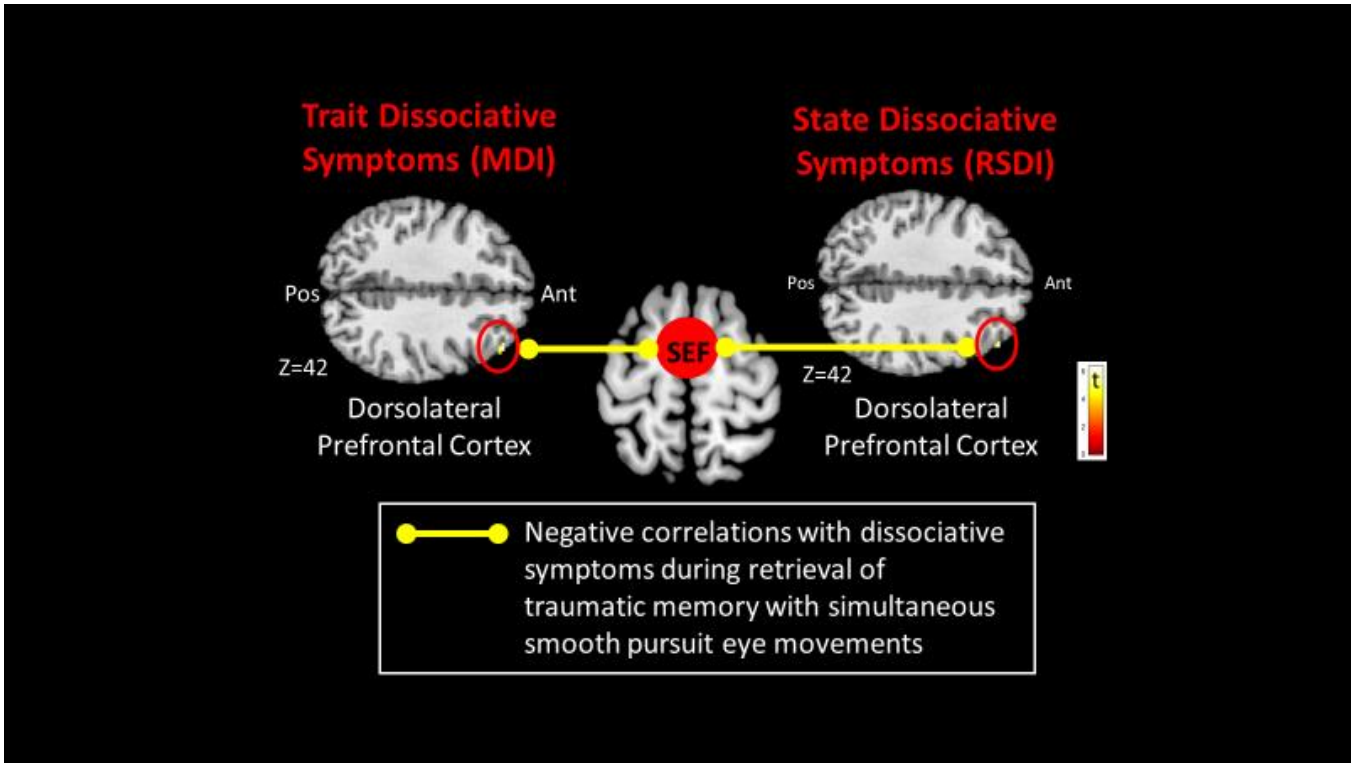

Figure 5.4 *Explorative negative functional connectivity correlations with clinical dissociative measures in the right supplementary eye field psychophysiological interaction during the traumatic memory retrieval condition.* During retrieval of a traumatic memory with horizontal smooth pursuit eye movements, trait dissociation (MDI) symptoms and state dissociation symptoms (RSDI) measures collected just prior to the scan correlated negatively with right supplementary eye field connectivity with the right dorsolateral prefrontal cortex. Results are shown at pFWE≤0.0125, k=10, corrected for multiple comparisons.

5.4 Discussion

In a pilot study aimed at enhancing our current understanding of the neurobiological mechanisms underlying EMDR therapy, we examined how oculomotion influences the neural circuitry engaged during retrieval of traumatic/stressful autobiographical memories in PTSD and healthy controls. We hypothesized initially that eye movements would activate the dorsal attentional network at the frontal and supplementary eye fields.

In turn, this network was expected to interact with frontoparietal brain regions involved in autobiographical memory retrieval, thus initializing a larger frontoparietal executive control network that recruits areas involved in higher-order cognitive demands, including emotion regulation. Overall, our results supported these hypotheses, demonstrating that frontoparietal regions involved in autobiographical memory retrieval and emotion regulation show connectivity with the right frontal and supplementary eye fields during the retrieval of a traumatic/stressful memory while performing concurrent horizontal saccadic and smooth pursuit eye movements. A full summary of study results can be found in the supplementary material. In keeping with previous studies (see Andrade et al., 1997; Barrowcliff et al., 2004), however, we discuss here only those results pertaining to the implementation of horizontal eye movements during retrieval of traumatic/stressful memories as these findings have direct relevance to identifying the neural mechanisms underlying EMDR. In addition, we highlight below the influence of simultaneous oculomotion during traumatic/stressful autobiographical memory retrieval on the recruitment of a frontoparietal executive control network that has the potential to facilitate top-down emotion regulation.

5.4.1 Top-Down Emotion Regulation

The findings of the present study point towards co-activation of the two functional subdivisions of the frontoparietal executive control network (Dixon et al. 2018), where ocular sensorimotor processing and introspection during traumatic/stressful autobiographical memory retrieval are thought to work in tandem to facilitate higher-order cognitive processes such as emotion regulation. Specifically, during traumatic/stressful memory retrieval with simultaneous horizontal smooth pursuit eye

movements, as compared to controls, the PTSD group showed increased right frontal and supplementary eye field connectivity with the right dorsolateral prefrontal cortex, as well as increased right supplementary eye field connectivity with the right dorsomedial prefrontal cortex.

Pagani et al. (2012), in trying to elucidate the role of eye movements in cognitive processing of traumatic memories during EMDR, suggest that the prefrontal cortex is central to this processing due to its involvement in self-referential processing of the emotional content underlying a memory. Indeed, self-referential processing is thought critical for event processing, as it aids in introspective reflection on a memory by providing context through interpretation of the emotion it evokes (Svoboda et al., 2006; St. Jacques et al., 2011). Here, the dorsolateral and dorsomedial prefrontal cortices are critical not only to the mediation of emotion regulation strategies to dampen negative emotions, but also for initiating the retrieval of an episodic memory (Andrews-Hanna et al., 2014; Frewen et al., 2017; Steinvorth, Corkin, & Halgren, 2006). Although individuals tend to integrate negative memories during REM sleep where the frontal lobe is largely inhibited (Hobson et al., 1998; Marshall et al., 2006; Nishida et al., 2009), Stickgold (2002) suggests eye movements may, conversely, engage the frontal lobe during the retrieval of episodic memories, thus enhancing the capacity for top-down emotion regulation. Critically, individuals with PTSD have been shown to have a decreased capacity for top-down emotion regulation (Frewen, Dozois, Neufeld, & Lanius, 2011), and thus, may require greater effort to recruit brain regions necessary for top-down emotion regulation as compared to healthy individuals. Accordingly, we suggest that engagement of the oculomotor frontoparietal network observed here among

individuals with PTSD may represent a compensatory neurobiological mechanism that facilitates downstream recruitment of regions impacted by emotion regulation, including the insula, in an effort to reduce the intense negative affect associated with a traumatic memory.

Brain regions involved in top-down emotion reappraisal, such as the dorsal prefrontal cortex, act on downstream structures, including the anterior and posterior regions of the insula (Goldin, McRae, Ramel, & Gross, 2008). Here, in the PTSD group as compared to in controls, during horizontal saccadic eye movements, the right supplementary eye field showed increased connectivity with the right anterior insula, a region thought central to identifying emotional feeling states. As compared to controls, the PTSD group reported more intense negative emotions following retrieval of a traumatic memory (Table 1). Hence, increased connectivity between the right supplementary eye field and the right insula may represent an increased attempt at regulation of intense emotion associated with traumatic memory retrieval in PTSD.

The anterior insula is thought to maintain one's sense of time; however, sensory overload from emotionally salient events may consume neural resources at the expense of the ability to assess the chronology of these events (Craig, 2009). This disruption may impact negatively memory processing, where the anterior insula is believed critical to the creation of a coherent emotional narrative of a memory with respect to time (Craig, 2009). Individuals with PTSD have been shown to suffer from a compromised ability to produce a coherent narrative of traumatic memories (Ehlers et al., 1998; Gray & Lombardo, 2001; van der Kolk & Fisler, 1995), and accordingly, may show reduced higher-order processing of its affective and sensory elements.

The increased right supplementary eye field recruitment of the right anterior insula in the PTSD group as compared to in controls suggests a potential role of eye movements in strengthening one's internal sense of time during retrieval of a traumatic memory. In turn, this enhanced chronological awareness may facilitate being able to more accurately retrieve a traumatic memory as an experience belonging to the past. Notably, these findings align with the concept of 'neuroentrainment' in EMDR (Coubard, 2015), which postulates rhythmic eye movements engage attentional processes to synchronize both affective and temporal components of traumatic memories.

Thus, among individuals with PTSD, the right supplementary eye field may: i) recruit the right anterior insula to assist in identifying a temporally coherent emotional narrative associated with the retrieval of a traumatic memory; and ii) recruit other cortical midline structures (e.g., dorsal prefrontal cortex) to assist in processing its intense negative emotional content.

As noted, as compared to the PTSD group, controls reported significantly less intense negative emotions following retrieval of a stressful memory while engaged in oculomotor movements (Table 1). We suggest that, among those who are not traumatized by a stressful experience, it may not be necessary to recruit additional cortical regions in an effort to engage top-down emotion regulation processes. As compared to individuals with PTSD, the healthy control group showed increased right frontal eye field connectivity with the right posterior insula only during retrieval of a stressful memory with simultaneous horizontal smooth pursuit eye movements. Pagani, Högberg, Fernandez, & Siracusano (2013) have emphasized previously the importance of EMDR in facilitating explicit cortical emotional processing of a traumatic memory over subcortical structures that carry

implicit affective components of a memory. Similarly, Corrigan & Grand (2013) suggest that top-down cortical integration of the episodic and the emotional components of a traumatic memory through EMDR may aid in memory reprocessing at the level of midbrain subcortical structures that help generate basic autonomic and instinctual responses to sensory input from the memory, such as the superior colliculus and the periaqueductal gray, where the latter may relay the implicit affective component of the memory through functional connections with the insula (Harricharan et al., 2016). Hence, during retrieval of a traumatic memory with simultaneous horizontal smooth pursuit eye movements, controls may require cortical control of the implicit negative affective intensity experienced at the level of the posterior insula only. In contrast, individuals with PTSD may require additional recruitment of higher-order emotion regulation brain regions (e.g., dorsolateral prefrontal cortex) to cope with the heightened emotional intensity experienced during retrieval.

On balance, we suggest that in individuals with PTSD as compared to in controls, horizontal eye movements may activate the right frontal and supplementary eye fields as an alternative mechanism to engage prefrontal regions involved in emotion regulation. These neural operations, in turn, are likely to assist in top-down reappraisal of a traumatic memory, thus reducing the negative affective intensity experienced upon its retrieval.

5.4.2 Dissociative Symptoms May Impede Emotion Regulation

PTSD patients with symptoms of depersonalization and derealisation often experience an altered perception of the self and its surroundings. In the present study, among individuals with PTSD, dissociative symptoms (MDI and RSDI) correlated *negatively* with right supplementary eye field connectivity with the right dorsolateral prefrontal cortex during

traumatic memory retrieval involving simultaneous horizontal smooth pursuit eye movements (Figure 5.4). Interestingly, a previous study by Bae, Kim, & Park, (2016) revealed poor treatment outcomes in patients with high scores on the Dissociative Experiences Scale (Bernstein & Putnam, 1986) when undergoing EMDR therapy. Taken together, we suggest that decreased ability of the oculomotor brain regions (i.e., supplementary and frontal eye fields) to engage regions involved in top-down emotion regulation, including the right dorsolateral prefrontal cortex, during traumatic memory retrieval may limit the efficacy of EMDR therapy in PTSD patients with significant dissociative symptoms.

5.4.3 Limitations and Future Directions

Several limitations of the current study need to be considered, including prominently its small sample size. Given that this was a pilot study, replication of the present study with a larger sample is warranted. A larger sample size will also be necessary to delineate any gender differences in activation of the oculomotor frontoparietal network during traumatic/stressful memory retrieval. Inclusion of a larger sample may also render it more feasible to include a trauma-exposed control group; however, it is often difficult to generate a comparably-sized sample group of traumatized controls that do not meet the lifetime criteria for one or more psychiatric disorders. Future studies are also required to elucidate the impact of each type of eye movement (i.e., horizontal versus vertical, smooth versus saccadic eye movements) in a larger sample. Notably, other types of bilateral stimulation, including tactile or auditory alternating bilateral stimulation, have been used in clinical practice with EMDR (González, Del Río-Casanova, & Justo-Alonso, 2017; Nieuwenhuis et al., 2013). Additional research is therefore necessary to determine whether

alternative bilateral stimulation methods show similar or different patterns of neural activation and of connectivity. Finally, given the potential of the present paradigm to identify the neural mechanisms underlying EMDR, it will be crucial to assess further the frontoparietal neural correlates of oculomotion, autobiographical memory and emotion regulation pre- and post-treatment among PTSD patients undergoing multiple sessions of EMDR (see Power et al., 2002; Rothbaum, Astin, & Marsteller, 2005).

5.4.4 Conclusions

The present study represents an important first step in identifying the role of the frontoparietal executive control network in the reprocessing of traumatic/stressful memories using eye movements. Here, we describe the influence of oculomotion on the recruitment of frontoparietal brain regions that impact top-down emotion regulatory processes during traumatic memory retrieval. In addition, we suggest that top-down emotion reappraisal strategies that occur in association with eye movements in PTSD may enhance self-referential processing to assist in reducing the negative emotional context associated with a memory. These processes may, in turn, facilitate integration of the exteroceptive and interoceptive details underlying traumatic memories, thus reducing what is often their time independent and fragmentary nature. Overall, these findings begin to shed light on the potential neurobiological mechanisms underlying EMDR's use as a treatment for PTSD.

5.5 References

Andrade, J., Kavanagh, D., & Baddeley, A. (1997). Eye-movements and visual imagery: A working memory approach to the treatment of post-traumatic stress disorder. *British Journal of Clinical Psychology, 36,* 209–223.

Andrews-Hanna, J. R., Saxe, R., & Yarkoni, T. (2014). Contributions of episodic retrieval and mentalizing to autobiographical thought: Evidence from functional neuroimaging, resting-state connectivity, and fMRI meta-analyses. *NeuroImage, 91,* 324–335.

Baddeley, A. (2010). Working memory. *Current Biology, 20*(4), R136-40.

Baddeley, A., & Hitch, G. (1974). Working memory. *Psychology of Learning and Motivation, 8,* 47–89.

Bae, H., Kim, D., & Park, Y. C. (2016). Dissociation predicts treatment response in eye movement desensitization and reprocessing for posttraumatic stress disorder. *Journal of Trauma & Dissociation, 17*(1), 112–130.

Barrowcliff, A. L., Gray, N. S., Freeman, T. C. A., & MacCulloch, M. J. (2004). Eye movements reduce the vividness, emotional valence and electrodermal arousal associated with negative autobiographical memories. *The Journal of Forensic Psychiatry and Psychology, 15*(2), 325–345.

Beck, A. T., Guth, D., Steer, R. A., & Ball, R. (1997). Screening for major depression disorders in medical inpatients with the Beck Depression Inventory for Primary Care. *Behaviour Research and Therapy, 35*(8), 785–791.

Beck, V. M., & Hollingworth, A. (2017). Competition in saccade target selection reveals attentional guidance by simultaneously active working memory representations. *Journal of Experimental Psychology:Human Perception and Performance, 43*(2), 225-231.

Bernstein, D., & Fink, L. (1998). Childhood trauma questionnaire: A retrospective self report: Manual. San Antonio, TX, US: The Psychological Corporation.

Bernstein, E. M., & Putnam, F. W. (1986). Development, reliability, and validity of a dissociation scale. *The Journal of Nervous and Mental Disease, 174*(12), 727 735.

Blake, D.D., Weathers, F. W., Nagy, L. M., Kaloupek, D. G., Gusman, F. D., Charney, D. S., & Keane, T. M. (1995). The development of a clinician-administered PTSD scale. *Journal of Traumatic Stress, 8*(1), 75–90.

Bremner, J. D., Krystal, J. H., Putnam, F. W., Southwick, S. M., Marmar, C., Charney, S., & Mazure, C. M. (1998). Measurement of dissociative states with the clinician-administered dissociative states scale (CADSS). *Journal of Traumatic Stress, 11*(1), 125–136.

Bremner, J. D., Narayan, M., Staib, L. H., Southwick, S. M., McGlashan, T., & Charney, D. S. (1999). Neural correlates of memories of childhood sexual abuse in women with and without posttraumatic stress disorder. *American Journal of Psychiatry, 156*(11), 1787–1795.

Brewin, C. R., Huntley, Z., & Whalley, M. G. (2012). Source memory errors associated with reports of posttraumatic flashbacks: A proof of concept study. *Cognition, 124(*2), 234–238.

Briere, J., Weathers, F. W., & Runtz, M. (2005). Is dissociation a multidimensional construct? Data from the Multiscale Dissociation Inventory. *Journal of Traumatic Stress, 18*(3), 221–231.

Burgess, N. (2006). Spatial memory: how egocentric and allocentric combine. *Trends in Cognitive Sciences, 10*(12), 551–557.

Burianova, H., McIntosh, A. R., & Grady, C. L. (2010). A common functional brain network for autobiographical, episodic, and semantic memory retrieval. *NeuroImage, 49*(1), 865–874.

Corbetta, M., & Shulman, G. L. (2002). Control of goal-directed and stimulus-driven attention in the brain. *Nature Reviews Neuroscience, 3*(3), 201–215.

Corrigan, F., & Grand, D. (2013). Brainspotting: Recruiting the midbrain for accessing and healing sensorimotor memories of traumatic activation. *Medical Hypotheses, 80*(6), 759–766.

Cotter, P., Meysner, L., & Lee, C. W. (2017). Participant experiences of eye movement desensitisation and reprocessing vs. cognitive behavioural therapy for grief: similarities and differences. *European Journal of Psychotraumatology*, *8*(1), 1375838.

Coubard, O. A. (2015). Eye Movement Desensitization and Reprocessing (EMDR) re examined as cognitive and emotional neuroentrainment. *Frontiers in Human Neuroscience*, 8, 1035.

Craig, A. D. B. (2009). How do you feel — now? The anterior insula and human awareness. *Nature Reviews Neuroscience, 10*(1), 59–70.

Dixon, M. L., De La Vega, A., Mills, C., Andrews-Hanna, J., Spreng, R. N., Cole, M. W., & Christoff, K. (2018). Heterogeneity within the frontoparietal control network and its relationship to the default and dorsal attention networks. *Proceedings of the National Academy of Sciences, 115*(7), E1598–E1607.

Ehlers, A., Clarke, D. M., Dunmore, E., Jaycox, L., Meadows, E., & Foa, E. B. (1998). Predicting response to exposure treatment in posttraumatic stress disorder: Role of mental defeat and alienation. *Journal of Traumatic Stress, 11*(3), 457–471.

Ehlers, A., Hackmann, A., & Michael, T. (2004). Intrusive re-experiencing in post traumatic stress disorder: Phenomenology, theory, and therapy. *Memory, 12*(4), 403–415.

Eklund, A., Nichols, T. E., & Knutsson, H. (2016). Cluster failure: why fMRI inferences for spatial extent have inflated false-positive rates. *Proceedings of the National Academy of Sciences, 113*(28), 7900-7905.

Eriksson, J., Vogel, E. K., Lansner, A., Bergström, F., & Nyberg, L. (2015). Neurocognitive architecture of working memory. *Neuron*, *88*(1), 33-46.

First, M., Spitzer, R., Gibbon, M., & Williams, J. (2002). Structured clinical interview for DSM-IV-TR axis I disorders, research version, non-patient edition. New York, NY: Biometrics Research, New York Psychiatric Institute.

Frewen, P. A., Dozois, D. J. A., Neufeld, R. W. J., & Lanius, R. A. (2011). Disturbances of emotional awareness and expression in posttraumatic stress disorder: Meta mood, emotion regulation, mindfulness, and interference of emotional expressiveness. *Psychological Trauma: Theory, Research, Practice, and Policy, 4*(2), 152–161.

Frewen, P., Thornley, E., Rabellino, D., & Lanius, R. (2017). Neuroimaging the traumatized self: fMRI reveals altered response in cortical midline structures and occipital cortex during visual and verbal self-and other-referential processing in women with PTSD. *European Journal of Psychotraumatology, 8*(1), 1314164.

Goldin, P. R., McRae, K., Ramel, W., & Gross, J. J. (2008). The neural bases of emotion regulation: Reappraisal and suppression of negative emotion. *Biological Psychiatry, 63*(6), 577–586.

González, A., Del Río-Casanova, L., & Justo-Alonso, A. (2017). Integrating neurobiology of emotion regulation and trauma therapy: Reflections on EMDR therapy. *Reviews in the Neurosciences, 28*(4), 431–440.

Gray, M. J., & Lombardo, T. W. (2001). Complexity of trauma narratives as an index of fragmented memory in PTSD: A critical analysis. *Applied Cognitive Psychology, 15*(7), S171–186.

Grosbras, M.-H., & Paus, T. (2002). Transcranial magnetic stimulation of the human frontal eye field: Effects on visual perception and attention. Journal of Cognitive *Neuroscience, 14*(7), 1109–1120.

Harricharan, S., Rabellino, D., Frewen, P. A., Densmore, M., Théberge, J., McKinnon, M. C., Schore, A.N., Lanius, R. A. (2016). fMRI functional connectivity of the

periaqueductal gray in PTSD and its dissociative subtype. *Brain and Behavior, 6*(12), e00579.

Hobson, J. A., Stickgold, R., & Pace-Schott, E. F. (1998). The neuropsychology of REM sleep dreaming. *Neuroreport, 9*(3), R1-R14.

Hopper, J. W., Frewen, P. A., Sack, M., Lanius, R. A., & van der Kolk, B. A. (2007). The responses to script-driven imagery scale (RSDI): Assessment of state posttraumatic symptoms for psychobiological and treatment research. *Journal of Psychopathology and Behavioral Assessment, 29*(4), 249–268.

Kurth, F., Zilles, K., Fox, P. T., Laird, A. R., & Eickhoff, S. B. (2010). A link between the systems: Functional differentiation and integration within the human insula revealed by meta-analysis. *Brain Structure and Function, 214*(5–6), 519–534.

Lanius, R. A., Williamson, P. C., Densmore, M., Boksman, K., Neufeld, R. W., Gati, J. S., & Menon, R. S. (2004). The nature of traumatic memories : A 4-T fMRI functional connectivity analysis. *American Journal of Psychiatry, 161*, 36-44.

Lencer, R., Nagel, M., Sprenger, A., Zapf, S., Erdmann, C., Heide, W., & Binkofski, F. (2004). Cortical mechanisms of smooth pursuit eye movements with target blanking. An fMRI study. *European Journal of Neuroscience, 19*(5), 1430-1436.

Littel, M., van Schie, K., & van den Hout, M. A. (2017). Exploring expectation effects in EMDR: does prior treatment knowledge affect the degrading effects of eye movements on memories?, *European Journal of Psychotraumatology, 8*(sup1), 1328954.

Maldjian, J. A., Laurienti, P. J., Kraft, R. A., & Burdette, J. H. (2003). An automated method for neuroanatomic and cytoarchitectonic atlas-based interrogation of fMRI data sets. *NeuroImage, 19*(3), 1233–1239. doi:10.1016/S1053 8119(03)00169-1

Marshall, L., Helgadóttir, H., Mölle, M., & Born, J. (2006). Boosting slow oscillations during sleep potentiates memory. *Nature, 444*(7119), 610.

Maxfield, L., Melnyk, W. T., & Hayman, G. C. (2008). A working memory exlanation for the effects of eye movements in EMDR. *Journal of EMDR Practice and Research, 2*(4), 247-261. d

Morawetz, C., Bode, S., Derntl, B., & Heekeren, H. R. (2017). The effect of strategies, goals and stimulus material on the neural mechanisms of emotion regulation: A meta-analysis of fMRI studies. *Neuroscience and Biobehavioral Reviews, 72*, 111–128.

Nieuwenhuis, S., Elzinga, B. M., Ras, P. H., Berends, F., Duijs, P., Samara, Z., & Slagter, H. A. (2013). Bilateral saccadic eye movements and tactile stimulation, but not auditory stimulation, enhance memory retrieval. Brain and Cognition, 81(1), 52-56.

Nishida, M., Pearsall, J., Buckner, R. L., & Walker, M. P. (2008). REM sleep, prefrontal theta, and the consolidation of human emotional memory. *Cerebral Cortex, 19*(5), 1158-1166.

Op den Kelder, R., Van den Akker, A. L., Geurts, H. M., Lindauer, R. J., & Overbeek, G. (2018). Executive functions in trauma-exposed youth: a meta-analysis. *European Journal of Psychotraumatology, 9*(1), 1450595.

Pagani, M., Di Lorenzo, G., Verardo, A. R., Nicolais, G., Monaco, L., Lauretti, G., … Siracusano, A. (2012). Neurobiological correlates of EMDR monitoring – An EEG study. *PLoS ONE, 7*(9), e45753.

Pagani, M., Högberg, G., Fernandez, I., & Siracusano, A. (2013). Correlates of EMDR therapy in functional and structural neuroimaging: A critical summary of recent findings. *Journal of EMDR Practice and Research, 7*(1), 29–38.

Pearson, D., & Sahraie, A. (2003). Oculomotor control and the maintenance of spatially and temporally distributed events in visuo-spatial working memory. *The Quarterly Journal of Experimental Psychology Section A, 56*(7), 1089-1111.

Picó-Pérez, M., Radua, J., Steward, T., Menchón, J. M., & Soriano-Mas, C. (2017). Emotion regulation in mood and anxiety disorders: A meta-analysis of fMRI cognitive reappraisal studies. *Progress in Neuropsychopharmacology and Biological Psychiatry*, *79*, 96–104.

Power, K., McGoldrick, T., Brown, K., Buchanan, R., Sharp, D., Swanson, V., & Karatzias, A. (2002). A controlled comparison of eye movement desensitization and reprocessing versus exposure plus cognitive restructuring versus waiting list in the treatment of post-traumatic stress disorder. *Clinical Psychology and Psychotherapy*, *9*, 299–318.

Rothbaum, B. O., Astin, M. C., & Marsteller, F. (2005). Prolonged exposure versus eye movement desensitization and reprocessing (EMDR) for PTSD rape victims. *Journal of Traumatic Stress*, *18*(6), 607–616.

Shapiro, F. (1989). Eye movement desensitization: A new treatment for post-traumatic stress disorder. *Journal of Behavior Therapy and Experimental Psychiatry*, *20*(3), 211–217.

Shipstead, Z., Harrison, T. L., & Engle, R. W. (2012). Working memory capacity and visual attention: Top-down and bottom-up guidance. *The Quarterly Journal of Experimental Psychology*, *65*(3), 401-407.

Spielberger, C. D. (2010). State-Trait Anxiety Inventory. In *The Corsini Encyclopedia of Psychology*. Hoboken, NJ: John Wiley & Sons, Inc.

St. Jacques, P. L., Kragel, P. A., & Rubin, D. C. (2011). Dynamic neural networks supporting memory retrieval. *Neuroimage*, *57*(2), 608-616.

Steinvorth, S., Corkin, S., & Halgren, E. (2006). Ecphory of autobiographical memories: An fMRI study of recent and remote memory retrieval. NeuroImage, 30(1), 285 298.

Stickgold, R. (2002). EMDR: A putative neurobiological mechanism of action. *Journal of Clinical Psychology*, *58*(1), 61-75.

Souza, A. S., & Oberauer, K. (2017). Time to process information in working memory improves episodic memory. *Journal of Memory and Language*, *96*, 155-167.

Svoboda, E., McKinnon, M. C., & Levine, B. (2006). The functional neuroanatomy of autobiographical memory: a meta-analysis. *Neuropsychologia, 44*(12), 2189 2208.

Szczepanski, S. M., Pinsk, M. A., Douglas, M. M., Kastner, S., & Saalmann, Y. B. (2013). Functional and structural architecture of the human dorsal frontoparietal attention network. *Proceedings of the National Academy of Sciences, 110*, 15806 15811.

Thomaes, K., Engelhard, I. M., Sijbrandij, M., Cath, D. C., & Van den Heuvel, O. A. (2016). Degrading traumatic memories with eye movements: A pilot functional MRI study in PTSD. *European Journal of Psychotraumatology, 7*(1), 31371.

Uncapher, M. R., & Wagner, A. D. (2009). Posterior parietal cortex and episodic encoding: insights from fMRI subsequent memory effects and dual-attention theory. *Neurobiology of Learning and Memory, 91*(2), 139-154.

Van der Kolk, B. A., & Fisler, R. (1995). Dissociation and the fragmentary nature of traumatic memories: Overview and exploratory study. *Journal of Traumatic Stress, 8*(4), 505–525.

Van der Kolk, B. A., Spinazzola, J., Blaustein, M. E., Hopper, J. W., Hopper, E. K., Korn, D. L., & Simpson, W. B. (2007). A Randomized clinical trial of eye movement desensitization and reprocessing (EMDR), fluoxetine, and pill placebo in the treatment of posttraumatic stress disorder: treatment effects and long-term maintenance. *Journal of Clinical Psychiatry*, *68*(1), 37–46.

Vernet, M., Quentin, R., Chanes, L., Mitsumasu, A., & Valero-cabré, A. (2014). Frontal eye field, where art thou? Anatomy, function, and non-invasive manipulation of frontal regions involved in eye movements and associated cognitive operations. *Frontiers in Integrative Neuroscience, 8*, 66.

Weathers, F.W., Blake, D.D., Schnurr, P.P., Kaloupek, D.G., Marx, B.P., & Keane, T.M. (2013). The Clinician-Administered PTSD Scale for DSM-5 (CAPS-5). Interview available from the National Center for PTSD at www.ptsd.va.gov.

Zilverstand, A., Parvaz, M. A., & Goldstein, R. Z. (2017). Neuroimaging cognitive reappraisal in clinical populations to define neural targets for enhancing emotion regulation. A systematic review. *NeuroImage, 151*(June 2016), 105–116.

Chapter 6

6 « Discussion of Findings and Conclusions»

This dissertation investigates the neural circuitry of subcortical and cortical brain regions associated with sensory processing in PTSD, its dissociative subtype, and healthy controls. In chapters 2 and 3, we investigated resting state functional connectivity patterns of brainstem structures central to interoceptive and exteroceptive processing, including the periaqueductal gray (Chapter 2) and vestibular nuclei (Chapter 3). Here, individuals with PTSD showed widespread periaqueductal grey resting-state connectivity with brain regions involved in emotional reactivity. The periaqueductal gray plays a critical role in autonomic nervous system regulation. Significant alterations in its connectivity patterns with limbic and cortical regions involved in emotional reactivity may therefore influence how interoceptive viscerosensory input is processed in individuals with PTSD. Furthermore, when compared to healthy individuals, PTSD was associated with decreased brainstem vestibular nuclei connectivity with the posterior insula, pointing towards decreased interoceptive awareness among individuals who suffer from PTSD (Chapter 3). Moreover, individuals with the dissociative subtype of PTSD showed limited brainstem vestibular nuclei connectivity with the temporoparietal junction, an area that has been linked previously to depersonalization and understanding one's own self-location in gravitational space, which may in turn impact exteroceptive sensory processing. In chapter 4, insula subregion resting-state connectivity was examined in PTSD, as the insula is thought to be a key node for relaying interoceptive and exteroceptive sensory information from the brainstem to the cortex. Here, when compared to healthy individuals, individuals with PTSD and its dissociative subtype

showed limited insula subregion resting-state connectivity with the frontal lobe. Notably, the insula is hypothesized to assist in identifying emotional states underlying incoming viscerosensory information and is believed critical for facilitating activation of frontal lobe structures in the central executive network, a network critical for higher-order cognitive tasks, including emotion regulation. Thus, decreased insula subregion connectivity with frontal lobe structures in PTSD as compared to healthy individuals may point to a decreased capacity to translate sensory information to frontal lobe structures involved in emotion regulation. In chapter 5, a task-based paradigm that involved performance of oculomotor movements during simultaneous traumatic memory recall was used to explore the impact of simultaneous exposure to interoceptive (traumatic memory recall) and exteroceptive (horizontal eye movements) sensory information among traumatized individuals. Here, activation of brain regions involved in the dorsal attentional network, including the frontal and supplementary eye fields, showed increased connectivity with frontoparietal cortical structures central to emotion regulation. Taken together, these findings point toward a potential neurobiological mechanism through which exposure to simultaneous exteroceptive and interoceptive sensory input may influence the frontoparietal cortical representation of a traumatic memory, thus decreasing the emotional intensity of the memory and aiding its reintegration into the embodied neural representation of one's self. The cumulative findings from each chapter of this dissertation have been summarized in the form of a hierarchy (Figure 6.1) that proposes a theoretical framework/model of sensory processing in PTSD.

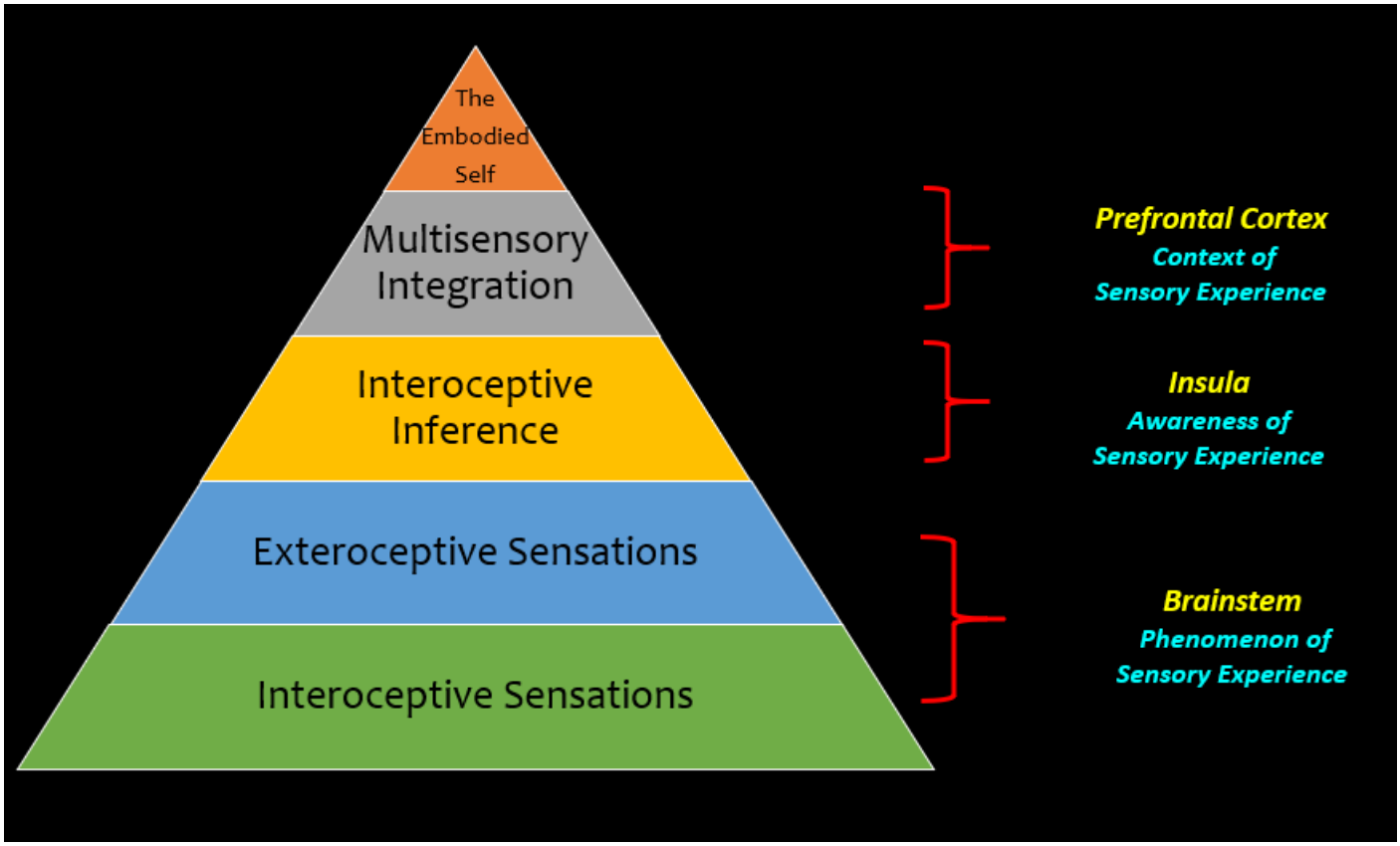

Figure 6.1 *Theoretical Framework for Sensory Processing in PTSD*

6.1 Interoceptive Sensations

At the base of the hierarchy, it is proposed that during rest, continuous sensory flow from the internal viscera and one's surroundings reaches the midbrain of the brainstem, thus evoking internal visceral sensations that provide primitive interoceptive sensory information to lay the foundation for bottom-up sensory processing to the cortex (see Panksepp, 2002; Northoff & Panksepp, 2008). Barrett & Simmons (2015) identified previously the periaqueductal grey as a key midbrain structure for receiving interoceptive information from within the body (also see Wiens, 2015). In the present investigation,

even at rest, individuals with PTSD showed widespread periaqueductal gray connectivity with areas involved in emotional reactivity (see chapter 2). Thus it appears that , even during rest, individuals with PTSD have a predisposition to activate the innate alarm system, a subcortical brain network that includes the periaqueductal gray, the amygdala, the cerebellum, the thalamus, and the prefrontal cortex and is hypothesized to facilitate fast defensive responses to a perceived threat (Liddell et al., 2005; Steuwe et al., 2013; Lanius et al., 2017). Hypervigilance of one's surroundings may, in turn, compromise the ability to process exteroceptive sensory information from the environment and thereby negatively affect the relationship between one's self and one's surroundings. Here, we hypothesize that primitive interoceptive sensations lay the foundation for which exteroceptive sensory information is interpreted, where internal visceral sensations may influence how sensory information from the external environment is relayed to the cortex.

6.2 Exteroceptive Sensations

Exteroceptive sensory information is continuously acquired from the environment to inform the relationship between one's self and one's surroundings (Hitier, Besnard, & Smith, 2014; Lopez, Halje, & Blanke, 2008). The vestibular system plays a crucial role in this process, as it is a subconscious system that consistently monitors one's position in gravitational space through the acquisition of both exteroceptive and interoceptive sensory information at the level of the brainstem vestibular nuclei (Guldin & Grusser, 1998; Farb, Segal, & Anderson, 2012). The vestibular system is critical for maintaining one's physical equilibrium where sensory information is eventually relayed to the parieto-insular vestibular cortex for both exteroceptive and interoceptive processing

(Lopez & Blanke, 2011). Ultimately, both exteroceptive and interoceptive information from the brainstem are thought to be utilized in tandem to facilitate multisensory integration at the level of the prefrontal cortex, thus allowing humans to develop mental constructs of the external world and guiding navigation through the environment (Lenggenhager & Lopez, 2015).

Notably, resting-state vestibular nuclei connectivity patterns in the dissociative subtype of PTSD (see chapter 3) provide critical insights into how depersonalization and derealization symptoms may negatively impact the capacities for exteroceptive sensory processing. Specifically, when compared to healthy individuals, the dissociative subtype showed limited vestibular nuclei connectivity with the temporoparietal junction within the parieto-insular vestibular cortex, a pattern of neural disruption that may negatively affect the ability to understand one's own self-orientation in space and can lead to feelings of disembodiment (Blanke, Slater, & Serino, 2015; Ionta et al., 2011; Pfeiffer, Serino, & Blanke, 2014). In addition, when again compared to healthy individuals, the dissociative subtype showed limited vestibular nuclei connectivity with the dorsolateral prefrontal cortex, which may negatively affect traumatized individuals' capacity for multisensory integration and navigation through their respective external environments.

Taken together, the current findings concerning the periaqueductual gray and the vestibular brainstem nuclei indicate that individuals with PTSD and its dissociative subtype experience significantly altered subcortical resting-state connectivity patterns with cortical structures that together may make them more susceptible to aberrations in sensory processing. In addition, these findings emphasize the importance of classifying individuals with PTSD separately based on the presence of the dissociative subtype,

where, at the cortical level, individuals with and without the dissociative subtype showed distinct alterations in the multisensory integration of interoceptive and exteroceptive information.

6.3 Interoceptive Inference

The insula is a critical structure for receiving both interoceptive viscerosensory input from the brainstem and is key for processing salient stimuli from the external environment (Barrett & Wager, 2006; Etkin & Wager, 2008; Menon, 2011). It is therefore a key node for the convergence of exteroceptive and interoceptive sensory information (Wiens, 2015) and is thought to make an interoceptive inference based on the sensory information that is received. The latter process would be postulated to move beyond the primary level of the *phenomenological* experience of sensory information at the brainstem and progress to a secondary level of *awareness* of an emotional experience at the level of the cortex. The insula may thus assist in making an interoceptive inference by identifying the emotional feelings underlying incoming viscerosensory input. Ultimately, we propose that awareness of an emotional feeling may aid in its translation to the central executive network, which encompasses the lateral frontoparietal cortex, and is necessary for identification of the contextual meaning of an emotional feeling (Seeley et al., 2007; Menon & Uddin, 2010; Wager et al., 2015). Specifically, the findings presented in chapter 4 revealed that during rest, when compared to PTSD and its dissociative subtype, healthy individuals displayed increased insula subregion connectivity to higher-order frontal areas, including the pre- and post-central gyri and the dorsolateral prefrontal cortex. By contrast, whereas individuals with PTSD showed increased connectivity with subcortical areas observed in hyperemotionality, the

dissociative subtype showed increased insula connectivity with structures involved in maintaining implicit memory. Overall, limited insula subregion connectivity to higher-order cortical structures for multisensory integration suggests strongly that individuals with PTSD lack the capacity to evaluate the contextual meaning of an interoceptive inference based on incoming exteroceptive and interoceptive sensory information. Given that the insula is central to emotion processing, it is further probable that disruption of insula subregion connectivity patterns among individuals with PTSD contributes to the distinctive patterns of emotion dysregulation observed among PTSD and its dissociative subtype, including hyperemotionality and emotional blunting states, respectively.

Taken together, the current findings overwhelmingly suggest that the insula plays a pivotal role in translating sensory information to higher-order frontal structures involved in the central executive network underlying higher-order cognitive functions, including emotion regulation. Ultimately, if increased insula connectivity with frontal lobe structures involved in the central executive network facilitates emotion regulation, rehabilitation of this connectivity pattern would be expected to aid in the reintegration of traumatic memories and in reduction of their emotional intensity, thus improving PTSD symptomatology.

6.4 Multisensory Integration and the Embodied Self

In the next phase of the hierarchy, it is proposed that multisensory integration at a cortical level is critical for interpretation of interoceptive inferences containing exteroceptive and interoceptive sensory information relayed from the brainstem. Here, integrating sensory information into one's own mental constructs can inform one's behavior in response to one's surroundings. As described above, the dorsal prefrontal cortex is thought critical for

multisensory integration (Aupperle, Melrose, Stein, & Paulus, 2012; Picó-Pérez, Radua, Steward, Menchón, & Soriano-Mas, 2017) and its activation is necessary for carrying out executive functioning tasks such as emotion regulation (Cromheeke & Mueller, 2014; Menon, 2011). In Chapter 5, oculomotor eye movements performed simultaneously with traumatic memory recall provided explicit exposure to both exteroceptive and interoceptive information. This activation of the dorsal attentional network through the frontal and supplementary eye fields is hypothesized to facilitate recruitment of neural structures involved in both the default-mode and central executive frontoparietal networks. The dorsal attentional network and the default-mode network are thought to work in tandem to facilitate further activation of the central executive network necessary to carry out higher-order cognitive tasks, including emotional regulatory processes (Pico-Perez et al., 2017) typically altered among individuals with PTSD (Andrews-Hanna, Smallwood, & Spreng, 2014; Frewen, Thornley, Rabellino, & Lanius, 2017; Steinvorth, Corkin, & Halgren, 2006). On balance, our finding suggests that exposure to simultaneous exteroceptive and interoceptive sensory stimuli through oculomotor eye movements performed simultaneous to traumatic memory recall engages the dorsal attentional network and default-mode frontoparietal networks that subsequently work in tandem to facilitate connectivity with structures in the central executive network, including the dorsolateral and dorsomedial prefrontal cortex, necessary for multisensory integration. Moreover, once the central executive network is engaged, it may recruit further neural regions critical for emotion regulation, thus assisting with the reintegration of a traumatic memory. Critically, the eventual reintegration of traumatic memories may facilitate one's attainment of the embodied self, the apex of the hierarchy, where one has

the ability to engage top-down cognitive processes that assist in coordinating behavioural responses to incoming exteroceptive and interoceptive information.

6.5 Limitations and Future Directions

While this dissertation employs broadly used neuroscientific research methods to study the neural circuitry underlying brain structures thought to be critical to sensory processing in individuals with PTSD, several limitations need to be considered. Firstly, while comorbidity of PTSD with other psychiatric disorders was acknowledged among recruited participants, the specificity of these findings to posttraumatic stress disorder requires further investigation. Secondly, future studies should aim to investigate the findings from the experimental chapters as a function of gender and also delineate further the effect of psychiatric medications on the differential patterns of neural connectivity that are addressed in the thesis. Finally, while this body of work addresses the role of neural connectivity between brain structures thought to be involved in the integration between mind and body, these data have yet to be related to physical markers that may elucidate significant findings about somatic manifestations that may occur as a direct result of post-traumatic stress disorder.

6.6 Conclusions

Overall, the findings of this dissertation reveal that individuals with PTSD experience aberrations in the neural circuitry necessary for processing both interoceptive and exteroceptive sensory information. We hypothesize that these observed alterations in interoceptive and exteroceptive neural processing may underlie, in part, the emotion dysregulation and maladaptive responses to chronic stress, including hypervigilance and

dissociative symptoms, observed in PTSD and its dissociative subtype. Moreover, when the foundation of the proposed sensory processing hierarchy outlined here is disrupted at the brainstem level in PTSD, this disruption may have cascading effects on its neural afferentation to higher-order cortical areas, such as the insula and the prefrontal cortex, thereby limiting one's ability to obtain an interoceptive inference and also one's capacity to perform multisensory integration for cognitively demanding tasks, such as emotion regulation. Future studies should aim to investigate further the impact of brainstem structures in post-traumatic stress disorder, through employing neuroimaging techniques that examine the brainstem at higher magnetic field strengths and using dynamic causal modelling techniques that determine the directionality of these processes. Overall, delineating the neural circuitry underlying the processing of sensory information in PTSD through the lens of exteroceptive and interoceptive information may offer valuable insights for understanding the pathogenesis of PTSD and may assist with delineating its neurobiological mechanisms. Identification if this circuitry also has the potential to shed light on clinical interventions, such as eye movement desensitization and reprocessing, shown previously to assist with the reintegration of traumatic memories and recovery from trauma.

6.7 References

Andrews-Hanna, J. R., Smallwood, J., & Spreng, R. N. (2014). The default network and self generated thought: component processes, dynamic control, and clinical relevance. *Annals of the New York Academy of Sciences*, *1316*(1), 29.

Aupperle, R. L., Melrose, A. J., Stein, M. B., & Paulus, M. P. (2012). Executive function and PTSD: disengaging from trauma. *Neuropharmacology*, *62*(2), 686-694.

Barrett, L. F., & Wager, T. D. (2006). The structure of emotion: Evidence from neuroimaging studies. *Current Directions in Psychological Science*, *15*(2), 79-83.

Blanke, O., Slater, M., & Serino, A. (2015). Behavioral, neural, and computational principles of bodily self-consciousness. *Neuron*, *88*(1), 145-166.

Cromheeke, S., & Mueller, S. C. (2014). Probing emotional influences on cognitive control: an ALE meta-analysis of cognition emotion interactions. *Brain Structure and Function*, *219*(3), 995-1008.

Etkin, A., & Wager, T. D. (2007). Functional neuroimaging of anxiety: a meta-analysis of emotional processing in PTSD, social anxiety disorder, and specific phobia. *American Journal of Psychiatry*, *164*(10), 1476-1488. https://doi.org/10.1176/appi.ajp.2007.07030504

Farb, N. A., Segal, Z. V., & Anderson, A. K. (2012). Attentional modulation of primary interoceptive and exteroceptive cortices. *Cerebral cortex*, *23*(1), 114-126

Frewen, P., Thornley, E., Rabellino, D., & Lanius, R. (2017). Neuroimaging the traumatized self: fMRI reveals altered response in cortical midline structures and occipital cortex during visual and verbal self-and other-referential processing in women with PTSD. *European journal of psychotraumatology*, *8*(1), 1314164.

Guldin, W. O., & Grüsser, O. J. (1998). Is there a vestibular cortex?. *Trends in neurosciences*, *21*(6), 254-259.hitir

Hitier, M., Besnard, S., & Smith, P. F. (2014). Vestibular pathways involved i cognition. *Frontiers in integrative neuroscience*, *8*, 59.ioiont

Ionta, S., Heydrich, L., Lenggenhager, B., Mouthon, M., Fornari, E., Chapuis, D., ... & Blanke, O. (2011). Multisensory mechanisms in temporo-parietal cortex support self-location and first-person perspective. *Neuron*, *70*(2), 363-374.

Lanius, R. A., Rabellino, D., Boyd, J. E., Harricharan, S., Frewen, P. A., & McKinnon, M. C. (2017). The innate alarm system in PTSD: conscious and subconscious processing of threat. *Current Opinion in Psychology*, *14*, 109-115.

Lenggenhager, Bigna; Lopez, Christophe (2015). Vestibular Contributions to the Sense of Body, Self, and Others. In: Metzinger, Thomas; Windt, Jennifer M. Open MIND. Frankfurt am Main: MIND Group, pp.1-38.

Liddell, B. J., Brown, K. J., Kemp, A. H., Barton, M. J., Das, P., Peduto, A., ... & Williams, L. M. (2005). A direct brainstem–amygdala–cortical 'alarm'system for subliminal signals of fear. *Neuroimage*, *24*(1), 235-243.

Lopez, C., & Blanke, O. (2011). The thalamocortical vestibular system in animals and humans. *Brain research reviews*, *67*(1-2), 119-146.

Lopez, C., Halje, P., & Blanke, O. (2008). Body ownership and embodiment: vestibular and multisensory mechanisms. *Neurophysiologie Clinique/Clinical Neurophysiology*, *38*(3), 149-161.

Menon, V. (2011). Large-scale brain networks and psychopathology: a unifying triple network model. *Trends in cognitive sciences*, *15*(10), 483-506.

Menon, V., & Uddin, L. Q. (2010). Saliency, switching, attention and control: a network model of insula function. *Brain Structure and Function*, *214*(5-6), 655-667.

Northoff, G., & Panksepp, J. (2008). The trans-species concept of self and the subcortical–cortical midline system. *Trends in cognitive sciences*, *12*(7), 259-264.

Panksepp, J. (2004). *Affective neuroscience: The foundations of human and animal emotions*. Oxford university press.

Picó-Pérez, M., Radua, J., Steward, T., Menchón, J. M., & Soriano-Mas, C. (2017). Emotion regulation in mood and anxiety disorders: A meta-analysis of fMRI cognitive reappraisal studies. *Progress in Neuro-Psychopharmacology and Biological Psychiatry*, *79*, 96-104.

Pfeiffer, C., Serino, A., & Blanke, O. (2014). The vestibular system: a spatial reference for bodily self-consciousness. *Frontiers in integrative neuroscience*, *8*, 31.

Seeley, W. W., Menon, V., Schatzberg, A. F., Keller, J., Glover, G. H., Kenna, H., ... & Greicius, M. D. (2007). Dissociable intrinsic connectivity networks for salience processing and executive control. *Journal of Neuroscience*, *27*(9), 2349-2356.

Steinvorth, S., Corkin, S., & Halgren, E. (2006). Ecphory of autobiographical memories: an fMRI study of recent and remote memory retrieval. *Neuroimage*, *30*(1), 285 298.

Steuwe, C., Daniels, J. K., Frewen, P. A., Densmore, M., Pannasch, S., Beblo, T., ... & Lanius, R. A. (2012). Effect of direct eye contact in PTSD related to interpersonal trauma: an fMRI study of activation of an innate alarm system. *Social Cognitive and Affective Neuroscience*, *9*(1), 88-97.

Wager, T. D., Kang, J., Johnson, T. D., Nichols, T. E., Satpute, A. B., & Barrett, L. F. (2015). A Bayesian model of category-specific emotional brain responses. *PLoS computational biology*, *11*(4), e1004066.

Wiens, S. (2005). Interoception in emotional experience. *Current opinion in neurology*, *18*(4), 442-447.

Appendices

Appendix A: Supplementary Material for Chapter 2

Supplementary Table 1 *Omnibus ANOVA Test for 3x2 Full Factorial*

Contrast	L/R	BA	Region	Cluster Size	p FWE	Z-Score	MNI Coordinates x	y	z
Group x ROI Interaction	R	6	Dorsal Anterior Cingulate Cortex	231	<0.001	4.81	12	-6	44
	R	6	Supplemental Motor			4.34	4	-10	54
	R	31	Mid-Cingulate Cortex			4.13	6	-20	46
	L	6	Pre-central Gyrus	62	0.004	4.16	-38	0	36
Main Effect of Group	L	6	Frontal Middle Gyrus	45514	<0.001	7.24	-26	-6	52
	L	24	Mid-Cingulate Gyrus			6.32	-4	16	36
	L	10	Frontal Middle Gyrus	50	0.014	4.27	-40	56	2
	L	10	Orbitomedial Prefrontal Cortex			4.06	-44	50	-4
Main Effect of PAG Subdivision	L		Cerebellar Lobules IV-V	915	<0.001	65535	-6	-38	-6
	R	23	Calcarine Sulcus	55	0.016	5.60	4	-56	12
	R	30	Calcarine Sulcus			3.69	16	-54	6
	R	24	Dorsal Anterior Cingulate	1703	<0.001	5.26	10	-20	44
	L	6	Supplemental Motor Area			5.09	-4	8	48
	L	41	Heschl Gyrus			5.08	-38	-26	14
	R	28	Hippocampus	457	<0.001	5.26	20	-34	0
	R	35	Parahippocampal Gyrus			4.78	36	-30	-14
	R	13	Anterior Insula	159	<0.001	4.85	48	2	0
	R	22	Superior Temporal Pole			4.10	56	10	-6
	R	8	Frontal Middle Gyrus	156	<0.001	4.52	32	14	36
	R	9	Frontal Middle Gyrus			4.11	30	30	34
	R	44	Inferior Frontal Operculum			4.09	42	12	34
	R	32	Dorsal Anterior Cingulate	77	0.002	4.24	12	24	36
	R	8	Superior Frontal Gyrus			3.69	6	28	44
	R	22	Superior Temporal Gyrus	58	0.012	4.21	50	-28	-2
	L	44	Anterior Insula	65	0.006	4.08	-36	14	12
	R	44	Middle Insula	69	0.005	4.08	34	6	14

Supplementary Table 1. *3 (Group) x 2 (PAG subdivision) Full Factorial ANOVA.*

Areas revealed in the full-factorial interaction between group (Control, PTSD-DS, PTSD+DS) and PAG subdivision (DL- and VL-PAG), as well as the main effects for each factor. Abbreviations: L/R, left or right hemispheres; BA, Brodmann area. Full factorial analysis of variance displayed FWE whole brain corrected clusters at $p<0.05$, k=50.

Supplementary Table 2: Results of Healthy Control PAG Functional Connectivity

Contrast	L/R	BA	Region	Cluster Size	p FWE	Z-Score	MNI Coordinates x	y	z
Within Control Group – DL-PAG	L		Cerebellar Lobules IV-V	135	<0.001	Inf	-6	-38	-6
	R		Cerebellar Lobule III			4.66	8	-40	-8
	L		Cerebellar Vermis			4.42	0	-46	-6
Within Control Group – VL-PAG			No suprathreshold clusters						
Control DL>VL-PAG	L		Cerebellar Lobules IV-V	61	0.020	6.89	-6	-38	-6
	L		Cerebellar Vermis			3.89	0	-50	-10
Control DL>VL-PAG			No suprathreshold clusters						
Control>PTSD-DS DL-PAG			No suprathreshold clusters						
Control>PTSD+DS DL-PAG			No suprathreshold clusters						
Control>PTSD-DS VL-PAG			No suprathreshold clusters						
Control>PTSD+DS VL-PAG			No suprathreshold clusters						

Patterns

Full factorial analysis of variance displayed FWE whole brain corrected clusters at $p<0.05$, k=50. Abbreviations: PTSD-DS, non-dissociative posttraumatic stress disorder patients; PTSD+DS, dissociative posttraumatic stress disorder patients; DL-PAG,

dorsolateral periaqueductal gray; VL-PAG, ventrolateral periaqueductal gray; L/R, left or right hemispheres; BA, Brodmann area.

Contrast	L/R	BA	Region	Cluster Size	p FWE	Z-Score	MNI Coordinates x	y	z
PTSD-DS>Control DL-PAG	L	44	Pre-central Gyrus	26318	<0.001	6.43	-58	8	24
	R	13	Rolandic Operculum			6.08	40	-8	18
	L	24	Dorsal Anterior Cingulate Cortex			5.88	0	-10	38
	R	54	Hippocampus	234	<0.001	6.04	24	-36	-2
	R		Thalamic Pulvinar			4.00	20	-32	12
	R		Cerebellar Lobules IV-V	595	<0.001	5.41	14	-56	-14
	R		Cerebellar Vermis			4.75	4	-52	-6
	L		Cerebellar Lobules IV-V			4.74	-12	-56	-14
	R	18	Calcarine Sulcus	102	<0.001	4.61	22	-60	4
	R	23	Calcarine Sulcus			4.15	12	-56	12
	R	30	Lingual Gyrus			3.84	8	-62	4
	R	40	Rolandic Operculum	70	0.011	4.54	48	-20	16
	R	41	Heschl Gyrus			3.75	52	-16	10
	R	41	Superior Temporal Gyrus			3.40	50	-30	12
	L	21	Middle Temporal Gyrus	55	0.032	4.26	-50	2	-30
	L	38	Middle Temporal Pole			3.46	-40	8	-30
PTSD-DS>Control VL-PAG	R	6	Mid-Cingulate Gyrus	18666	<0.001	6.24	-20	0	42
	R	23	Mid-Cingulate Gyrus			5.67	2	-18	34
	R	6	Supplemental Motor			5.64	12	0	56
	R		Cerebellar Lobule VI	55	0.032	5.57	18	-64	-18
	L	18	Lingual Gyrus	157	<0.001	5.18	-16	-62	2
	L	23	Precuneus			4.36	-4	-54	18
	L	23	Calcarine Sulcus			3.69	-12	-58	10
	R	54	Hippocampus	134	<0.001	4.71	32	-36	-8
	R	18	Lingual Gyrus			4.04	22	-48	0
	L	43	Rolandic Operculum	55	0.032	4.67	-44	-14	22
	L		Cerebellar Vermis	104	0.001	4.47	-2	-58	-10
	L		Cerebellar Lobules IV-V			4.30	-6	-58	-18
	L	10	Orbitomedial Prefrontal Cortex	84	0.004	4.06	-40	48	-10

Supplementary Table 3: *PTSD versus Healthy Controls PAG Functional Connectivity Patterns*

Contrast	L/R	BA	Region	Cluster Size	p FWE	Z-Score	MNI Coordinates x	y	z
PTSD+DS>Control DL-PAG	L	6	Pre-central Gyrus	26486	<0.001	6.09	-28	-12	48
	L	24	Frontal Middle Gyrus			5.94	-30	8	42
	R	6	Supplemental Motor			5.85	10	4	52
	R	10	Frontal Middle	110	0.001	4.06	32	58	-2
	R	11	Orbitomedial Prefrontal			6.58	26	48	-12
PTSD+DS>Control VL-PAG	L	6	Frontal Middle Gyrus	23618	<0.001	5.99	-26	-10	48
	R	6	Dorsal Anterior Cingulate Cortex			5.35	14	28	42
	R	21	Middle Temporal Gyrus	770	<0.001	4.92	44	-40	-2
	R	19	Lingual Gyrus			4.83	20	-54	-8
	R	38	Superior Temporal Pole	110	0.001	4.43	52	16	-16
	R	10	Superior Orbitofrontal Gyrus	112	0.001	3.96	30	56	-4
	R	10	Orbitmedial Prefrontal Cortex			3.64	22	58	-12

Supplementary Table 4: *PTSD+DS versus Healthy Controls PAG Functional Connectivity Patterns*

Full factorial analysis of variance displayed FWE whole brain corrected clusters at $p<0.05$, k=50. Abbreviations: PTSD-DS, non-dissociative posttraumatic stress disorder patients; PTSD+DS, dissociative posttraumatic stress disorder patients; DL-PAG, dorsolateral periaqueductal gray; VL-PAG, ventrolateral periaqueductal gray; L/R, left or right hemispheres; BA, Brodmann area.

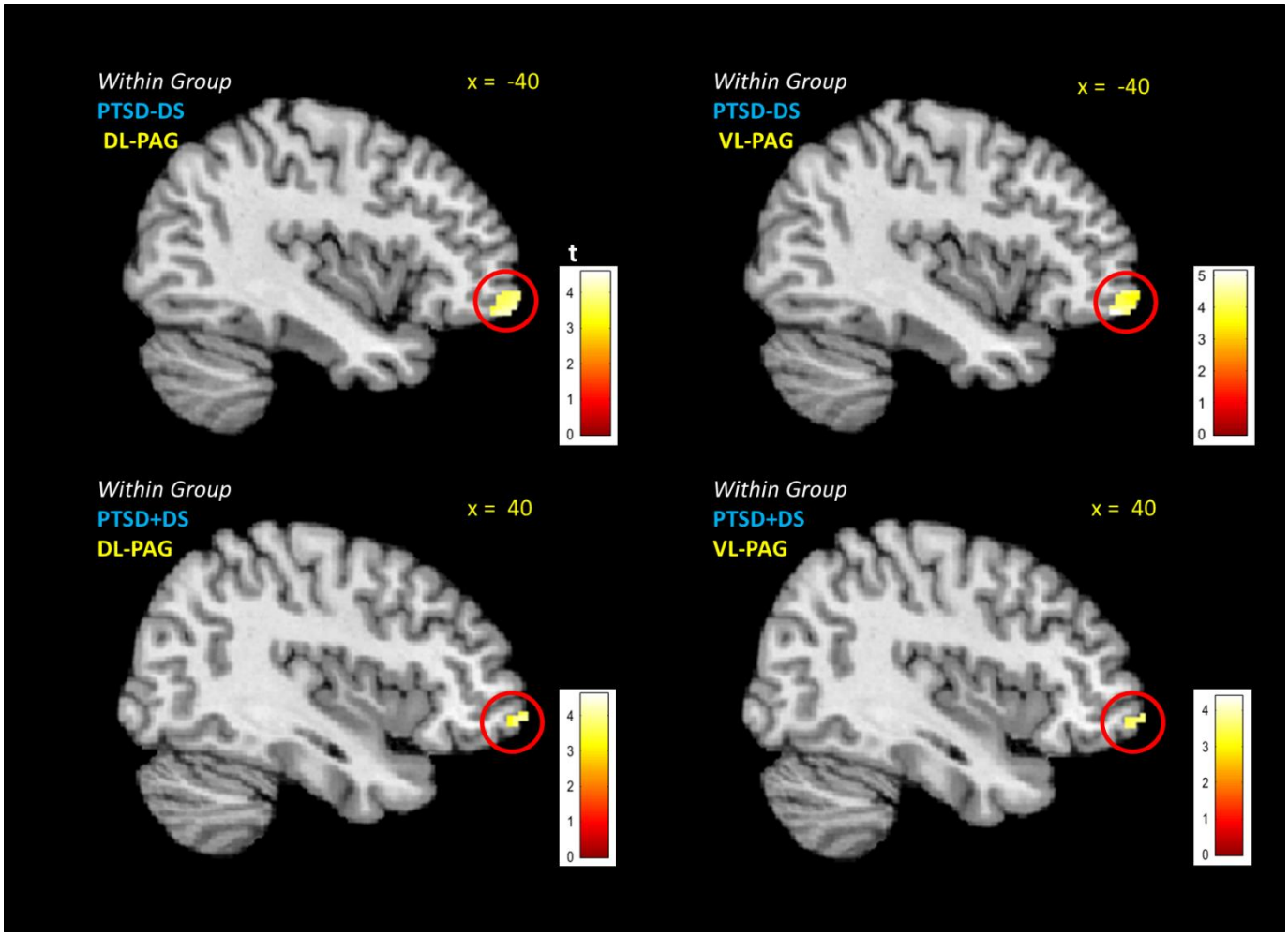

Supplemental Figure 2. Orbitomedial Prefrontal Cortex. PTSD-DS and PTSD+DS patient groups demonstrated both DL- and VL-PAG functional connectivity with the orbitomedial prefrontal cortex (red circles) during resting state. FWE whole brain cluster corrected at $p<0.05$, k=50.

Abbreviations: PTSD-DS, non-dissociative posttraumatic stress disorder patients; PTSD+DS, dissociative posttraumatic stress disorder patients; DL-PAG, dorsolateral periaqueductal gray; VL-PAG, ventrolateral periaqueductal gray; L, left hemisphere; R, right hemisphere.

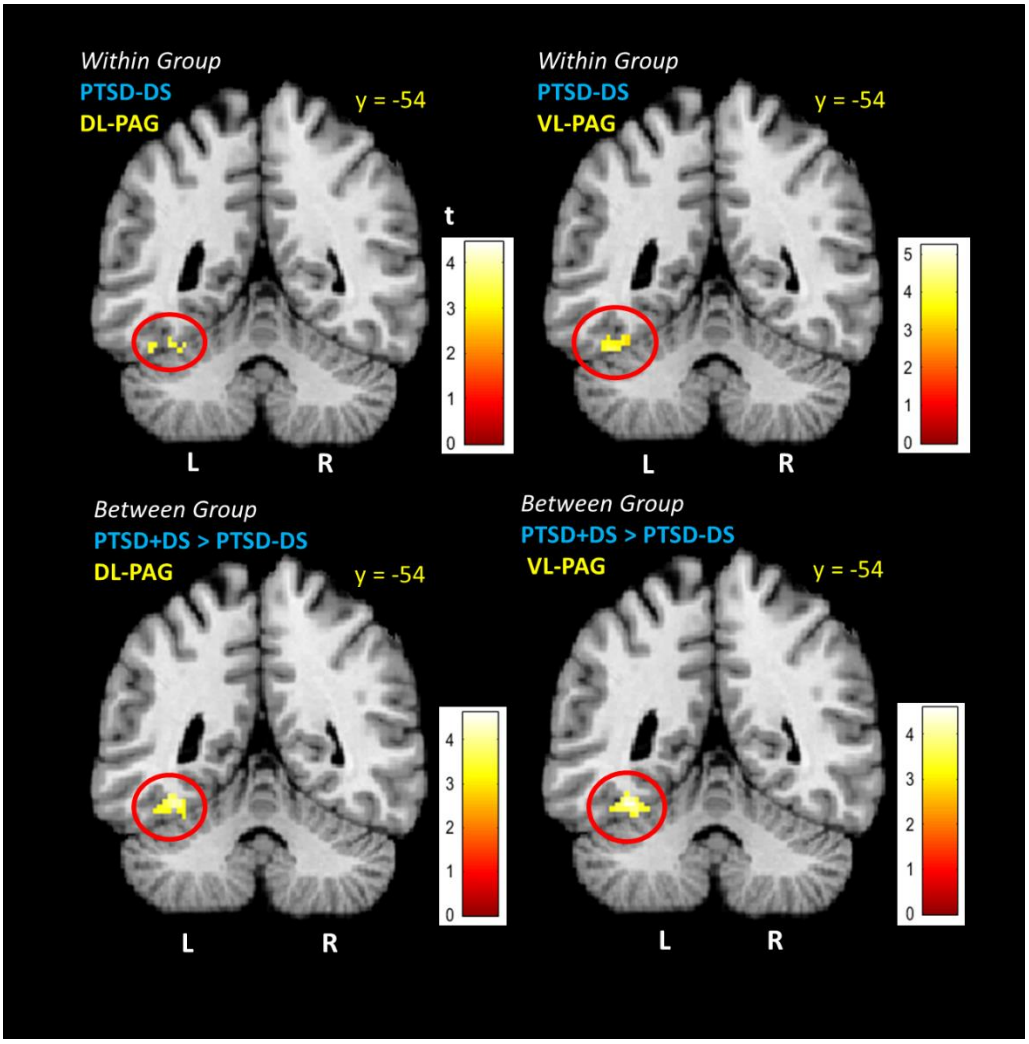

Supplementary Figure 3. Fusiform Gyrus. Both PTSD-DS and PTSD+DS demonstrated both DL- and VL-PAG functional connectivity with the left fusiform gyrus (red circles) during resting state. PTSD-DS also demonstrated connectivity with the right fusiform gyrus (not shown). FWE whole brain cluster corrected at $p<0.05$, k=50.

Abbreviations: PTSD-DS, non-dissociative posttraumatic stress disorder patients; PTSD+DS, dissociative posttraumatic stress disorder patients; DL-PAG, dorsolateral periaqueductal gray; VL-PAG, ventrolateral periaqueductal gray; L, left hemisphere; R, right hemisphere.

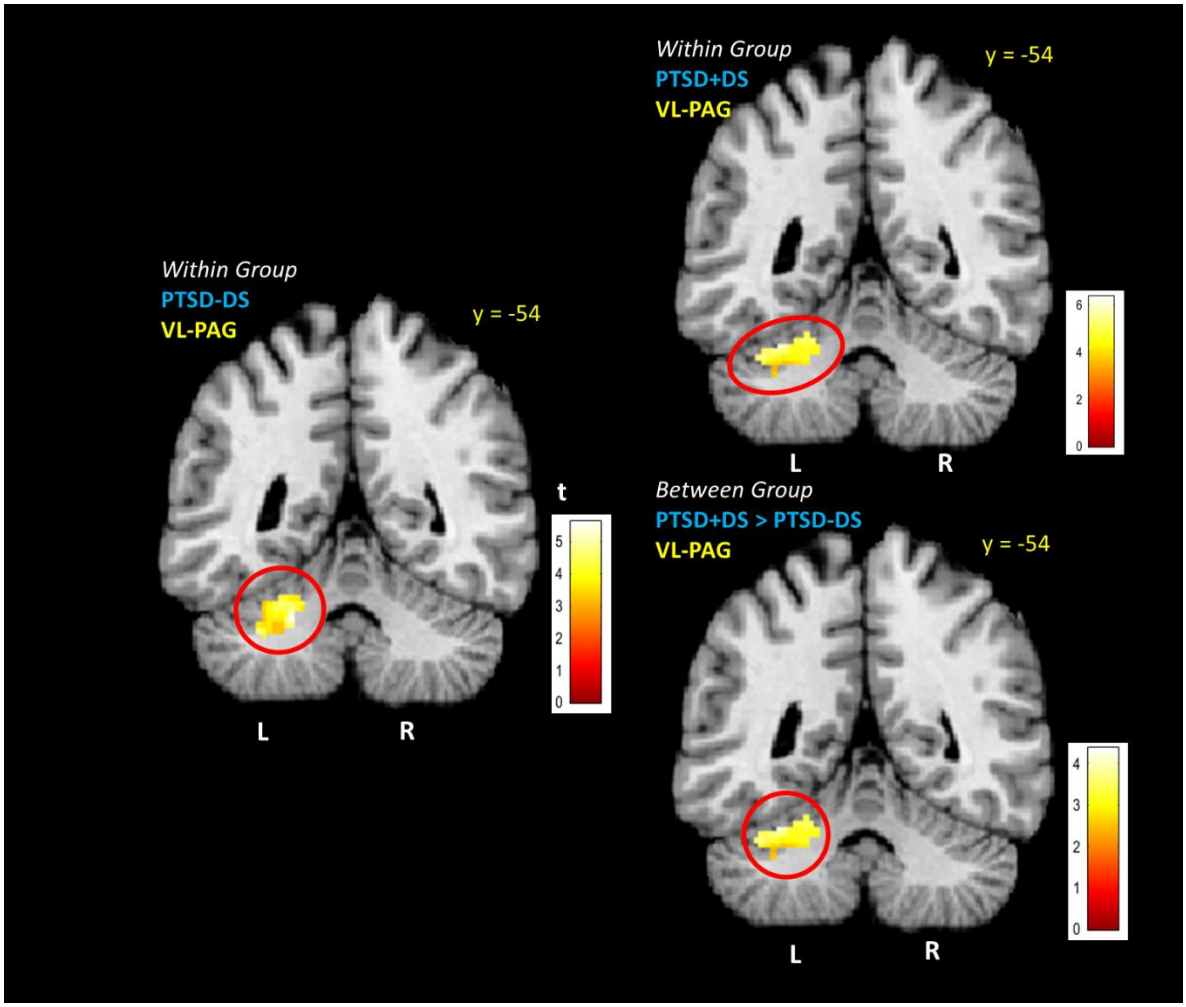

Supplementary Figure 4. Cerebellar Lobule VI. PTSD-DS demonstrated VL-PAG functional connectivity with cerebellar lobule VI (red circles), however PTSD+DS demonstrated both DL- and VL-PAG functional connectivity in the same area. PTSD+DS showed greater vlPAG functional connectivity with lobule VI when compared to PTSD-DS. Full factorial analysis of variance displayed FWE whole brain corrected clusters at $p<0.05$, k=50.

Abbreviations: PTSD-DS, non-dissociative posttraumatic stress disorder patients; PTSD+DS, dissociative posttraumatic stress disorder patients; DL-PAG, dorsolateral periaqueductal gray; VL-PAG, ventrolateral periaqueductal gray; L, left hemisphere; R, right hemisphere

Appendix B: Supplementary Material for Chapter 3

Supplementary Table 1. *Omnibus ANOVA Results from 3 (Group) x 2 (Region of Interest) Full Factorial ANOVA*

Contrast	LR	BA	Region	k	pFWE	Z	MNI Coordinates		
							x	y	z
Interaction Group x ROI	L	44	Supramarginal Gyrus	123	0.007	4.80	-56	24	26
	R	10	Superior Frontal Gyrus	62	0.031	4.45	30	66	0
Main Effect ROI	R	20	Inferior Temporal Gyrus	617	0.005	4.84	50	-32	-18
	R	38	Superior Temporal Pole		0.023	4.51	34	16	-30
	R	21	Middle Temporal Gyrus		0.029	4.44	60	-14	-20
	L		Cerebellar Lobule VI (Culmen)	27	0.003	4.57	-28	-50	-32
	L	10	Superior Frontal Gyrus	111	0.040	4.37	-12	68	6
	R	10	Superior Frontal Gyrus	311	0.041	4.36	22	68	10
Main Effect Group	R	40	Supramarginal Gyrus	12	0.008	4.78	66	-28	28

Areas revealed in the full-factorial interaction between group (PTSD, PTSD+DS, Controls) and vestibular nuclei (LVN and RVN), as well as the main effects for each factor. Full factorial analysis of variance displayed FWE whole-brain voxel-corrected at $p<0.05$, $k=10$. Peak coordinates without *k* (cluster size) values listed are subpeaks of the nearest *k* value listed above.

Abbreviations: ROI, region-of-interest; L, left hemisphere; R, right hemisphere; BA, Brodmann Area; *k*, Cluster Size.

Within Group Functional Connectivity Patterns

i.) PTSD

PTSD demonstrated LVN and RVN functional connectivity with the cerebellar lobule VI, the bilateral posterior insula, the right supramarginal gyrus, and the right superior frontal gyrus (BA 8) (Table II, Fig.1). There was also LVN and RVN connectivity with both the left medial dorsal and the right pulvinar thalamic nuclei, with additional RVN connectivity with the right medial dorsal and the medial geniculate thalamic nuclei. By contrast, LVN connectivity was observed with the cerebellar vermis, the right middle temporal gyrus, the right posterior cingulate cortex, and with premotor regions such as the left supplemental motor area and the right mid-cingulate (Table II). There was additional RVN connectivity with the left supramarginal gyrus, the right hippocampus, as well as various occipital regions such as the right fusiform and lingual gyri, as well as the right calcarine sulcus.

ii.) PTSD+DS

PTSD+DS demonstrated LVN and RVN functional connectivity with the cerebellar lobule VI, the left posterior insula, and the right thalamic pulvinar nuclei (Table II; Fig.1). Both LVN and RVN also demonstrated connectivity with multiple occipital brain

regions, including the left fusiform gyrus and the right calcarine sulcus, with additional RVN connectivity with the bilateral lingual gyrus. There was additional LVN connectivity with the right hippocampus. By contrast, RVN connectivity was observed with the cerebellar lobule I and the left middle temporal gyrus (Table II).

iii.) Controls

Healthy controls demonstrated LVN and RVN connectivity with the cerebellar lobule VI, the bilateral posterior insula, the left supramarginal gyrus, and the right superior frontal gyrus (BA 8) (Fig.1, Table II). There was both LVN and RVN connectivity with the left medial dorsal and the right pulvinar thalamic nuclei, with additional LVN connectivity with the right medial dorsal nuclei. In addition, LVN and RVN connectivity was observed with the primary motor (right precentral gyrus) and the premotor areas (right mid-cingulate; additional RVN connectivity with bilateral supplemental motor areas), as well as with the left primary auditory cortex (Heschl's gyrus) (Table II).

Supplementary Table 2. *LVN and RVN Functional Connectivity Within Participant Group*

Contrast	**L R**	**B A**	**Region**	**k**	**vFWE**	**Z**	**MNI Coordinates**		
							x	**y**	**z**
Within PTSD LVN	L		Cerebellar Lobule VI	5508 8	<0.001	Inf	-26	-48	-28
	L		Cerebellar Vermis		<0.001	Inf	-2	-60	-20
	R	23	Mid-Cingulate		<0.001	7.6 6	6	-40	36

	R	23	Posterior Cingulate Gyrus		<0.001	7.38	10	-42	32
	L	13	Posterior Insula		<0.001	6.08	-36	-24	10
	R	40	Supramarginal Gyrus		0.006	6.03	38	-28	36
	R	13	Posterior Insula		0.001	5.16	36	-26	12
	R	50	Pulvinar Thalamus	42	<0.001	6.72	10	-26	8
	L	50	Medial Dorsal Thalamus		<0.001	6.34	-8	-22	8
	R	19	Middle Temporal Gyrus	15	<0.001	5.68	42	-62	2
	R	8	Superior Frontal Gyrus	21	0.006	4.82	26	24	54
	L	6	Supplemental Motor Area	17	0.031	4.41	-8	-2	76
Within PTSD RVN	R		Cerebellar Lobule VI	58833	<0.001	Inf	28	-52	-32
	R	54	Hippocampus		<0.001	7.80	30	-32	-4
	R	23	Calcarine Sulcus		<0.001	7.49	14	-56	10
	R	37	Fusiform Gyrus		<0.001	7.69	30	-58	-8
	R	37	Lingual Gyrus		<0.001	7.50	6	-44	-14
	R	8	Superior		<0.001	5.9	6	16	48

			Frontal Gyrus			9			
	L	13	Posterior Insula		<0.001	5.73	-36	-26	10
	R	13	Posterior Insula		<0.001	5.54	34	-18	16
	R	50	Medial Dorsal Thalamus	42	<0.001	6.44	10	-26	8
	L	50	Medial Geniculate Thalamus		<0.001	6.31	-2	-20	4
	L	50	Medial Dorsal Thalamus		<0.001	6.02	-8	-22	8
	R	50	Pulvinar Thalamus		<0.001	5.34	10	-28	2
	R	40	Supramarginal Gyrus	15	<0.001	6.21	66	-28	28
	L	40	Supramarginal Gyrus	34	0.002	5.00	-62	-26	42
Within PTSD+DS LVN	L		Cerebellar Lobule VI	12674	<0.001	7.35	-38	-50	-28
	L	37	Fusiform Gyrus		<0.001	6.21	-24	-38	-20
	R	54	Hippocampus		<0.001	5.96	30	-32	-4
	L	13	Posterior Insula		0.011	4.67	-36	-24	16
	R	23	Calcarine Sulcus	49	<0.001	5.35	14	-56	10
	R	50	Pulvinar Thalamus	28	0.001	5.19	12	-26	6

Within PTSD+DS RVN	L	37	Fusiform Gyrus	20043	<0.001	Inf	-40	-46	-22
	L		Cerebellar Lobule VI		<0.001	Inf	-38	-48	-28
	L		Cerebellar Lobule I Crus		<0.001	6.94	-44	-52	-28
	L	13	Posterior Insula		0.001	5.22	-40	-26	12
	L	20	Middle Temporal Gyrus		<0.001	6.22	-50	-32	-16
	L	19	Lingual Gyrus		<0.001	6.00	-24	-52	-8
	R	23	Calcarine Sulcus	94	<0.001	6.24	14	-56	10
	R	18	Lingual Gyrus		0.038	4.36	24	-58	2
	R	50	Pulvinar Thalamus	42	0.004	4.91	10	-28	2
Within Ctrl LVN	L		Cerebellar Lobule VI	58927	<0.001	Inf	-28	-48	-30
	L	13	Posterior Insula		<0.001	7.60	-38	-22	14
	L	41	Superior Temporal Gyrus		<0.001	7.49	-60	-8	2
	R	24	Mid-Cingulate Gyrus		<0.001	7.17	2	-18	46
	L	41	Heschl Gyrus		<0.001	7.13	-52	-12	8
	L	37	Fusiform		<0.001	7.0	-38	-46	-22

			Gyrus			8			
	L	4	Precentral Gyrus		<0.001	6.95	-30	-20	48
	R	8	Superior Frontal Gyrus		<0.001	6.81	24	22	44
	L	40	Supramarginal Gyrus		<0.001	5.92	-52	-24	14
	R	13	Posterior Insula		0.001	5.18	34	-26	16
	L	50	Medial Dorsal Thalamus	40	<0.001	5.84	-8	-22	8
	R	50	Medial Dorsal Thalamus		0.004	4.87	8	-22	8
	R	50	Pulvinar Thalamus		0.007	4.76	10	-26	8
	L	40	Inferior Parietal	30	0.017	4.55	-38	-38	46
	R	6	Precentral Gyrus		0.030	4.42	20	-24	76
Within Ctrl RVN	R	31	Mid-Cingulate Gyrus	58896	<0.001	7.51	4	-24	44
	L	13	Posterior Insula		<0.001	7.46	-36	-20	12
	L	24	Supplemental Motor Area		<0.001	7.16	-2	-12	50
	L		Cerebellum Lobule VI		<0.001	6.99	-40	-42	-28
	L	41	Heschl Gyrus		<0.001	6.87	-48	-20	6
	R	13	Posterior Insula		<0.001	5.83	34	-26	16

	L	40	Supramarginal Gyrus		<0.001	5.62	-48	-22	24
	L	50	Medial Dorsal Thalamus	42	<0.001	5.37	-8	-22	8
	R	50	Pulvinar Thalamus		0.002	5.09	12	-26	6
	R	8	Superior Frontal Gyrus	73	0.002	5.03	26	24	54
	R	6	Supplemental Motor Area	181	0.002	5.00	20	-10	74
	R	6	Precentral Gyrus		0.023	4.44	20	-24	76
	L	40	Inferior Parietal	27	0.020	4.52	-38	-38	46

Post-hoc one-sample t-tests based on full-factorial analysis (reported at family-wise error whole-brain voxel-corrected at $p<.05$, $k=10$). Peak coordinates without *k* (cluster size) values listed are subpeaks of the nearest *k* value listed above.

Abbreviations: PTSD, posttraumatic stress disorder; PTSD+DS, posttraumatic stress disorder with the dissociative subtype; Ctrl, healthy controls; LVN, left vestibular nuclei; RVN, right vestibular nuclei; L, left hemisphere; R, right hemisphere; BA, Brodmann Area; *k*, Cluster Size; v-FWE, family-wise error voxel-corrected.

Appendix C: Supplementary Material for Chapter 4

Supplementary Table 1. *Results from* the *omnibus 3 x 12 (Particpant Group x Regions-of-Interest) ANOVA*

Contrast	**L R**	**B A**	**Region**	**k**	**vFWE**	**Z**	**MNI Coordinates x y z**		
Two-Way Interaction Participant Group x Regions-of-Interest									
	L/ R	31	Precuneus	693	< .001	5.59	0	-58	20
	R	18	Lingual Gyrus	Of 693	.001	5.35	2	-64	8
	L/ R	23	Posterior Cingulate Cortex	Of 693	.002	5.22	0	-50	30
	L	47	Rolandic Operculum	484	.002	3.49	-46	16	-6
	L	6	Precentral Gyrus	701	.012	3.25	-10	-16	76
	R	13	Posterior Insula	859	.024	3.15	44	-2	-6
	R	51	Pallidum	Of 859	.044	3.06	26	-14	-12
	R	6	Superior Frontal Gyrus	272	.027	3.13	18	12	56
	L	48	Caudate	171	.028	3.13	-10	16	6
Main Effect: Participant									

group									
	R	48	Caudate	1952	< .001	5.95	10	10	2
	R	51	Pallidum	Of 1952	.01	4.84	20	2	2
	L	18	Lingual Gyrus	12863	< .001	5.85	-16	-72	-4
	L	18	Cuneus	Of 12863	.001	5.32	-4	-74	18
	R	54	Hippocampus	735	.026	4.63	22	-34	0
	L	6	Precentral Gyrus	75	.048	4.48	-44	0	46
Main Effect: Regions-of-interest									
	R	13	Posterior Insula	93566	< .001	*Inf*	36	-20	6
	L	13	Posterior Insula	Of 93566	< .001	*Inf*	-38	-8	-8
	R	17	Calcarine Cortex	32	< .001	6.19	12	-94	0

Results from the omnibus 3 x 12 (Particpant Group x Regions-of-Interest) ANOVA (reported at family-wise error whole-brain voxel-corrected at $pFWE < .05$, $k = 10$). Cluster sizes (*k*) listed as "Of *x*" are subpeaks of the nearest "*x*" *k*-value listed above.

Abbreviations: PTSD posttraumatic stress disorder; PTSD+DS, posttraumatic stress disorder with the dissociative subtype; rdAIns, right dorsal anterior insula; rvAIns, right ventral anterior insula; ldAIns, left dorsal anterior insula; lvAIns, left ventral anterior insula; rdPIns, right dorsal posterior insula rvPIns, right ventral posterior insula; ldPIns, left dorsal posterior insula; lvPIns, left ventral posterior insula; L, left hemisphere; R, right hemisphere; BA, Brodmann Area; *k*, Cluster Size; *vFWE*, family-wise error voxel-corrected; MNI, Montréal Neurological Institute.

Supplementary Table 2: *Results from 3 (Group) x 2 (Hemisphere) x 2 (Axis) x 3 (Insula Subregion) Full Factorial Main Effects and Interactions*

Contrast	**L R**	**B A**	**Region**	**k**	**vFWE**	**Z**	**MNI Coordinates**		
							x	**y**	**z**
Four-Way Interaction (3 x 2 x 2 x 3) **Grp x Hem x Axis x Sub**			*None*						
Three-Way Interaction (3 x 2 x 3) **Grp x Hem x Sub**			*None*						
Three-Way Interaction (3 x 2 x 3) **Grp x Hem x Axis**			*None*						
Two-Way Interaction Grp x Hem									
	R	1	Central Operculum	22365	< .001	Inf	46	-20	24
	R	1	Postcentral Gyrus	Of 22635	< .001	Inf	38	-28	38
	R	6	Superior Frontal Gyrus	Of 22635	< .001	Inf	20	10	56

	L	30	Posterior Cingulate Cortex	32	< .001	7.12	-2	-48	14
	L	36	Parahippocampal Gyrus	118	< .001	6.28	-30	-16	-26
	L	20	Inferior Temporal Gyrus	Of 118	< .001	6.26	-40	-22	-26
	R	38	Temporal Pole	27	< .001	6.03	42	20	-38
	R		Cerebellar Lobule VI	124	< .001	5.86	38	-44	-28
	R	37	Fusiform Gyrus	Of 124	< .001	5.47	46	-56	-24
	R		Cerebellar Lobule IX	Of 124	.003	5.09	32	-42	-36
	R		Cerebellar Lobule IV	74	< .001	5.85	6	-48	-2
	R	37	Fusiform Gyrus	45	< .001	5.69	52	-68	-12
	L	38	Temporal Pole	33	< .001	5.61	-42	22	-24
	R	31	Precuneus	70	< .001	5.55	4	-42	54
	R	10	Medial Prefrontal Cortex	22	< .001	5.46	10	68	4
	R	37	Fusiform Gyrus	20	.002	5.24	64	-50	-8
	L	8	Dorsolateral Prefrontal Cortex	43	.002	5.23	-26	22	54
Two-Way Interaction Grp x Axis									
	L	38	Temporal Pole	54	< .001	6.16	-58	4	-22
	R	18	Lingual Gyrus	47	< .001	6.14	4	-60	8
Two-Way Interaction									

Grp x Sub									
	LR	31	Precuneus	301	< .001	6.63	0	-58	22
	R	17	Lingual Gyrus	Of 301	.002	5.18	2	-68	12
	R	37	Fusiform Gyrus	325	< .001	6.16	48	-48	-20
	L		Cerebellar Lobule IV	199	< .001	6.09	-20	-62	-34
	L		Cerebellar Lobule IX	Of 199	< .001	5.59	-14	-70	-34
	L		Cerebellar Lobule VII	Of 199	.003	5.14	-44	-60	-34
	R	47	Anterior Orbital Gyrus	282	< .001	6.03	34	44	-16
	R	10	Orbitolateral Prefrontal Cortex	Of 282	< .001	5.93	38	58	-4
	R	11	Medial Orbital Gyrus	Of 282	< .001	5.86	14	60	-16
	R	49	Amygdala	75	< .001	5.98	30	-2	-16
	R	9	Dorsolateral Prefrontal Cortex	135	< .001	5.74	54	28	16
	R	49	Basal Forebrain	38	< .001	5.63	14	4	-16
	R	37	Fusiform Gyrus	50	< .001	5.43	38	-68	-18
	R	40	Supramarginal Gyrus	52	< .001	5.33	44	-30	38
	R	22	Superior Temporal Gyrus	52	.001	5.30	60	-36	10
	R	9	Medial Prefrontal Cortex	71	.003	5.11	8	48	42
	R	39	Angular Gyrus	22	.004	5.05	42	-50	24

Main Effect: **group**									
	R	51	Pallidum	36394	< .001	Inf	10	4	-4
	R	48	Caudate	Of 36394	< .001	Inf	10	10	2
	L	20	Inferior Temporal Gyrus	3233	< .001	Inf	-58	-10	-32
	L	6	Precentral Gyrus	Of 3233	< .001	Inf	-44	0	46
	L	6	Postcentral Gyrus	Of 3233	< .001	Inf	-56	-8	28
	L	10	Ventrolateral Prefrontal Cortex	54	< .001	6.61	-26	54	-14
	R	24	Mid-Cingulate Cortex	495	< .001	6.51	14	-18	42
	L	24	Mid-Cingulate Cortex	38	< .001	5.99	-8	-18	40
	R	40	Supramarginal Gyrus	22	< .001	5.85	66	-30	32
	R	21	Middle Temporal Gyrus	29	< .001	5.63	64	-2	-24
	L	8	Dorsolateral Prefrontal Cortex	57	< .001	5.60	-38	14	38
	L	1	Postcentral Gyrus	20	< .001	5.42	-44	-28	56
	L	40	Supramarginal Gyrus	86	.001	5.35	-44	-44	50
	R	10	Dorsolateral Prefrontal Cortex	72	.002	5.18	40	58	8

Main Effect: hemisphere									
	R	13	Ventral Mid Insula	25885	< .001	Inf	40	-6	0
	R	13	Dorsal Posterior Insula	Of 25885	< .001	Inf	38	-14	12
	R	41	Central Operculum	Of 25885	< .001	Inf	48	-18	12
	L	13	Ventral Mid Insula	29016	< .001	Inf	-40	-2	-12
	L	13	Dorsal Mid Insula	Of 29016	< .001	Inf	-40	-10	4
	L	13	Ventral Anterior Insula	Of 29016	< .001	Inf	-38	4	-2
	L		Cerebellar Lobule VI	65	< .001	5.68	-26	-52	-32
	L	5	Postcentral Gyrus	66	< .001	5.54	-26	-34	66
	L	37	Fusiform Gyrus	65	.001	5.28	-26	-42	-20
	L	10	Medial Prefrontal Cortex	20	.003	5.07	-12	60	-12
Main Effect: axis									
	R	13	Ventral Anterior Insula	40181	< .001	Inf	36	12	-18
	R	13	Ventral Mid Insula	Of 40181	< .001	Inf	40	4	-14
	R	13	Ventral Mid Insula	Of 40181	< .001	Inf	42	-8	-8

	R	6	Superior Frontal Gyrus	38	.002	5.18	24	10	54
	L	22	Superior Temporal Gyrus	34	.003	5.08	-50	-42	20
Main Effect: subregion									
	R	13	Dorsal Posterior Insula	135293	< .001	Inf	36	-18	10
	R	13	Dorsal Posterior Insula	Of 135293	< .001	Inf	-36	-20	10
	R	13	Dorsal Mid Insula	Of 135293	< .001	Inf	18	-4	16

Omnibus ANOVA F-test summary of the 3 x 2 x 2 x 3 (participant group x hemisphere x axis x subregion) full-factorial analysis (reported at family-wise error whole-brain voxel-corrected at $pFWE < .05$, $k = 10$). Cluster sizes (k) listed as "Of x" are subpeaks of the nearest "x" k-value listed above.

Abbreviations: PTSD posttraumatic stress disorder; PTSD+DS, posttraumatic stress disorder with the dissociative subtype; rdAIns, right dorsal anterior insula; rvAIns, right ventral anterior insula; ldAIns, left dorsal anterior insula; lvAIns, left ventral anterior insula; rdPIns, right dorsal posterior insula rvPIns, right ventral posterior insula; ldPIns, left dorsal posterior insula; lvPIns, left ventral posterior insula; L, left hemisphere; R, right hemisphere; BA, Brodmann Area; *k*, Cluster Size; vFWE, family-wise error voxel-corrected; MNI, Montréal Neurological Institute.

Supplementary Table 3: *Post-hoc One Sample t-tests for Within Group Functional Connectivity*

Contrast	**L R**	**B A**	**Region**	**k**	**vFWE**	**Z**	**MNI Coordinates**

							x	y	z
Healthy controls									
rdAIns	R	13	Dorsal Anterior Insula	99918	< .001	Inf	34	20	4
rvAIns	R	13	Ventral Anterior Insula	10912	< .001	Inf	34	14	-14
rdMIns	R	13	Dorsal Mid Insula	11715	< .001	Inf	38	4	4
rvMIns	R	13	Ventral Mid Insula	11747	< .001	Inf	38	-4	-6
rdPIns	R	13	Dorsal Posterior insula	12266	< .001	Inf	36	-10	14
rvPIns	R	13	Ventral Posterior Insula	13884	< .001	Inf	34	-22	14
ldAIns	L	13	Dorsal Anterior Insula	89508	< .001	Inf	-36	16	-2
lvAIns	L	13	Ventral Anterior Insula	93696	< .001	Inf	-32	14	-14
ldMIns	L	13	Dorsal Mid Insula	98047	< .001	Inf	-38	4	0
lvMIns	L	13	Ventral Mid Insula	10675	< .001	Inf	-38	-8	-6
ldPIns	L	13	Dorsal Posterior Insula	11953	< .001	Inf	-40	-8	12
lvPIns	L	13	Ventral Posterior Insula	15502	< .001	Inf	-36	-20	10
PTSD									
rdAIns	R	13	Dorsal Anterior Insula	12069	< .001	Inf	36	16	-2

rvAIns	R	13	Ventral Anterior Insula	11715	< .001	Inf	34	14	-16
rdMIns	R	13	Dorsal Mid Insula	12957	< .001	Inf	34	6	8
rvMIns		13	Ventral Mid Insula	12207	< .001	Inf	40	-4	-8
rdPIns	R	13	Dorsal Posterior Insula	13634	< .001	Inf	36	-10	14
rvPIns	R	13	Ventral Posterior Insula	14313	< .001	Inf	38	-14	4
ldAIns	L	13	Dorsal Anterior Insula	12393	< .001	Inf	-32	18	4
lvAIns	L	13	Ventral Anterior Insula	12566	< .001	Inf	-32	14	-14
ldMIns	L	13	Dorsal Mid Insula	13085	< .001	Inf	-36	4	4
lvMIns	L	13	Ventral Mid Insula	13298	< .001	Inf	-38	-8	-8
ldPIns	L	13	Dorsal Posterior Insula	13384	< .001	Inf	-42	-4	2
lvPIns	L	13	Ventral Posterior Insula	14605	< .001	Inf	-36	-18	2
PTSD+DS									
rdAIns	R	13	Dorsal Anterior Insula	99071	< .001	Inf	40	18	-4
rvAIns	R	13	Ventral Anterior Insula	95554	< .001	Inf	36	12	-16
rdMIns	R	13	Dorsal Mid Insula	13302	< .001	Inf	40	8	-2
rvMIns	R	13	Ventral Mid	12403	< .001	Inf	38	6	-14

			Insula						
rdPIns	R	13	Dorsal Posterior Insula	15254	< .001	Inf	40	-4	0
rvPIns	R	13	Ventral Posterior Insula	14762	< .001	Inf	36	-20	6
ldAIns	L	13	Dorsal Anterior Insula	11127	< .001	Inf	-34	20	0
lvAIns	L	13	Ventral Anterior Insula	10837	< .001	Inf	-34	12	-16
ldMIns	L	13	Dorsal Mid Insula	13115	< .001	Inf	-40	6	0
lvMIns	L	13	Ventral Mid Insula	13361	< .001	Inf	-38	-6	-8
ldPIns	L	13	Dorsal Posterior Insula	15208	< .001	Inf	-42	-6	2
lvPIns	L	13	Ventral Posterior Insula	16139	< .001	Inf	-36	-18	6

Post-hoc one-sample *t*-tests detailing results from the 3 x 12 full-factorial analysis (reported at family-wise error whole-brain voxel-corrected at $pFWE < .05$, $k = 10$). Cluster sizes (*k*) listed as "Of *x*" are subpeaks of the nearest "*x*" k-value listed above.

Abbreviations: PTSD posttraumatic stress disorder; PTSD+DS, posttraumatic stress disorder with the dissociative subtype; rdAIns, right dorsal anterior insula; rvAIns, right ventral anterior insula; ldAIns, left dorsal anterior insula; lvAIns, left ventral anterior insula; rdPIns, right dorsal posterior insula rvPIns, right ventral posterior insula; ldPIns, left dorsal posterior insula; lvPIns, left ventral posterior insula; L, left hemisphere; R, right hemisphere; BA, Brodmann Area; *k*, Cluster Size; vFWE, family-wise error voxel-corrected; MNI, Montréal Neurological Institute.

Supplementary Table 4: *Post-hoc One Sample t-tests for Between Group Functional Connectivity Differences for the Mid-Insula*

- **Post-hoc analysis for anterior and posterior subregion group differences is detailed in the main manuscript.**

Contrast	L R	B A	Region	k	vFWE	Z	MNI Coordinates x	y	z
PTSD> PTSD+DS									
rdMIns			*ns*						
rvMIns			*ns*						
ldMIns	L	51	Pallidum	26	.002	5.24	-16	6	0
lvMIns	R	50	Ventral Anterior Thalamus	107	< .001	6.33	8	2	-4
	R	51	Pallidum		< .001	5.74	14	8	-2
	L	51	Pallidum	236	< .001	5.96	-20	-2	2
					< .001				
PTSD+DS> PTSD					< .001				
rdMIns	L		Cerebellar Lobule II	512	< .001	5.97	-8	-80	-28
	L		Cerebellar Lobule I	Of 512	< .001	5.53	-18	-78	-24
	L	19	Lingual Gyrus	167	< .001	5.86	-16	-68	-4
	L	19	Middle Occipital Gyrus	1086	< .001	5.50	-28	-86	14

	L	18	Cuneus	Of 1086	< .001	5.36	-6	-74	18
	L	19	Inferior Occipital Gyrus	44	.002	5.20	-38	-64	-12
	R		Cerebellar Lobule I	48	.002	5.18	20	-82	-22
rvMIns	L	18	Lingual Gyrus	2789	< .001	5.66	-18	-68	-4
	L	19	Middle Occipital Gyrus	Of 2789	< .001	5.54	-26	-86	14
	L	39	Angular Gyrus	81	< .001	5.42	-48	-44	22
	L	7	Precuneus	53	.004	5.01	-8	-62	50
ldMIns			*ns*						
lvMIns	L		Cerebellar Lobule VI	34	< .001	5.49	-38	-62	-24
PTSD > healthy controls									
rdMIns	R	48	Caudate	143	.001	5.28	10	10	0
rvMIns	L	24	Rostral Anterior Cingulate Cortex	249	.001	5.33	-2	26	-6
ldMIns	R	50	Pulvinar Thalamus	2139	< .001	7.35	20	-30	14

	L	54	Hippocampus	Of 2139	< .001	6.00	-26	-34	-2
	R	48	Caudate	465	< .001	6.48	10	8	4
	L	50	Mediodorsal Thalamus	Of 465	.001	5.26	-4	0	-2
lvMIns	R	50	Ventral Anterior Thalamus	2521	< .001	7.59	6	2	-4
	R	49	Putamen	Of 2521	< .001	6.92	16	8	4
	L	54	Hippocampus	128	< .001	5.97	-28	-34	0
	R		Periaqueductal Gray	60	.002	5.13	6	-26	-10
	L	50	Midline Thalamus	54	.003	5.09	-8	-18	18
PTSD+DS> healthy controls									
rdMIns	L	19	Fusiform Gyrus	230	< .001	5.67	-14	-66	-6
	R	19	Lingual Gyrus	27	< .001	5.51	16	-66	-2
	R	19	Lingual Gyrus	21	< .001	5.44	12	-74	0
	L	18	Cuneus	228	.001	5.25	-2	-82	18
	L	19	Middle Occipital Gyrus	Of 228	.002	5.16	-28	-84	14
	L	19	Superior Occipital Gyrus	Of 228	.003	5.13	-12	-88	24
	R	17	Calcarine Cortex	22	.002	5.22	16	-64	12

rvMIns			*ns*						
ldMIns	R	19	Cuneus	5433	< .001	6.50	10	-78	34
	R	18	Lingual Gyrus	Of 5433	< .001	5.99	4	-64	8
	R	13	Ventral Anterior Insula	85	.001	5.31	48	16	-4
	R	13	Ventral Mid Insula	41	.001	5.26	46	-8	-2
	L		Cerebellar Lobule	21	.005	4.99	-38	-64	-24
lvMIns	L		Cerebellar Lobule	688	< .001	6.17	-6	-62	-8
	L	18	Lingual Gyrus	Of 688	< .001	5.76	-16	-68	-6
	L	18	Inferior Occipital Gyrus	Of 688	.002	5.13	-30	-84	-6
	L		Cerebellar Lobule	450	< .001	5.89	-38	-64	-24
	R		Cerebellar Lobule	Of 450	< .001	5.70	14	-68	-30
	L		Cerebellar Lobule	Of 450	< .001	5.69	-20	-80	-24
	R	18	Cuneus	2314	< .001	5.64	14	-74	26
	R	17	Calcarine Cortex	Of 2314	< .001	5.64	10	-64	14
	R	13	Ventral Mid Insula	73	< .001	5.38	46	-8	-2

healthy controls > PTSD									
rdMIns	L		Precentral Gyrus	62	< .001	5.79	-44	0	46
	L		Middle Temporal Gyrus	79	< .001	5.76	-58	-36	-8
	L		Postcentral Gyrus	126	< .001	5.73	-58	-8	26
	L		Central Operculum	Of 126	.003	5.12	-58	-12	14
	L		Precentral Gyrus	102	.001	5.41	-50	0	20
	L		Superior Temporal Gyrus	27	.002	5.14	-64	-16	-6
rvMIns			*ns*						
ldMIns			*ns*						
lvMIns			*ns*						
healthy controls > PTSD+DS									
rdMIns	R	4	Postcentral Gyrus	331	< .001	5.69	34	-18	42
	L	1	Postcentral Gyrus	145	.003	5.07	-52	-22	30
rvMIns	L	1	Postcentral	58	< .001	5.44	-52	-22	30

			Gyrus						
	L	4	Central Operculum	206	< .001	5.34	-44	-12	18
	L	13	Dorsal Posterior Insula	Of 206	.001	5.28	-34	-14	18
ldMIns	L	40	Postcentral Gyrus	117	< .001	5.34	-48	-20	34
lvMIns	L	6	Precentral Gyrus	27	.004	5.03	-40	-2	32

Between group post-hoc two-sample *t*-tests detailing differences in mid-insula functional connectivity patterns in PTSD groups (PTSD and PTSD+DS) versus healthy controls based on the 3 x 12 full-factorial analysis (reported at family-wise error whole-brain voxel-corrected at *p*FWE < .05, *k* = 10). Cluster sizes (*k*) listed as "Of *x*" are subpeaks of the nearest "*x*" k-value listed above.

Abbreviations: PTSD posttraumatic stress disorder; PTSD+DS, posttraumatic stress disorder with the dissociative subtype; rdAIns, right dorsal anterior insula; rvAIns, right ventral anterior insula; ldAIns, left dorsal anterior insula; lvAIns, left ventral anterior insula; rdPIns, right dorsal posterior insula rvPIns, right ventral posterior insula; ldPIns, left dorsal posterior insula; lvPIns, left ventral posterior insula; L, left hemisphere; R, right hemisphere; BA, Brodmann Area; *k*, Cluster Size; vFWE, family-wise error voxel-corrected; MNI, Montréal Neurological Institute.

Appendix D: Supplementary Material for Chapter 5

Supplementary Table 1. *Subtraction Analyses F-tests*

	LR	BA	Region	k	vFWE	Z-Score	MNI Coordinates		
							x	y	z
Omnibus ANOVA test	R	19	Inferior Occipital Gyrus	34008	<0.001	Inf	44	-64	4
	L	19	Inferior Occipital Gyrus		<0.001	Inf	-46	-68	8
	L	18	Cuneus		<0.001	Inf	-2	-80	20
	R	6	Frontal Eye Field	3486	<0.001	Inf	46	0	56
	L	6	Frontal Eye Field	4109	<0.001	Inf	-44	-6	56
	L	44	Inferior Frontal Operculum		<0.001	5.88	-54	10	4
	L	10	Orbitolateral Prefrontal Cortex		<0.001	5.73	-42	50	-14
	R	6	Supplementary Eye Field	949	<0.001	7.61	2	2	62
	R	8	Supplementary Motor Cortex		0.034	4.92	2	16	50
	R	7	Superior Parietal Lobule	79	0.019	5.05	22	-44	76
Main Effect of Group	**NS**								
Main Effect of Motion	L/R	18	Cuneus	18641	<0.001	Inf	0	-80	20
	R	17	Lingual Gyrus		<0.001	Inf	2	-80	4
	L	18	Lingual Gyrus		<0.001	Inf	-10	-76	-10
	L	17	Calcarine Cortex		<0.001	Inf	-10	-72	10
	R	17	Calcarine Cortex		<0.001	Inf	10	-82	4

	L	19	Superior Occipital Gyrus		<0.001	Inf	18	-86	26
	R	18	Superior Occipital Gyrus		<0.001	Inf	-10	-72	24
	L	6	Precentral Gyrus	575	<0.001	7.26	-44	-8	56
	R	6	Precentral Gyrus	833	<0.001	6.73	46	-4	54
	R	4	Postcentral Gyrus		0.004	5.42	36	-16	40
	L	7	Superior Parietal Lobule	335	0.002	5.42	-30	-52	58
	L	24	Mid-Cingulate Gyrus	79	0.004	5.40	-12	-20	40
	L	6	Supplemental Eye Field	141	0.024	5.04	-4	-4	62
Main Effect of Memory	L	19	Occipital-Fusiform Gyrus	116	0.049	4.86	-34	-76	-20
Interaction: Group x Motion	**NS**								
Interaction: Memory x Motion	**NS**								
Interaction: Group x Memory x Motion	**NS**								

Abbreviations: LR, left/right hemisphere; BA, Brodmann Area; k, cluster size; vFWE, voxel-wise family-wise error corrected; MNI, Montréal Neurological Institute; **NS**, not significant.

Supplementary Table 2. *Within Condition T-tests for Subtraction Analysis*

	L R	B A	Region	k	vFWE	Z-Score	MNI Coordinates x y z		
No Memory									
Controls									
Central Fixation Dot	**N S**								
Horizontal Smooth Pursuit	L/ R	18	Cuneus	1432 0	<0.001	Inf	0	-80	20
	R	17	Calcarine Cortex				8	-64	10
	L	17	Calcarine Cortex		<0.001	Inf	-12	-68	8
	R	17	Inferior Occipital Gyrus		<0.001	Inf	8	-74	6
	R	19	Superior Occipital Gyrus		<0.001	Inf	18	-84	26
	L	19	Lingual Gyrus		<0.001	Inf	-12	-66	-2
	L	19	Inferior Occipital Gyrus		<0.001	Inf	-42	-68	4
	R	6	Frontal Eye Field	1475	<0.001	6.73	48	-2	52
	L	6	Frontal Eye Field	568	0.003	5.44	-42	-8	48
	L	40	Parietal Operculum	272	0.004	5.39	-50	-40	26
	R	7	Superior Parietal Lobule	1567	0.005	5.31	28	-42	42
	R	22	Superior Temporal Gyrus		0.013	5.11	66	-30	18

	L	7	Superior Parietal Lobule	393	0.007	5.25	-28	-50	54
	R	31	Medial Precentral Gyrus	121	0.007	5.24	12	-26	42
Horizontal Saccadic	L	19	Lingual Gyrus	6242	<0.001	7.75	-16	-64	-2
	L	17	Calcarine Cortex		<0.001	7.29	-16	-68	6
	L	18	Cuneus		<0.001	7.01	-2	-78	24
	R	19	Inferior Occipital Gyrus		<0.001	6.65	42	-66	8
	R	19	Lingual Gyrus		<0.001	6.57	14	-60	-8
	R	19	Superior Occipital Gyrus		0.002	5.50	18	-84	26
	R	37	Middle Temporal Gyrus		0.002	5.46	56	-62	2
	L	37	Inferior Occipital Gyrus	525	<0.001	6.03	-50	-74	2
	R	6	Frontal Eye Field	837	<0.001	5.74	48	-2	56
	R	22	Superior Temporal Gyrus	322	0.001	5.58	66	-38	12
	L	40	Parietal Operculum	113	0.006	5.28	-52	-40	26
	L	6	Frontal Eye Field	415	0.007	5.26	-42	-8	56
Vertical Saccadic	R	19	Inferior Occipital Gyrus	9169	<0.001	7.78	42	-64	6
	R	18	Calcarine Cortex		<0.001	7.61	8	-64	6
	L/R	18	Cuneus		<0.001	7.18	0	-80	20

	R		Cerebellar Lobule VI		<0.001	6.89	14	-60	-10
	R	19	Lingual Gyrus		<0.001	6.56	22	-68	-4
	L	19	Lingual Gyrus		<0.001	6.47	-16	-62	0
	R	19	Superior Occipital Gyrus		<0.001	6.16	16	-84	26
	L	37	Superior Occipital Gyrus		<0.001	5.89	50	-72	0
	R	6	Frontal Eye Field	1391	<0.001	7.15	48	-2	54
	L	19	Inferior Occipital Gyrus	700	<0.001	6.32	-52	-72	6
	L	19	Middle Temporal Gyrus		<0.001	6.07	-42	-64	6
	R	22	Superior Temporal Gyrus	446	<0.001	5.88	64	-38	14
	L	6	Frontal Eye Field	602	<0.001	5.78	-46	-6	54
	L	6	Supplementary Eye Field	452	0.003	5.45	-2	-4	66
PTSD									
Central Fixation Dot	R	37	Occipital-Fusiform Gyrus	282	0.020	5.02	34	-70	-14
Horizontal Smooth Pursuit	L	19	Middle Temporal Gyrus	15927	<0.001	Inf	-46	-68	6
	R	19	Superior Occipital Gyrus		<0.001	Inf	20	-84	28
	R	18	Cuneus		<0.001	Inf	4	-76	18
	R	17	Calcarine Cortex		<0.001	Inf	18	-66	8

	L	17	Calcarine Cortex		<0.001	Inf	-12	-72	10
	L	18	Cuneus		<0.001	Inf	-6	-82	20
	L	19	Superior Occipital Gyrus		<0.001	Inf	-20	-86	28
	L	17	Precuneus		<0.001	7.42	-8	-80	4
	R	37	Inferior Occipital Gyrus		<0.001	7.08	50	-66	0
	L	7	Superior Parietal Lobule	577	<0.001	5.78	-28	-58	58
	R	6	Frontal Eye Field	605	0.001	5.57	44	-2	56
	L	6	Frontal Eye Field	541	0.020	5.02	-40	-4	56
Horizontal Saccadic	R	17	Calcarine Cortex	7072	<0.001	6.58	14	-70	12
	L	17	Calcarine Cortex		<0.001	6.52	-14	-70	8
	R	18	Cuneus		<0.001	6.16	4	-78	16
	L	18	Cuneus		<0.001	5.95	-2	-80	22
	R	19	Superior Occipital Gyrus		<0.001	5.92	20	-86	30
	R	37	Inferior Occipital Gyrus		0.006	5.27	54	-66	2
	L	19	Superior Occipital Gyrus		0.018	5.04	-20	-86	26
	R	19	Lingual Gyrus		0.022	5.00	16	-56	0
	L	19	Occipital-Fusiform Gyrus		0.028	4.95	-26	-72	-8
	L	19	Middle Temporal Gyrus	1616	<0.001	5.99	-44	-66	8
	L	19	Superior		0.011	5.14	-44	-66	8

			Temporal Gyrus						
	L	19	Inferior Occipital Gyrus		0.038	4.87	-46	-80	2
	L	6	Frontal Eye Field	417	0.005	5.30	-48	-8	50
Vertical Saccadic	L	19	Inferior Occipital Gyrus		<0.001	Inf	-44	-68	6
	R	19	Superior Occipital Gyrus	12037	<0.001	7.18	20	-84	28
	R	19	Middle Temporal Gyrus		<0.001	7.08	42	-62	2
	L	19	Superior Occipital Gyrus		<0.001	6.75	20	-84	28
	R	17	Cuneus		<0.001	6.54	4	-82	10
	L	18	Cuneus		<0.001	6.53	-6	-84	18
	R	37	Inferior Occipital Gyrus		<0.001	6.16	52	-66	0
	L	17	Calcarine Cortex		<0.001	6.05	-4	-92	10
	L	19	Occipital-Fusiform Gyrus		<0.001	5.91	-24	-70	-12
	R	7	Superior Parietal Lobule		<0.001	5.88	30	-56	54
	R	6	Frontal Eye Field	797	<0.001	5.23	44	0	58
	L	6	Frontal Eye Field	993	0.007	5.10	52	4	48
	R	6	Supplemental Motor Cortex	312	0.014	4.39	4	2	60
	L	7	Superior Parietal Lobule	604	0.014	5.00	-32	-52	58

Neutral Memory									
Controls									
Central Fixation Dot	R	18	Inferior Occipital Gyrus	1682	<0.001	7.13	30	-94	-4
	R	18	Occipital Pole		0.005	5.33	26	-98	4
	R	37	Fusiform Gyrus		0.011	5.15	36	-62	-20
	R	37	Occipital-Fusiform Gyrus		0.033	5.07	36	-78	-16
	L	18	Inferior Occipital Gyrus	1504	<0.001	6.08	-26	-84	-10
	L	18	Occipital-Fusiform Gyrus		<0.001	5.99	-24	-88	-10
	L	18	Occipital Pole		0.002	5.53	-24	-98	2
	R	7	Superior Parietal Lobule	237	0.026	4.96	36	-60	62
Horizontal Smooth Pursuit	R	17	Calcarine Cortex	15136	<0.001	Inf	10	-66	14
	L/R	18	Cuneus		<0.001	Inf	0	-76	14
	R	19	Inferior Occipital Gyrus		<0.001	Inf	44	-64	4
	L	17	Lingual Gyrus		<0.001	Inf	-12	-80	2
	R	18	Superior Occipital Gyrus		<0.001	Inf	20	-90	16
	L	18	Superior Occipital Gyrus		<0.001	Inf	-18	-90	16
	R	6	Frontal Eye Field	762	<0.001	6.32	48	0	56
	L	6	Frontal Eye Field	524	0.009	5.19	-48	-4	54

	R	7	Superior Parietal Lobule	642	0.017	5.06	26	-50	46
Horizontal Saccadic	R	17	Calcarine Cortex	12100	<0.001	7.45	4	-76	4
	L	18	Cuneus		<0.001	6.86	-2	-80	18
	L	19	Lingual Gyrus		<0.001	6.72	-24	-64	-8
	L	18	Calcarine Cortex		<0.001	6.69	-10	-80	-8
	R	19	Middle Temporal Gyrus		<0.001	6.28	46	-62	6
	R	18	Superior Occipital Gyrus		0.001	5.73	18	-90	18
	L	19	Middle Temporal Gyrus		0.001	5.63	-50	-66	8
	L	7	Superior Parietal Lobule	512	0.001	5.66	-30	-48	44
	R	6	Frontal Eye Field	657	0.002	5.51	48	2	36
	L	6	Frontal Eye Field	551	0.010	5.17	-48	-2	52
Vertical Saccadic	L	18	Lingual Gyrus	13598	<0.001	7.10	-4	-78	0
	R	19	Calcarine Cortex		<0.001	6.62	12	-64	-8
	L	18	Occipital-Fusiform Gyrus		<0.001	6.56	-22	-74	-6
	R	18	Superior Occipital Gyrus		<0.001	6.48	20	-88	18
	R	19	Inferior Occipital Gyrus		<0.001	6.35	46	-64	4

	R	19	Lingual Gyrus		<0.001	6.32	24	-70	-4
	L/R	17	Cuneus		<0.001	6.31	0	-84	-4
	R	6	Frontal Eye Field	473	<0.001	5.92	48	0	56
	L	6	Frontal Eye Field	573	0.005	5.32	-44	-6	56
	L	7	Superior Parietal Lobule	231	0.018	5.05	-30	-52	54
PTSD									
Central Fixation Dot	R	18	Inferior Occipital Gyrus	3436	<0.001	5.95	32	-90	2
	R	18	Occipital-Fusiform Gyrus		<0.001	5.86	28	-64	14
	R	37	Fusiform Gyrus		0.007	5.26	40	-54	-10
	R		Cerebellar Lobule VI		0.038	4.88	30	-80	-20
	R	18	Lingual Gyrus		0.048	4.83	14	-92	-12
	L	37	Fusiform Gyrus	2076	0.004	5.32	-42	-56	-22
	L	18	Inferior Occipital Gyrus		0.011	5.15	-28	-92	10
	L	19	Occipital-Fusiform Gyrus		0.024	4.97	-36	-72	-16
Horizontal Smooth Pursuit	L	19	Superior Occipital Gyrus	13434	<0.001	7.33	-20	-90	26
	L	19	Inferior Occipital Gyrus		<0.001	6.88	-42	-70	6
	L	17	Calcarine Cortex		<0.001	6.85	-6	-88	2

	R	17	Calcarine Cortex		<0.001	6.78	10	-82	4
	L	18	Cuneus		<0.001	6.74	-4	-82	20
	R	17	Lingual Gyrus		<0.001	6.67	4	-72	8
	R	19	Inferior Occipital Gyrus		<0.001	6.66	42	-66	2
	L	18	Lingual Gyrus		<0.001	6.55	-10	-80	0
	R		Cerebellar Lobule VI		<0.001	6.47	26	-68	-18
Horizontal Saccadic	R	17	Calcarine Cortex	7072	<0.001	6.58	14	-70	12
	L	17	Calcarine Cortex		<0.001	6.52	-2	-84	6
	R	18	Cuneus		<0.001	6.16	4	-78	16
	R	19	Superior Occipital Gyrus		<0.001	5.92	20	-86	30
	L	19	Lingual Gyrus		<0.001	5.87	-14	-64	-6
	R	23	Precuneus		0.002	5.48	24	-56	6
	R	37	Inferior Occipital Gyrus		0.006	5.27	54	-66	2
	L	19	Superior Occipital Gyrus		0.018	5.04	-20	-86	26
	R	19	Lingual Gyrus		0.022	5.00	16	-56	0
	L	19	Occipital-Fusiform Gyrus		0.028	4.95	-26	-72	-8
	R	47	Inferior Orbitofrontal Cortex	253	0.040	4.87	48	42	-18
Vertical Saccadic	R	37	Occipital-	1132	<0.001	Inf	24	-68	-14

			Fusiform Gyrus	1					
	R		Cerebellar Lobule VI		<0.001	6.45	16	-74	-16
	R	17	Calcarine Cortex		<0.001	6.42	10	-86	10
	L	18	Occipital-Fusiform Gyrus		<0.001	6.31	-22	-70	-14
	R	17	Lingual Gyrus		<0.001	6.11	4	-80	2
	R	19	Inferior Occipital Gyrus			5.90	44	-68	2
	L	18	Cuneus			5.92	-4	-82	18
	L	19	Lingual Gyrus		0.001	5.71	-18	-64	-8
Traumatic Memory									
Controls									
Central Fixation Dot			**NS**						
Horizontal Smooth Pursuit	L/R	18	Cuneus	12148	<0.001	Inf	0	-74	22
	R	17	Calcarine Cortex		<0.001	Inf	12	-84	0
	L	17	Lingual Gyrus		<0.001	Inf	-12	-80	2
	L	17	Calcarine Cortex		<0.001	6.98	-6	-88	-2
	R	19	Middle Temporal Gyrus		<0.001	6.92	42	-62	4
	L	6	Frontal Eye Field	336	0.004	5.34	-46	-6	58
Horizontal Saccadic	R	17	Calcarine Cortex	3943	<0.001	6.15	12	-88	2
	R	17	Lingual Gyrus		<0.001	6.09	2	-72	12

	L	18	Occipital-Fusiform Gyrus		<0.001	5.72	-24	-74	-14
	L/R	18	Cuneus		0.001	5.63	0	-74	20
	L	17	Calcarine Cortex		0.001	5.59	-10	-80	6
	L	18	Lingual Gyrus		0.018	5.04	-16	-70	-12
Vertical Saccadic	R	19	Calcarine Cortex	5788	<0.001	5.89	14	-62	4
	L	18	Lingual Gyrus		0.001	5.76	-18	-74	-12
	L	18	Occipital-Fusiform Gyrus		0.001	5.70	-24	-72	-12
	R	18	Cuneus		0.001	5.65	6	-90	12
	L	19	Middle Occipital Gyrus		0.003	5.42	-50	-70	10
	L	19	Inferior Occipital Gyrus		0.003	5.41	-52	-74	8
	L	17	Calcarine Cortex		0.029	4.94	-10	-66	8
	L	6	Frontal Eye Field	92	0.002	5.47	-46	-6	58
	R	37	Middle Temporal Gyrus	380	0.004	5034	44	-62	4
PTSD									
Central Fixation Dot	R	37	Occipital-Fusiform Gyrus	1263	<0.001	5.89	39	-62	-18
	L	19	Occipital-Fusiform Gyrus	1123	0.002	5.50	-36	-72	-18
	R	6	Supplementary Eye Field	343	0.006	5.28	2	0	62

Horizontal Smooth Pursuit	R	17	Calcarine Cortex	19891	<0.001	Inf	10	-86	6
	L	17	Calcarine Cortex		<0.001	Inf	-6	-86	2
	L	19	Inferior Occipital Gyrus		<0.001	Inf	-44	-70	4
	L	18	Cuneus		<0.001	7.68	-4	-82	20
	L	19	Occipital-Fusiform Gyrus		<0.001	7.54	-36	-74	-18
	R		Cerebellar Lobule VI		<0.001	7.48	14	-76	-16
	R	19	Superior Occipital Gyrus		<0.001	7.26	20	-82	24
	L	19	Superior Occipital Gyrus		<0.001	7.09	-20	-90	26
	R	37	Fusiform Gyrus		<0.001	7.07	26	-66	-16
	L	7	Superior Parietal Lobule		0.001	5.56	-28	-60	62
	L	6	Frontal Eye Field	627	0.003	5.39	-42	-4	58
	R	6	Frontal Eye Field	236	0.022	5.14	44	0	56
	L/R	7	Precuneus	149	<0.001*	5.56	0	-62	54
Horizontal Saccadic	R	17	Calcarine Cortex	8588	<0.001	7.14	10	-86	6
	L	17	Calcarine Cortex		<0.001	6.72	-12	-72	8
	R	17	Lingual Gyrus		<0.001	6.54	2	-76	4
	R	18	Cuneus		<0.001	6.16	4	-88	12
	L	18	Calcarine Cortex		<0.001	6.06	-6	-72	6

	L		Cerebellar Lobule VI		0.004	5.36	-20	-74	-18
	R		Cerebellar Lobule VI		0.005	5.32	16	-74	-16
	L	7	Superior Parietal Lobule	163	0.043	4.85	-36	-58	58
Vertical Saccadic	R		Cerebellar Lobule VI	1680 2	<0.001	7.80	24	-66	-16
	L	19	Inferior Occipital Gyrus		<0.001	7.10	-42	-68	6
	L		Cerebellar Lobule VI		<0.001	6.94	-20	-72	-18
	R	17	Calcarine Cortex		<0.001	6.81	8	-88	6
	L/ R	17	Cuneus		<0.001	6.79	0	-86	12
	L	19	Occipital-Fusiform Gyrus		<0.001	6.73	-24	-70	-16
	R	19	Superior Occipital Gyrus		<0.001	6.57	20	-82	26
	R	19	Occipital-Fusiform Gyrus		<0.001	6.35	38	-64	-16
	R	17	Lingual Gyrus		<0.001	6.29	2	-90	2
	L	7	Precuneus	47	0.003*	4.23	-2	-58	54

Abbreviations: LR, left/right hemisphere; BA, Brodmann Area; k, cluster size; vFWE, voxel-wise family-wise error corrected; MNI, Montréal Neurological Institute; **NS,** not significant

Supplementary Table 3. *Between-Group T-tests for Subtraction Analysis*

	LR	BA	Region	k	vFWE	Z-Score	MNI Coordinates x	y	z
Between Group									
PTSD>Control No Memory Condition Horizontal Saccadic	L	21	Superior Temporal Gyrus	200	0.013	5.12	-48	-48	10
PTSD>Controls Traumatic Memory Horizontal Smooth Pursuit	L/R	7	Precuneus	40	0.004*	4.08	0	-58	52
Between Motion Type									
No Memory									
Controls									
Horizontal Smooth Pursuit > Central Fixation Dot	R	17	Calcarine Cortex	17601	<0.001	Inf	8	-66	12
	L/R	18	Cuneus		<0.001	Inf	0	-76	14
	L	17	Lingual Gyrus		<0.001	Inf	-2	-76	2
	R	18	Superior Occipital Gyrus		<0.001	Inf	20	-88	18
	L	6	Frontal Eye Field	407	0.001	5.67	-46	-8	58
	R	6	Frontal Eye Field	634	0.002	5.50	48	-2	52
	R	7	Precuneus	11	0.004*	4.07	2	-74	46
Horizontal Saccadic > Central Fixation Dot	R	17	Lingual Gyrus	10484	<0.001	Inf	2	-78	4
	R	17	Calcarine Cortex		<0.001	Inf	8	-68	14

	L	17	Calcarine Cortex		<0.001	Inf	-6	-74	10
	L	18	Cuneus		<0.001	Inf	-2	-78	24
	L	18	Lingual Gyrus		<0.001	7.55	-12	-78	-12
Horizontal Smooth Pursuit > Horizontal Saccadic	R	18	Superior Occipital Gyrus		<0.001	6.84	18	-88	18
	R	17	Cuneus	3806	0.002	5.77	2	-72	12
	L	18	Calcarine Cortex		0.005	5.33	-12	-84	-4
	L	18	Lingual Gyrus		0.007	5.25	-2	-68	4
	L	18	Superior Occipital Gyrus		0.013	5.11	-18	-92	16
	R	18	Occipital Pole		0.046	4.83	20	-94	18
	R	13	Posterior Insula	10	0.008*	3.93	30	-20	12
PTSD									
Horizontal Smooth Pursuit > Central Fixation Dot	L	18	Cuneus	9233	<0.001	Inf	-2	-82	22
	L	17	Calcarine Cortex		<0.001	Inf	-12	-72	8
	R	19	Superior Occipital Gyrus		<0.001	Inf	20	-84	28
	R	17	Lingual Gyrus		<0.001	7.71	2	-72	8
	L	19	Superior Occipital Gyrus		<0.001	7.52	-20	-90	26
	R	17	Calcarine Cortex		<0.001	7.45	16	-70	12
	L	19	Precuneus		<0.001	7.07	-8	-80	42
	L	19	Middle Temporal Gyrus	375	0.013	5.11	-48	-68	6

	R	19	Middle Temporal Gyrus	387	0.016	5.06	42	-62	2
Horizontal Saccadic > Central Fixation Dot	L/R	17	Lingual Gyrus	6530	<0.001	7.63	0	-82	4
	L	18	Cuneus		<0.001	6.76	-2	-82	22
	R	18	Calcarine Cortex		<0.001	6.76	8	-86	22
	L	17	Calcarine Cortex		<0.001	6.43	-12	-72	8
	R	19	Superior Occipital Gyrus		<0.001	6.23	20	-86	30
	L	19	Lingual Gyrus		<0.001	6.12	-12	-62	-4
Central Fixation Dot > Horizontal Saccadic	R	18	Inferior Occipital Gyrus	323	0.006	5.28	26	-94	0
	L	18	Inferior Occipital Gyrus	124	0.033	4.91	-20	-98	-6
Neutral Memory									
Controls									
Horizontal Smooth Pursuit > Central Fixation Dot	R	18	Cuneus	9129	<0.001	Inf	2	-74	20
	R	17	Calcarine Cortex		<0.001	Inf	8	-76	4
	R	17	Lingual Gyrus		<0.001	Inf	2	-78	2
	R	19	Superior Occipital Gyrus		<0.001	7.70	18	-86	26
	L	18	Calcarine Cortex		<0.001	7.45	-10	-86	-2
	L	18	Middle Occipital Gyrus		<0.001	7.24	-18	-90	16
	R	19	Inferior Occipital Gyrus	340	0.001	5.55	44	-64	4

Horizontal Saccadic > Central Fixation Dot	R	17	Calcarine Cortex	7697	<0.001	Inf	4	-72	10
	L/R	18	Cuneus		<0.001	Inf	0	-78	20
	L	18	Calcarine Cortex		<0.001	Inf	-8	-74	10
	L	19	Lingual Gyrus		<0.001	7.36	-12	-66	-2
	R	18	Lingual Gyrus		<0.001	6.13	10	-58	4
Central Fixation Dot > Horizontal Smooth Pursuit	R	18	Occipital Pole	78	0.006	5.26	28	-96	-4
PTSD									
Horizontal Smooth Pursuit > Central Fixation Dot	L	19	Cuneus	5316	<0.001	6.65	-2	-82	22
	L	17	Calcarine Cortex		<0.001	6.53	-12	-72	8
	R	17	Calcarine Cortex		<0.001	6.30	12	-82	4
	L	18	Superior Occipital Gyrus		<0.001	6.22	-20	-90	24
	R	17	Lingual Gyrus		0.001	5.69	2	-86	1
	R	19	Superior Occipital Gyrus		0.001	5.67	20	-82	24
	L	18	Lingual Gyrus		0.001	5.59	-8	-78	2
	L	19	Inferior Occipital Gyrus	209	0.031	4.92	-42	-70	6
Horizontal Saccadic > Central Fixation Dot	L	17	Calcarine Cortex	2577	<0.001	5.82	-12	-72	8
	R	17	Lingual Gyrus		<0.001	5.71	4	-84	0
	L	17	Cuneus		0.009	5.20	-4	-80	22
	R	18	Calcarine Cortex		0.014	5.09	14	-70	14

Central Fixation Dot > Horizontal Smooth Pursuit	L	18	Occipital Pole	43	0.037	4.88	-20	-100	-6
Traumatic Memory									
Controls									
Horizontal Smooth Pursuit > Central Fixation Dot	L/R	18	Cuneus	11527	<0.001	Inf	0	-76	14
	R	17	Calcarine Cortex		<0.001	Inf	10	-88	2
	L	18	Lingual Gyrus		<0.001	Inf	-10	-80	-10
	R	19	Superior Occipital Gyrus		<0.001	Inf	18	-88	28
	L	17	Calcarine Cortex		<0.001	Inf	-6	-88	0
	L	18	Middle Occipital Gyrus		<0.001	Inf	-18	-92	16
	R	19	Middle Temporal Gyrus	382	<0.001	6.30	42	-60	4
	R	6	Frontal Eye Field	257	0.002	5.47	44	-8	46
	R	7	Precuneus	26	0.003*	4.22	2	-72	42
Horizontal Saccadic > Central Fixation Dot	R	17	Calcarine Cortex	5839	<0.001	7.54	4	-72	14
	R	18	Lingual Gyrus		<0.001	7.51	2	-80	4
	L	18	Cuneus		<0.001	6.93	-2	-80	18
	L	17	Calcarine Cortex		<0.001	6.28	-10	-82	8
	L	18	Lingual Gyrus		0.001	5.81	-8	-78	-10
	R	19	Superior Occipital Gyrus		0.005	5.32	20	-88	26

	L	6	Frontal Eye Field	42	0.048	4.82	-46	-6	58
Central Fixation Dot > Horizontal Saccadic	R	18	**Inferior Occipital Gyrus**	151	0.038	4.88	28	-96	0
Horizontal Smooth Pursuit > Horizontal Saccadic	L	18	**Superior Occipital Gyrus**	3581	<0.001	5.77	-18	-90	14
	L	18	**Lingual Gyrus**		0.001	5.70	-12	-80	-14
	L	18	**Calcarine Cortex**		0.005	5.30	-14	-82	-2
	L	18	**Cuneus**		0.023	4.99	-2	-80	26
	R	18	**Middle Occipital Gyrus**		0.041	4.86	20	-90	16
	R	19	**Middle Temporal Gyrus**	115	0.015	5.08	38	-62	4
PTSD									
Horizontal Smooth Pursuit > Central Fixation Dot	R	17	Calcarine Cortex	11284	<0.001	Inf	10	-84	4
	L	17	Calcarine Cortex		<0.001	Inf	-6	-86	2
	L/R	17	Cuneus		<0.001	Inf	0	-82	8
	L	18	Superior Occipital Gyrus		<0.001	Inf	-6	-82	20
	L	17	Occipital Pole		<0.001	Inf	-8	-94	6
	R	18	Superior Occipital Gyrus		<0.001	7.42	2	-82	26
	L	19	Inferior Occipital Gyrus	566	<0.001	6.82	-48	-72	6
Horizontal Saccadic > Central Fixation Dot	R	17	Calcarine Cortex	3536	<0.001	6.27	10	-84	4

	L	17	Calcarine Cortex		<0.001	6.00	-12	-72	8
	R	17	Lingual Gyrus		<0.001	5.97	4	-86	0
	L	18	Cuneus		0.001	5.61	-2	-80	20
Central Fixation Dot > Horizontal Saccadic	L	18	Occipital Pole	229	0.047	4.83	-22	-100	-2
Horizontal Smooth Pursuit > Horizontal Saccadic	L	18	Occipital Pole	590	0.001	5.17	-16	-94	6
	R	8	Dorsolateral Prefrontal Cortex	2348	0.036	4.89	36	30	50
	R	7	Precuneus	40	0.008	3.85	4	-60	40
Between Memory	**NS**								
Between Group, Between Motion, Within Memory	**NS**								
Between Group, Within Motion, Between Memory	**NS**								
Within Group, Between Motion, Between Memory									
Control Traumatic>Neutral Memory Central Fixation Dot > Horizontal Saccadic	L	11	Rostral Anterior Cingulate Cortex	25	0.044	4.84	-12	28	-16
PTSD Traumatic>No Memory Horizontal Smooth Pursuit > Horizontal Saccadic	R	39	Angular Gyrus	95	0.032	4.92	50	-56	52

	R	8	Dorsolateral Prefrontal Cortex	12	0.003*	4.13	36	28	52
Between Group, Between Motion, Between Memory	**NS**								

Abbreviations: LR, left/right hemisphere; BA, Brodmann Area; k, cluster size; vFWE, voxel-wise family-wise error corrected; MNI, Montréal Neurological Institute; NS, not significant

Supplementary Table 4. *Right Frontal Eye Field Psychophysiological Interaction F-tests*

	LR	**BA**	**Region**	**k**	**vFWE**	**Z-Score**	**MNI Coordinates**		
							x	**y**	**z**
Average ANOVA effect	L		Angular Gyrus	549	0.010	5.23	-44	-66	36
	R		Precentral Gyrus	182	0.011	5.21	28	-8	56
	L		Precuneus	1094	0.023	5.06	-4	-60	34
Main Effect of Group	**NS**								
Main Effect of Memory	**NS**								
Main Effect of Motion	**NS**								
Interaction:	**NS**								

Group x Motion									
Interaction: Memory x Motion	**NS**								
Interaction: Group x Memory x Motion	**NS**								

Abbreviations: LR, left/right hemisphere; BA, Brodmann Area; k, cluster size; vFWE, voxel-wise family-wise error corrected; MNI, Montréal Neurological Institute; NS, not significant

Supplementary Table 5. *Right Supplementary Eye Field Psychophysiological Interaction F-tests*

	LR	**BA**	**Region**	**k**	**vFWE**	**Z-Score**	**MNI Coordinates**		
							x	**y**	**z**
Average ANOVA Effect	R	6	Precentral Gyrus	3497	0.002	5.61	38	-10	54
	L	6	Superior Frontal Gyrus		0.025	5.04	-14	14	66
	L	6	Middle Frontal Gyrus		0.030	5.00	-46	4	46
	L	7	Superior Parietal Lobule	799	0.036	4.96	-22	-52	52
Main Effect of Group	**NS**								

Main Effect of Memory	L	18	Lingual Gyrus	896	0.027	4.96	-6	-86	-8
Main Effect of Motion	**NS**								
Interaction: GroupxMotion	R	39	Angular Gyrus	543	0.041	4.96	48	-58	38
Interaction: Memory x Motion	**NS**								
Interaction: GroupxMemoryxMotion	**NS**								

Abbreviations: LR, left/right hemisphere; BA, Brodmann Area; k, cluster size; vFWE, voxel-wise family-wise error corrected; MNI, Montréal Neurological Institute; NS, not significant

Curriculum Vitae

Name: Sherain Harricharan

Post-secondary Education and Degrees:

The University of Western Ontario
London, Ontario, Canada
2010-2015
BSc, Honors Specialization in Biology, Major in Medical Sciences

Schulich School of Medicine and Dentistry
The University of Western Ontario
London, Ontario, Canada
2015-present
Doctoral Candidate, Department of Neuroscience

Honours and Awards:

MITACS Accelerate Scholarship — September 2018-present

Western Graduate Research Scholarship — September 2015-present

Best Student Oral Presentation — June 22, 2017
London Psychiatric Academic Research Day
Schulich School of Medicine & Dentistry

Related Work Experience

Neuroscience 9500: Principles of Neuroscience — September – December 2016
Teaching Assistant for Dr. Arthur Brown
Department of Neuroscience, Schulich School of Medicine and Dentistry

AnatCell 4451F: Integrative Neuroscience — September – December 2015
Teaching Assistant for Dr. Susanne Schmid
Department of Anatomy and Cell Biology, Schulich School of Medicine and Dentistry
Western University

Publications:

Harricharan, S., Rabellino, D., Frewen, P.A., Densmore, M., Théberge, J., Mckinnon, M.C., Schore, A.N., Lanius, R.A. 2016. fMRI functional connectivity of the periaqueductal gray in PTSD and its dissociative subtype. Brain Behav, 6: e00579, 1-16.

Harricharan, S., Nicholson, A. A., Densmore, M., Théberge, J., McKinnon, M. C., Neufeld, R. W., & Lanius, R. A. 2017. Sensory overload and imbalance: Resting-state vestibular connectivity in PTSD and its dissociative subtype. Neuropsychologia, 106: 169-178. Impact Factor: 3.197.

Harricharan, S., McKinnon, M.C., Tursich, M., Densmore, M., Frewen, P., Théberge, J., van der Kolk, B., Lanius, R. A. (2019). A pilot study examining overlapping frontoparietal networks in response to oculomotion and traumatic autobiographical memory retrieval: Implications for eye movement desensitization and reprocessing. European Journal of Psychotraumatology.

Harricharan, S., Nicholson, A.A., Thome, J., Densmore, M., McKinnon, M.C., Théberge, J., Frewen, P.A., Neufeld, R.W.J., Lanius, R.A. (2019; in press). PTSD and its dissociative subtype through the lens of the insula: Anterior and posterior insula resting-state functional connectivity and its predictive validity using machine learning. Psychophysiology.

Lanius, R. A., Rabellino, D., Boyd, J. E., Harricharan, S., Frewen, P. A., & McKinnon, M. C. 2017. The innate alarm system in PTSD: conscious and subconscious processing of threat. Current Opinion in Psychology, 14: 109-115.

Nicholson, A. A., Friston, K. J., Zeidman, P., Harricharan, S., McKinnon, M. C., Densmore, M., Neufeld, R.W., Théberge, J., Corrigan, F., Jetly, R., Spiegel, D. (2017). Dynamic causal modeling in PTSD and its dissociative subtype: Bottom–up versus top–down processing within fear and emotion regulation circuitry. Human Brain Mapping, 38: 5551-5561.

Rabellino, D., Densmore, M., Harricharan, S., Jean, T., McKinnon, M. C., & Lanius, R. A. 2017. Resting-state functional connectivity of the bed nucleus of the stria terminalis in post-traumatic stress disorder and its dissociative subtype. Human Brain Mapping. In press.

Rabellino, D., Harricharan, S., Frewen, P. A., Burin, D., McKinnon, M. C., & Lanius, R. A. (2016). “I can't tell whether it's my hand”: a pilot study of the neurophenomenology of body representation during the rubber hand illusion in trauma-related disorders. Eur J Psychotraumatol, 7: 32918.

Olivé, I., Densmore, M., Harricharan, S., Théberge, J., McKinnon, M. C., & Lanius, R. 2018. Superior colliculus resting state networks in post-traumatic stress disorder and its dissociative subtype. Human Brain Mapping 39: 563-574.

Tursich, M., Neufeld, R. W. J., Frewen, P. A., Harricharan, S., Kibler, J. L., Rhind, S. G., & Lanius, R. A. (2014). Association of trauma exposure with proinflammatory activity: a transdiagnostic meta-analysis. Transl Psychiatry, 4(7), e413. Impact Factor: 5.601. My role was to serve as a co-reviewer along with the first author for studies included in the meta-analysis.

Academic Presentations

Annual Society of Biological Psychiatry Conference May 16-19, 2019
Title: The Vestibular System in Posttraumatic Stress Disorder
Symposium Presentation
Chicago, Illinois

Annual ISSTD Conference March 28-April 1, 2019
Title: The Vestibular System in Posttraumatic Stress Disorder
Symposium Presentation
New York City, New York

International Trauma Conference May 30-June 2, 2018
Title: The Vestibular System in Posttraumatic Stress Disorder
**Keynote Speech*
Boston, Massachussetts

Neuropsychiatry Rounds September 8, 2017
Title: fMRI resting state functional connectivity of the periaqueductal gray in posttraumatic stress disorder and its dissociative subtype

Department of Psychiatry, Schulich School of Medicine and Dentistry
London, Ontario

London Psychiatry Academic Research Day June 22, 2017
Title: Sensory Overload and Imbalance: Resting-State Vestibular Connectivity in PTSD
Department of Psychiatry, Schulich School of Medicine and Dentistry
London, Ontario
*Received award for best student oral presentation

International Trauma Conference May 31-June 3, 2017
Title: The Vestibular System in Posttraumatic Stress Disorder
Workshop
Boston, Massachussetts

London Health Research Day March 28, 2017
Title: Sensory Overload and Imbalance: Resting-State Vestibular Connectivity in PTSD
Lawson Health Research Institute
London, Ontario

London Psychiatry Academic Research Day June 23, 2016
Title: fMRI resting state functional connectivity of the periaqueductal gray in posttraumatic stress disorder and its dissociative subtype
Department of Psychiatry, Schulich School of Medicine and Dentistry
London, Ontario